

Molecular mechanisms of M cell signalling in the small intestine

By

Ana Klisurić

Bachelor of Health Sciences (Honours; Physiology)

A thesis submitted for the degree of

Doctor of Philosophy

School of Pharmacy and Medical Sciences

Division of Health Sciences

March 2023

Table of Contents

List of Figures iv
List of Tables xi
Abbreviations xii
Declaration xv
Acknowledgements xvi
Funding xvii
Thesis Summary xviii
Abstract, Hypothesis and Aims xxi
Thesis Outline xxiv
Chapter 1 Introduction 25
1.1 The Physiology of the Gastrointestinal Tract 26
1.2 Crypt-Villus Subunit 29
1.3 The Cellular Composition of the Small Intestinal Epithelial Barrier 29
1.4 Immunity in the GIT 43
1.5 Brief Review of Literature Pertaining to the Study of Intestinal M Cells 45
1.6 References 47
Chapter 2 Identifying human and murine M cells *in vitro* 55
2.1 Abstract 56
2.2 Introduction 57
2.3 Morphological Indicators of M Cell Presence 63
2.4 Cell Surface Markers 67
2.5 Functional Indicators of M cell Presence 75
2.6 Conclusion 76
2.7 References 78
Chapter 3 Follicle-associated epithelial organoids as a platform for assessing M cell-mediated nanoparticle uptake 84
3.1 Abstract 85
3.2 Introduction 86
3.3 Materials and Methods 89
3.4 Results 94
3.5 Discussion 110
3.6 Conclusion 112
3.7 References 114
Chapter 4 Outstanding questions in intestinal M cell biology 117
4.1 Abstract 118
4.2 Introduction 119

4.3 Mechanisms of transcytosis 123
4.4 M cell subtypes 127
4.5 Conclusion 131
4.6 References 134
Chapter 5 Osteoprotegerin negatively regulates M cell differentiation 139
5.1 Abstract 140
5.2 Introduction 141
5.3 Materials and Methods 143
5.4 Results 145
5.5 Discussion 153
5.6 Conclusion 154
5.7 References 156
Chapter 6 Stem cells, signalling gradients and cellular differentiation 160
6.1 Intestinal stem cell niche 161
6.2 Signalling gradients along the crypt-villus axis 162
6.3 Lineage commitment 164
6.4 Signalling gradients in the Peyer's Patches 167
6.5 References 170
Chapter 7 Gastrointestinal mucus regulates particulate uptake in human *in vitro* models of the small intestinal epithelium 173
7.1 Abstract 174
7.2 Introduction 175
7.3 Materials and Methods 177
7.4 Results 182
7.5 Discussion 195
7.6 Conclusion 198
7.7 References 200
Chapter 8 Discussion and conclusion 202
8.1 Discussion 202
8.2 Conclusion 209
8.4 References 210
Appendix I: Publication Contributions and Permissions 213

List of Figures

Chapter 1

Figure 1: The gastrointestinal tract has four broad functions relating to the processing of ingested materials; ingestion, digestion, absorption and elimination. The digestive process begins with **(1)** the ingestion of food through the oral cavity, **(2)** the digestion of ingested food by mechanical and chemical means in the oral cavity, the stomach and the small intestine, **(3)** the absorption of nutrients from digested products primarily in the small intestine, but also, to a lesser extent, in the large intestine, and **(4)** the elimination of waste products, termed feces, from the large intestine by the anus. The structure of the epithelial barrier and the function of the cells lining the mucosa differs according to the region. At the histological level, the oral mucosa, where little absorption occurs, consists of highly keratinized, stratified, squamous epithelial cells. The gastric mucosa consists of a monolayer of columnar epithelial cells which secrete digestive enzymes to help breakdown food, and mucus, to protect the epithelium from the acidic gastrointestinal pH. The surface of the epithelium is distinguishable by numerous irregular gastric pits encircling gastric glands that are responsible primarily for the secretion of digestive acids. The small intestine is organised into distinct crypt-villus structural units; this increases the surface area available for absorption. The mucosa of the large intestine is less adapted to absorption, smoother in appearance and void of the small intestinal villi.

Figure 2: The crypt-villus subunit is composed of six mature cell types and two progenitor cell populations. The six mature cell types are subdivided into either the absorptive or the secretory lineage. Cells that develop along the absorptive lineage are limited to enterocytes, which are the most abundant cell type and are present throughout the epithelium. Secretory cells are further subdivided into Enteroendocrine cells, goblet cells, tuft cells and Paneth cells. The first three, Enteroendocrine cells, goblet cells and tuft cells, are present predominantly above the crypt-villus junction. Paneth cells migrate into the crypts upon differentiation, settling among the ISCs. M cells are present in the epithelium directly overlying the lymphoid follicles of the gut.

Figure 3: Lgr5+ stem cells are located at the base of the intestinal crypts and can reconstitute the epithelium in its entirety. Upper panel shows (b-c) LacZ staining (blue) of small intestinal

sections derived from mice carrying *LacZ* integrated into the last exon of the *LGR5* gene. Staining shows that LacZ is restricted to 6-8 cells dispersed at the bottom of the intestinal crypts. Lower panel (d-e) shows intestinal sections from a *Lgr5-EGFPIRES-creERT2* knock-in mouse crossed with the *Rosa26-lacZ* reporter mouse 5 days after tamoxifen injection (d) and 60 days after tamoxifen injection (e). Figure adapted, with permission, from results published by Barker & Clevers (2007).

Chapter 2

Figure 1: The differentiation of M cells is triggered by ligation of the RANK receptor expressed by cells of the intestinal epithelium to its ligand, RANKL. This causes the activation of TRAF6-mediated NF-kB signalling and the induction of Ets transcription factor SpiB. M cells express different markers during early and late stage development, with Gp2 being indicative of fully differentiated, mature M cells. Cytokines secreted by the follicle-associated epithelium, such as CCL20 and CCL9, have a chemotaxic effect toward CD11b+ dendritic cells that are present in the subepithelial dome.

Figure 2: M cells constitutively expressed by the follicle-associated epithelium express the mature M cell marker Gp2. They differentiate in response to RANKL stimulation and induction of *SpiB*. Alternatively, regular villous enterocytes can be prompted to differentiate into an 'villous' M cells that are only partially reminiscent of the M cell phenotype. Villous M cells are not restricted to the follicle-associated epithelium, express different markers and develop independently of *SpiB*. They are void of Gp2 expression and thus have an impaired transcytotic ability.

Chapter 3

Figure 1: Comparison of the cell-line-based co-culture versus RANKL-treated murine small intestinal organoids as an *in vitro* model of the follicle-associated epithelium (FAE). **(A)** Schematic of the two models. The Transwell co-culture is the current industry gold standard for *in vitro* modelling of the FAE. It consists of an epithelial cell line monolayer cultured for 21d on a semi-permeable membrane suspended in a Transwell; M cell differentiation is induced by co-culturing the epithelial cells with a cell line of hematopoietic origin in the lower compartment. Organoids are derived from mouse small intestinal (MsSI) stem cells and cultured for 5-7d in a hydrogel substrate; M cell differentiation is induced with soluble

RANKL. **(B)** Quantitative RT-qPCR analysis of transcriptional expression of M cell specific genes, normalised to β-actin. Mature M cell marker *Gp2,* and transcriptional factor regulating M cell differentiation, *SpiB*, are both upregulated significantly in RANKL-treated organoids compared to control organoids ($p=0.0153$ and $p>0.0001$, respectively). This effect is not observed in *SpiB*$^{-/-}$ organoids. Immature M cell marker, *Marcskl1,* is upregulated in RANKL-treated organoids, however this effect is *SpiB*-independent. *Gp2* expression is negligible across all models containing Caco-2 cells.. *SpiB* is upregulated in Caco-2/ LAZ 221 co-cultures ($p=0.0118$) and Caco-2/JY co-cultures, but not in RANKL-treated Caco-2 cells. *Marcskl1* is upregulated in RANKL-treated Caco-2 cells and in Caco-2/JY co-cultures.

Figure 2: Characterization of the murine organoid model of the intestinal follicle-associated epithelium. M cell differentiation was induced by activation of RANK/RANKL signalling, triggered by the supplementation of soluble RANKL into culture media. **(A)** Organoids cultured in regular 'ENR' media and RANKL-treated organoids retained a comparable morphology after 5d in culture, as evaluated by brightfield microscopy. **(B)** Representative confocal microscopy images of organoids after 5-7 days in culture revealed strong expression of Gp2, a terminal M cell differentiation marker, on the apical surface of cells of organoids that had been exposed to RANKL-supplemented 'ENR' media. Specific, apical Gp2 expression was not observed on cells of control organoids cultured in 'ENR' media only. Images are representative optical slices from a maximal projection of a Z-stack.

Figure 3: Characterization of polystyrene nanoparticles before and after conjugation to UEA-1. Transmission electron microscopy images of particles **(A)** before and **(B)** after conjugation to UEA-1 showing lack of aggregation. **(C)** Hydrodynamic diameters for the control (PS_{200}-PEG) and UEA-1 conjugated particles (PS_{200}-PEG-UEA-1). **(D)** XPS elemental survey spectra before and after conjugation to UEA-1 showing a significant increase in N% at 400eV.

Figure 4: Uptake of control and UEA-1 modified in WT mouse organoids cultured in either 'ENR' media or 'ENR' media supplemented with RANKL. **(A)** Schematic of microinjection and picture of injected organoids. **(B)** Representative quantification of uptake; an average of three experiments. **(C)** Representative FACS plots. Gate indicates double positive cell population; particles that have uptaken a bead (488- x axis) and particles that are positive for UEA-1 (561-y axis). Uptake of control particles is approximately double (x2.25) in organoids cultured in 'ENR+RANKL' media compared to 'ENR' cultured organoids. With

UEA-1 modified particles, the entire cell population, for both 'ENR' and 'ENR+RANKL' organoids, shifts leftwards into the double positive gate. There is a significant increase in uptake in both 'ENR' and 'ENR+RANKL' organoids, compared to non-modified particles. Uptake is consistently highest with UEA-1 modified particles in the 'ENR+RANKL' model. Experiment performed in quadruplicate. **(D)** Confocal images of binding of UEA-1 lectin by organoids cultured in 'ENR' media (upper panel) and organoids cultured in 'ENR+RANKL' media (lower panel). UEA-1 binds to organoids in both media conditions. **(E)** Internalization of microinjected particles co-localised with Gp2.

Supplementary Figure 1: Visualization of 'M-like cells' generated by the Caco-2/B cell co-culture by transmission electron microscopy. **(A, B)** Caco-2 cells grown in monolayers present with an organised brush border and a dense cytoplasm. **(C, D) '**M-like cells' generated from Caco-2 cells through co-culture with Raji B lymphocytes were identified by disrupted brush border, fewer microvilli and cytoplasmic vacuoles. Scale bars; 1 μm **(A, B),** 2 μm **(C, D).**

Chapter 5

Figure 1: OPG negatively regulates the M cell differentiation. **(A)** WT and *TNFRSF11B* $^{-/-}$ mouse small intestinal organoids were cultured with and without RANKL for 7 days. **(B)** The transcriptional expression of M cell specific genes, *Gp2* and *SpiB*, was evaluated; *Gp2* was elevated in a statistically significant manner between control and RANKL-treated *TNFRSF11B* $^{-/-}$ organoids (p=0.0171) and between RANKL-treated WT organoids and RANKL-treated *TNFRSF11B* $^{-/-}$ organoids (p=0.0222). *SpiB* was elevated in a statistically significant manner between control and RANKL-treated WT organoids (p=0.0376) and between control and RANKL-treated *TNFRSF11B* $^{-/-}$ organoids (p=0.0130). **(C)** The difference in protein expression of mature M cell marker Gp2 was assessed between the four groups; untreated WT and *TNFRSF11B* $^{-/-}$ organoids showed no Gp2 expression, RANKL-treated WT organoids showed some Gp2 expression and RANKL-treated *TNFRSF11B* $^{-/-}$ organoids showed a high level of Gp2 positivity.

Figure 2: Small intestinal organoids secrete OPG in response to exogenous RANKL.
(A) Transcriptional expression of *TNFRSF11B* is elevated in small intestinal organoids derived from WT mice treated with 200ng/ml of soluble RANKL, compared to untreated control organoids (p=0.3210). No transcriptional expression of *TNFRSF11B* was observed

in *TNFRSF11B* $^{-/-}$ organoids. **(B)** The transcriptional expression of mature M cells marker *Gp2* and *SpiB* rose in a RANKL dependent manner, peaking at 1ug/ml. The expression of *TNFRSF11B* also rose in a RANKL dose dependent manner. **(C)** Representative confocal images suggest that OPG secretion is not strictly restricted to Gp2+ M cells.

Chapter 6

Figure 1: Signalling gradients along the crypt villus axis. The base of the intestinal crypts experiences high levels of Wnt signalling. Wnt, and its potentiator R-spondin, are secreted by mesenchymal cells and Paneth cells. Wnt signalling helps maintain active stem cell proliferation. As Wnt ligands are poorly soluble, their exerted effect tapers off with increasing distance from the crypt bottom. In contrast, BMP signalling is highest at the base of the villous tips. Mesenchymal cells above the crypt-villus junction secrete BMP proteins that allow for the induction of differentiated cell types. To attenuate this effect at the crypt base, several cell types secrete BMP inhibitors such as Gremlin 1 (Grem 1), Gremlin 2 (Grem 2) and Chordin-like 1 (CHRDL1) protein.

Chapter 7

Figure 1: The absorptive capacity of Caco-2 cells, HT29 cells and HT29-MTX cells, represented as a mean fluorescence intensity value, as assessed using IFC. **(A)** Caco-2 cells display the highest uptake of 200nm amine-modified FluoSpheres, followed by HT29 cells, and then HT29-MTX cells. A one-way ANOVA analysis of the three groups determined the difference in absorptive capacity between the three cell types was statistically significant, p=0.0003. Results represent average values from three separate experiments, (n=3). **(B)** An IFC representative image of the fluorescence curve of the three cell populations; Caco-2 (green), HT29 (blue) and HT29-MTX (red).

Figure 2: The absorptive capacity of Caco-2 cells, HT29 cells and HT29-MTX cells before and after the dislodgement of the mucus from the cell surface through physical agitation and washing, represented as a mean fluorescence intensity value as assessed using IFC. **(A)** The washing of the Caco-2 cells did not result in a difference in uptake capacity. The washing of the HT29 cells and the HT29-MTX cells resulted in a statistically significant increase in the uptake capacity of the cells (p=0.0123 and p=0.0287, respectively). Results represent average values from three separate experiments, (n=3). **(B)** Alcian blue staining of HT29

and HT29-MTX monolayers before and after washing. Before washing, HT29-MTX cells display a higher level of mucus staining. After washing, HT29-MTX cells retain staining, whereas HT29 cells are completely void of mucus.

Figure 3: Transmission electron microscope (TEM) images of **(A)** aminated polystyrene FluoSpheres prior to any surface modification, **(B)** PEGylated, aminated polystyrene FluoSpheres and **(C)** 6-PGA modified, aminated polystyrene FluoSpheres. TEM analysis revealed no significant differences in the morphology, size and distribution of the particles before and after modification. The TEM images reveal a monodispersed particle population before and after modification, with no visible aggregation. Size distribution measurement of particles before and after modification in aqueous media was measured by dynamic light scattering and revealed that the particles maintained a narrow size range and did not aggregate. **(D)** The results show that the aminated polystyrene particles had a narrow size distribution with an average diameter of 235 nm (intensity distribution). Coating the particles with PEG polymers or 6-PGA molecules resulted in a slight increase in their average hydrodynamic diameter (251 nm for PEGylation and 270 nm for 6-PGA modification, respectively), as summarised in Table E **(E)**.

Figure 4: XPS analysis was used to confirm the successful modification of the particles and quantify the amounts of PEG and 6-PGA present after the conjugation process. **(A-B)** XPS elemental composition analysis and C 1s high resolution spectra of polystyrene particles with different surface modifications. The dash lines in the C 1s spectra indicate the CC/CH (285 eV, yellow) and CO (286.5 eV, green) components. A significant increase in the oxygen (O) and decrease in nitrogen (N) signals were detected for the PEGylated particles in comparison with the aminated particles. C 1s high resolution spectra also show an increase in the CO component, which can be attributed to the PEG chains. The ratio of CO to CC/CH in the C 1s signal was higher for PEGylated particles compared to the aminated control particles, suggesting successful PEGylation. For 6-PGA modified particles, an increase in the O component, from the GA molecule, was observed for the 6-PGA modified particles compared to control particles. C 1s high resolution spectra also confirmed the presence of 6-PGA, as shown by the increase in the ratio of CO to CC/CH component. **(C)** Zeta potential values of different polystyrene particles in PBS buffer (0.1×, the concentration of electrolytes is 15 mM).

Figure 5: The PEGylation of polystyrene FluoSpheres increases uptake in a statistically significant manner in all mucus models, compared to the non-PEGylated controls. **(A)** The four models with varying amounts of mucus were cultured for 10-12 days and exposed to a solution of control, non-PEGylated particles or PEGylated particles for 1 hour. PEGylated particles were uptaken by the cells at a higher rate in models characterised by higher levels of mucus, as determined by a Student t-test (*p>0.05). **(B)** Control particles or 6-PGA modified particles were exposed to HT29-MTX monolayers, the highest mucus containing model, for 1 hour. Uptake, assessed using IFC, was significantly higher with 6-PGA modified particles compared to the control particles (*p>0.05). Results represent the average of three separate experiments, n=3.

List of Tables

Chapter 2

Table 1: Commonly used and recently published variations of in vitro models of the follicle-associated epithelium and examples of M cell identification techniques used.

Table 2: M cell markers identified specifically in the gut-associated lymphoid tissue epithelium of different species.

Abbreviations

AMP: anti-microbial peptides

APC: antigen presenting cell

APC*: adenomatous polyposis coli

BMP: bone morphogenic protein

CBC: crypt base columnar

CCK: cholecystokinin

CCL20: chemokine (C-C motif) ligand 20

CCR6: C-C motif chemokine receptor 6

CFTR: cystic fibrosis transmembrane conductance regulator

CD: Crohn's disease

CHRDL1: Chordin-like protein 1

DAPT: N-[N-(3, 5-difluorophenacetyl)-l-alanyl]-s-phenylglycinet-butyl ester

DLL1: delta-like canonical Notch ligand 1

DLS: dynamic light scattering

DOCK2: dedicator of cytokinesis 2

DSS: dextrane sulfate sodium

EDC: 1-Ethyl-3-(3-dimethylaminopropyl)-carbodiimide

EEC: Enteroendocrine cell

EGF: epidermal growth factor

ERRB1: ephrinB1

FAE: follicle-associated epithelium

GALT: gut-associated mucosal lymphoid tissue

GC: Goblet cell

GFI1B: growth factor independent 1B

GFP: green fluorescent protein

GHRL: ghrelin

GI: gastrointestinal

GIP: gastric inhibitory peptide

GIT: gastrointestinal tract

GLP1: glucagon-like peptide 1

GP2: glycoprotein 2

GPI: glycosylphosphatidylinositol

GREM1: Gremlin 1

GREM2: Gremlin 2

IBD: inflammatory bowel disease

IL22BP: interleukin 22 binding protein

ILC2: innate lymphoid type 2 cells

ILC3: innate lymphoid type 2 cells

ISC: intestinal stem cell

IV: intravenous

IWP2: N-(6-Methyl-2-benzothiazolyl)-2-[(3,4,6,7-tetrahydro-4-oxo-3-phenylthieno[3,2-d]pyrimidin-2-yl)thio]-acetamide

LGR5: leucine-rich repeat-containing G-protein coupled receptor 5

LP: lamina propria

$LT\alpha_1\beta_2$: lymphotoxin $\alpha_1\beta_2$

LTi: lymphoid tissue inducer cell

LTo: lymphoid tissue organizer cell

M cell: microfold or membranous cell

MALT: mucosa-associated lymphoid tissue

MAP: muco-adhesive particles

Marcskl1: myristoylated alanine-rich C-kinase substrate kinase linked 1

MCi: M cell inducer

MHC: major histocompatibility complex

MPP: muco-penetrative particles

Ms: mouse

N: nitrogen

NHS: N-hydroxysuccinimide

O: oxygen

ODD: oral drug delivery

O-MALT: organized mucosal associated lymphoid tissue

OPG: osteoprotegerin

PAMP: pathogen-associated molecular pattern

PSD: particle size distribution

PNA: peanut agglutinin

POU2F3: POU domain, class 2, transcription factor 3

PP: Peyer’s Patch

PrPc: cellular prion protein

PrPSc: scrapie prion protein

PRR: pathogen recognition receptor

PSNP: polystyrene nanoparticles

PYY: peptide YY

RANK: receptor activator of nuclear factor kappa-B

RANKL: receptor activator of nuclear factor kappa-B ligand

Rpbj: recombination signal binding protein for immunoglobulin kappa J region

SI: small intestine

SLAA: sialyl Lewis A antigen

T2DM: type 2 diabetes mellitus

T4SS: type IV secretion systems

TAC: transit-amplifying cells

TEM: transmission electron microscopy

TC: tuft cell

TGFα: transforming growth factor- α

TF: transcription factor

TJ: tight junction

TLR: toll-like receptor

TRAF6: tumour necrosis factor receptor-associated factor 6

UEA-1: Ulex Europeaus Agglutinin 1

UC: ulcerative colitis

WGA: wheat germ agglutinin

WT: wild type

XPS: X-ray photoelectron spectroscopy

ZO-1: zonula occludens-1

Declaration

This thesis presents work carried out by myself and does not incorporate without acknowledgment any material previously submitted for a degree or diploma in any university; to the best of my knowledge it does not contain any materials previously published or written by another person except where due reference is made in the text; and all substantive contributions by others to the work presented, including jointly authored publications, are clearly acknowledged.



Ana Klisuric

02/03/2023

Acknowledgements

Firstly, I would like to thank my PhD supervisors Professor Benjamin Thierry, Professor Rachel Gibson and Professor Clive Prestidge for their support, patience and guidance, scientifically, professionally and personally, throughout my candidature. I would also like to extend my gratitude to all the members of the Bionanoengineering Laboratory, past and present; it has been a pleasure sharing this journey with you.

To Professor Hans Clevers, who graciously invited me to his laboratory and taught me more than I thought possible in one year; I cannot thank you enough. To Dr. Yotam Bar Ephraim- thank you for showing me the ropes and always being there to answer my many questions. And finally, to the rest of the Clevers lab; it was a pleasure and an honour working alongside such talented scientists.

To my family in Australia and overseas, thank you for your endless support and encouragement. To my darling sister Božica, thank you for your unique sense of humour. Thank you Ujko Srbo, Ujna Sladjo, Ivana and Miloše, for teaching me that 15,000km is no distance at all. Thank you Deda Miloše for teaching me how to tell time, forcing me to read endless passages of text and igniting in me a love of crosswords and Sudoku; thank you Baba Miro, though you weren't here to watch over me in person, I felt your presence every step of the way. To Deda Ilija and Baba Boja; thank you for always having my back. To the rest of my enormous family; thank you. I would name you all individually, but I might exceed the thesis character length.

To Jacqueline, my dearest friend, thank you for being my person, for your reliability, support and your friendship. Thank you to all the kind and inspiring women I'm delighted to call friends.

To my parents, Djurdjica and Milivoj, thank you for teaching me the importance of resilience and strength. Thank you for encouraging and supporting my educational journey from the very beginning. Most of all, thank you for inspiring me through your actions, not just your words. I dedicate this thesis to you.

Funding

The work conducted in this thesis was funded by ARC Linkage Grant (LP150100032), the Endeavour Leadership Foundation, a University of South Australia Student Mobility Grant and the ONCODE Institute.

Thesis Summary

The following thesis explores the mechanisms of M cell differentiation and function.

Chapter 1 serves as a general introduction to the field of intestinal epithelial biology. The purpose of this introduction is to convey the molecular complexity of the intestinal epithelium, the various cell types within it and how they function in relation to one another and the mucosal immune system. Specific emphasis is placed on conveying the differences between the follicle-associated epithelium and the regular epithelium in order to provide a clear rationale for the necessity of establishing an *in vitro* model of the follicle-associated epithelium that accurately reflects its physiological and molecular complexity.

Chapter 2, a published *Highlight Article* from issue 244 of the *Journal of Experimental Medicine and Biology,* entitled "Identifying human and murine M cells *in vitro,"* is a comprehensive analysis of the literature in the field which identified numerous discrepancies in models of M cells and corresponding identification methods. This critical review postulates M cells generated via various methods differ significantly in gene and protein expression, despite a superficial similarity in function. This key point is explored further in **Chapter 3**, which addresses discrepancies in M cell markers between different models. Specifically, this chapter proposes that Caco-2-derived M cells are not a good representation of true M cells. In contrast, M cells generated from organoids are a faithful representation of *in vivo* M cells in terms of established gene and protein markers. Furthermore, this chapter describes a reproducible method for utilising organoid-derived M cells to study the rate of uptake of nanoparticles. The method involves injecting a nanoparticle solution into the enclosed lumen of the M cell-containing organoids and analysing the rate of nanoparticle uptake using fluorescence-activated cell sorting. Together, **Chapter 2** and **Chapter 3** provide evidence, from both a critical review of the literature and from experimental data, that the commonly used methods to generate M-like cells and test their functionality are poor compared to the *in vivo* context. Furthermore, **Chapter 3** provides experimental evidence that surface modification of nanoparticles can increase the rate of uptake by M cells.

In vivo studies of intestinal M cells are hampered by their rarity. As such, much of the data pertaining to M cells, particularly M cell function, is derived from cell line-based assays. Previous chapters have explored the limitations of these methods, generating still more questions about the apparently divergent developmental pathways of intestinal M cells. These questions are investigated in depth in **Chapter 4**. Entitled *"*Outstanding questions in

M cell biology," this chapter critically analyses the current literature to identify unanswered questions surrounding M cells and can be used to guide future investigative efforts in this field.

Chapter 5 utilises the M cell model described in **Chapter 3** to investigate regulatory mechanisms of M cell development. This chapter utilises techniques such as measuring RNA expression levels of M cell markers in wild-type and gene knockout organoids to explore how the number and function of M cells is maintained in the intestine. Osteoprotegerin, a soluble protein that forms a part of the RANK/RANKL/OPG axis, is implicated as having a major regulatory role in M cell biology.

The purpose of **Chapter 6**, a review chapter entitled "Stem cells, signalling gradients and cellular differentiation", is to provide a better understanding as to why *in vivo* M cells differ so significantly from the 'M cells' generated from cell line-based assays reported in the literature. This chapter explores the various signalling gradients and mechanisms essential for the normal development of M cells, and more broadly all intestinal epithelial cells, *in vivo.* The chapter also summarises the numerous pathways required for cellular differentiation *in vivo,* providing crucial insights into intestinal stem cell biology and, ultimately, context as to why cell line-based models are incapable of generating true M cells.

Various parts of this thesis discuss the limitations of cell lines in modelling M cells *in vitro*. Despite this, certain features of the intestinal epithelium, such as the intestinal mucus, can be replicated in a limited capacity by cell lines *in vitro*. **Chapter 7** utilises cell lines to generate intestinal epithelial models featuring varying levels of mucus. These models provide an appropriate platform for the study of the involvement of mucus in particle transport. Furthermore, utilising cell lines to study mucus/particle interaction may be a more practical approach than organoids, as goblet cell enrichment in organoids necessitates modifications to the culture protocol that introduces various extraneous variables into the otherwise well-characterised system. This is discussed further in **Chapter 8**, a chapter containing the discussion and conclusion for this thesis.

Chapters 3, 4 and **5** are the product of work conducted at the Hubrecht Institute in the Netherlands. This work was completed under the direct supervision of Professor Hans Clevers, Professor Benjamin Thierry and postdoctoral researcher Dr. Yotam Bar-Ephraim. At the time of completion of this thesis, these chapters are being prepared for publication in

collaboration with Professor Clevers, Professor Benjamin Thierry and Dr. Bar-Ephraim. This work was funded by the Endeavour Leadership Foundation and a University of South Australia Student Mobility Grant. **Chapters 2**, **4** and **7** were funded by an ARC Linkage Grant (LP150100032) and the University of South Australia Postgraduate Award.

All chapters were conducted under the supervision of Professor Benjamin Thierry, Professor Rachel Gibson and Professor Clive Prestidge.

The work conducted in this PhD is crucial to advancing the knowledge of M cells and providing advanced platforms that can be utilised for future work in this field.

Abstract, Hypothesis and Aims

Abstract

The epithelium overlying the organised lymphoid follicles of the gut differs from villous epithelium in that it has a diminished mucus layer and the presence of antigen-sampling M cells, an epithelial cell population specialised for transcytosis. The reduced mucus layer enables luminal antigens to interact more readily with the epithelium, including M cells. Owing to their unique morphology and expression of cell-specific capture receptors, M cells are capable of transcytosing luminal antigens swiftly and efficiently. Following M cell-mediated transcytosis, antigens are presented to immune cells located in the subepithelial lymphoid tissues. This triggers the rapid induction of a mucosal immune response.

Due to their ability to transcytose luminal antigens at a higher rate than surrounding epithelial cells, the functional mechanisms of M cells have garnered significant interest. This is especially relevant to the field of oral drug delivery, where understanding the transcytotic mechanisms of M cells could lead to improved and more effective drug delivery systems. Currently, lack of insight into the molecular mechanisms regulating the absorption of particles across the small intestinal epithelial barrier has hindered the development of therapeutically optimal oral drug delivery systems within the pharmaceutical industry. Leveraging M cell-mediated transcytotic pathways may enable the development of the next generation of oral pharmaceuticals.

M cells comprise between 5-10% of all cells within the follicle-associated epithelium. Due to their scarcity, M cells have proven difficult to study. Isolation and purification of M cells from *in vivo* tissues generally does not yield sufficient cell numbers to conduct statistically significant studies. Thus, the most convenient and efficient method for studying M cells is *in vitro.* In an attempt to enable the *in vitro* study of M cells, Kerneis and colleagues (1997) pioneered a co-culture system consisting of differentiated Caco-2 cells and freshly isolated Peyer's Patch lymphocytes; the biochemical factors released by lymphocytes purportedly induced the differentiation of Caco-2 cells to M cells, as evaluated by changes in apical morphology. In the subsequent 25 years, several additional models have been published in an attempt to recapitulate the complex microenvironment of the Peyer's Patch and facilitate the *in vitro* study of M cells. The most frequently published models comprise of Caco-2 monolayers cultured on a porous membrane with Raji B cells cultured in suspension

underneath. Other models include (i) organoid cultures where M cells are differentiated through RANKL stimulation, (ii) co-cultures of epithelial cells with hematopoietic B cells and (iii) inducing M cell differentiation from enterocytes through exposure to a pathogenic challenge such as cholera toxin (CT) or certain types of enterobacteria. Though these cells often recapitulate the characteristic M cell morphology, it is unclear how similar the M cells generated through these various developmental pathways are to terminally-differentiated, Gp-2+ M cells found in the human follicle-associated epithelium *in vivo*. In the case of the frequently published Caco-2/Raji co-culture, several reports suggest that the M cells generated through the co-culture system lack the genomic and proteomic signature of fully-differentiated *in vivo* M cells.

The overarching purpose of this PhD thesis was to advance the understanding of the role of intestinal M cells in particulate uptake. Practically, this necessitated the critical analysis of currently used models for studying M cells *in vitro* and the development of an advanced model that can provide better insight into the molecular mechanisms underlying M cell differentiation and function.

This work has achieved several significant contributions to the field of intestinal epithelial biology and the study of M cells. It provides a comprehensive introduction to the complexity of the intestinal epithelium and highlights the differences between follicle-associated epithelium and regular epithelium, justifying the need for an accurate in vitro model. Through a critical analysis of existing literature and experimental data, it convincingly demonstrates the limitations of commonly used M cell models and highlights the utility of organoid-derived M cells for studying nanoparticle uptake. The study raises important questions in M cell biology and explores the regulatory mechanisms behind M cell development. It also sheds light on the complex signaling gradients and differentiation processes involved in M cell development in vivo. By investigating the role of mucus in particle transport, the work offers insights into the interaction between epithelial cells and particles. In summary, this research significantly advances our understanding of M cell biology, providing clarity on the limitations of existing models and offering new perspectives for future investigations.

Aim

The aim of this PhD thesis was to develop an advanced model of the follicle-associated epithelium in order to advance the understanding of

(1) The role of intestinal M cells in particulate uptake and
(2) The mechanisms of M cell differentiation and function.

Aim 1

Critically evaluate the models currently available for studying the molecular and functional mechanisms of M cells, outlining potential advantages and disadvantages.

Aim 2

Using knowledge gained from Aim 1, develop an advanced *in vitro* model for studying the follicle-associated epithelium. Development of the model should take into consideration gastrointestinal physiology and a methodology for evaluating M cell function in the context of nanoparticle uptake.

Aim 3

Using the model developed in Aim 2, investigate the molecular mechanisms of differentiation of M cells.

Aim 4

Investigate the functional mechanisms of enterocytes and M cells using a range of engineered nanoparticles.

Hypothesis

The development of a physiologically and more molecularly accurate *in vitro* model of the small intestinal epithelial barrier will provide insight into the molecular mechanisms regulating M cell differentiation and function.

Thesis Outline

Chapter	Chapter Title	Aims Addressed
1	Introduction	-
2	Identifying human and murine M cells *in vitro*	1
3	Follicle-associated epithelial organoids as a platform for assessing M cell-mediated nanoparticle uptake	1, 2 and 4
4	Outstanding questions in M cell biology	1 and 3
5	Osteoprotegerin negatively regulates M cell differentiation	2 and 3
6	Stem cells, signalling gradients and cellular differentiation	3
7	Gastrointestinal mucus regulates particulate uptake in human *in vitro* models of the small intestinal epithelium	4
8	Discussion and conclusion	-

Chapter 1 Introduction

The aim of this thesis is to gain a comprehensive understanding of the intricate structure of the small intestinal epithelial barrier from both the physiological and the molecular perspective, with the aim of producing an *in vitro* model of this complex system. Accordingly, this chapter covers the following topics:

1. The anatomy and physiology of the gastrointestinal tract and the structure of the epithelial barrier.
2. The molecular composition of the epithelial barrier, with a focus on the roles of various cell types in maintaining the barrier's integrity, which has important implications for oral drug delivery.

1.1 The Physiology of the Gastrointestinal Tract

The human gastrointestinal tract (GIT) performs several functions, primarily relating to the digestion of ingested foodstuffs and absorption of nutrients into systemic circulation. [1-4] Anatomically, the gastrointestinal tract (GIT) commences at the oral cavity, proceeding through the pharynx, the esophagus, the stomach, the small intestine (SI), the large intestine, the rectum, and concluding at the anus. Structurally, the GIT is a continuous hollow tube with a wall composed of four concentrically-arranged tissue layers. [2] The outermost layer, the serosa, is a smooth membrane consisting of a thin layer of mesothelial cells and connective tissue. The next layer, the muscularis, is composed of several sheets of smooth muscle responsible for peristalsis; wave-like contractions that help propel food through the GIT. The middle layer, the submucosa, is composed of connective tissue rich in blood and lymph components, nerve fibfers and various immune cells. The innermost layer, the mucosa, consists of a monolayer of epithelial cells supported by a loose matrix of vascularised connective tissue termed the lamina propria (LP). [5] The mucosa is the primary interface between the external environment and the internal structures of the body. The epithelial cells lining the mucosa form a semipermeable barrier that mediates the passage of luminal contents into the subepithelial space. [2, 4, 5]

The oral cavity, where food and other orally ingested compounds enter the mouth, marks the initiation of both the GIT and the digestive process. Here, ingested food is processed chemically and mechanically, primarily through mastication by the teeth and lubrication with mucus and salivary gland excretions. [2] Next, the pharynx, a musculo-membranous tube, serves as the opening to the esophagus. During swallowing, the nasopharynx and larynx close, allowing the food to be directed into the esophageal tube. The esophagus is a long, muscular tube that uses peristaltic motion to propel the food into the stomach. The stomach is the primary site of chemical and mechanical digestion. Here, continuous secretion of gastric acid maintains a relatively low regional pH (1.5-3.5). [5] The acidic environment and high enzymatic activity allow for the efficient chemical breakdown of foodstuffs. Additionally, in the stomach wall, the sheets of muscle that comprise the muscularis consist of an inner oblique muscle layer, a middle circular layer and an external longitudinal layer. This robust muscularis propagates mechanical digestion by contracting and relaxing the three muscle layers, assisting in the mixing and churning motion of the stomach. The chemically and mechanically digested food then proceeds to the small intestine, where ~90% of the absorption takes place.

The small intestine is further segmented into the duodenum, the jejunum and the ileum. [4-6] The first part of the small intestine, the duodenum, receives the stomach contents, known as chyme, combining them with digestive materials from the pancreas and the liver. In this region, the acidic pH of the chyme is neutralised by the alkaline pH of the duodenum. Absorption is initiated, primarily that of calcium, magnesium and iron [7], before the chyme progresses to the next segment. The next segment, the jejunum, is the site of absorption of most other nutrients. The final segment, the ileum, is the site of absorption of vitamin B_{12}, bile salts and any residual digestive by-products from the jejunum. [4]

The epithelium of the small intestine is ordered into distinct crypt-villus structural units. [8] Cells of the epithelium are generated in the crypt region and lost by apoptosis at the tips of the villi, which are finger-like projections extending into the lumen. [9] Individual cells comprising the epithelial barrier have microscopic cellular protrusions termed microvilli. The entirety of the mucosa is folded into crescentic folds termed plicae circulares. These folds are particularly prominent towards the distal end of the duodenum and the jejunum. Collectively, the plicae circulares, the crypt-villus subunits and the microvilli serve to increase the absorptive surface area of the small intestine, enabling more efficient absorption. [2]

The large intestine is the site of water absorption and formation of feces, which are subsequently expelled from the GIT via the anus. These organs, together with the various accessory organs of digestion (salivary glands, pancreas, liver) are collectively responsible for digestion and absorption from the point of ingestion to the point of expulsion. The GIT organs involved in the broad functions of ingestion, digestion, absorption and elimination, and the microscopic histological structure of the mucosal barrier, are summarised in **Figure 1**.

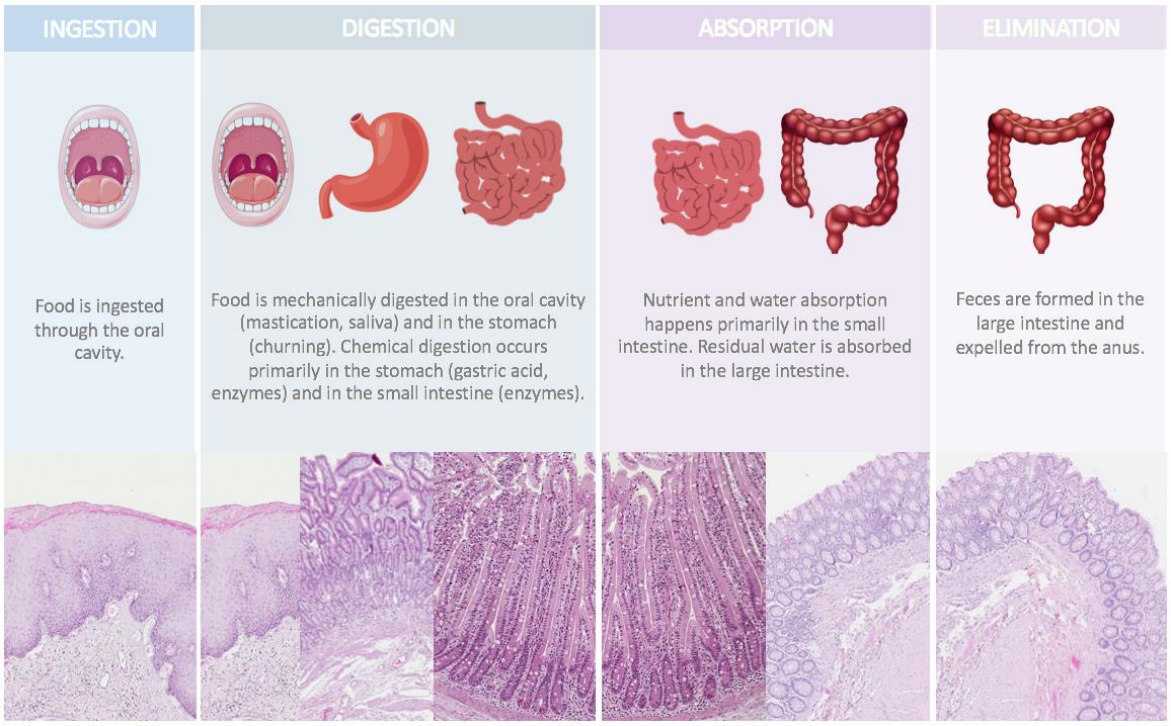

Figure 1: The gastrointestinal tract has four broad functions relating to the processing of ingested materials; ingestion, digestion, absorption and elimination. The digestive process begins with **(1)** the ingestion of food through the oral cavity, **(2)** the digestion of ingested food by mechanical and chemical means in the oral cavity, the stomach and the small intestine, **(3)** the absorption of nutrients from digested products primarily in the small intestine, but also, to a lesser extent, in the large intestine, and **(4)** the elimination of waste products, termed feces, from the large intestine by the anus. The structure of the epithelial barrier and the function of the cells lining the mucosa differs according to the region. At the histological level, the oral mucosa, where little absorption occurs, consists of highly keratinized, stratified, squamous epithelial cells. The gastric mucosa consists of a monolayer of columnar epithelial cells which secrete digestive enzymes to help breakdown food, and mucus, to protect the epithelium from the acidic gastrointestinal pH. The surface of the epithelium is distinguishable by numerous irregular gastric pits encircling gastric glands that are responsible primarily for the secretion of digestive acids. The small intestine is organised into distinct crypt-villus structural units; this increases the surface area available for absorption. The mucosa of the large intestine is less adapted to absorption, smoother in appearance and void of the small intestinal villi.

1.2 Crypt-Villus Subunit

The tissue architecture of the intestinal epithelium facilitates the primary function of the region. The small intestinal epithelium is the primary site of nutrient absorption; thus the epithelium is arranged into millions of distinct crypt-villus subunits. The villi are finger-like protrusions extending into the lumen of the GIT; the concave invaginations between the villi are called crypts. [10, 11] The density of the crypt-villus subunits decreases in a proximal to distal progression, resulting in less surface area available for absorption. The colon is void of villi entirely. The surface of the intestinal mucosa is lined by a monolayer of polarized epithelial cells held together by interacting proteins. The interacting proteins create fusion points between individual cells, effectively forming a resistant paracellular barrier.

The small intestinal mucosa is highly permeable and, as such, facilitates the greatest interchange between the external and internal environments. The epithelium must maintain an efficient rate of absorption of luminal contents, whilst simultaneously precluding the passage of harmful substances. To achieve this delicate balance, six mature cell types work to both absorb and protect. [12] These cells are regenerated by a highly proliferative pool of progenitor cells, known as transit-amplifying cells (TACs), that are produced from a pool of intestinal stem cells (ISCs) located at the base of the intestinal crypts. [13]

1.3 The Cellular Composition of the Small Intestinal Epithelial Barrier

The epithelium of the small intestine is one of the most rapidly renewing tissues in the body. [14] The cells comprising the epithelium are generated from a pool of continuously cycling intestinal stem cells. These ISCs are located at the base of the intestinal crypts and can be identified by the expression of surface marker leucine-rich repeat-containing G-protein coupled receptor 5 (Lgr5+). [8, 15]

Lgr5+ stem cells replenish the intestinal epithelium by generating a pool of highly proliferative TACs. TACs, considered an ‘intermediary cell population’, subsequently differentiate into the six mature cell types that comprise the epithelial wall. [12, 16] The six cell types mature along two main differentiation lineages; absorptive or secretory. [17] Absorptive enterocytes constitute the majority of cells contained within the intestinal barrier (~80%), whilst secretory cells, further subcategorised into Enteroendocrine cells (EECs), Paneth cells, goblet cells and tuft cells, collectively comprise ~20% of the epithelial wall.

[12, 17] It is unclear whether M cells, the last remaining cell type, belong to the absorptive or secretory lineage.

Absorptive enterocytes are responsible for nutrient absorption, whereas secretory cells, discussed in greater detail in subsequent sections, are primarily responsible for the secretion of several important substances. These include hormones that regulate metabolic functions (EECs), secretion of ligands that regulate the signalling pathways necessary for the maintenance of the stem cell niche (Paneth cells), secretion of protective mucus (goblet cells) and secretion of immune-reactive factors (tuft cells). [12, 18-22] Additionally, specialised, transcytotically-active M cells can be found in the follicle-associated epithelium (FAE) overlying lymphoid structures of the gut; their developmental origins remain uncharacterised. [23-25] Finally, the 'stem cell pool' located at the base of the intestinal crypts includes bona fide ISCs and the intermediary progenitor population, the TACs. Together, the ISCs and TACs are the source of all cellular renewal. [15, 26]

The six mature cell types and the stem cell pool symbiotically work to maintain homeostasis. The functional importance of each cell type is reflected in its positioning within the crypt-villus subunit; multiple signalling gradients differentially expressed along the crypt-villus axis maintain a robust stem cell population, drive lineage commitment of progenitor cells and maintain the correct proportions of each cell type. [17, 27-30] Enterocytes are present throughout the epithelium. EECs, goblet cells and tuft cells are present predominantly above the crypt-villus junction. [12] Goblet cells, which secrete a protective mucus, are most abundantly expressed near the villous tip, as this region undergoes most exposure to luminal contents. [22] EECs secrete hormones that regulate metabolic functions, whilst tuft cells secrete interleukins and other defense molecules in response to immuno-stimulatory factors. [19, 31] The number of these stimulus-responsive cells varies greatly during disease and infection, affirming their role as sentinels of immune regulation in the gut. The crypts are primarily reserved for ISCs, TACs and the last remaining secretory cell type, the Paneth cells. Paneth cells secrete essential ligands that maintain a robust stem cell population, as well as anti-microbial peptides (AMPs) that repel invading bacteria from the stem cell niche. [12, 20, 32] Their regulation of ISCs is contact-dependent, and their number is tightly regulated.

Beyond the crypt-villus subunit, accretions of lymph tissue develop as domal protrusions of the mucosa. These dome-like structures, termed the Peyer's Patches (PPs), are the most

convenient point of access to the mucosal immune system. [33-35] The epithelium covering the PPs is also uniquely adapted to facilitate this function. Goblet cells are largely absent, resulting in a significantly thinner layer of glycocalyx covering the apical cell surface, and an additional cell population, the M cell, is present. M cells comprise ~10% of the epithelium in this region and exhibit a greater capacity for transcytosis than the surrounding epithelium. The location of each cell type is represented schematically in **Figure 2**; the signalling pathways and factors influencing cell differentiation are discussed in subsequent sections.

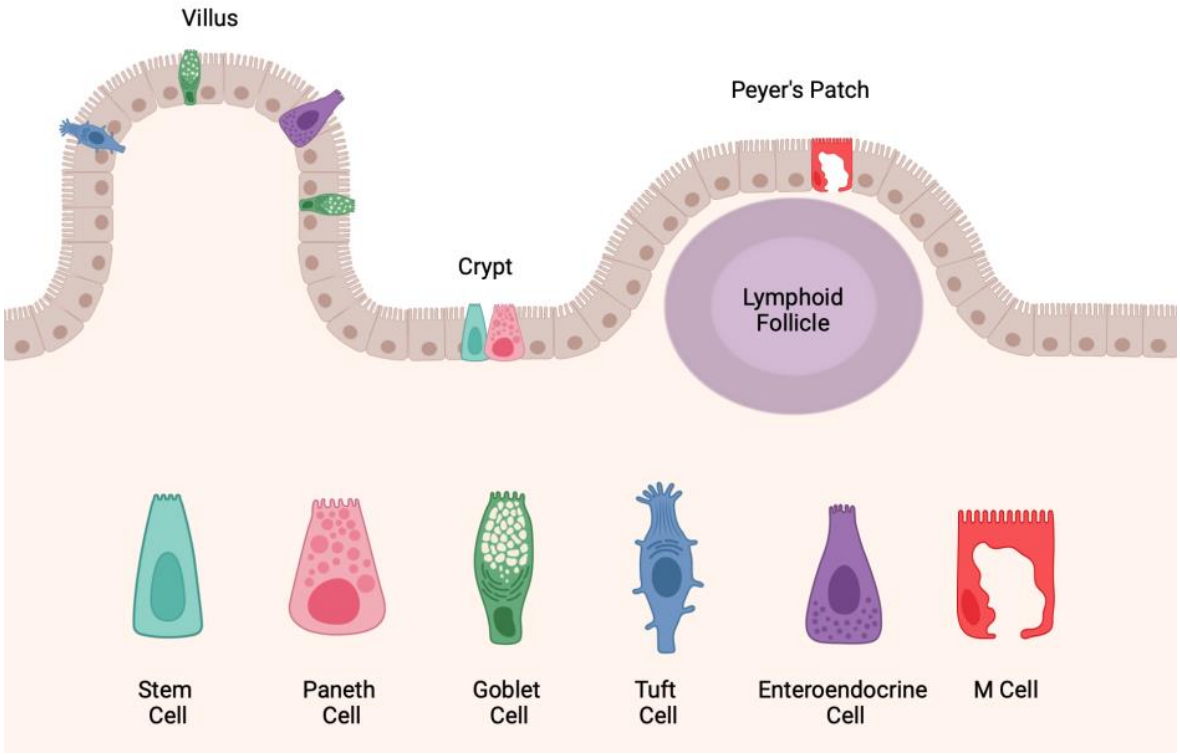

Figure 2: The crypt-villus subunit is composed of six mature cell types and two progenitor cell populations. The six mature cell types are subdivided into either the absorptive or the secretory lineage. Cells that develop along the absorptive lineage are limited to enterocytes, which are the most abundant cell type and are present throughout the epithelium. Secretory cells are further subdivided into Enteroendocrine cells, goblet cells, tuft cells and Paneth cells. The first three, Enteroendocrine cells, goblet cells and tuft cells, are present predominantly above the crypt-villus junction. Paneth cells migrate into the crypts upon differentiation, settling among the ISCs. M cells are present in the epithelium directly overlying the lymphoid follicles of the gut.

1.3.1 Enterocytes

Enterocytes comprise majority of the intestinal epithelium, accounting for approximately 80% of all cells present within the barrier. [26] As the most abundant cell type, enterocytes are tasked with the critical function of establishing and maintaining an effective epithelial barrier, whilst also performing a range of other vital functions. [36-38]

The primary purpose of the epithelial barrier is to spatially segregate the contents of the intestinal lumen and the underlying immune environment through a selectively permeable physical barrier; this function is crucial for precluding the host microbiota from continuously activating the mucosal immune system. Cells within the epithelial barrier are conjoined through the interaction of various adhesion proteins. The integrity of the intestinal barrier is dependent on cellular proximity, which is in turn mediated by the apical junctional complex comprised of tight junctions (TJs) and subjacent adherens junctions. TJs, comprised of transmembrane proteins, scaffolding proteins and regulatory molecules, limit solute flux in the paracellular space and, as such, are the main determinants of paracellular transport. [37] Adherens junctions, composed of the cadherin protein family, stabilise cell-to-cell contact, regulate the actin cytoskeleton and mediate intercellular communication. [39] Breaches in the integrity of the barrier results in unregulated interaction between immune cells and luminal contents creating chronic inflammation; this is known to be a hallmark feature of several debilitating gut pathologies such as Crohn's disease and ulcerative colitis. [37, 38, 40, 41] Collectively, these adhesion points between adjacent cells function to maintain an effective barrier that seals the paracellular space, safeguarding the sub-epithelial lamina propria and associated lymphoid structures from luminal antigens.

Commitment to the enterocyte lineage was thought to be regulated by activation of the Notch signalling pathway. [29, 42] However, it appears as though activation of Notch is only essential to repress commitment to the secretory lineage; in the absence of Notch, progenitor cells differentiate to absorptive enterocytes by default. [29, 43, 44] A more thorough discussion of the regulation of lineage commitment can be found in **Chapter 6.**

Functionally, enterocytes absorb nutrients, ions and bile acids via transporters expressed on the cell membrane; in the absence of specific transporters, enterocytes are mostly impermeable to hydrophilic solutes. The apical surface of the entire small intestinal barrier, excepting the PPs, is covered by a thick, loose layer of mucus that is actively and

continuously secreted by goblet cells. However, enterocytes also express a thinner, carbohydrate-enriched glycocalyx. The glycocalyx is composed of secreted, heavily glycosylated proteins anchored to the surface of the cells and harbors a wealth of digestive enzymes. [45, 46]

Historically, enterocytes were studied mostly pertaining to absorption, digestion and barrier maintenance. However, it is now understood that enterocytes also have an active role in mediating GI immunity. [47-49] In addition to the digestion of luminal nutrients, enterocytes can chemically digest luminal contents, cross-communicating with cells of the immune system to induce oral tolerance, i.e. a state of non-reactivity to innocuous luminal stimuli and microbial species. The chemical digestion of luminal nutrients by enterocytes ensures the degradation of epitopes that can stimulate immune response to innocuous stimuli, thereby contributing significantly to oral tolerance. [47-49] This enterocyte-mediated process is a key feature of oral tolerance and homeostasis.

1.3.2 Intestinal Stem Cells

The intestinal epithelium undergoes continuous and rapid self-renewal, indicating an active and robust stem cell population. [26] Past research has produced an operational definition of stem cell characteristics; stem cells are relatively quiescent and do not differentiate directly into mature cell lineages. [15, 17, 27, 44, 50] Instead, they divide asymmetrically, producing one stem cell and one pluripotent, rapidly proliferating cell committed to terminal cellular differentiation. This highly proliferative 'transit' cell population divides rapidly, forming a pool of transit amplifying cells that are able to differentiate into all cell lineages. [51, 52]

Proliferative ability of the stem cell population is regulated by several factors. Tcf4, a potent downstream effector of the Wingless/Wnt signalling pathway, has been deemed crucial to maintaining cellular proliferation in the intestine. A study by Korinek & Clevers demonstrated that disruption of the *Tcf7l2* gene encoding for Tcf4 in mice leads to a lack of crypt stem cells in the small intestine. *Tcf7l2*$^{-/-}$ mice died shortly after birth and their neonatal epithelium was composed entirely of differentiated, non-dividing cells. [53] Building on this finding, Barker & Clevers proposed that Wnt signalling was a key pathway regulating stem cell proliferation in the intestine; they compiled a list of Wnt target genes and analysed their expression in the intestine to select possible candidates for stem cell specific markers. The *LGR5* gene was uniquely expressed by a small number of cells at the base of the intestinal

crypts. [9, 15] Next, they generated a knock-in allele of green fluorescent protein (GFP), *(EGFP)-IRES-creERT2*, cassette into the first ATG codon of the *LGR5* gene. Analysis of GFP-tagged *LGR5* expression in homozygous mice revealed that *LGR5*$^{+}$ cells could reconstitute all of the cells of the intestinal epithelium. [9] Representative figures adapted from the seminal paper are displayed, with permission, in **Figure 3**.

In summary, Lgr5+ stem cells, located at the base of the intestinal crypts, continuously cycle to produce transit amplifying cells (TACs) that, upon several rapid rounds of division, then go on to reconstitute the intestinal epithelium in its entirety. [9] These cells can be isolated and cultured *in vitro* under optimised conditions to create fully-functional mini-organs, or 'organoids', that recapitulate the molecular and physiological make-up of the original organ. [8]

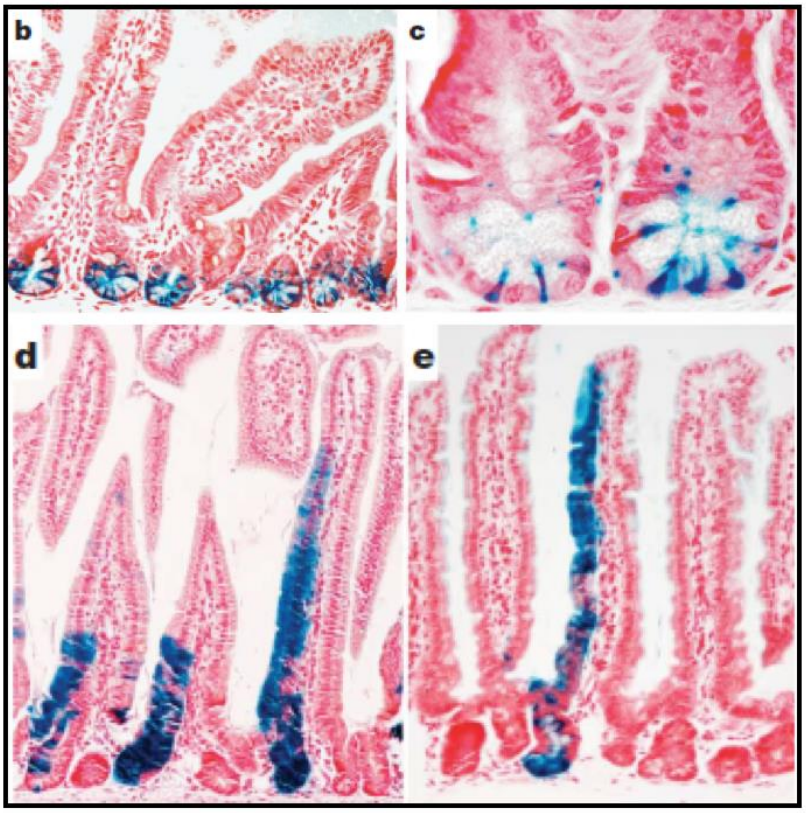

Figure 3: Lgr5+ stem cells are located at the base of the intestinal crypts and can reconstitute the epithelium in its entirety. Upper panel shows (b-c) LacZ staining (blue) of small intestinal sections derived from mice carrying *LacZ* integrated into the last exon of the *LGR5* gene. Staining shows that LacZ is restricted to 6-8 cells dispersed at the bottom of the intestinal crypts. Lower panel (d-e) shows intestinal sections from a *Lgr5-EGFPIRES-creERT2* knock-in mouse crossed with the *Rosa26-lacZ* reporter mouse 5 days after tamoxifen injection (d) and 60 days after tamoxifen injection (e). Figure adapted, with permission, from results published by Barker & Clevers (2007).

1.3.3 Transit Amplifying Cells

Due to the relatively quiescent nature of true stem cells, proliferative tissues require the presence of an intermediary progenitor cell population. [50] This observation was first brought forth by Laszlo G. Lajtha (1979), who proposed that rather than differentiating directly into specific cell types, stem cells produce precursor cell populations that divide rapidly creating a pool of undifferentiated cells. [50] TACs, unlike their stem cell progenitors, proliferate swiftly, undergoing several rounds of cell division prior to differentiating into a specific lineage. As such, TACs are functionally responsible for the renewal of the intestinal epithelium, whereas true stem cells technically only maintain their number and regenerative ability and produce TACs. [13, 16] Upon completing a set number of cell divisions, well established molecular and genetic cues guide the differentiation of TACs into one of the epithelial cell lineages. [42-44] TACs that commit to the lineage of Paneth cells remain at the base of the crypts, whereas the rest migrate up the crypt-villus axis, responding to different signal transduction pathways and protein gradients, to differentiate into one of the remaining epithelial cell populations.

Within the mouse small intestine, TACs divide approximately every 12-16h, generating approximately 300 cells per crypt, per day. [54] Recent studies suggest that interleukin (IL) 22 promotes TAC proliferation at the expense of Lgr5+ stem cell survival. [55] A study conducted in IL22-treated mouse SI organoids showed that IL22 greatly increased the size of the organoids but diminished organoid survival after passaging. This indicates high proliferative ability despite an impaired stem cell compartment, i.e. impaired Lgr5+ stem cell survival, but an active TAC population. This was reflected in the expression of corresponding gene markers, with reduced expression of ISC markers (*Lgr5*, *Ascl2, Olfm4, Sox9*), but an increased expression of proliferative marker *Ki67,* the stem and TAC marker *Prom 1/*CD133 and the TAC-specific marker *Zfp652*. [56] This repression of IL22-induced ISC survival, which was mirrored *in vivo*, correlated with a suppression of IL22-induced Wnt and Notch signalling. [55] Taken together, the data suggests that IL22 is crucial for regeneration of the intestinal epithelium under inflammatory conditions by promoting TAC differentiation from ISCs.

1.3.4 Paneth Cells

Easily discernible by their prominent secretory granules, these specialised epithelial cells migrate downward from the TAC pool upon differentiation, settling adjacent to the stem cells. Interspersed between the ISCs, these secretory cells are essential to the maintenance of the stem cell niche and maintaining efficient mucosal immunity. Upon exposure to bacteria through MyD88-dependent TLR activation, these long-lived cells (18-23 days) secrete a variety of antimicrobial peptides (AMPs), defensins and proteins that exert potent antimicrobial activity and mediate host-microbe interactions. [57] Factors secreted by Paneth cells are essential to protecting and maintaining the stem cell niche. The first tangible evidence of this was provided by Sato & Clevers (2011). Confocal imaging of cross sections of the small intestinal crypts of *Lgr5-EGFP-ires-creERT2* mice revealed that ISCs and Paneth cells were distributed in such a way that maximised heterotypic contact. [21] This phenomenon was also observed in *in vitro* organoid cultures. This direct cell-cell contact of ISCs and Paneth cells suggested that the two cell types likely exchange contact-dependent signals in a symbiotic manner. Gene expression profiling experiments revealed that Paneth cells expressed several genes that are important for stem cell maintenance including *Wnt3, Egf* and the Notch ligand *Dll1*. [21, 28]

Interestingly, human *in vitro* organoid culture requires the exogenous addition of Wnt3a and EGF; Wnt3a and EGF regulate the expansion potential of organoid cultures. [8, 21] These exogenously added proteins mimic the signals produced by Paneth cells *in vivo.* The same study used several *in vivo* models with a genetic loss of Paneth cells (*Gfi1*$^{-/-}$ mice, *CR2-tox176* mice and *Sox9* $^{-/-}$ mice) to investigate whether Paneth cells were unequivocally crucial for maintenance of the stem cell niche and found that, in the absence of Paneth cells, ISCs disappeared. In fact, the presence of ISCs was proportional and dependent on the number of Paneth cells. As such, Paneth cells are not only key players in the regulation of host-microbe interactions through MyD88-dependent secretion of various AMPs and other protective molecules; they also play an essential role in providing the necessary signals to maintain the 'stemness' of the ISCs niche.

Paneth cells protect the host organism from enteric pathogens via antimicrobial secretions and shape the profile of the microbiome. [32, 57] These functions are overlapping, with enteric pathogens altering the microbial profile significantly and innate microbial species protecting the host via colonization resistance. In humans, Paneth cells secrete human defensin (HD) 5 and 6, lysozymes, secretory phospholipase A_2 and regenerating islet-derived protein IIIA. [58-60] HD5 and HD6 are the most abundant AMPs; HD5 plays an important

role in protection against pathogens and shaping the microbial profile, whilst HD6, until recently, appeared to have no direct anti-microbial activity. However it has emerged that HD6 blocks the ability of *Salmonella enterica* serovar Typhimurium from invading the epithelium. [58] Collectively, Paneth cell secretions are important in maintaining the antimicrobial gradient that protects the stem cell niche.

1.3.5 Enteroendocrine Cells

Enteroendocrine cells act as sensory sentinels of luminal contents; they produce peptide hormones, cytokines and other factors that help mediate digestion and mucosal immunity in response to stimuli such as nutrients, microbial metabolites and pathogens. These rare cells comprise approximately 1% of the total GI epithelium and produce upwards of 15 different hormones which are differentially expressed between crypts and villi. [19] Until recently, it was believed that EECs were comprised of approximately 15 distinct subtypes, each committed to producing a specific hormone. This was challenged by a recent study which found that EECs can change their secretory profile as they migrate up the crypt-villus axis. [19] The study applied single cell mRNA sequencing to organoids induced to differentiate along the EEC lineage through exogenous addition of bone morphogenic protein (BMP). It was found that the hormone expression profile of individual EECs was influenced by the levels of BMP; crypt-borne EECs gradually migrate from a BMP-low to a BMP-high environment, switching hormone expression profile along the way. As such, it appears that there are fewer EEC lineages than was previously thought and that EECs exhibit significant hormonal plasticity. [19]

EEC secretions are of particular importance when it comes to food metabolism. After ingestion of food, by-products of digested chyme (e.g. glucose, amino acids, fatty acids) and microbial fermentation stimulate nutrient-sensing EECs through a range of signalling pathways (e.g. G-coupled protein receptors, nutrient transporters, ion channels). This stimulates the rapid release of glucagon-like peptide-1 (GLP-1) and gastric inhibitory polypeptide (GIP), which, in turn, stimulate insulin secretion. Due to their ability to stimulate blood glucose levels, GLP-1 receptor agonists are currently used to treat type 2 diabetes mellitus (T2DM) and obesity. [61, 62]

EEC-secreted hormones also modulate the rate of nutrient absorption; gastric emptying is a tightly regulated process that matches the rate at which the duodenum can absorb incoming

nutrients. This process is regulated by cholecystokinin (Cck), glucagon-like peptide 1 (GLP-1) and peptide YY (PYY). GLP-1 and PYY secretion increases when food is absorbed distally in the small intestine, this slows gastric emptying allowing more thorough absorption to take place in the proximal SI. Another important function of GLP-1 agonists used in the treatment of T2DM is the ability to slow gastric emptying resulting in slower glucose entry into circulation. [7, 62] Proximally located EECs produce hormones in response to incoming nutrients, whereas distally located EECs, which experience little to no absorption, produce hormones mostly in response to microbial products. [7]

In the context of food metabolism, most EEC-secreted hormones are considered either orexigenic, meaning they promote hunger, or anorexigenic, meaning they promote satiety. Orexigenic hormones are fewer; ghrelin (GHRL), secreted in the stomach in anticipation of a meal, is thought to exert orexigenic effects. [63] Cck, GLP-1 and PYY, which rise in response to food consumption, are thought to exert anorexigenic effects. As such, EECs play a central role in modulating the body's response to ingested food through the secretion of hormones with overlapping and complementary functions.

1.3.6 Goblet Cells

Goblet cells are specialised for the secretion of mucin, providing the mucosal surfaces of the body with a viscous, mucus lining that serves as a protective barrier against luminal microbes. [22] Within the small intestine, goblet cells account for approximately 10% of all epithelial cells. They increase in prevalence toward the distal segment of the small intestine. As the prevalence of these cells varies throughout the intestine, the composition of mucus within the GIT varies by region as well. [22, 64] Within the small intestine, the primary site of absorption, the mucus is single-layered and loosely attached to complement the organs' absorptive function.

It has been observed that mucus secretion can vary under pathologic conditions. Mucus secretion increases when goblet cells are stimulated by noxious stimuli; cholinergic agonists (e.g. acetylcholine, carbachol) trigger a rapid, transient increase in mucus secretion that returns to baseline after 30 minutes. [65] Hypersecretion under stress is most evident further down the crypt-villus axis, with the villous tip goblet cells markedly less responsive to stimuli. Hypersecretion in response to noxious stimuli is likely an attempt to rapidly expel pathogens from invading the crypt base, where the ISCs reside. [22] Not surprisingly,

stimulating villous goblet cells and surface colonic goblet cells does not trigger the same response as these cells are either spatially distant from the subepithelial immune cell network or overlying a firmer, more impenetrable mucus layer, respectively. [22, 66, 67]

It is not definitively clear why goblet cell location impacts their reactivity to stimuli. It is reasonable to assume that signalling gradients predominant at the base of the crypts may play a role. Another possible explanation is that crypt dwelling goblet cells undergo more exposure to antimicrobial peptides secreted by neighbouring Paneth cells and are thus more sensitive to invading microbes. This hypothesis is supported by the fact that goblet cell hyperplasia and mucus hypersecretion are hallmarks of parasitic helminth infections. [68, 69] Goblet cell dysfunction is also a hallmark of inflammatory bowel diseases; goblet cell differentiation is stimulated primarily by HATH1 (human homolog of Math1) and KLF4. In ulcerative colitis goblet cell differentiation is impaired by defects in these same genes. [70] Evidence suggests that mucus secreting goblet cells are more than just passive players in mucosal immunity and warrant further study.

Within the SI, aside from providing a physical protective barrier from potentially harmful luminal antigens, the mucus layer is rich with complex carbohydrate moieties that protect epithelial cells from proteolytic degradation by host enzymes, i.e. ‘self-digestion.’ Mucus, along with antimicrobial peptides secreted by Paneth cells, creates an antibacterial gradient that prevents the microbial species from damaging the stem cell niche and penetrating the sub-epithelial space. [20, 57] These antimicrobial peptides within the small intestine are extremely important as the consistency of the small intestinal mucus is loose and porous, unlike in other regions, so microbes have greater access to epithelial cells.

As well as mucus secretion, goblet cells also play a role in antigen presentation to the subepithelial immune cells. Small intestinal goblet cells are capable of endocytosing low molecular weight soluble antigens and presenting them to tolerogenic CD103+ dendritic cells. [71] This finding challenges the earlier notion that goblet cells have a purely secretory function and represent goblet cells as a multifaceted, versatile cell type. This function appears to be restricted to SI goblet cells; it is likely that goblet cell-mediated endocytosis is absent in the colon due to the firm, inner mucus layer and the abundance of microbes in the upper layer. [71]

1.3.7 Tuft Cells

Tuft cells, the mechano-sensory sentinels of the intestine, are a rare epithelial cell subpopulation that is crucial to type 2 mucosal immunity. These rare cells, often referred to as 'brush' cells, are morphologically recognizable by a 'tuft' of long, blunt microvilli, cytoskeletal rootlets that extend basally and a rich apical vesicle network. Though present in most mucosal tissues, tuft cells are best characterised in the SI where they are known to derive from Lgr5+ stem cells. Unlike other differentiated progeny of ISCs, tuft cells continue to express Lgr5 post differentiation. [72, 73] POU class 2 homeobox 3 (POU2F3) and growth factor -independent 1B (GF1B) have been implicated as master regulator genes of tuft cell differentiation; *Pou2f3*$^{-/-}$ mice are devoid of tuft cell, whilst all other epithelial cell lineages appear unaffected within the small intestine. [18]

Despite a shared morphology, it appears as though tuft cells in different tissues and even in different regions of the same tissue display some heterogeneity. RNA sequencing of EPCAM^{+}/IL-25^{+} tuft cells from different tissues sought to identify a common transcriptional signature. Though the transcriptional signature identified several shared markers (*IL25, Dlck1, Trpm5, Ptgs1,* among others), RNA sequencing also revealed significant inter and intra-tissue diversity. [12] This heterogeneity led to the creation of two tuft cell categories; Tuft-1 and Tuft-2 cells. Tuft-1 cells exhibit a transcriptional signature with genes related to neuronal development, whilst Tuft-2 cells express immune-related genes. Among the immune related genes expressed by Tuft-2 cells is *Ptprc* encoding for the pan immune marker CD45; this is the first known instance of CD45+ cells from a non-hematopoetic lineage. [12]

Tuft cells play a key role in mediating host responses to parasitic infections through type 2 immune circuits. Helminth parasite or protozoa infection in WT mice results in goblet and tuft cell hyperplasia; in mice lacking *Pou2f3, Trpm or gustducin*, signalling receptors expressed by tuft cells specifically, tuft cell mediated type 2 immune response is abrogated. [18] Tuft cells activate group 2 innate lymphoid cells (ILC2s) via IL25, which leads to an increase in IL13, which then acts on epithelial progenitors to promote linage commitment towards tuft and goblet cells. [74] As a result of this immune circuit, parasitic infections are generally characterised by tuft cell hyperplasia.

1.3.8 M Cells

M cells, an antigen sampling population of epithelial cells found in the follicle-associated epithelium overlying GI lymphoid structures, are crucial to the induction of a mucosal immune response. [23, 75] M cells constitute approximately 5-10% of the FAE, with M cell number and density varying slightly across species and at different ages; mice tend to have more M cells than humans, and functional maturation of M cells decreases significantly with age. [76] These rare cells are specialized for transcytosis; they capture luminal antigens through their unique morphological features and apically expressed capture receptors, and subsequently present them to the underlying immune cell network. [25, 77, 78]

M cells are distinguishable through numerous distinctive morphological and functional features. These include a disorganised apical brush border with distinct gaps in microvilli, numerous vacuoles and basolateral invaginations harbouring pockets of lymphocytes. [78] Lack of an organised brush border allows luminal antigens ready access to apically expressed capture receptors such as Gp2. [79, 80] The basolateral invaginations serve to reduce the intracellular distance for captured antigens and enable quicker exposure to immune-competent antigen-presenting cells located in the subepithelial space. [81-83]
Due to their rarity, M cells have proven difficult to study and numerous outstanding questions in M cell biology remain unanswered. A more complete discussion on M cell function, model systems used to study M cells and the outstanding questions in M cell biology can be found in subsequent chapters.

1.4 Immunity in the GIT

The intestinal epithelium and underlying immune structures undergo constant exposure to antigens, pathogens and commensal microbes. The vast luminal burden experienced by the GIT necessitates a robust and measured immune response that can efficiently neutralize harmful pathogens whilst adopting tolerance against innocuous antigens. [75, 84] This delicate immune balance requires a cooperative effort on behalf of all the cell types present within the mucosa and the surrounding mesenchyme. Whilst there are specialised accretions of dedicated gut-associated lymphoid tissues (GALT) that serve as focal points of gut immunity, the entirety of the mucosa features an abundance of immune-competent cells that continuously monitor and sample luminal contents. [85]

GALT forms a physiological part of the wider mucosa-associated lymphoid tissue (MALT) network that works within the body to protect mucosal tissues from invasion by harmful pathogens. Within the gut, GALT structures, consisting of concentrated regions of immunocompetent cells, comprise the Waldeyer's tonsillar ring, aggregates of lymphoid tissue in the appendix and intestines, isolated lymphoid follicles scattered throughout the epithelium and the Peyer's Patches. [75] PPs, domal aggregates of immune-competent cells that project into the lumen, and the overlying follicle-associated epithelium, are central to inducing mucosal immunity. [86] The lamina propria (LP) directly underlies the villous epithelium forming a loose, mesh-like bed of connective tissue rich with various myeloid and lymphoid cells including lymphocytes, fibroblasts, plasma cells, macrophages and dendritic cells, among others. Luminal antigens, pathogens and other particulates are transported into the underlying immunocompetent environment via numerous trans- and endo-cytotic pathways that are associated with different cell types. [38]

M cells act as immune-sensory sentinels of gastrointestinal immune responses. [23] Positioned advantageously above an immunocompetent environment, M cells can transport luminal antigens into the subepithelial space rapidly, making them an effective gateway to the mucosal immune system. Upon M cell-mediated antigen transcytosis, immune cells contained within the inductive lymphoid tissues of the gut collaborate to orchestrate an immune response. [23, 87] In the subepithelial space, in close contact with the epithelium, are antigen-presenting cells (APCs) such as macrophages, dendritic cells and B cells. Antigen sampling cells within the epithelium capture luminal antigens and present them to the underlying immune cells within the LP. Pathogen recognition receptors (PRRs) on APCs recognize pathogen-associated molecular patterns (PAMPs), triggering the initiation of a mucosal immune response. This in turn activates T cell immune responses and IgA secretion by plasma cells. Activated T cells produce several cytokines, such as IL-17 and IL-22, which promote production of antimicrobial molecules by intestinal epithelial cells to regulate microbial species. [88, 89] M cell-mediated transcytosis is an essential process in inducing mucosal immunity. In mice infected with *Salmonella* Typhimurium, antigen-specific T-cell responses are greatly reduced when M cells are not present. [80, 90]

Due to their critical role in inducing antigen-specific mucosal immune responses, M cells are regarded as promising targets for orally delivered drugs. [91, 92] Efforts to target M cell-specific capture receptors and/or enhance M cell-mediated transcytosis demonstrate that targeting M cells may be a promising strategy for increasing bioavailability of orally

delivered drugs. [92, 93] This necessitates the development of convenient and molecularly accurate biomimetic models to facilitate the *in vitro* study of M cell function.

1.5 Brief Review of Literature Pertaining to the Study of Intestinal M Cells

A search in the "PubMed" database reveals two primary models employed in the literature to study M cell function. The first is based on a model pioneered by Kerneis et al. (1997) in which human colon adenocarcinoma-derived Caco-2 cells were co-cultured with murine Peyer's Patch lymphocytes resulting in the conversion of Caco-2 cells into cells exhibiting some M cell features, including increased transcytosis. [94] The original paper, cited 758 times at the time of writing this thesis, has provided a useful and convenient platform for the study of the superficial functional features of FAE M cells. Numerous papers have employed the co-culture technique, using a range of cells of hematopoietic origin in place of primary lymphocytes, with the aim of demystifying the functional features of M cells and, by extension, exploiting these features to formulate better oral drugs. [95-106]

The second model was made possible by two previous discoveries; **(1)** the identification of the LGR5 G-protein coupled receptor as the molecular marker of ISCs and **(2)** the subsequent isolation and culture of intestinal stem cells into 3D organoids under optimized conditions. [8, 15] These enabled the long-term culture and study of intestinal stem cells and their progeny *in vitro*, giving rise to an abundance of genomic and functional data for each population of intestinal cells, including M cells. Organoids derived from ISCs according to the original culture protocol spontaneously give rise to stem cells, Paneth cells, TA cells and epithelial cells. [8] The addition and/or withdrawal of exogenous factors mimicking the *in vivo* microenvironment and signalling gradients is necessary to direct differentiation along the goblet cell, Enteroendocrine cell, tuft cell and M cell lineage. To enrich organoids for goblet and Enteroendocrine cells, inhibiting Notch signalling is vital. As discussed previously, balanced Notch and Wnt signalling are crucial for proper maintenance of the crypt-villus subunit. Blocking Notch leads to an overrepresentation of cells belonging to the secretory lineage. Exogenous addition of γ-secretase inhibitor DAPT indirectly inhibits Notch, allowing for the overexpression of secretory cells. The goblet cell lineage can be further promoted through addition of IL-13 and the Enteroendocrine lineage can be promoted through the withdrawal of noggin and addition of BMP. [19]

Three years ensuing the initial generation of organoids, De Lau et al. (2012) published the finding that true M cells can be induced in organoids through exogenous stimulation with RANKL; this was also confirmed in human organoids. [107, 108] Subsequent comparisons between the cell line-based co-culture model and the organoid-based model highlighted important differences in basic biology; whilst Caco-2 derived 'M cells' exhibited some features that could be likened to true PP M cells, they are not transcriptionally or functionally representative of *in vivo* M cells. The complex biological microenvironment, including crucial signalling gradients and exogenous cues that differ along the crypt-villus subunit, play a critical role in cell lineage commitment. These key differences then instigated a new line of questioning; if these 'M-like cells' generated through the cell line-derived co-culture method did exhibit functional similarities but were not true M cells, what were they? Is the same process relevant *in vivo?* In accordance with these findings, the basis of this thesis has changed over time; the focus has shifted from studying Caco-2 derived 'M-like cells' to organoid-derived true PP M cells. However, numerous outstanding questions in M cell biology remain unanswered. Additionally, the cell line-based model remains in widespread use, with findings generally attributed to have relevance for true PP M cells, further confusing the field.

Subsequent chapters will discuss several topics; **(i)** the challenges associated with identifying M cells across various *in vitro* models, **(ii)** important questions in M cell biology that remain unanswered, **(iii)** the precise regulation of M cell number and function through various signalling pathways and **(iv)** the use of M cells derived from ISCs in organoids for functional studies. The thesis will address the discrepancies that have hindered progress in the field of M cell research thus far and contribute to the understanding of the differentiation and function of genuine Peyer's Patch M cells. Finally, this thesis will propose specific guidelines for future work in this field.

1.6 References

1. Ferguson, C.M., *An Overview of the Gastrointestinal System*, in *Clinical Methods: The History, Physical, and Laboratory Examinations*, rd, et al., Editors. 1990: Boston.
2. Cheng, L.K., et al., *Gastrointestinal system.* Wiley Interdiscip Rev Syst Biol Med, 2010. **2**(1): p. 65-79.
3. Kararli, T.T., *Comparison of the gastrointestinal anatomy, physiology, and biochemistry of humans and commonly used laboratory animals.* Biopharm Drug Dispos, 1995. **16**(5): p. 351-80.
4. Kiela, P.R. and F.K. Ghishan, *Physiology of Intestinal Absorption and Secretion.* Best Pract Res Clin Gastroenterol, 2016. **30**(2): p. 145-59.
5. Ogobuiro, I. and F. Tuma, *Physiology, Gastrointestinal*, in *StatPearls*. 2020: Treasure Island (FL).
6. Sarna, S.K. and M.F. Otterson, *Small intestinal physiology and pathophysiology.* Gastroenterol Clin North Am, 1989. **18**(2): p. 375-404.
7. Wu, T., et al., *Gut motility and enteroendocrine secretion.* Curr Opin Pharmacol, 2013. **13**(6): p. 928-34.
8. Sato, T., et al., *Single Lgr5 stem cells build crypt-villus structures in vitro without a mesenchymal niche.* Nature, 2009. **459**(7244): p. 262-5.
9. Sumigray, K.D., M. Terwilliger, and T. Lechler, *Morphogenesis and Compartmentalization of the Intestinal Crypt.* Dev Cell, 2018. **45**(2): p. 183-197 e5.
10. Bonis, V., C. Rossell, and H. Gehart, *The Intestinal Epithelium - Fluid Fate and Rigid Structure From Crypt Bottom to Villus Tip.* Front Cell Dev Biol, 2021. **9**: p. 661931.
11. Haber, A.L., et al., *A single-cell survey of the small intestinal epithelium.* Nature, 2017. **551**(7680): p. 333-339.
12. Hsu, Y.C., L. Li, and E. Fuchs, *Transit-amplifying cells orchestrate stem cell activity and tissue regeneration.* Cell, 2014. **157**(4): p. 935-49.
13. Reynolds, A., et al., *Canonical Wnt signals combined with suppressed TGFbeta/BMP pathways promote renewal of the native human colonic epithelium.* Gut, 2014. **63**(4): p. 610-21.
14. Barker, N., et al., *Identification of stem cells in small intestine and colon by marker gene Lgr5.* Nature, 2007. **449**(7165): p. 1003-7.

15. Rangel-Huerta, E. and E. Maldonado, *Transit-Amplifying Cells in the Fast Lane from Stem Cells towards Differentiation.* Stem Cells Int, 2017. **2017**: p. 7602951.
16. Gehart, H. and H. Clevers, *Tales from the crypt: new insights into intestinal stem cells.* Nat Rev Gastroenterol Hepatol, 2019. **16**(1): p. 19-34.
17. Gerbe, F., et al., *Intestinal epithelial tuft cells initiate type 2 mucosal immunity to helminth parasites.* Nature, 2016. **529**(7585): p. 226-30.
18. Beumer, J., et al., *Enteroendocrine cells switch hormone expression along the crypt-to-villus BMP signalling gradient.* Nat Cell Biol, 2018. **20**(8): p. 909-916.
19. Clevers, H.C. and C.L. Bevins, *Paneth cells: maestros of the small intestinal crypts.* Annu Rev Physiol, 2013. **75**: p. 289-311.
20. Sato, T., et al., *Paneth cells constitute the niche for Lgr5 stem cells in intestinal crypts.* Nature, 2011. **469**(7330): p. 415-8.
21. Johansson, M.E. and G.C. Hansson, *Immunological aspects of intestinal mucus and mucins.* Nat Rev Immunol, 2016. **16**(10): p. 639-49.
22. Mabbott, N.A., et al., *Microfold (M) cells: important immunosurveillance posts in the intestinal epithelium.* Mucosal Immunol, 2013. **6**(4): p. 666-77.
23. Klisuric, A., et al., *Highlight Article: Identifying human and murine M cells in vitro.* Exp Biol Med (Maywood), 2019. **244**(7): p. 554-564.
24. Lo, D.D., *Vigilance or Subversion? Constitutive and Inducible M Cells in Mucosal Tissues.* Trends Immunol, 2018. **39**(3): p. 185-195.
25. Cheng, H. and C.P. Leblond, *Origin, differentiation and renewal of the four main epithelial cell types in the mouse small intestine. V. Unitarian Theory of the origin of the four epithelial cell types.* Am J Anat, 1974. **141**(4): p. 537-61.
26. Clevers, H., *The intestinal crypt, a prototype stem cell compartment.* Cell, 2013. **154**(2): p. 274-84.
27. Gregorieff, A., et al., *Expression pattern of Wnt signaling components in the adult intestine.* Gastroenterology, 2005. **129**(2): p. 626-38.
28. Stanger, B.Z., et al., *Direct regulation of intestinal fate by Notch.* Proc Natl Acad Sci U S A, 2005. **102**(35): p. 12443-8.
29. Yang, Q., et al., *Requirement of Math1 for secretory cell lineage commitment in the mouse intestine.* Science, 2001. **294**(5549): p. 2155-8.
30. Bjerknes, M. and H. Cheng, *Neurogenin 3 and the enteroendocrine cell lineage in the adult mouse small intestinal epithelium.* Dev Biol, 2006. **300**(2): p. 722-35.
31. Bevins, C.L. and N.H. Salzman, *Paneth cells, antimicrobial peptides and maintenance of intestinal homeostasis.* Nat Rev Microbiol, 2011. **9**(5): p. 356-68.

32. Faulk, W.P., et al., *Peyer's pacthes: morphologic studies.* Cell Immunology, 1970. **1**: p. 500-520.
33. Gullberg, E. and J.D. Soderholm, *Peyer's patches and M cells as potential sites of the inflammatory onset in Crohn's disease.* Ann N Y Acad Sci, 2006. **1072**: p. 218-32.
34. Jung, C., J.P. Hugot, and F. Barreau, *Peyer's Patches: The Immune Sensors of the Intestine.* Int J Inflam, 2010. **2010**: p. 823710.
35. Dickson, I., *Enterocyte zonation along the intestinal villus reveals a division of labour.* Nat Rev Gastroenterol Hepatol, 2018. **15**(12): p. 717.
36. Okumura, R. and K. Takeda, *Roles of intestinal epithelial cells in the maintenance of gut homeostasis.* Exp Mol Med, 2017. **49**(5): p. e338.
37. Vancamelbeke, M. and S. Vermeire, *The intestinal barrier: a fundamental role in health and disease.* Expert Rev Gastroenterol Hepatol, 2017. **11**(9): p. 821-834.
38. Groschwitz, K.R. and S.P. Hogan, *Intestinal barrier function: molecular regulation and disease pathogenesis.* J Allergy Clin Immunol, 2009. **124**(1): p. 3-20; quiz 21-2.
39. Hollander, D., et al., *Increased intestinal permeability in patients with Crohn's disease and their relatives. A possible etiologic factor.* Ann Intern Med, 1986. **105**(6): p. 883-5.
40. Fujimura, Y., R. Kamoi, and M. Iida, *Pathogenesis of aphthoid ulcers in Crohn's disease: correlative findings by magnifying colonoscopy, electron microscopy, and immunohistochemistry.* Gut, 1996. **38**(5): p. 724-32.
41. Demitrack, E.S. and L.C. Samuelson, *Notch regulation of gastrointestinal stem cells.* J Physiol, 2016. **594**(17): p. 4791-803.
42. Zecchini, V., et al., *Notch signaling regulates the differentiation of post-mitotic intestinal epithelial cells.* Genes Dev, 2005. **19**(14): p. 1686-91.
43. Sancho, R., C.A. Cremona, and A. Behrens, *Stem cell and progenitor fate in the mammalian intestine: Notch and lateral inhibition in homeostasis and disease.* EMBO Rep, 2015. **16**(5): p. 571-81.
44. Frey, A., et al., *Role of the glycocalyx in regulating access of microparticles to apical plasma membranes of intestinal epithelial cells: implications for microbial attachment and oral vaccine targeting.* J Exp Med, 1996. **184**(3): p. 1045-59.
45. Reitsma, S., et al., *The endothelial glycocalyx: composition, functions, and visualization.* Pflugers Arch, 2007. **454**(3): p. 345-59.
46. Miron, N. and V. Cristea, *Enterocytes: active cells in tolerance to food and microbial antigens in the gut.* Clin Exp Immunol, 2012. **167**(3): p. 405-12.

47. Kaiserlian, D., K. Vidal, and J.P. Revillard, *Murine enterocytes can present soluble antigen to specific class II-restricted CD4+ T cells.* Eur J Immunol, 1989. **19**(8): p. 1513-6.
48. Hershberg, R.M. and L.F. Mayer, *Antigen processing and presentation by intestinal epithelial cells - polarity and complexity.* Immunol Today, 2000. **21**(3): p. 123-8.
49. Lajtha, L.G., *Stem cell concepts.* Nouv Rev Fr Hematol, 1979. **21**(1): p. 59-65.
50. Srinivasan, T., et al., *Notch signalling regulates asymmetric division and inter-conversion between lgr5 and bmi1 expressing intestinal stem cells.* Sci Rep, 2016. **6**: p. 26069.
51. Barker, N., *Adult intestinal stem cells: critical drivers of epithelial homeostasis and regeneration.* Nat Rev Mol Cell Biol, 2014. **15**(1): p. 19-33.
52. Korinek, V., et al., *Depletion of epithelial stem-cell compartments in the small intestine of mice lacking Tcf-4.* Nat Genet, 1998. **19**(4): p. 379-83.
53. Barker, N., et al., *Very long-term self-renewal of small intestine, colon, and hair follicles from cycling Lgr5+ve stem cells.* Cold Spring Harb Symp Quant Biol, 2008. **73**: p. 351-6.
54. Marshman, E., C. Booth, and C.S. Potten, *The intestinal epithelial stem cell.* Bioessays, 2002. **24**(1): p. 91-8.
55. Zha, J.M., et al., *Interleukin 22 Expands Transit-Amplifying Cells While Depleting Lgr5(+) Stem Cells via Inhibition of Wnt and Notch Signaling.* Cell Mol Gastroenterol Hepatol, 2019. **7**(2): p. 255-274.
56. Zwarycz, B., et al., *IL22 Inhibits Epithelial Stem Cell Expansion in an Ileal Organoid Model.* Cell Mol Gastroenterol Hepatol, 2019. **7**(1): p. 1-17.
57. van Es, J.H. and H. Clevers, *Paneth cells.* Curr Biol, 2014. **24**(12): p. R547-R548.
58. Chu, H., et al., *Human alpha-defensin 6 promotes mucosal innate immunity through self-assembled peptide nanonets.* Science, 2012. **337**(6093): p. 477-81.
59. Ghosh, D., et al., *Paneth cell trypsin is the processing enzyme for human defensin-5.* Nat Immunol, 2002. **3**(6): p. 583-90.
60. Salzman, N.H., et al., *Protection against enteric salmonellosis in transgenic mice expressing a human intestinal defensin.* Nature, 2003. **422**(6931): p. 522-6.
61. Yan, K.S., et al., *Intestinal Enteroendocrine Lineage Cells Possess Homeostatic and Injury-Inducible Stem Cell Activity.* Cell Stem Cell, 2017. **21**(1): p. 78-90 e6.
62. Andersen, A., et al., *[Glucagon-like peptide 1 receptor agonists for the treatment of Type 2 diabetes].* Ugeskr Laeger, 2019. **181**(12).
63. Muller, T.D., et al., *Ghrelin.* Mol Metab, 2015. **4**(6): p. 437-60.

64. Johansson, M.E., J.M. Larsson, and G.C. Hansson, *The two mucus layers of colon are organized by the MUC2 mucin, whereas the outer layer is a legislator of host-microbial interactions.* Proc Natl Acad Sci U S A, 2011. **108 Suppl 1**: p. 4659-65.
65. Gustafsson, J.K., et al., *An ex vivo method for studying mucus formation, properties, and thickness in human colonic biopsies and mouse small and large intestinal explants.* Am J Physiol Gastrointest Liver Physiol, 2012. **302**(4): p. G430-8.
66. Birchenough, G.M., et al., *New developments in goblet cell mucus secretion and function.* Mucosal Immunol, 2015. **8**(4): p. 712-9.
67. Nystrom, E.E.L., et al., *An intercrypt subpopulation of goblet cells is essential for colonic mucus barrier function.* Science, 2021. **372**(6539).
68. Marillier, R.G., et al., *IL-4/IL-13 independent goblet cell hyperplasia in experimental helminth infections.* BMC Immunol, 2008. **9**: p. 11.
69. Oeser, K., C. Schwartz, and D. Voehringer, *Conditional IL-4/IL-13-deficient mice reveal a critical role of innate immune cells for protective immunity against gastrointestinal helminths.* Mucosal Immunol, 2015. **8**(3): p. 672-82.
70. Gersemann, M., et al., *Differences in goblet cell differentiation between Crohn's disease and ulcerative colitis.* Differentiation, 2009. **77**(1): p. 84-94.
71. McDole, J.R., et al., *Goblet cells deliver luminal antigen to CD103+ dendritic cells in the small intestine.* Nature, 2012. **483**(7389): p. 345-9.
72. Itzkovitz, S., et al., *Single-molecule transcript counting of stem-cell markers in the mouse intestine.* Nat Cell Biol, 2011. **14**(1): p. 106-14.
73. McKinley, E.T., et al., *Optimized multiplex immunofluorescence single-cell analysis reveals tuft cell heterogeneity.* JCI Insight, 2017. **2**(11).
74. von Moltke, J., et al., *Tuft-cell-derived IL-25 regulates an intestinal ILC2-epithelial response circuit.* Nature, 2016. **529**(7585): p. 221-5.
75. McGhee, J.R. and K. Fujihashi, *Inside the mucosal immune system.* PLoS Biol, 2012. **10**(9): p. e1001397.
76. Kobayashi, A., et al., *The functional maturation of M cells is dramatically reduced in the Peyer's patches of aged mice.* Mucosal Immunol, 2013. **6**(5): p. 1027-37.
77. Kanaya, T., et al., *Development of intestinal M cells and follicle-associated epithelium is regulated by TRAF6-mediated NF-kappaB signaling.* J Exp Med, 2018. **215**(2): p. 501-519.
78. Owen, R.L. and A.L. Jones, *Epithelial cell specialization within human Peyer's patches: an ultrastructural study of intestinal lymphoid follicles.* Gastroenterology, 1974. **66**(2): p. 189-203.

79. Ohno, H. and K. Hase, *Glycoprotein 2 (GP2): grabbing the FimH bacteria into M cells for mucosal immunity.* Gut Microbes, 2010. **1**(6): p. 407-10.
80. Hase, K., et al., *Uptake through glycoprotein 2 of FimH(+) bacteria by M cells initiates mucosal immune response.* Nature, 2009. **462**(7270): p. 226-30.
81. Gebert, A., et al., *Antigen transport into Peyer's patches: increased uptake by constant numbers of M cells.* Am J Pathol, 2004. **164**(1): p. 65-72.
82. Owen, R.L., et al., *M cell transport of Vibrio cholerae from the intestinal lumen into Peyer's patches: a mechanism for antigen sampling and for microbial transepithelial migration.* J Infect Dis, 1986. **153**(6): p. 1108-18.
83. Jang, M.H., et al., *Intestinal villous M cells: an antigen entry site in the mucosal epithelium.* Proc Natl Acad Sci U S A, 2004. **101**(16): p. 6110-5.
84. Holmgren, J. and C. Czerkinsky, *Mucosal immunity and vaccines.* Nat Med, 2005. **11**(4 Suppl): p. S45-53.
85. Obata, Y., et al., *Epithelial-stromal interaction via Notch signaling is essential for the full maturation of gut-associated lymphoid tissues.* EMBO Rep, 2014. **15**(12): p. 1297-304.
86. Terahara, K., et al., *Comprehensive gene expression profiling of Peyer's patch M cells, villous M-like cells, and intestinal epithelial cells.* J Immunol, 2008. **180**(12): p. 7840-6.
87. Heppner, F.L., et al., *Transepithelial prion transport by M cells.* Nat Med, 2001. **7**(9): p. 976-7.
88. McDermott, A.J. and G.B. Huffnagle, *The microbiome and regulation of mucosal immunity.* Immunology, 2014. **142**(1): p. 24-31.
89. Zhang, X., et al., *Interleukin22 regulates the homeostasis of the intestinal epithelium during inflammation.* Int J Mol Med, 2019. **43**(4): p. 1657-1668.
90. Clark, M.A., et al., *Preferential interaction of Salmonella typhimurium with mouse Peyer's patch M cells.* Res Microbiol, 1994. **145**(7): p. 543-52.
91. Devriendt, B., et al., *Crossing the barrier: Targeting epithelial receptors for enhanced oral vaccine delivery.* J Control Release, 2012. **160**(3): p. 431-9.
92. Kim, S.H. and Y.S. Jang, *Antigen targeting to M cells for enhancing the efficacy of mucosal vaccines.* Exp Mol Med, 2014. **46**: p. e85.
93. Azizi, A., et al., *Enhancing oral vaccine potency by targeting intestinal M cells.* PLoS Pathog, 2010. **6**(11): p. e1001147.
94. Kerneis, S., et al., *Conversion by Peyer's patch lymphocytes of human enterocytes into M cells that transport bacteria.* Science, 1997. **277**(5328): p. 949-52.

95. Beloqui, A., et al., *A human intestinal M-cell-like model for investigating particle, antigen and microorganism translocation.* Nat Protoc, 2017. **12**(7): p. 1387-1399.
96. Beloqui, A., A. des Rieux, and V. Preat, *Mechanisms of transport of polymeric and lipidic nanoparticles across the intestinal barrier.* Adv Drug Deliv Rev, 2016. **106**(Pt B): p. 242-255.
97. des Rieux, A., et al., *An improved in vitro model of human intestinal follicle-associated epithelium to study nanoparticle transport by M cells.* Eur J Pharm Sci, 2007. **30**(5): p. 380-91.
98. des Rieux, A., et al., *Transport of nanoparticles across an in vitro model of the human intestinal follicle associated epithelium.* Eur J Pharm Sci, 2005. **25**(4-5): p. 455-65.
99. Loo, Y., et al., *Comparative study of nanoparticle-mediated transfection in different GI epithelium co-culture models.* J Control Release, 2012. **160**(1): p. 48-56.
100. Gagnon, M., et al., *Comparison of the Caco-2, HT-29 and the mucus-secreting HT29-MTX intestinal cell models to investigate Salmonella adhesion and invasion.* J Microbiol Methods, 2013. **94**(3): p. 274-9.
101. Rochereau, N., et al., *Dectin-1 is essential for reverse transcytosis of glycosylated SIgA-antigen complexes by intestinal M cells.* PLoS Biol, 2013. **11**(9): p. e1001658.
102. Schimpel, C., et al., *Development of an advanced intestinal in vitro triple culture permeability model to study transport of nanoparticles.* Mol Pharm, 2014. **11**(3): p. 808-18.
103. Araujo, F. and B. Sarmento, *Towards the characterization of an in vitro triple co-culture intestine cell model for permeability studies.* Int J Pharm, 2013. **458**(1): p. 128-34.
104. Pielage, J.F., et al., *Reversible differentiation of Caco-2 cells reveals galectin-9 as a surface marker molecule for human follicle-associated epithelia and M cell-like cells.* Int J Biochem Cell Biol, 2007. **39**(10): p. 1886-901.
105. Lai, Y.H. and M.J. D'Souza, *Microparticle transport in the human intestinal M cell model.* J Drug Target, 2008. **16**(1): p. 36-42.
106. Masuda, K., A. Kajikawa, and S. Igimi, *Establishment and Evaluation of an in vitro M Cell Model using C2BBe1 Cells and Raji Cells.* Biosci Microflora, 2011. **30**(2): p. 37-44.
107. Rouch, J.D., et al., *Development of Functional Microfold (M) Cells from Intestinal Stem Cells in Primary Human Enteroids.* PLoS One, 2016. **11**(1): p. e0148216.

108. de Lau, W., et al., *Peyer's patch M cells derived from Lgr5(+) stem cells require SpiB and are induced by RankL in cultured "miniguts"*. Mol Cell Biol, 2012. **32**(18): p. 3639-47.

Chapter 2 Identifying human and murine M cells *in vitro*

This chapter has been reproduced from the following publication with permission from the Journal of Experimental Biology and Medicine (Appendix I):

Klisuric A, Thierry B, Delon L, Prestidge CA, Gibson RJ. Identifying human and murine M cells in vitro. Experimental Biology and Medicine. 2019;244(7):554-564. doi:10.1177/1535370219838674

This chapter seeks to summarize and critically evaluate the various models currently in use to assess M cell function *in vitro*, thus addressing Aim 1.

2.1 Abstract

M cells are an epithelial cell population found in the follicle-associated epithelium overlying gut-associated lymphoid tissues. They are specialised in the transcytosis of luminal antigens. Their transcytotic capacity and location in an immunocompetent environment has prompted the study of these cells as possible targets for oral drug delivery systems. Currently, the models most commonly used to study M cells are restricted to in vivo experiments conducted in mice, and in vitro studies conducted in models comprised either of primary epithelial cells or established cell lines of murine or human origin. In vitro models of the follicle-associated epithelium can be constructed in several ways. Small intestinal Lgr5+ stem cells can be cultured into a 3D organoid structure where M cells are induced with RANKL administration. Additionally, in vitro models containing an "M cell-like" population can be obtained through co-culturing intestinal epithelial cells with cells of lymphocytic origin to induce the M cell phenotype. The evaluation of the efficiency of the variations of these models and their relevance to the in vivo human system is hampered by the lack of a universal M cell marker. This issue has also hindered the advancement of M cell-specific targeting approaches aimed at improving the bioavailability of orally administered compounds. This critical review discusses the different approaches utilized in the literature to identify M cells, their efficiency, reliability and relevance, in the context of commonly used models of the follicle- associated epithelium. The outcome of this review is a clearly defined and universally recognized criteria for the assessment of the relevance of models of the follicle-associated models currently used.

2.2 Introduction

The gastrointestinal (GI) mucosal surface functions as the primary interface between the internal and external environment, absorbing luminal nutrients, serving a protective role against invading pathogens and mediating the gastrointestinal immune response. [1] The innermost layer of the GI mucosa is comprised of a monolayer of polarized epithelial cells conjoined by tight junctions (TJs), forming an effective barrier preventing the invasion of luminal pathogens into the body. [1, 2] Due to the considerable bacterial burden imposed onto the GI mucosa, the mucosal immune system and its associated lymphoid structures, collectively termed the gut-associated lymphoid tissues (GALT), play an important role in maintaining homeostasis and mediating mucosal immune responses. GALT structures include isolated lymphoid follicles (ILFs) scattered throughout the epithelium of the small intestine and aggregated lymphoid nodules called the Peyer's Patches (PPs). [3]

PPs are aggregated nodules of lymphoid tissue composed of three distinct regions: the follicular area, the inter-follicular area and the follicle-associated epithelium (FAE). [3] The follicular and interfollicular regions are comprised of organised lymphoid follicles with proliferating B lymphocytes, follicular dendritic cells and macrophages, with a germinal center forming the core of each follicle. [3] The FAE is the name given to the epithelium directly overlying GALT. The complex interplay between the cells of the FAE and associated lymphocytes are central to inducing the mucosal immune response. [3-5] The FAE differs from the regular villous epithelium, containing a large number of lymphocytes, fewer goblet cells and a subpopulation of specialised epithelial cells called the M (microfold or membranous) cells. [6-8]

M cells are specialised epithelial cells expressed in many mucosal tissues of the body; most prominently in the GI tract and the airways. Within the small intestine, M cells are located primarily in the epithelium covering the PPs and account for less than 5-10% of all the cells of the FAE, with the number of mature M cells decreasing with age. [9] These cells are highly specialised for the transcytosis of luminal contents into the underlying immuno-competent environment. [10] Due to their specialised function for the uptake of luminal antigens, M cells have long been considered an attractive target for delivery of mucosal vaccines and biologics. [11-13] Lineage tracing experiments using mice expressing a *LacZ* reporter gene under the control of the Lgr5 promoter have shown that M cells derive from Lgr5+ stem cells that reside at the bottom of the intestinal crypts. [6] It is postulated that M

cell differentiation is regulated by several different factors including the binding of receptor activator of NF-κB ligand (RANKL), secreted by sub-epithelial stromal cells, to the RANK receptor expressed by epithelial cells (**Figure 1**). Studies have reported RANKL-deficient mice have a significantly diminished number of M cells in the FAE and consequently exhibit impaired transcytosis. Subsequent administration of recombinant RANKL can restore M cell numbers and functionality. [6, 14] Though it is well established that the ligation of RANK by RANKL and the subsequent activation of the NF-kB pathway is essential for the differentiation of M cells, until recently the intracellular signalling mechanisms involved remained unclear. Recently, a study used TNF receptor associated factor (TRAF) 6-deficient mice to evaluate the role of TRAF6 in M cell differentiation. TRAF6 is known to play a crucial role in the RANK-mediated activation of the canonical NF-kB pathway. [15] Mice lacking TRAF6 specifically in the intestinal epithelium (TRAF6 $^{IEC-KO}$) were generated by crossing mice with LoxP-flanked *Traf6* alleles with *Villin*-Cre transgenic mice. The expression of M cell specific markers was silenced in the PP FAE of TRAF6 $^{IEC-KO}$ mice throughout the length of the GIT, indicating that TRAF6-mediated activation of the canonical NFkB pathway was crucial to M cell development. [16] This observation was further confirmed using human TRAF6-/- organoids generated by the CRISPR/Cas9 system; M cell specific marker expression was silenced. Downstream of RANK/RANKL signalling, research suggests SpiB, a highly conserved transcription factor belonging to the Ets (E26 transformation specific) family, is responsible for M cell differentiation, with SpiB -/- mice presenting with impaired PP formation and few to no detectable M cells. [6, 17] SpiB -/- mice also display a significantly diminished expression of several previously reported M cell specific genes. [18] SpiB also appears to be implicated in human M cell development, with *in vitro* organoid cultures grown from human tissue showing an increased transcriptional expression of M cell specific genes in response to RANKL stimulation. [7, 16] This research highlights the central role of SpiB in regulating the development of functional, mature M cells, though more recently it has been postulated that M cells can develop via SpiB-independent pathways. [18, 19]

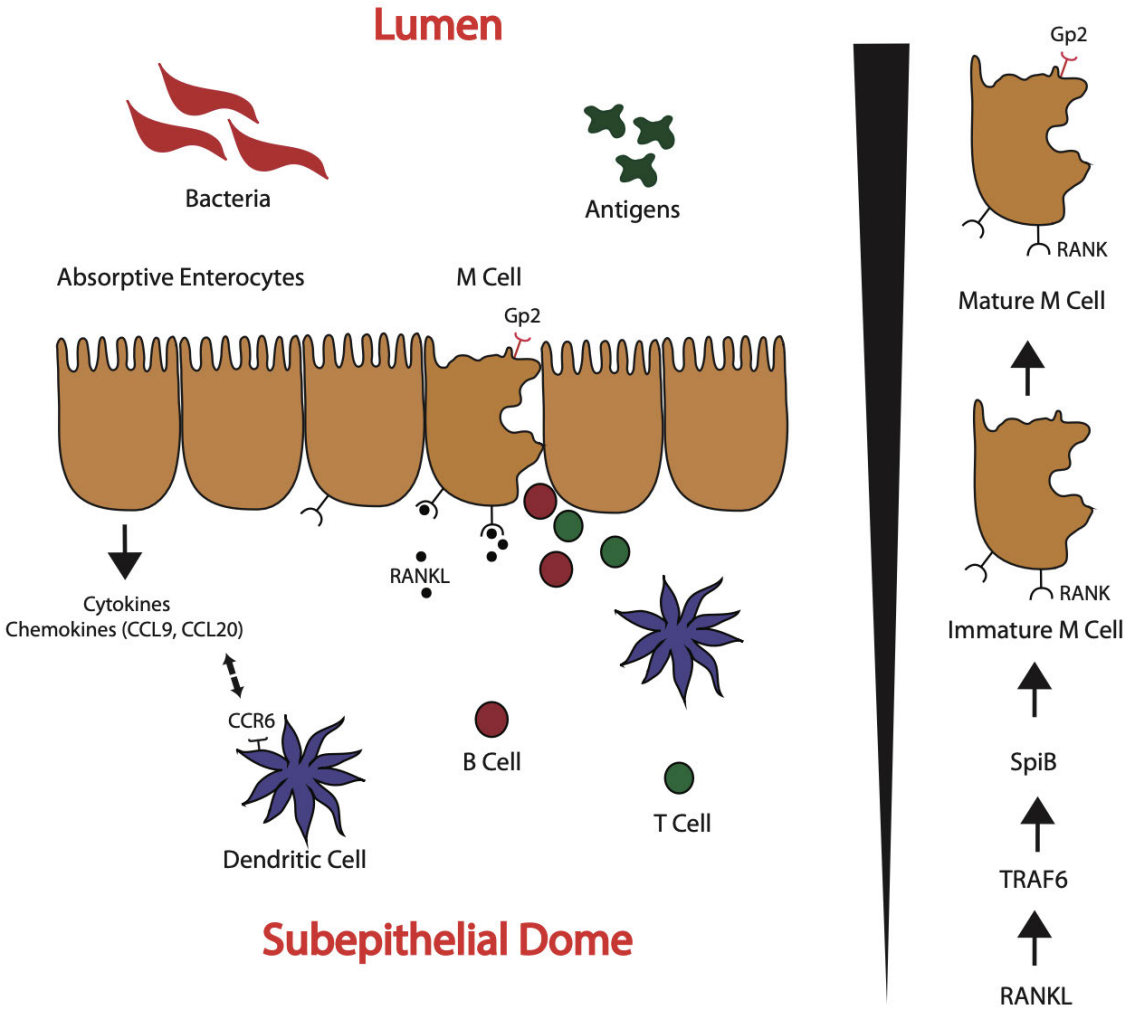

Figure 1: The differentiation of M cells is triggered by ligation of the RANK receptor expressed by cells of the intestinal epithelium to its ligand, RANKL. This causes the activation of TRAF6-mediated NF-kB signalling and the induction of Ets transcription factor SpiB. M cells express different markers during early and late stage development, with Gp2 being indicative of fully differentiated, mature M cells. Cytokines secreted by the follicle-associated epithelium, such as CCL20 and CCL9, have a chemotaxic effect toward CD11b+ dendritic cells that are present in the subepithelial dome.

In the past several years, it has become evident that M cell differentiation remains a complex and incompletely understood process. Studies suggest that independently of SpiB, villous epithelial cells can develop an M cell-like morphology and function upon exposure to *Salmonella* Typhimirium and cholera toxin (CT). [20, 21] These 'villous' M cells express some, but not all, M cell marker genes, though it is unclear how similar in function they are to the PP M cells. In addition to this, SpiB -/- mice display a significantly diminished expression of the human and murine M cell-specific gene *Gp2* and the reported M cell specific gene *Umod*. However, other reported M cell specific genes *Fut1, Marcskl1* and *Pglyrp1*, remained comparably expressed both in WT mice and SpiB -/- mice. [18] These data suggests that a subset of cells phenotypically similar to M cells may differentiate independently of SpiB. [18, 19] Despite this, SpiB is essential for the functional and structural maturation of M cells. [18] The villous 'M cells' that develop independently of SpiB, often in response to a pathogen, do not display all of the hallmarks of mature M cells, including expression of Gp2 which is widely considered a terminal differentiation marker of human and murine M cells. As such these cells may in fact be deemed a separate cell population altogether, or a less functionally mature version of PP M cells. [18, 22, 23] Additionally, M cells generated independently of SpiB have an impaired ability for the uptake of particles compared to PP M cells, indicating a less functional phenotype than SpiB-regulated PP M cells. [6, 18] This is equally true in other mucosal areas of the body; in the nasal-associated lymphoid tissues (NALT), CT can induce epithelial precursors to differentiate into M cells within a timeframe of several hours. [24] In the colon, inflammation triggered by exposure to *Citrobacter rodentium* can also induce the development of M cells. [25] These induced villous 'M cells' do not faithfully recapitulate the genetic and proteomic signature of true PP M cells. [18] Though several studies have demonstrated the integral role M cells play in initiating the mucosal immune response, it is also clear that the diversity of factors that can lead to the differentiation of M cells encompass a complex and not yet fully understood process that likely has a significant impact on the phenotypic and genotypic profile observed. [19, 22, 26] A more comprehensive examination of the various developmental origins of M cells is outside the scope of this critical review. However, it is crucial to convey here that there appear to be different developmental origins of M cells, and this likely explains why there is no 'blanket' M cell marker which applies across all of the models published in the literature.

Most biologics, including peptide and protein-based drugs, are delivered parenterally due to their poor GI permeability and oral bioavailability. [11] Oral delivery is preferred due to cost effectiveness and better patient compliance, hence there is considerable current interest in

formulating oral delivery systems which improve bioavailability of biological agents. Specific interest in developing oral delivery systems that target M cells has led to an increased demand for understanding of the molecular mechanisms regulating M cell function. As a result, M cells have been studied extensively in many species in both *in vivo* and *in vitro* systems, with varying degrees of success. [7, 10, 13, 27-35] The most commonly used and best validated models for the *in vivo* study of M cells are murine models. In mice, several reported studies have successfully targeted murine M cell markers to enhance the bioavailability of an orally delivered compound *in vivo.* [11, 13] However, variance between M cell markers and M cell frequency in different species suggests that the use of data obtained from non-human models may not be relevant to human clinical applications. As such, numerous *in vitro* models have been developed to allow for the evaluation of agents designed to exploit the characteristics of M cells. A commonly used and easily reproducible human *in vitro* model of the FAE uses the intestinal colon-derived cell line Caco-2 co-cultured with B cells, most often Raji cells, to induce the M cell phenotype. [29, 36] The two cell populations are typically cultured in a Transwell system separated by a porous membrane, as described previously. [36-38] The co-culturing of these two cell types induces the differentiation of a highly transcytotic sub-population of cells with a similar functional profile to the small intestinal PP M cells. It remains unclear how similar these cells are to PP M cells. [39] Commonly used and/or recently reported variations of the *in vitro* culture-based model initially pioneered by Gullberg et al. [37] are summarized in ***Table 1***. Multiple approaches have been used in an attempt to identify M cells in such co-culture models. These include electron microscopy [6, 29], binding of lectins (UEA-1, WGA and PNA) [40], expression of glycoproteins (Gp-2) [10], alkaline phosphatase activity [36] and expression of cellular adhesion markers such as NCAM and VCAM. [21, 37] Although it is well established that Gp-2 is the only marker of mature M cells cross-reactive between human and mouse known-to-date [10, 30], Caco-2/Raji co-culture based systems have not successfully applied this marker systematically in the literature. This poses additional questions in regards to the possible genetic and proteomic disparities between *in vivo* human PP M cells and the 'M-like cells' generated through the Caco/Raji co-culture. [19] As a result of these discrepancies in published data, it is imperative to establish a method of benchmarking *in vitro* models against one another to determine the overall relevance of different methods to the *in vivo* system.

Model	M cell identification methods	Reference
Caco-2 cells are seeded on the apical membrane of Transwell inserts. The cells are cultured for 4–6 days and the model is inverted. Raji cells are added to the basolateral compartment of the inverted model on days 14–16 of culture. The co-culture is maintained for a further 4–6 days.	• Functional transport studies between Caco-2 monoculture controls and co-cultures • TEM • SEM	36,44
Caco-2 cells are seeded on the apical membrane of Transwell inserts. The cells are cultured for 14 days. Raji cells are added to the basolateral compartment on day 14 of culture. The co-culture is maintained for a further 4–6 days.	• Functional transport studies between Caco-2 monoculture controls and co-cultures • Immunofluorescence staining of β-1 integrins	38
Caco-2 and HT29-MTX cells are seeded on the apical membrane and allowed to reach confluence. Raji cells added to the basolateral compartment on day 14 of culture. The triple-culture is maintained for a further 4–6 days.	• Distribution of alkaline phosphatase on apical cell surface • Immunofluorescence evaluation of degree of binding of WGA • SEM	43,73,74
Caco-2 cells are pretreated with 25 ng/ml of epidermal growth (EGF) factor for 24 h. Then, Raji cells and EGF pretreated Caco-2 cells are allowed to interact in detached condition for 2 h at a 1:1 ratio and then plated in culture plates. Cells are cultured for 14 days.	• Functional transport studies between Caco-2 monoculture controls and co-cultures • Phase contrast imaging • SEM	29
Organoids are cultured from primary murine epithelial crypt stem cells. RANKL is added at a concentration of 200 ng/nl for 72 h to stimulate M cell differentiation.	• Immunofluorescence of clusterin • Immunofluorescence staining of UEA-1 and annexin V • TEM • SEM • Functional uptake studies of beads • Expression of M cell genes	6
Epithelial organoids are cultured from primary human small intestinal crypts. RANKL is added at a concentration of 200 ng/nl for 72 h to stimulate M cell differentiation.	• Immunofluorescence staining of Gp2, E-Cadherin and EPCAM • Functional uptake studies of microparticles • Expression of M cell genes	7

Table 1: Commonly used and recently published variations of *in vitro* models of the follicle-associated epithelium and examples of M cell identification techniques used.

Other models of the FAE include organoid and enteroid cultures; in an attempt to advance the standard Caco-2/Raji co-culture, a murine 3D organoid model of the FAE was introduced in which M cell differentiation was induced with soluble RANKL treatment. [6] This model used murine primary small intestinal epithelial cells to culture an epithelial organoid structure representative of the intestinal epithelial barrier. Subsequently, M cells were induced using soluble RANKL, which resulted in an increase of the genetic expression of both *SpiB* and *Gp-2*. To improve the translatability of this model, in 2016 Rouch et al. introduced a similar enteroid model with RANKL-induced M cells grown from human intestinal crypt cells, observing similar upregulation of M cell markers in response to RANKL. [7] Enteroid and organoid cultures are potentially more biologically relevant than the colon-derived Caco-2 cell line-based model as they are grown from primary, healthy tissue and findings using these models may therefore be more translatable to the human *in vivo* environment than cell line-based models and murine cultures. This is particularly due to the expression of M cell markers in the organoid and enteroid cultures that have not been validated in the cell line-based systems. [6, 7]

As stated previously, a major impediment to studies involving M cells is the lack of a reliable and specific M cell marker that applies across all established models. Different pathways of M cell differentiation may indicate an inherent difference in the genetic and proteomic signatures, thus perhaps making a universal marker unlikely. Thus far, the identification of M cells in the literature has relied on a number of different strategies, making it difficult to compare data across different models and studies. As such it is imperative to describe a reliable and specific M cell identification approach that will apply across both human and murine *in vitro* models, as they are most commonly used to study M cells. This critical review aims to discuss the various methods employed in the literature for confirming the presence of human and murine M cells in *in vitro* models of the FAE.

2.3 Morphological Indicators of M Cell Presence

2.3.1 Application of Electron Microscopy

The unique morphology of the M cell was first described in 1973 and compared between three different systems; the rabbit appendix, the chicken bursa of Fabricius and the mouse Peyer's Patches. [41] Transmission electron microscopy (TEM) revealed a morphologically distinct cell type associated with follicular lymphoid structures that exhibited increased

capability of transporting ferritin and India ink tracers from the lumen of the small intestine. [41] Among the many morphological and structural differences displayed by M cells, the most obvious are a denser cytoplasm, irregular microvilli formation, vesicles in the apical cytoplasm and an overall reduction in size of the cell. These parameters are still used frequently to identify M cells in *in vitro* human M cell models. [29, 38, 42] Indeed, due to the lack of a universally-applicable gene or protein markers, the most definitive way of confirming M cell presence is to visualize M cells with electron microscopy. For example, TEM is often used to visualize the characteristic disrupted brush border phenotype associated with the apical membrane of M cells. [43, 44] Scanning electron microscopy (SEM) is also frequently used to visualize the apical cellular surface in an attempt to distinguish well-formed microvilli of regular epithelial cells from the mal-formed, disrupted brush border of M cells. [23, 29, 43] Loss of features associated with the epithelial cell phenotype, including increase in the expression of annexin V [6], may imply these cells undergo a differentiation process that resembles a partial epithelial to mesenchymal (EMT) transition. [45] Morphological assessment may be the most reliable way of confirming the presence of a highly transcytotic cell population because, despite the variance in markers, the morphological characteristics of both fully mature PP M cells and villous 'M cells' are relatively consistent. [22] However, though useful as a visual guide providing information about the morphologic appearance of the cell, TEM and SEM are laborious and cost inefficient techniques which provide mostly qualitative information. [46] The data acquired is hard to quantify objectively and as such it is generally accepted that the sole use of TEM or SEM is not sufficient and needs to be accompanied by other methods. [47]

2.3.2 Cytoskeletal Structure

The cell cytoskeleton is comprised of organised networks of interacting filamentous proteins that serve three main functions; they maintain spatial organization of the internal cellular space, they generate forces enabling cell movement and change of shape and they connect the cell to the external environment. [48] There are three main filamentous proteins collectively comprising the building blocks of the cell cytoskeleton; actin filaments, microtubules and intermediate filaments. [48] All three cytoskeletal proteins are able to reorganise in response to external cues and thus rearrange the intracellular compartments. Actin filaments in particular are less rigid than other interacting proteins, yet able to assemble highly organised, stiff structures in the presence of cross-linkers. Actin filaments support protrusions, such as intestinal epithelial microvilli, and can generate forces involved

in changing cellular shape, as is observed during phagocytotic events. [48] Furthermore, the actin cytoskeleton is subject to continuous assembly and disassembly in response to local signalling cues. During endocytosis, signals released by the invaginating plasma membrane trigger the disassembly and reorganization of local actin filaments allowing the membrane region to form an endocytotic vesicle. [48] The unique morphology of the M cells' disrupted apical brush border has been reported on frequently; electron microscopy techniques have revealed the loss of organization in the apical microvilli of M cells and the invaginations in the cells' basolateral surface. [49] The partial loss of apical microvilli suggests rearrangement of the internal actin filaments supporting microvilli protrusions, and as such actin filament stains can give indication of the presence of M cells. Phalloidin, a high-affinity filamentous actin probe, or villin, an actin binding protein, are among common immunohistological stains that can be used to stain epithelial cell monolayers in which discontinuous staining indirectly suggests the presence of M cells. [50] Recently, a study investigated the role of allograft inflammatory factor 1 (Aif1) in M cell mediated transcytosis after observing the depletion of Aif1 in *SpiB* $^{-/-}$ mice. Using *Aif1*$^{-/-}$ mice, the study showed that although *Aif1* deficiency did not impact the amount of Gp2+ M cells, it significantly impeded their uptake capacity of both microparticles and *Yersinia enterocolitica* and S. Typhimurium. [51] This was initially hypothesized to be a result of actin remodeling, as previous studies had shown that Aif1 is implicated in the cytosketelal development of cells [52, 53], however Aif1 deficiency did not alter the ultrastructural appearance of M cells nor their frequency, yet still remained crucial for antigen uptake.

Species	M cell markers	Reference
Human	Gp2	7,27,29
	Clusterin (?)	
	Morphological indicators	
	Functional capacity	
Mouse	Gp2	10,13,28,30, 31
	UEA-1	
	Clusterin	
	Annexin V (immature)	
	Morphological indicators	
	Functional capacity	
Rabbit	Vimentin	32,33
Pig	Cytokeratin 18	34
Rat	Cytokeratin 8	35

Table 2: M cell markers identified specifically in the gut-associated lymphoid tissue epithelium of different species.

2.4 Cell Surface Markers

2.4.1 Lectins

2.4.1.1 UEA-1 and WGA

Ulex europaeus agglutinin (UEA) 1 is a lectin which binds to glycoproteins and glycolipids containing α-linked fucose residues. [11] Several research studies have shown that UEA-1 is able to bind to sites of α-1,2 fucosylation on murine M cells with high affinity. [13, 21, 40] UEA-1 was first established as a positive marker for murine M cells in 1993 by Clark et al. who used fixed mouse small intestinal PPs to compare four lectins for their binding affinity to M cells within the FAE: UEA-1, psophocarpus tetragonolobus (WBA), arachis hypogaea (PNA) and triticum vulgaris (WGA). They reported UEA-1 bound strongly to M cells, without cross-binding with goblet cells and enterocytes. WBA exhibited similar staining patterns as UEA-1, but with a much weaker staining intensity. PNA was found to bind with strong affinity to goblet cells but not to any other cell type, whilst WGA was found to stain goblet cells strongly, enterocytes moderately and M cells not at all. [31] As such, UEA-1 was reported to be a strong, positive M cell marker and WGA a reliable negative M cell marker for murine M cells in PPs. [31] However, a number of subsequent studies have reported that UEA-1 also binds strongly to goblet cells, which is inconsistent with the initial observation of Clark. [22, 54, 55] Currently, UEA-1 is used as a marker of goblet cells. Though goblet cells bind UEA-1, they also binds WGA, therefore M cells can be differentiated from goblet cells in murine models by co-staining with an additional marker. UEA-1 and WGA have been used to identify M cells in murine models frequently, though utilization of these known murine markers in human systems is infrequent in the literature and has yielded variable results. One study showed decreased staining in the co-cultures, which directly contradicts the observations made in murine systems [56], whilst another showed a relatively large amount of non-specific binding across both monocultures and co-cultures. [30] This indicates UEA-1 may not be a reliable marker for human M cells generated through the standard co-culture.

Building on the work conducted in murine systems, fluorescent latex microspheres were coated with either UEA-1 or several different agents and their interaction with murine M cells measured using a murine intestinal gut loop model. [13] The microspheres were injected into gut loops excised from female BALB/c mice. Out of all the agents trialed, only

UEA-1 coated microspheres demonstrated selective binding to M cells, being internalized at a 100-fold greater rate than the control BSA-coated microspheres. Furthermore, it was found that binding of UEA-1 with a-L-fucose prior to exposing the microspheres to M cells resulted in a similar level of binding as in the controls, suggesting UEA-1 interacted specifically with the carbohydrate receptor on M cells. [13] This work prompted abundant interest in M-cell specific targeting of bioactive agents. For example, microparticles containing an antigen and with and without UEA-1, were introduced into four mice intramuscularly or mucosally through oral, nasal or rectal administration and immunoglobulin [22] isotypes generated were measured by an ELISA test. Though, as expected, intramuscular administration elicited the highest Ig response, microparticles targeted using UEA-1 significantly enhanced the immune response in all mucosal routes trialled. [11]

In recent years several studies have reported successful lectin-mediated M cell targeting approaches in murine models. [11, 13, 21] Notably, human studies in this area are relatively few. Russell-Jones et al. reported enhanced transport of microspheres functionalized with different lectins in Caco-2 monolayers [57], but otherwise there is a lack of data regarding M cell targeting in human models. Despite the reported successful applications of UEA-1-mediated targeting of M cells in non-human systems, little is known about this transcytotic pathway. [30] As such, there is a need for well-characterized, reproducible human models of the FAE to further study the molecular mechanisms of M-cell mediated transcytosis. [58]

2.4.1.2 NKM 16-2-4

NKM 16-2-4 is a monoclonal antibody (mAb) first developed in 2007 in an effort to develop a marker for the α(1,2) fucose containing carbohydrate moiety that is more specific than UEA-1. NKM 16-2-4 has been shown to bind to murine M cells with a greater affinity than UEA-1. [59] The mAb NKM 16-2-4 conjugated to FITC was introduced into rat intestinal loop models containing PPs. Within 10 minutes of administration, NKM 16-2-4 specifically attached to the apical surface of M cells in the dome region of the PPs, whereas the rat IgG control did not, as assessed through confocal imaging of stained sections. As a result of the intended increased specificity, the mAb did not cross-bind to goblet cells. [59] The intended use of the NKM 16-2-4 mAb was to serve as an M cell targeting agent specifically for murine systems. It has since been used to identify M cells in both human and murine *in vitro* FAE models, though use in human models is infrequent and generates variable results. [10, 30]

2.4.2 Proteins

2.4.2.1 Clusterin

Clusterin, also known as apolipoprotein J, is a highly conserved, disulfide-linked heterodimeric glycoprotein previously shown to be strongly expressed in murine PPs. [27] Normal villous epithelium samples and FAE samples were extracted from BALB/c mice and gene expression profiles were compared using microarray analysis. Clusterin was found to have a 7.76-fold increased expression in the FAE compared to the normal villous epithelium. This finding prompted a more comprehensive investigation into the expression of clusterin in inductive sites of human mucosal associated lymphoid tissue. [27] Clusterin expression was investigated in fixed surgical resection specimens of human non-pathologic terminal ileum containing PPs, colon, appendix, palatine and nasopharyngeal tonsils using immunohistochemistry and cryo-immunogold electron microscopy. [27] In human PPs, clusterin marked subcellular cytosolic space of cells thought to be M cells. To ensure the stained cells were M cells, a combination of high resolution immunofluorescence imaging and cryo-immunogold electron microscopy was conducted with results confirming clusterin was immunoreactive in the cytosol of M-like cells with the characteristic M cell phenotype. Although this suggests clusterin may be expressed in the cytosol of human M cells, Verburgghe et al. used Caco-2 cells as a positive control for the clusterin antibody. [27] Caco-2 cells do express the *CLU* gene encoding for clusterin. [60] As such, although clusterin may mark human PP M cells, it may lack specificity as a marker for M cells generated in an *in vitro* Caco-2/Raji cell-based model. Despite this, clusterin was recently used to mark M cells in a proposed, novel Caco-2/Raji co-culture protocol published by Chaikhumwang et al. [29] (refer to ***Table 1***). They reported no clusterin expression in Caco-2 cells alone, as demonstrated by Western blotting. [29] This disparity in published data indicates more studies are required to determine whether clusterin can be used as a reliable human M cell marker across various human models.

2.4.2.2 Annexin V

Annexin V (or annexin A5) is a cellular protein belonging to the annexin family of calcium-dependent phospholipid binding proteins. [61] Annexin V is most frequently known for its function as an apoptotic marker; it is used commonly in flow cytometry to detect apoptotic cells due to its ability to bind phosphatidylserine (PtdSer) on the outer leaflet of the plasma

membrane. [28] Expression of PtdSet on the cellular membrane is an integral step in apoptosis as it signals nearby phagocytes to action. In 2004, a novel study proposed PtdSer may form a part of a yet undescribed pinocytotic pathway. [62] The study observed the internalization of annexin V into anti-Fas (an apoptosis signal receptor) stimulated Jurkat cells in a PtdSer dependent manner, whereby annexin V was transported into the cell and redistributed throughout the cytoplasm in endocytotic vesicles. [62]

The FAE-specific genetic expression of annexin V was reported by two different groups. [28, 63] Gene expression profiles of the FAE and normal villous epithelium of BALB/c mice were compared through microarray analysis. The analysis revealed that within the FAE, 91 genes were upregulated and 4 downregulated by at least two-fold. This subset of genes was further confirmed through quantitative RT-qPCR. [28] The *Anxa5* gene encoding Annexin V was upregulated more than 3 times in the FAE compared to the VE, as determined by microarray analysis. *Anxa5* was the second most expressed gene in the FAE, behind the gene encoding for clusterin. Immunohistochemical analyses revealed that whilst the VE was completely negative for annexin V immunoreactivity, strong immunoreactivity of annexin V co-localising with UEA-1 was observed within the FAE. Other studies have shown that annexin V binds to the lipopolysaccharide of gram negative bacteria reducing endotoxin activity, suggesting that annexin V may play a role in M cell mediated bacteria uptake. [61] It appears that the role of annexin V as an M cell marker functions independently of SpiB, and thus may be more indicative of an immature/proliferating M cell phenotype. A 2012 study used RT-qPCR to evaluate mRNA expression of M cell specific genes in WT and SpiB -/- mice. The transcriptional expression of M cell specific genes Gp2, CCL9, M-Sec and Sgne-1 was completely ablated in SpiB-/- mice and this expression was not restored by subsequent RANKL administration. [17] In contrast, mRNA expression for Marcksl1 and annexin V was maintained the SpiB -/- mice. [17] This observation suggests Gp2, CCL9, M-Sec and Sgne-1 are regulated by SpiB, whereas Marcksl1 and annexin V appear to be SpiB-independent and thus may be markers of a less mature M cell phenotype. [17]

In 2012, de Lau et al. developed an *in vitro* 'M cell' organoid model using cells derived from either wildtype (WT) or SpiB-deficient mice that were stimulated with recombinant RANKL to induce M cell differentiation. [6] RANKL stimulation resulted in an increase of the genetic expression of *SpiB* within 24 hours, as well as other M cell markers including *Gp-2*. This advanced model was validated using immunohistochemical analyses of UEA-1, annexin V and Gp-2, alongside transcriptional analyses of RANK, SpiB, Gp-2 and annexin V. [6]

Though likely to be effective in murine models, annexin V remains unexplored in human systems. However, as previously highlighted, it is possible that annexin V, a known EMT marker, may be a marker of the phenotypic transition that epithelial cells undergo in order to adopt the 'M cell' phenotype.

2.4.2.3 Glycoprotein-2

Glycoprotein-2 (Gp-2) is a protein secreted from intracellular zymogen granules and anchored to the cell membrane through glycosylphosphatidylinositol (GPI) linkages. [64] Gp-2 binds pathogens, including enterobacteria, and is thus central in mediating innate immunity. [10] Though initially thought to be expressed solely on mammalian pancreatic acinar cells [64], microarray analysis conducted on the FAE and normal intestinal epithelium of mouse PP's has demonstrated an increased expression of *Gp-2* mRNA on the FAE. [63] Additionally Gp-2 has been shown to be localised on M cells of the FAE through *in situ* hybridization and immunostaining experiments showing co-localization of Gp-2 with UEA-1. [10] Comparison of immunostaining of mouse and human PP showed similar staining patterns in the FAE overlying the PP, with co-localization with another proposed human M cell marker clusterin. [10] Thus Gp-2 may be the only M cell marker cross reactive between human and mouse that is currently available. [10] Gp-2 selectively binds to the FimH region of the type I pili on the outer membrane of bacteria including *E. coli.* In the absence of Gp-2, the transport of type I piliated bacteria across the FAE is impeded. [10] The expression of Gp2 was implicated as a pivotal factor in the transcytotic function of M cells in a 2015 study by Kimura and Iwanaga (2015). Briefly, they assessed the uptake capacity of two subsets of M cells; Gp2-high 'mature' M cells and M cells expressing a purported early M cell marker Tfnaip2, with low Gp2 expression. Ligated intestinal loop assays using 20nm fluorescent latex beads revealed that the beads were internalized mostly by Gp2-high cells and only occasionally by Gp2-low cells. [65] This suggests that Gp2 expression by M cells is crucial for high transcytotic capacity. [65]

Though it has been previously reported *SpiB-/-* mice lack Gp-2 expressing M cells in the FAE, it has also been suggested the M cell phenotype can be induced in regular absorptive epithelial cells via a *SpiB* independent pathway. [18, 19] One study showed that villous intestinal epithelial cells (IECs) could adopt an M cell phenotype when presented with an immunological challenge in the form of CT and *Salmonella* Thyphirium. [20, 22] These CT-induced 'M cells', designated as such due to being UEA-1^{+}, NKM 16-2-4^{+} and $CD45^{-}$, showed a different expression pattern of protein markers and cytokines as compared to PP

M cells and normal IECs. Despite this, they were capable of increased transcytosis and developed an M cell-like morphology. In SpiB-dependent PP M cells, Gp-2 was highly expressed and co-localised with UEA-1, whereas in CT-induced 'M cells' it was entirely absent. This is also true of another reported M cell marker Marcksl1. Additionally, cytokines that were abundantly expressed in PP M cells were only moderately expressed in CT-induced 'M cells'; as an example, CCL9 was upregulated over 124 times in PP M cells compared to IECs, and only 7 times in CT-induced 'M cells'. This indicated that SpiB-dependent M cells of the FAE and SpiB-independent 'M cells' may have different proteomic and genetic expression profiles, and a different functional capacity. [18, 22] Taken together, it is likely that SpiB regulates Gp-2 expression, and additionally that, due to their lower numbers, absence of crucial markers and diminished functional capacity, these SpiB–independent 'M cells' may not have a mature, fully differentiated M cell phenotype.

In the context of the *in vitro* models used to study the FAE, both mouse and human organoid cultures have successfully used Gp-2 to identify M cells. [6, 7] However, it has been reported that neither the *SpiB* gene nor the *Gp-2* gene are expressed in Caco-2 cells. [5] This indicates that 'M cells' generated through the Caco-2/Raji co-culture method are likely differentiated by a SpiB-independent pathway and as such may not be fully mature nor functionally similar to $Gp2^+$ PP M cells. Interestingly, one study does show the presence of Gp-2 on the apical surface of 'M cells' generated through a Caco-2/Raji co-culture, but the study lacks gene expression data. [30] Except in this instance, Gp-2 staining of Caco-2/Raji co-cultures has not been successfully demonstrated in the literature. As such, Gp-2 can be used as a reliable, human and murine M cell marker, but the absence of Gp-2 in a particular model may indicate the presence of 'M-like' cells generated independently of SpiB. It is important to note that though mechanisms of action of these cells may be similar, not enough is known about this subpopulation of cells to assume that they are a molecularly relevant model of the *in vivo* FAE microenvironment. Immortalized cell-line-based models are limited in their ability to recapitulate healthy human and murine tissues. Due to this, the *in vitro* organoid system cultured from isolated Lgr5+ intestinal stem cells and stimulated by RANKL appears to be a more appropriate model of the FAE, with reference to the genetic and proteomic signature reminiscent of *in vivo* PP M cells. The organoid system, pioneered by the Clevers group, is a controlled, *in vitro* organ model that, as a consequence of being cultured from primary stem cells, recapitulates much of the complexity of the original organ. Small intestinal organoids have, under certain growth conditions, been shown to spontaneously develop a crypt-villous structure and give rise to all of the main cell types found in the intestinal

epithelium. [66] In the *in vitro* M cell organoid model presented by de Lau et al. (2012), Gp2 expression is demonstrated at both the genetic and proteomic level indicating the presence of mature, terminally differentiated M cell population. [6] This, coupled with the observation that Gp2 expression has not been definitively confirmed in the Caco/Raji co-culture model, suggests that the organoid system is a far more accurate representation of the FAE.

Peyer's Patch M Cells	Villous M Cells
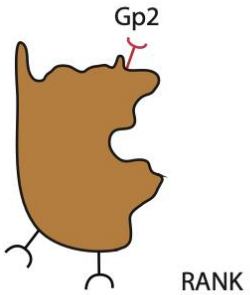	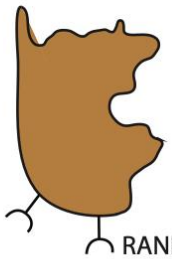
SpiB-dependent Express mature M cell marker Gp2 Constitutively expressed Differentiate in response to RANKL stimulation Highly transcytotic Located in the FAE overlying Peyer's Patches	SpiB-independent Express immature M cell markers (e.g. annexin V and Marcksl1) Inducible by pathogenic or virulent stimuli (e.g. cholera toxin) Impaired transcytotic capacity Found throughout the villous epithelium

Figure 2: M cells constitutively expressed by the follicle-associated epithelium express the mature M cell marker Gp2. They differentiate in response to RANKL stimulation and induction of *SpiB*. Alternatively, regular villous enterocytes can be prompted to differentiate into an 'villous' M cells that are only partially reminiscent of the M cell phenotype. Villous M cells are not restricted to the follicle-associated epithelium, express different markers and develop independently of *SpiB*. They are void of Gp2 expression and thus have an impaired transcytotic ability.

2.5 Functional Indicators of M cell Presence

2.5.1 Transcytotic Capacity

The interest in studying M cells is prompted by their increased ability to transcytose luminal antigens and the potential applications of this to targeted oral vaccine delivery strategies. In the absence of a confirmed M cell protein marker, the most reliable indicator of M cell presence is the transcytotic capacity of the cells. [36, 43] Functional studies evaluating the degree of uptake and transcytosis of particles are regularly used in *in vitro* models to confirm the presence of an M-cell like population. It is reported that in human cell-line-based assays in which M-like cells are induced through co-culturing epithelial cells with lymphoblastic cells, the presence of induced M-like cells can increase transcytotic capacity by approximately 800 times. [36] Furthermore, it is believed the transcytotic capacity of M cells is further exacerbated through contact with pathogenic materials. Through TEM, it has been shown that radiolabeled *Vibrio chloerae* were up taken by M cells in the PPs' of white rabbits, and that neutralization of *Vibrio chloerae* through acidification, heat, formalin or UV radiation reversed this effect. [67] It has also been shown that various strains of enterohemorrhagic *Escherichia coli* interact with *ex vivo* murine PPs, increasing their absorptive capacity, using the intestinal gut loop model. [10, 26] *In vitro* functional transport studies are a relatively simple method of confirming M cell presence by evaluating the absorptive capacity of the cell, providing also that the monolayer integrity remains intact.

2.5.2 Alkaline Phosphatase

Alkaline phosphatase is a homodimeric protein enzyme secreted bi-directionally by villous enterocytes and is integral to the digestive function of enterocyte cells. [68] Many *in vitro* models of the FAE utilize the Caco-2 cell line to represent the absorptive enterocytes of the *in vivo* small intestinal epithelium. [36] Caco-2 cells spontaneously differentiate into polarized enterocyte-like cells expressing high levels of brush border enzymes typical of small intestinal absorptive enterocytes. [69] The activity of brush border digestive enzymes, such as alkaline phosphatase, peptidases and disaccharides, gradually increase as cells mature and reach confluence. Thus, the conversion of enterocyte-like cells to "M cells" generally involves a loss of digestive function and a decrease in the expression of digestive enzymes including alkaline phosphatase. [68] This suggests a decrease in alkaline phosphatase activity could serve as a negative marker of M cells. Smith et al. (1987) were

among the first to attempt to quantify M cells in mice by investigating the decrease in alkaline phosphatase activity. [70] They examined the difference in number of M cells in BALB/c mice when the mice were transferred from a specific pathogen-free environment to a normal animal house environment. To quantify M cell numbers, they hypothesized that cells with the least amount of alkaline phosphatase activity were most likely to be M cells. This was supported by the observation that cells with the least amount of alkaline phosphatase activity change in numbers in a predictable fashion after the transfer of mice from a specific pathogen free environment into a normal animal house environment. This observation led them to suggest alkaline phosphatase is indicative of conversion of enterocyte-like cells into M cells.

Currently, many human *in vitro* models quantify alkaline phosphatase activity in order to measure the activity of intestinal cell lines. [42, 69, 71] In the context of the Caco-2/Raji co-culture model, a decrease in alkaline phosphatase activity is generally attributed to the presence of M cells. [42] Negative markers can be useful as complementary data to more established M cell identification methods, but cannot definitively be attributed to M cell conversion as a loss of brush border digestive enzymes indicates a decrease in digestive function of the original cell line and not necessarily the presence of M cells.

2.6 Conclusion

In vitro studies of the molecular mechanisms of function of the follicle-associated epithelium are made difficult by the lack of a universal M-cell specific marker that evaluates the degree of conversion of M cells and their transcytotic capacity. M cells are vital to mediating the intestinal immune response by regulating access of microorganisms and antigens circulating in the gut lumen to the underlying immune tissue. Despite their central role in intestinal immunity, the molecular mechanisms regulating the actions of these cells are still poorly understood. The importance of further study into the molecular actions of M cells is highlighted by the fact over 95% of human pathogenic microroganisms gain entry into host cells by crossing epithelial barriers. [2] Thus, inducing mucosal immunity by targeting M cells directly would be highly beneficial, despite the low number of M cells found *in vivo*. This critical review has discussed commonly used M cell markers, and outlined the necessity for developing a standardized approach to make the study of the M like cells generated in vitro more reliable. The current trend of using only imaging techniques or enzyme activity assays is not sufficient to demonstrate conclusively the conversion of enterocytes to mature M cells. Alternatively, the use of functional experiments showing elevated transport in M

cell models compared to control models does not definitively confirm that the results observed are due to M cell activity without confirmation of M cell presence. Due to the lack of a single, universal M cell marker, an approach utilising several techniques is recommended to confirm the presence of M cells, and expression of Gp2 in human and murine models can be considered indicative of a mature M cell population. Understanding the molecular mechanisms regulating M cells will be a crucial step towards advancing our knowledge of intestinal immunity and developing novel strategies to improve oral delivery of biologically active compounds.

2.7 References

1. Vighi, G., et al., *Allergy and the gastrointestinal system.* Clin Exp Immunol, 2008. **153 Suppl 1**: p. 3-6.
2. Azegami, T., Y. Yuki, and H. Kiyono, *Challenges in mucosal vaccines for the control of infectious diseases.* Int Immunol, 2014. **26**(9): p. 517-28.
3. Jung, C., J.P. Hugot, and F. Barreau, *Peyer's Patches: The Immune Sensors of the Intestine.* Int J Inflam, 2010. **2010**: p. 823710.
4. Lavelle, E.C. and D.T. O'Hagan, *Delivery systems and adjuvants for oral vaccines.* Expert Opin Drug Deliv, 2006. **3**(6): p. 747-62.
5. Mabbott, N.A., et al., *Microfold (M) cells: important immunosurveillance posts in the intestinal epithelium.* Mucosal Immunol, 2013. **6**(4): p. 666-77.
6. de Lau, W., et al., *Peyer's patch M cells derived from Lgr5(+) stem cells require SpiB and are induced by RankL in cultured "miniguts".* Mol Cell Biol, 2012. **32**(18): p. 3639-47.
7. Rouch, J.D., et al., *Development of Functional Microfold (M) Cells from Intestinal Stem Cells in Primary Human Enteroids.* PLoS One, 2016. **11**(1): p. e0148216.
8. Haber, A.L., et al., *A single-cell survey of the small intestinal epithelium.* Nature, 2017. **551**(7680): p. 333-339.
9. Kobayashi, A., et al., *The functional maturation of M cells is dramatically reduced in the Peyer's patches of aged mice.* Mucosal Immunol, 2013. **6**(5): p. 1027-37.
10. Hase, K., et al., *Uptake through glycoprotein 2 of FimH(+) bacteria by M cells initiates mucosal immune response.* Nature, 2009. **462**(7270): p. 226-30.
11. Manocha, M., et al., *Enhanced mucosal and systemic immune response with intranasal immunization of mice with HIV peptides entrapped in PLG microparticles in combination with Ulex Europaeus-I lectin as M cell target.* Vaccine, 2005. **23**(48-49): p. 5599-617.
12. Azizi, A., et al., *Enhancing oral vaccine potency by targeting intestinal M cells.* PLoS Pathog, 2010. **6**(11): p. e1001147.
13. Foster, N., et al., *Ulex europaeus 1 lectin targets microspheres to mouse Peyer's patch M-cells in vivo.* Vaccine, 1998. **16**(5): p. 536-41.
14. Knoop, K.A., et al., *RANKL is necessary and sufficient to initiate development of antigen-sampling M cells in the intestinal epithelium.* J Immunol, 2009. **183**(9): p. 5738-47.

15. Walsh, M.C. and Y. Choi, *Biology of the RANKL-RANK-OPG System in Immunity, Bone, and Beyond.* Front Immunol, 2014. **5**: p. 511.
16. Kanaya, T., et al., *Development of intestinal M cells and follicle-associated epithelium is regulated by TRAF6-mediated NF-kappaB signaling.* J Exp Med, 2018. **215**(2): p. 501-519.
17. Kanaya, T., et al., *The Ets transcription factor Spi-B is essential for the differentiation of intestinal microfold cells.* Nat Immunol, 2012. **13**(8): p. 729-36.
18. Sato, S., et al., *Transcription factor Spi-B-dependent and -independent pathways for the development of Peyer's patch M cells.* Mucosal Immunol, 2013. **6**(4): p. 838-46.
19. Lo, D.D., *Vigilance or Subversion? Constitutive and Inducible M Cells in Mucosal Tissues.* Trends Immunol, 2018. **39**(3): p. 185-195.
20. Tahoun, A., et al., *Salmonella transforms follicle-associated epithelial cells into M cells to promote intestinal invasion.* Cell Host Microbe, 2012. **12**(5): p. 645-56.
21. Kim, S.H. and Y.S. Jang, *Antigen targeting to M cells for enhancing the efficacy of mucosal vaccines.* Exp Mol Med, 2014. **46**: p. e85.
22. Terahara, K., et al., *Comprehensive gene expression profiling of Peyer's patch M cells, villous M-like cells, and intestinal epithelial cells.* J Immunol, 2008. **180**(12): p. 7840-6.
23. Jang, M.H., et al., *Intestinal villous M cells: an antigen entry site in the mucosal epithelium.* Proc Natl Acad Sci U S A, 2004. **101**(16): p. 6110-5.
24. Wang, J., et al., *Convergent and divergent development among M cell lineages in mouse mucosal epithelium.* J Immunol, 2011. **187**(10): p. 5277-85.
25. Neyt, K., et al., *Early IL-1 Signaling Promotes iBALT Induction after Influenza Virus Infection.* Front Immunol, 2016. **7**: p. 312.
26. Etienne-Mesmin, L., et al., *Interactions with M Cells and Macrophages as Key Steps in the Pathogenesis of Enterohemorragic Escherichia coli Infections.* Plos One, 2011. **6**(8).
27. Verbrugghe, P., et al., *Clusterin in human gut-associated lymphoid tissue, tonsils, and adenoids: localization to M cells and follicular dendritic cells.* Histochem Cell Biol, 2008. **129**(3): p. 311-20.
28. Verbrugghe, P., et al., *Murine M cells express annexin V specifically.* J Pathol, 2006. **209**(2): p. 240-9.
29. Chaikhumwang, P., et al., *A new cell-to-cell interaction model for epithelial microfold cell formation and the enhancing effect of epidermal growth factor.* Eur J Pharm Sci, 2017. **106**: p. 49-61.

30. Kim, S.H., et al., *The M cell-targeting ligand promotes antigen delivery and induces antigen-specific immune responses in mucosal vaccination.* J Immunol, 2010. **185**(10): p. 5787-95.
31. Clark, M.A., et al., *Differential expression of lectin-binding sites defines mouse intestinal M-cells.* J Histochem Cytochem, 1993. **41**(11): p. 1679-87.
32. Gebert, A., G. Hach, and H. Bartels, *Co-localization of vimentin and cytokeratins in M-cells of rabbit gut-associated lymphoid tissue (GALT).* Cell Tissue Res, 1992. **269**(2): p. 331-40.
33. Iwatsuki, H., C. Ogawa, and M. Suda, *Vimentin-positive cells in the villus epithelium of the rabbit small intestine.* Histochem Cell Biol, 2002. **117**(4): p. 363-70.
34. Gebert, A., H.J. Rothkotter, and R. Pabst, *Cytokeratin 18 is an M-cell marker in porcine Peyer's patches.* Cell Tissue Res, 1994. **276**(2): p. 213-21.
35. Rautenberg, K., et al., *Immunocytochemical characterization of the follicle-associated epithelium of Peyer's patches: anti-cytokeratin 8 antibody (clone 4.1.18) as a molecular marker for rat M cells.* Eur J Cell Biol, 1996. **71**(4): p. 363-70.
36. Beloqui, A., et al., *A human intestinal M-cell-like model for investigating particle, antigen and microorganism translocation.* Nat Protoc, 2017. **12**(7): p. 1387-1399.
37. Gullberg, E., et al., *Expression of specific markers and particle transport in a new human intestinal M-cell model.* Biochem Biophys Res Commun, 2000. **279**(3): p. 808-13.
38. des Rieux, A., et al., *Transport of nanoparticles across an in vitro model of the human intestinal follicle associated epithelium.* Eur J Pharm Sci, 2005. **25**(4-5): p. 455-65.
39. Beloqui, A., A. des Rieux, and V. Preat, *Mechanisms of transport of polymeric and lipidic nanoparticles across the intestinal barrier.* Adv Drug Deliv Rev, 2016. **106**(Pt B): p. 242-255.
40. Chionh, Y.T., et al., *M-cell targeting of whole killed bacteria induces protective immunity against gastrointestinal pathogens.* Infect Immun, 2009. **77**(7): p. 2962-70.
41. Bockman, D.E. and M.D. Cooper, *Pinocytosis by epithelium associated with lymphoid follicles in the bursa of Fabricius, appendix, and Peyer's patches. An electron microscopic study.* Am J Anat, 1973. **136**(4): p. 455-77.
42. Schimpel, C., et al., *Development of an advanced intestinal in vitro triple culture permeability model to study transport of nanoparticles.* Mol Pharm, 2014. **11**(3): p. 808-18.

43. des Rieux, A., et al., *An improved in vitro model of human intestinal follicle-associated epithelium to study nanoparticle transport by M cells.* Eur J Pharm Sci, 2007. **30**(5): p. 380-91.
44. Rochereau, N., et al., *Dectin-1 is essential for reverse transcytosis of glycosylated SIgA-antigen complexes by intestinal M cells.* PLoS Biol, 2013. **11**(9): p. e1001658.
45. Knoop, K.A., et al., *Distinct developmental requirements for isolated lymphoid follicle formation in the small and large intestine: RANKL is essential only in the small intestine.* Am J Pathol, 2011. **179**(4): p. 1861-71.
46. Ferris, M.M., et al., *Quantitative intercomparison of transmission electron microscopy, flow cytometry, and epifluorescence microscopy for nanometric particle analysis.* Anal Biochem, 2002. **304**(2): p. 249-56.
47. Muhlfeld, C., et al., *Visualization and quantitative analysis of nanoparticles in the respiratory tract by transmission electron microscopy.* Part Fibre Toxicol, 2007. **4**: p. 11.
48. Fletcher, D.A. and R.D. Mullins, *Cell mechanics and the cytoskeleton.* Nature, 2010. **463**(7280): p. 485-92.
49. Kimura, S., *Molecular insights into the mechanisms of M-cell differentiation and transcytosis in the mucosa-associated lymphoid tissues.* Anat Sci Int, 2017.
50. Albac, S., et al., *Candida albicans is able to use M cells as a portal of entry across the intestinal barrier in vitro.* Cell Microbiol, 2016. **18**(2): p. 195-210.
51. Kishikawa, S., et al., *Allograft inflammatory factor 1 is a regulator of transcytosis in M cells.* Nat Commun, 2017. **8**: p. 14509.
52. Ohsawa, K., et al., *Involvement of Iba1 in membrane ruffling and phagocytosis of macrophages/microglia.* J Cell Sci, 2000. **113 (Pt 17)**: p. 3073-84.
53. Mishima, T., et al., *Allograft inflammatory factor-1 augments macrophage phagocytotic activity and accelerates the progression of atherosclerosis in ApoE-/- mice.* Int J Mol Med, 2008. **21**(2): p. 181-7.
54. Ermund, A., et al., *Mucus properties and goblet cell quantification in mouse, rat and human ileal Peyer's patches.* PLoS One, 2013. **8**(12): p. e83688.
55. Kandori, H., et al., *Histochemical, lectin-histochemical and morphometrical characteristics of intestinal goblet cells of germfree and conventional mice.* Exp Anim, 1996. **45**(2): p. 155-60.
56. Pielage, J.F., et al., *Reversible differentiation of Caco-2 cells reveals galectin-9 as a surface marker molecule for human follicle-associated epithelia and M cell-like cells.* Int J Biochem Cell Biol, 2007. **39**(10): p. 1886-901.

57. Russell-Jones, G.J., H. Veitch, and L. Arthur, *Lectin-mediated transport of nanoparticles across Caco-2 and OK cells.* Int J Pharm, 1999. **190**(2): p. 165-74.
58. Brayden, D.J., *Oral vaccination in man using antigens in particles: current status.* Eur J Pharm Sci, 2001. **14**(3): p. 183-9.
59. Nochi, T., et al., *A novel M cell-specific carbohydrate-targeted mucosal vaccine effectively induces antigen-specific immune responses.* J Exp Med, 2007. **204**(12): p. 2789-96.
60. Rodriguez-Pineiro, A.M., et al., *Secreted clusterin in colon tumor cell models and its potential as diagnostic marker for colorectal cancer.* Cancer Invest, 2012. **30**(1): p. 72-8.
61. Rand, M.L., et al., *Diannexin, an annexin A5 homodimer, binds phosphatidylserine with high affinity and is a potent inhibitor of platelet-mediated events during thrombus formation.* J Thromb Haemost, 2012. **10**(6): p. 1109-19.
62. Kenis, H., et al., *Cell surface-expressed phosphatidylserine and annexin A5 open a novel portal of cell entry.* J Biol Chem, 2004. **279**(50): p. 52623-9.
63. Hase, K., et al., *Distinct gene expression profiles characterize cellular phenotypes of follicle-associated epithelium and M cells.* DNA Res, 2005. **12**(2): p. 127-37.
64. Hoops, T.C. and M.J. Rindler, *Isolation of the cDNA encoding glycoprotein-2 (GP-2), the major zymogen granule membrane protein. Homology to uromodulin/Tamm-Horsfall protein.* J Biol Chem, 1991. **266**(7): p. 4257-63.
65. Kimura, S., et al., *Visualization of the entire differentiation process of murine M cells: suppression of their maturation in cecal patches.* Mucosal Immunol, 2015. **8**(3): p. 650-60.
66. Sato, T., et al., *Single Lgr5 stem cells build crypt-villus structures in vitro without a mesenchymal niche.* Nature, 2009. **459**(7244): p. 262-5.
67. Owen, R.L., et al., *M cell transport of Vibrio cholerae from the intestinal lumen into Peyer's patches: a mechanism for antigen sampling and for microbial transepithelial migration.* J Infect Dis, 1986. **153**(6): p. 1108-18.
68. Lowe, D. and S. John, *Alkaline Phosphatase*, in *StatPearls*. 2018: Treasure Island (FL).
69. Ferruzza, S., et al., *A protocol for in situ enzyme assays to assess the differentiation of human intestinal Caco-2 cells.* Toxicol In Vitro, 2012. **26**(8): p. 1247-51.
70. Smith, M.W., P.S. James, and D.R. Tivey, *M cell numbers increase after transfer of SPF mice to a normal animal house environment.* Am J Pathol, 1987. **128**(3): p. 385-9.

71. Nollevaux, G., et al., *Development of a serum-free co-culture of human intestinal epithelium cell-lines (Caco-2/HT29-5M21).* BMC Cell Biol, 2006. **7**: p. 20.

Chapter 3 Follicle-associated epithelial organoids as a platform for assessing M cell-mediated nanoparticle uptake

The primary objective of this thesis is to develop an advanced *in vitro* model of the follicle-associated epithelium and to establish a methodology for evaluating the function of M cells.

Building upon the previous chapters' analysis of the epithelial barrier's structure from both a physiological and a molecular perspective, this chapter presents an advanced *in vitro* model of the small intestinal epithelium that incorporates true M cells, and a corresponding protocol for M cell function assessment. Accordingly, Aims 1, 2 and 4 are addressed.

3.1 Abstract

M cells are specialised epithelial cells that play a crucial role in the induction of the mucosal immune response by rapidly transcytosing luminal antigens to underlying lymphoid follicles. Their ability to swiftly transcytose luminal antigens to subepithelial immune cells have prompted interest in the study of these cells as potential targets for biopharmaceutical delivery. However, the absence of biologically relevant *in vitro* models to assess the rate of uptake has been a limiting factor in this field. To overcome this obstacle, the Clevers laboratory has previously developed an organoid model of the follicle-associated epithelium containing RANKL-induced, differentiated M cells. In this study, we demonstrate the utility of this murine small intestinal organoid culture system in evaluating the rate of uptake of surface-modified polystyrene nanoparticles (PSNP) as model nanocarriers for oral drug delivery. By comparing the uptake of control PSNP and UEA-1-conjugated PSNP between normal small intestinal organoids and M cell-containing small intestinal organoids, we show that Gp2+ M cells are primarily responsible for the increased uptake. Our findings highlight the potential of this organoid model to bridge the gap between current 2D monoculture systems and *in vivo* animal testing for the assessment of oral drug delivery efficacy.

3.2 Introduction

The recent advances in the use of biopharmaceuticals to treat a wide range of diseases has spurred a renewed interest in developing more specific and less invasive methods for delivering these treatments into systemic circulation. [1] Currently, intravenous (IV) administration is the most commonly used delivery route for administration of biopharmaceuticals as it provides high bioavailability and triggers a rapid systemic immune response. Despite this, IV administration of biopharmaceuticals is costly, inconvenient and ineffective at eliciting a rapid mucosal immune response in comparison to oral drug delivery (ODD) systems. [2-4] However, despite being the preferred method, ODD systems remain suboptimal as bioavailability of orally administered compounds is often too low to be therapeutically effective. This is particularly relevant for protein- and peptide-based drugs as their bioactive payload is subjected to low pH and enzymatic degradation in the stomach, they have a short plasma half-life and face difficulty penetrating the epithelial barrier in the small intestine. [2] To overcome the challenges associated with ODD systems, nanoparticle carriers have recently emerged as a promising vehicle for orally delivered compounds. [4, 5] Polymeric nanoparticle carriers encapsulate their biological payload, protecting it from enzymatic degradation and thereby increasing residence time in the body and, by extension, the bioavailability of the drug. Additionally, the polymer nanocarrier surface is amenable to chemical modifications, increasing the potential for specific targeting within the gastrointestinal tract (GIT).

The concept of specific targeting involves leveraging a unique feature of a molecular target to increase binding, enhance penetration through biological barriers and improve biodistribution. In the context of the GIT, specialised microfold (M) cells within the follicle-associated epithelium (FAE) overlying the Peyer's Patches (PPs) and other lymphoid structures are considered an attractive target for ODD systems. These rare cells comprise approximately 5-10% of the cells of the FAE and are highly specialised for the transcytosis of luminal antigens. [6, 7] Following transcytosis, the compound is presented to the hematopoietic cells residing in the sub-epithelial dome of the PPs, eliciting a potent mucosal immune response. The developmental origins and mechanisms of action of M cells remain improperly understood, primarily because their rarity makes them difficult to study; it is known that they differentiate in response to the RANK/RANKL dependent activation of the TRAF6-mediated NF-kB pathway. [8-10] Several preliminary animal studies suggest that specific targeting of particles to M cells may improve bioavailability. [11, 12] Hindering

progress in this promising field is the lack of relevant and predictive *in vitro* models used in the early stages of drug development to evaluate mechanisms of uptake and determine the most promising carrier systems and targeting strategies.

In addition to animal studies, which are both resource-intensive, ethically contentious, and biologically complex, researchers commonly utilize *in vitro* models to predict the rate of uptake by intestinal epithelial cells and M cells. These models typically use cell lines with absorptive properties, such as Caco-2 and T84 cells, to estimate uptake. To recapitulate the complex microenvironment of the PPs and the M cell-containing FAE, these intestinal cell lines are often co-cultured with cells of hematopoietic origin. [13, 14] It has been postulated that these cell-line-based co-cultures induce the differentiation of 'M-like cells' in a subset of epithelial cells in response to soluble factors released by hematopoietic cells. Although in widespread use, these models have been acknowledged for not encompassing all the cellular components of the *in vivo* intestinal barrier. Furthermore, there is limited characterization data to support the notion that these "M-like cell" are similar to true PP M cells. [15, 16] As such, they are currently an unreliable prognostic tool for predicting the *in vivo* absorption of orally administered compounds by M cells.

The Clevers laboratory have previously established long-term culture conditions under which crypt fragments containing stem cells derived from the mouse small intestine expand *in vitro* indefinitely. [17] The expanding crypts generate three-dimensional crypt-villus-like epithelial structures that contain all of the differentiated cell types found *in vivo*. The laboratory has also established that *SpiB*-dependent M cells can be induced within small intestinal organoids through the supplementation of culture media with soluble RANKL. [18] This study proposes the utilization of small intestinal organoids as a novel *in vitro* model for the assessment of targeted particle uptake. We describe a simple, improved *in vitro* model for the testing of targeted particle uptake and demonstrate the functionality of this model by using modified nanoparticles targeted to M cells to evaluate the differences in the rate of uptake, and the extent to which the uptake is facilitated by M cells. We compare this model to the current gold standard co-culture model to establish the relevance of 'M cells' generated from co-culture methods.

The consensus in pharmaceutical research is that there is an urgent need for *in vitro* models that accurately recapitulate the *in vivo* gastrointestinal environment and facilitate preliminary testing of pharmaceutical compounds. This would ease the reliance of pharmaceutical testing

on complex and costly animal models, and provide a convenient, reproducible tool for the *in vitro* testing of ODD systems that are prognostic of *in vivo* performance. In the present study, we demonstrate that the transcriptional and proteomic profile of 'M cells' generated by the frequently used Caco-2/B cell co-culture is different from *in vivo* M cells. As such, the cell-line-based models that have been used thus far are not biologically relevant and may explain why many drug candidates fail preclinical and clinical testing due to inadequate *in vitro* data. The time and cost exhaustive consequence of these failures highlights the need for translational *in vitro* models that are more representative of the *in vivo* intestinal environment. The organoid-based model presented in this paper can serve as a useful tool to evaluate the potential for ODD systems that target protective nanocarriers to defined molecular targets.

3.3 Materials and Methods

Cell Culture

Cells were maintained in 75cm^2 sterile cell culture flasks (Corning Life Sciences) at 37°C with 5% CO_2. Caco-2 cells were maintained in Dulbecco's Modified Eagle Medium/Nutrient Mixture F12 Ham (DMEM/F12, Sigma Aldrich) containing 15mM HEPES and sodium bicarbonate, supplemented with 1% L-glutamine, 1% penicillin/streptomycin, 10% FBS and 1% non-essential amino acids. LAZ 221 and JY cells were maintained in RPMI-1640 medium with sodium bicarbonate (Sigma Aldrich, Cat: R0883), supplemented with 1% penicillin/streptomycin and 10% FBS. For co-cultures, Caco-2 cells were seeded on the apical side of a polyester membrane (1.12 cm^2, 0.4 mm-pore) suspended in a Transwell (Corning Life Sciences). Caco-2 cells were seeded in the apical chamber at a density of 1 x 10^5/1.12cm^2, with the basal chamber containing 3ml of cell-free media. For co-culture experiments, after 14 days in culture, a suspension of 1 x 10^6 either LAZ 221 or JY cells were added to basal compartment in 3ml of growth media. The co-culture was maintained for a further 5-7 days. For RANKL differentiation experiments, the Caco-2 cell growth media was supplemented with 200ng/ml recombinant human soluble RANK ligand (sRANKL) (Peprotech) on day 14 of culture. The culture was maintained for a further 5-7 days. All cell lines were used between 10-30 passages.

Organoid Culture

Organoids were harvested from the small intestine of WT and *SpiB* $^{-/-}$ mice as described previously. [19] Briefly, crypts were isolated by digestion in a chelation buffer for 30 minutes at 4°C. Organoids were plated in Basal Membrane Extract (Trevigen) and cultured in 'ENR' media consisting of Dulbecco's Modified Eagle's medium/F12 supplemented with penicillin/streptomycin, 10 mM HEPES, Glutamax, B27 (GIBCO), 1 mM N-acetylcysteine (Sigma), 50 ng/ml murine recombinant epidermal growth factor (Peprotech), R-spondin1 (conditioned medium, 5% of final volume) and Noggin (conditioned medium, 5% of final volume). Organoids were cultured for 5-7 days after passaging. To induce the differentiation of M cells in organoids, ENR medium was supplemented with 200ng/ml of murine sRANK ligand for 72 h (Peprotech).

Transmission Electron Microscopy for Cell Morphology

Cells were seeded on Transwell inserts comprised of an apical and basolateral compartment and separated by a polyester membrane with 0.4μm pores (Corning Life Sciences). For the Caco-2 monolayer controls, Caco-2 cells were seeded in the apical chamber at a density of 1 x 10^5/1.12cm^2, with the basal chamber containing 3ml of cell-free media. Cells were cultured for 19-21 days. Medium in the apical chamber was changed every 48 hours, medium in the basolateral chamber was changed twice a week. For the Caco-2/B cell co-culture, Caco-2 cells were seeded in the apical chamber at a density of 1 x 10^5/1.12cm^2 and maintained identically to the monolayer controls. After 14 days a suspension of 1 x 10^6 Raji-B cells was added to basal compartment in 3ml of growth media. TEER was measured daily using an EVOM2 epithelial volt-ohm-meter to monitor cell monolayer stability. After 19-20 days, the cells were washed and fixed overnight in 4% paraformaldehyde/1.25% glutaraldehyde (electron microscopy grade) in 1X PBS (4% sucrose; pH 7.2). Membranes were washed with 1X PBS (PBS+4% sucrose) for 5 minutes, then postfixed in 2% osmium tetroxide (w/v) for 1 h. Monolayers were then dehydrated through graded ethanols, removed from the inserts using a scalpel and embedded in resin. Embedded membranes were left to polymerize at 70 C for 24 h. Polymerized samples were then cut into 80mm thick sections on a Leica Ultracut Microtome using a diamond knife. Sections were picked up on 200 mesh copper/palladium grids and stained with uranyl acetate and Lead Citrate. Grids were then visualized using the Philips CM200 transmission electron microscope. Monolayers were assessed for the presence of a cell monolayer (quality control step to exclude possible multilayer formation), the presence of tight junctions and cell morphology (columnar shape, polarization of cells, apical microvilli organization and organelle distribution). Monolayers with stable TEER values over 1000 /cm^2 were used in all experiments.

Conjugation of UEA-1 to polystyrene nanoparticles

UEA-1 (Sigma Aldrich) was covalently conjugated to flourescent polystyrene nanoparticles (FluoSpheres™ Amine-Modified Microspheres, 0.2 μm, yellow-green fluorescent, Molecular Probes) through a carboxylated PEG adlayer. Carboxylated PEG (20 mg) was activated using EDC-HCl (3.2 mg) and NHS (4.8 mg) dissolved in 2-ethanesulfonic acid (MES) buffer (2 mL) and reacted to the amine nanoparticles. The nanoparticle suspension was centrifuged twice in PBS and the supernatant removed to eliminate free PEG). The terminal PEG carboxylic groups on the PEGylated nanoparticles (2mg) were activated again

using EDC and NHS to conjugate the UEA-1 lectin (0.5 mg). The conjugated particles were thoroughly washed and stored at 4C until used. Particles were stored at 4°C until use. All reagants were obtained from Sigma Aldrich.

Transmission Electron Microscopy for Particle Analysis

Transmission electron microscopy analysis was used to determine average size, surface morphology and dispersion state of particles. A drop of undiluted product was placed onto ultrathin Formvar-coated 200-mesh copper grids and allowed to air dry. Particles were visualized using a TEM (JEOL JEM-2100F-HR, Transmission Electron Microscope, Japan) at an accelerating voltage of 200kV.

Dynamic Light Scattering and Zeta Potential Measurements

Dynamic light scattering (DLS) (Zetasizer Nano-ZS instrument (Malvern Instruments Ltd, UK)) was used to determine particle size distribution (PSD). The parameters were as follows; material refractive index 1.600, the dispersant was water, material absorption 0.010, viscosity 0.8872 cP. Each sample was measured at 25 °C in triplicate with an equilibration step of 120 s. Zeta potential was also measured using a Zetasizer Nano-ZS instrument (Malvern Instruments Ltd, UK) and recorded in a plastic cuvette with an equilibration time of 120 s.

Uptake Studies

To evaluate the uptake of nanoparticles by the small intestinal WT and *SpiB* -/- organoids, organoids were cultured for 5-7 days in either ENR medium or ENR medium supplemented with 200ng/ml sRANKL. A 0.5mg/ml suspension of either PEGylated (control) or UEA-1 conjugated 200nm sized fluorescent PSNP was microinjected into the lumens of control and sRANKL treated WT organoids. The injections were performed using a microinjector and capillary needles. The particle suspension was mixed with 1µl of fast-red immediately prior to injecting to aid in the macroscopic visualization of injected organoids. Then, an equal number of organoids per well and condition were microinjected. Organoids were incubated for 30 minutes at 37°C with 5% CO_2. Then, BME was dissolved using ice-cold PBS, organoids were collected in 1ml of TRYPLE and subsequently mechanically disassociated

using a glass pipette. Organoids were incubated at 37°C for 3 minutes. Then, organoids were pelleted by centrifugation for 5 minutes at 300g, re-suspended in 4% paraformaldehyde and fixed for 10 minutes at RT. After fixation, organoids were pelleted by centrifugation again ad resuspended in 100ul of FACS buffer (PBS, 1% BSA). Percentage of cells that had uptaken the nanoparticles was evaluated using FACS.

Flow cytometry

For analyzing PSNP uptake by flow cytometry, organoids were dissociated using TRYPLE for 5 minutes at 37°C and subsequent mechanical dissociation. Where indicated, cells would be stained with biotinylated UEA-1 lectin followed by streptavidin-561 (Invitrogen) or using anti-mouse GP2 antibody INSERT followed by anti-rat-561 (Invitrogen). Analysis was done using a FACSAria, FACSFusion (both BD) or a Cytoflex (Beckman Coulter). Data analysis was done using FACSDiva (BD) or FlowJo (Tristar) software.

Immunostaining

Immunostainings were performed as described previously. [20] Briefly, whole organoids were collected by dissolving the BME with ice-cold PBS and fixed overnight in 4% paraformaldehyde at 4°C. Organoids were washed twice with ice-cold PBS and blocked for 1h at RT in PBS containing 2% normal donkey serum (Jackson ImmunoResearch). After blocking, organoids were washed again and then permeabilized using PBS containing 1% Triton X-100 (Sigma Aldrich) for 30 minutes at RT. Then, organoids were resuspended in blocking buffer containing primary antibodies overnight at 4°C. Primary antibody used to detect Gp2 was mouse anti rat Gp2 (D278-3, MBL). The primary antibody was combined with Phalloidin-488 (Life Technologies) and UEA-1. The next day, organoids were again washed twice and subsequently incubated with the corresponding secondary antibodies in blocking buffer containing DAPI (1:1000; Invitrogen). Secondary antibodies used were donkey anti rat Alexa Flour 488 (LN0803245, LabNed) to visualize Gp2 and donkey anti goat streptavidin Alexa Flour 568 (610182, BD Biosciences) to visualize UEA-1. Sections were embedded in Vectashield (Vector Labs) and imaged using a Sp8 confocal microscope (Leica). Image analysis was performed using ImageJ/Fiji software.

Reverse Transcriptase (RT) quantitative PCR

RNA was isolated using the RNAeasy Mini Kit (Qiagen) according to the manufacturer's instructions. RNA (1 μg) was subjected to reverse transcription using Oligo dT primer and Superscript IV reverse transcriptase (18090050, Thermo Fisher Scientific), as per the manufacturer's instructions. cDNA was used for the RT-qPCR, performed with SYBR Green PCR Master Mix (Thermo Fisher Scientific). Gene analysis was conducted using a Bio-Rad RT-qPCR machine as previously described, [21] with reactions performed in triplicate. Primers used in this study are listed in *Table 1* and *Table 2* of the Appendix. Levels of mRNA expression were normalized to the expression of a reference gene, as calculated using the $2^{-}\Delta\Delta CT$ method.

Statistical Analysis

The GraphPad Prism 5 software (La Jolla, CA, USA, http://graphpad.com) was used for statistical analysis of data. Student *t*-tests or one-way ANOVAs were used throughout the study, where indicated, to evaluate statistical significance. Statistical significance is represented as * $p<0.05$.

3.4 Results

M cells generated through the Caco-2/B cell co-culture are distinct from *in vivo* M cells

Due to the widespread use of Caco-2/B cell co-cultures to model the follicle-associated epithelium M cells, we compared the M cells produced by the FAE organoid model with the 'M-like cells' generated through the Caco-2/B cell co-culture **(Figure 1, A).** First, we compared the transcriptional expression of mature M cell marker *Gp2*, transcription factor *SpiB* and the immature M cell marker *Marcskl1* between four groups; **(1)** Caco-2 cell monolayers, **(2)** Caco-2 cells treated with sRANKL, **(3)** Caco-2 cells co-cultured with LAZ 221 cells and **(4)** Caco-2 cells co-cultured with JY cells, as described. [22] The expression of *Gp2* at the transcriptional level was negligible across all groups, indicating that Caco-2 cells could not form fully mature, Gp2+ M cells through sRANKL stimulation, nor through soluble factors released by the B cell components **(Figure 1, B, lower panel).** The expression of *SpiB* was upregulated in the Caco-2 cells co-cultured with B cells; the Caco-2/LAZ 221 co-culture yielded the most significant increase in *SpiB* when compared to the control monolayers ($p=0.0118$). Caco-2 cells treated with sRANKL did not show any *SpiB* upregulation, indicating that the 'M cells' generated through this co-culture are not RANKL dependent, diverging significantly from the *in vivo* M cell developmental pathway. *Marcksl1* is not a M cell specific gene, but it is upregulated significantly during the early stages of M cell differentiation. *Marcskl1* was upregulated in both the sRANKL treated Caco-2 cells and the Caco-2 cells co-cultured with JY cells. This provides additional evidence to support the hypothesis that 'M cells' derived from Caco-2 cells, whether via the conventional RANKL pathway or through the frequently employed co-culture with hematopoietic cells, do not represent genuine M cells. Instead, they appear to resemble an immature M cell-like population that develops through an alternative developmental pathway. Given that numerous prior studies have noted the development of a highly transcytotic M cell-like population in Caco-2 co-culture with B cells, we aimed to confirm the presence of these cells within the monolayer, even in the absence of Gp2 positivity. [13, 22-24] TEM images of control Caco-2 cell monolayers show a monolayer of cells with organised microvilli held together by tight junctions with a regular dispersion of organelles in the cytoplasm **(Supplementary Figure 1).** A small subset of cells within the monolayer did display an M cell-like morphology; the apical surface of these cells displayed an irregular and disorganised brush border and large vacuoles within the cytoplasm.

Figure 1

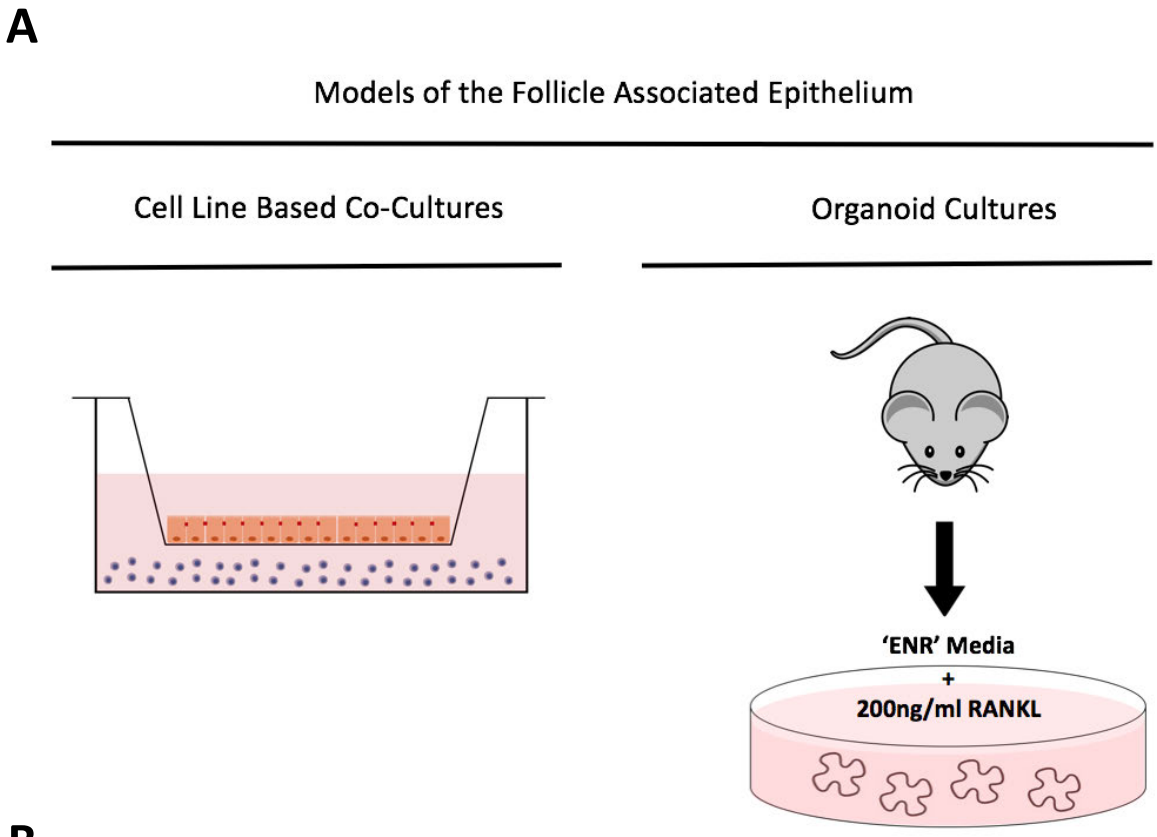
A
Models of the Follicle Associated Epithelium
Cell Line Based Co-Cultures
Organoid Cultures
'ENR' Media
+
200ng/ml RANKL

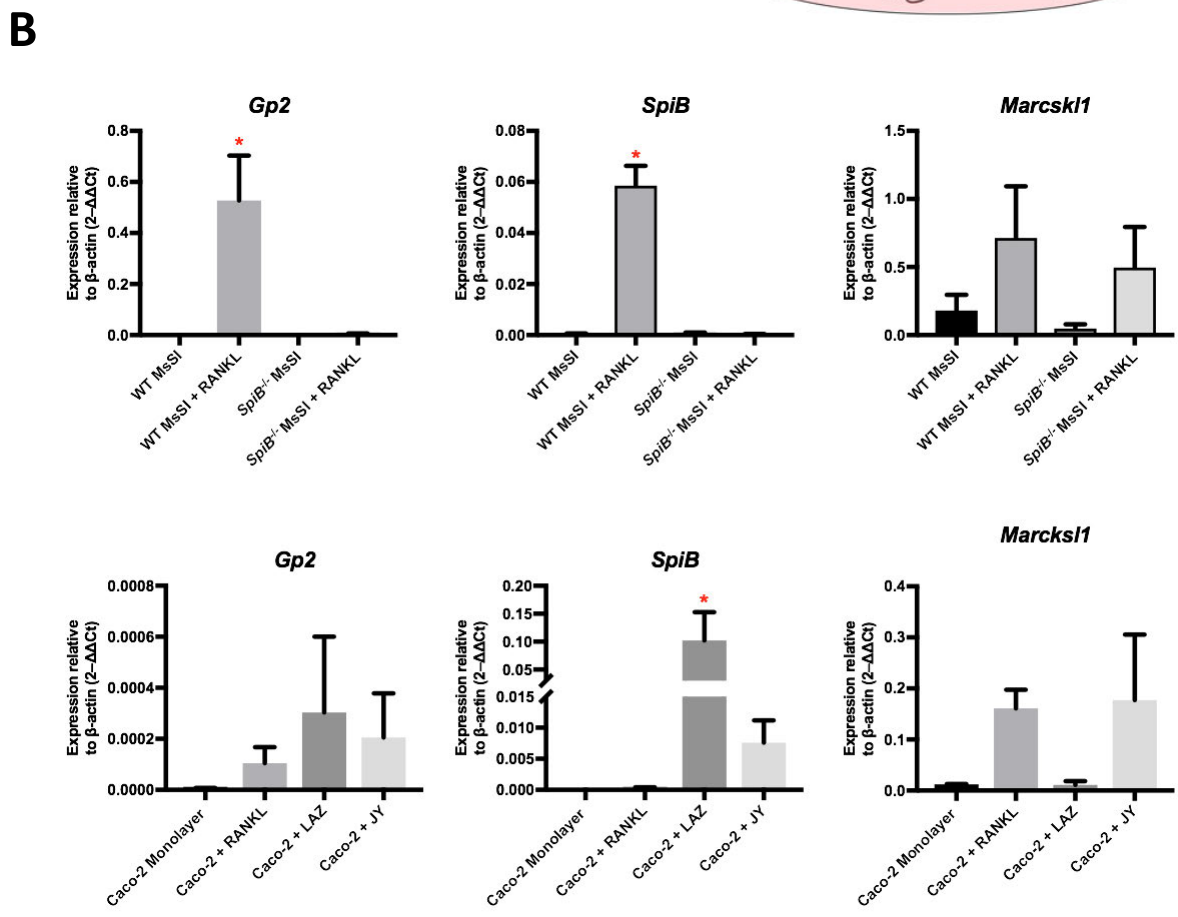
B
Gp2
SpiB
Marcskl1
Expression relative to β-actin (2−ΔΔCt)
WT MsSI
WT MsSI + RANKL
SpiB−/− MsSI
SpiB−/− MsSI + RANKL
Gp2
SpiB
Marcksl1
Caco-2 Monolayer
Caco-2 + RANKL
Caco-2 + LAZ
Caco-2 + JY

Figure 1: Comparison of the cell-line-based co-culture versus RANKL-treated murine small intestinal organoids as an *in vitro* model of the follicle-associated epithelium (FAE). **(A)** Schematic of the two models. The Transwell co-culture is the current industry gold standard for *in vitro* modelling of the FAE. It consists of an epithelial cell line monolayer cultured for 21d on a semi-permeable membrane suspended in a Transwell; M cell differentiation is induced by co-culturing the epithelial cells with a cell line of hematopoietic origin in the lower compartment. Organoids are derived from mouse small intestinal (MsSI) stem cells and cultured for 5-7d in a hydrogel substrate; M cell differentiation is induced with soluble RANKL. **(B)** Quantitative RT-qPCR analysis of transcriptional expression of M cell specific genes, normalized to β-actin. Mature M cell marker *Gp2,* and transcriptional factor regulating M cell differentiation, *SpiB,* are both upregulated significantly in RANKL-treated organoids compared to control organoids ($p=0.0153$ and $p>0.0001$, respectively). This effect is not observed in *SpiB*$^{-/-}$ organoids. Immature M cell marker, *Marcskl1,* is upregulated in RANKL-treated organoids, however this effect is *SpiB*-independent. *Gp2* expression is negligible across all models containing Caco-2 cells. *SpiB* is upregulated in Caco-2/ LAZ 221 co-cultures ($p=0.0118$) and Caco-2/JY co-cultures, but not in RANKL-treated Caco-2 cells. *Marcskl1* is upregulated in RANKL-treated Caco-2 cells and in Caco-2/JY co-cultures.

M cells generated through RANK/RANKL pathway activation in small intestinal organoids express M cell genes *Gp2* and *SpiB*

As reported previously, treatment of WT murine small intestinal organoids with sRANKL induced the differentiation of intestinal M cells *in vitro.* [18] To ensure sRANKL treated organoids produced M cells, we performed RT-qPCR for M cell specific genes *SpiB* and *Gp2*. We also tested the transcriptional expression of *Marcskl1*, shown previously to be highly expressed on both mature and immature, *SpiB*-independent M cells. [25] All RT-qPCR experiments were done on *SpiB*$^{-/-}$ (control and sRANKL-treated) organoids in parallel, to ensure the differentiation of M cells was *SpiB* dependent, as in the FAE *in vivo*. *Gp2* and *SpiB* were upregulated in a statistically significant manner ($p=0.0153$ and $p<0.0001$ respectively) in the sRANKL treated WT organoids compared to the control WT organoids **(Figure 1, B).** As expected, *Gp2* and *SpiB* expression was not detected in either the control nor sRANKL treated *SpiB*$^{-/-}$ organoids, confirming M cells within the organoid model were *SpiB*-dependent. We also tested the transcriptional expression of *Marcskl1*, a gene that was reported to be expressed by both traditional PP M cells and immature, transcytotic cells that develop independently of *SpiB* in response to RANKL. As expected, *Marcskl1* expression was increased in the sRANKL treated WT organoids compared to the control WT organoids. *Marcskl1* also increased in a similar fashion in the sRANKL *SpiB*$^{-/-}$ organoids, confirming its divergence from the traditional *SpiB*-dependent developmental pathway of Peyer's Patch M cells. To confirm the expression of Gp2 at the protein level, control and sRANKL treated organoids were stained for the Gp2 protein. Only WT sRANKL treated organoids showed positive Gp2 staining **(Figure 2, B).** This confirms that sRANKL treated organoids contain *SpiB*-dependent, Gp2+ M cells. These M cells, unlike the 'M-like cells' generated by the commonly used co-culture of Caco-2 and B cells, have a similar transcriptional profile to *in vivo* M cells. We monitored the morphology of the organoids microscopically to ensure the organoids maintained the same phenotype between the control and sRANKL treated conditions. Both the control and sRANKL treated WT organoids exhibited self-organising crypt-villus units, with the characteristic 'budding' after 2-3 days in culture; there were no microscopically evident morphological differences between the two conditions **(Figure 2, A).**

Figure 2

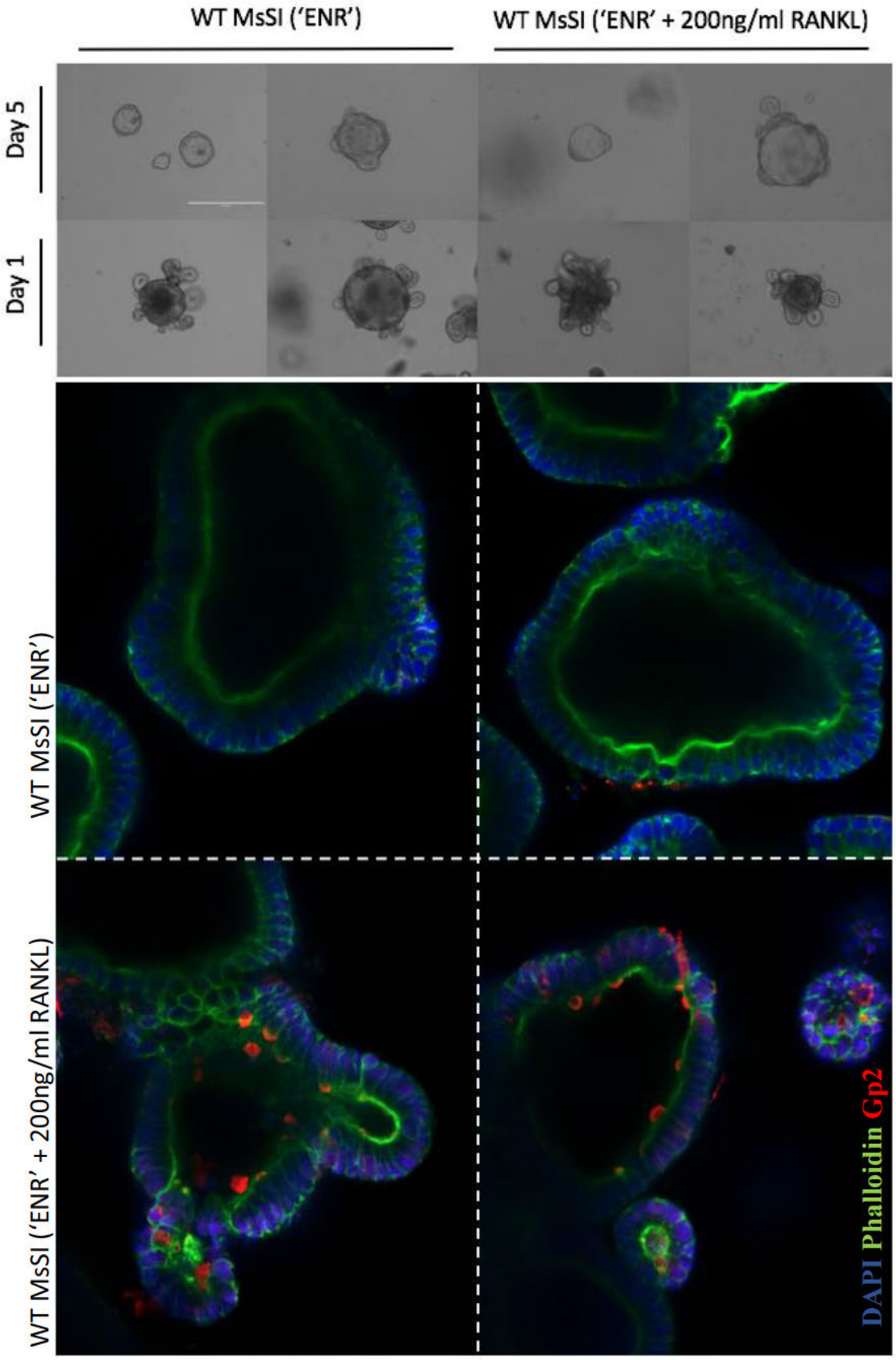
WT MsSI ('ENR')
WT MsSI ('ENR' + 200ng/ml RANKL)
Day 5
Day 1
WT MsSI ('ENR')
WT MsSI ('ENR' + 200ng/ml RANKL)
DAPI Phalloidin Gp2

Figure 2: Characterization of the murine organoid model of the intestinal follicle-associated epithelium. M cell differentiation was induced by activation of RANK/RANKL signalling, triggered by the supplementation of soluble RANKL into culture media. **(A)** Organoids cultured in regular 'ENR' media and RANKL-treated organoids retained a comparable morphology after 5d in culture, as evaluated by brightfield microscopy. **(B)** Representative confocal microscopy images of organoids after 5-7 days in culture revealed strong expression of Gp2, a terminal M cell differentiation marker, on the apical surface of cells of organoids that had been exposed to RANKL-supplemented 'ENR' media. Specific, apical Gp2 expression was not observed on cells of control organoids cultured in 'ENR' media only. Images are representative optical slices from a maximal projection of a Z-stack.

Model polymeric nanoparticles and their conjugation to UEA-1 for M cell targeting

The UEA-1 lectin binds to the α-1,2 fucose residues that are reportedly enriched on the apical membrane of M cells. [26] Targeting M cells to improve the efficacy of orally delivered vaccines has shown promising results in previous studies. [26-29] Specifically, UEA-1-modified nanoparticles have shown favourable results in increasing M cell-mediated uptake. [30, 31] We wanted to test the potential of UEA-1-modified PSNP to target M cells in an organoid model of the FAE. We used 200 nm sized, fluorescent polystyrene microspheres that were either conjugated with PEG (control particles) or PEG-UEA-1. Prior to use in functional experiments, the physicochemical properties of both control and modified particles were assessed. TEM images showed a monodispersed particle population; no formation of aggregates was observed **(Figure 3, A).** Dynamic light scattering (DLS) was used to assess the size distribution of the particles in aqueous media and revealed that both the control particles and UEA-1 modified particles fell within a narrow polydispersity range **(Figure 3, C).** This indicates the conjugation process was controlled and that formation of aggregates was prevented under the current conjugation method. X-ray photoelectron spectroscopy (XPS) elemental analysis was conducted to investigate the surface chemical properties of the particles and to quantify the amount of UEA-1 after conjugation **(Figure 3, D).** A significant increase in oxygen (O) and decrease in nitrogen (N) (from 1.6% to 6.3%) signals were measured for the UEA-1 conjugated particles compared to the PEGylated particles. The control particles had a zeta potential of +18 mV, likely due to the ionization of remaining free $–NH_2$ groups. The charge of the UEA-1 conjugated particles decreased to -5 mV, potentially due to the further screening afforded by the lectin. Collectively, these results indicate successful conjugation and the presence of UEA-1 on the surface of the modified particles intended to target M cells.

Figure 3

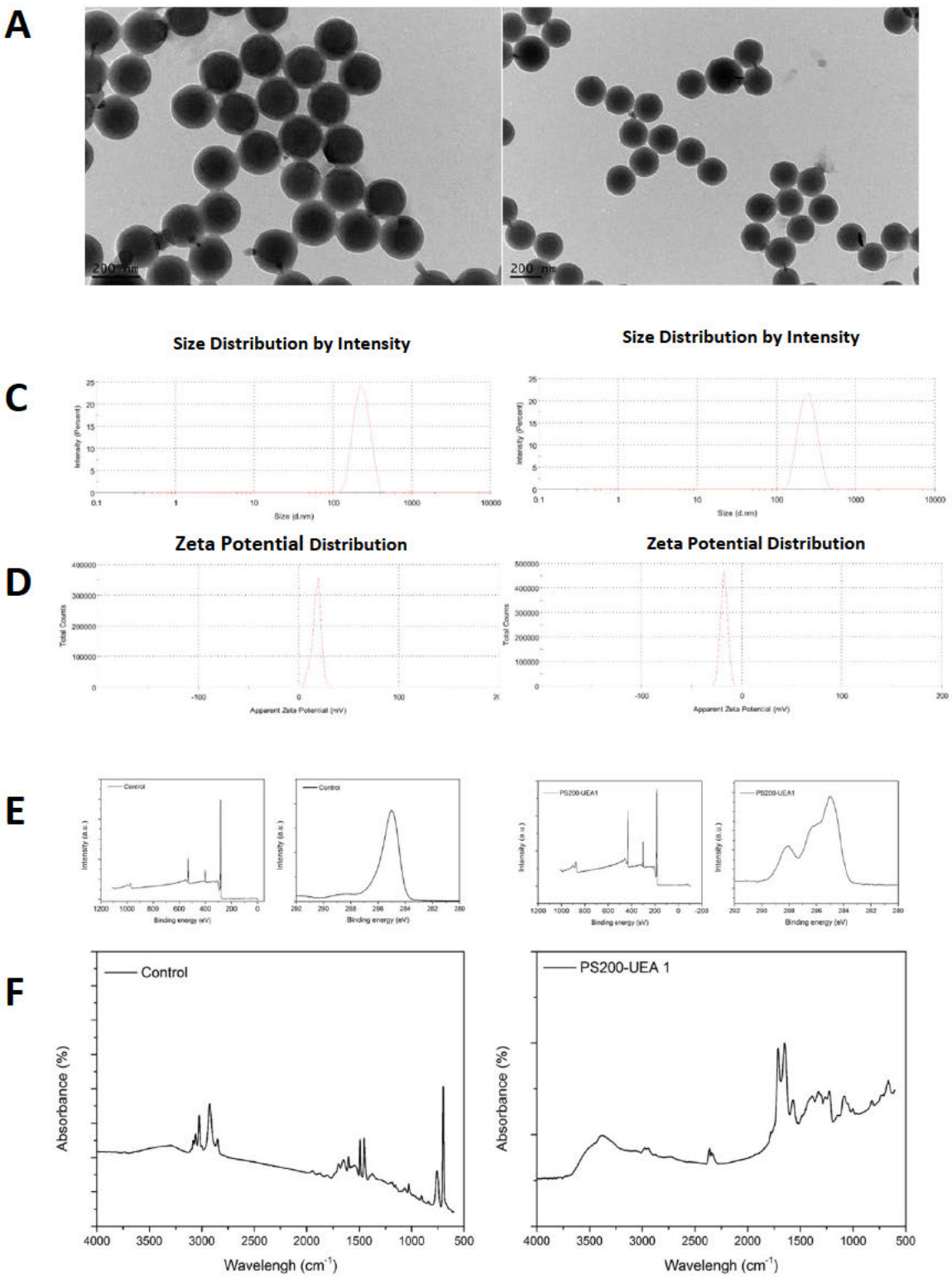
A
200 nm
200 nm
C
Size Distribution by Intensity
Size Distribution by Intensity
Intensity (Percent)
Size (d.nm)
D
Zeta Potential Distribution
Zeta Potential Distribution
Total Counts
Apparent Zeta Potential (mV)
E
Control
Control
PS200-UEA1
PS200-UEA1
Intensity (a.u.)
Binding energy (eV)
F
Control
PS200-UEA 1
Absorbance (%)
Wavelengh (cm-1)
4000
3500
3000
2500
2000
1500
1000
500

Figure 3: Characterization of polystyrene nanoparticles before and after conjugation to UEA-1. Transmission electron microscopy images of particles **(A)** before and **(B)** after conjugation to UEA-1 showing lack of aggregation. **(C)** Hydrodynamic diameters for the control (PS_{200}-PEG) and UEA-1 conjugated particles (PS_{200}-PEG-UEA-1). **(D)** XPS elemental survey spectra before and after conjugation to UEA-1 showing a significant increase in N% at 400eV.

UEA-1 conjugated nanoparticles are up-taken at a greater rate than control nanoparticles

Due to the desirability of M cell-specific targeting in the field of oral drug development, all nanoparticles were tested in normal small intestinal control organoids and sRANKL-treated organoids in order to evaluate the difference in the rate of uptake that may occur between normal intestinal epithelium and the follicle-associated epithelium. Organoids were injected as summarized schematically in **Figure 4 (A).** Uptake of particles and UEA-1 positivity were analysed in conjunction. As shown in Figure 4, control nanoparticles in control WT organoids showed least uptake. The percentage of cells that were positive for both UEA-1 and internalized particles (++) was 10.73% **(Figure 4, top left).** In the FAE organoid model, using control particles, 24.15% of the cells displayed positivity for both UEA-1 and the particles **(Figure 4, top right).** The percentage of cells showing UEA-1 positivity (y-axis) was slightly higher in the sRANKL-treated FAE organoid model. With the UEA-1 conjugated particles, uptake increased considerably. In the control small intestinal organoids **(Figure 4, bottom left),** though the cell population maintained a similar level of UEA-1 positivity (y-axis), the percentage of cells that had internalized nanoparticles increased significantly to 69.48%. In the FAE organoid model, using UEA-1 conjugated particles, 88.14% of cells were double positive for UEA-1 and the nanoparticles. This result was maintained with repetition **(Figure 4, B).** The percentage of cells taking up nanoparticles increased considerably when UEA-1 conjugated nanoparticles were used; the cell population shifts towards the top-right **(Figure 4, C; x-axis).** These results indicate that conjugation of UEA-1 to PSNPs increases uptake in both control organoids and FAE organoids. As conjugation to UEA-1 increased uptake in both control and sRANKL treated organoids, we stained the organoids with UEA-1 lectin to see whether expression was restricted to M cell containing organoids. Both control and sRANKL treated organoids displayed high levels of UEA-1 staining **(Figure 4, D).**

Figure 4

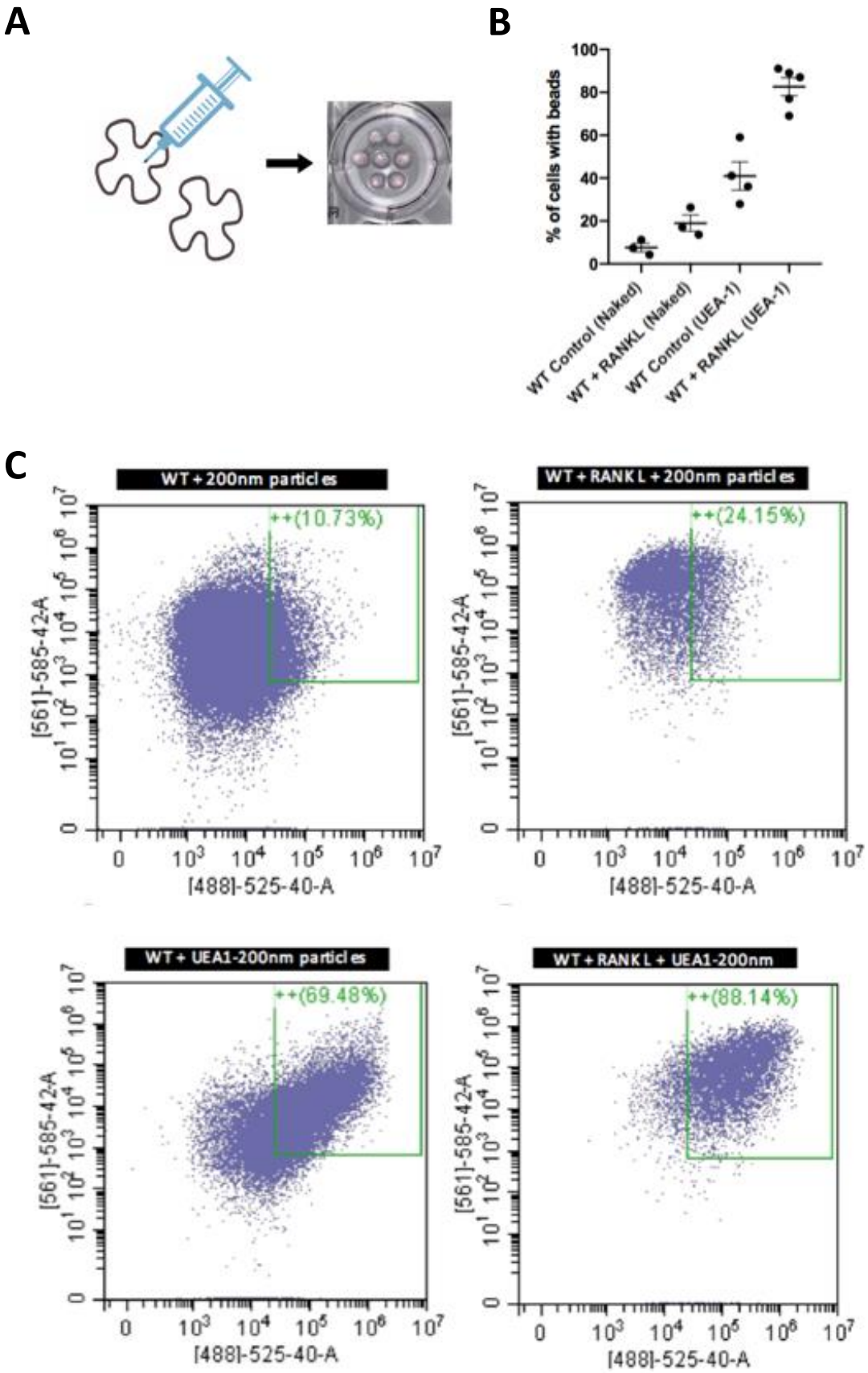
A
B
% of cells with beads
100
80
60
40
20
0
WT Control (Naked)
WT + RANKL (Naked)
WT Control (UEA-1)
WT + RANKL (UEA-1)
C
WT + 200nm particles
++(10.73%)
WT + RANKL + 200nm particles
++(24.15%)
WT + UEA1-200nm particles
++(69.48%)
WT + RANKL + UEA1-200nm
++(88.14%)
[561]-585-42-A
[488]-525-40-A

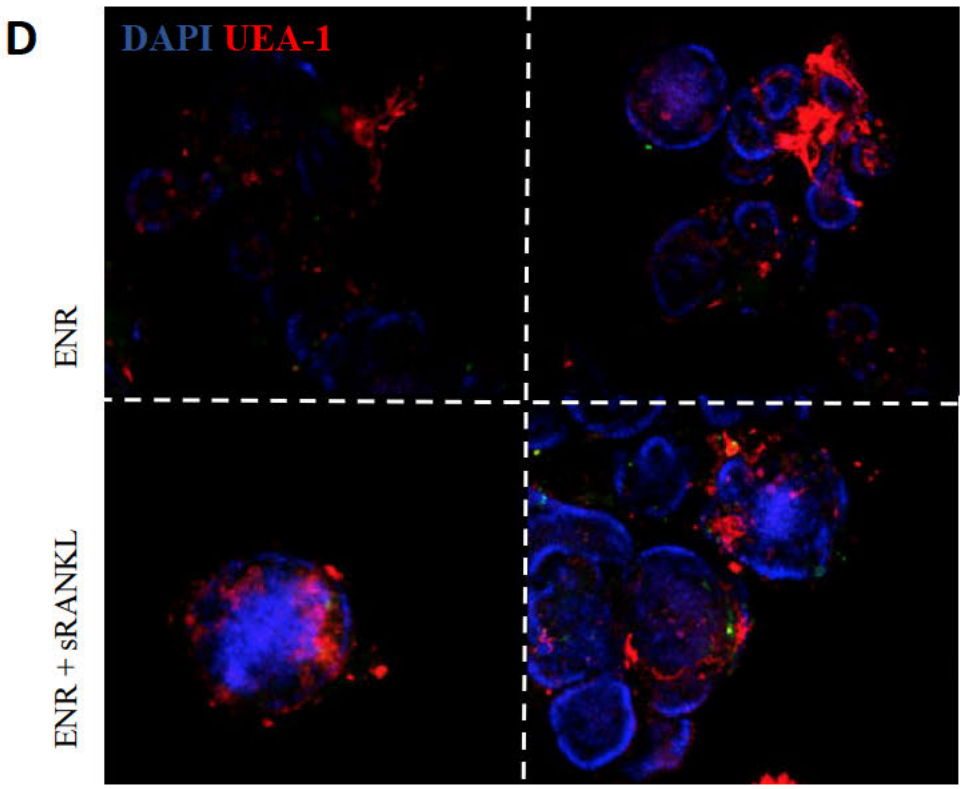
D
DAPI UEA-1
ENR
ENR + sRANKL

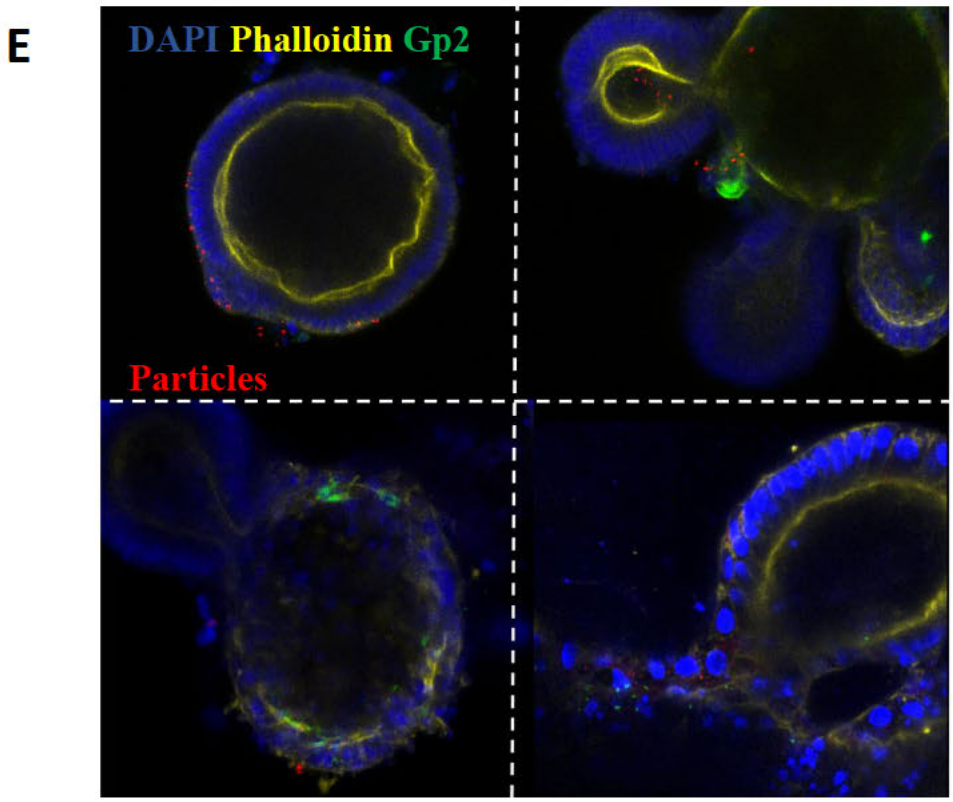
E
DAPI Phalloidin Gp2
Particles

Figure 4: Uptake of control and UEA-1 modified nanoparticles in WT mouse organoids cultured in either 'ENR' media or 'ENR' media supplemented with RANKL. **(A)** Schematic of microinjection and picture of injected organoids. **(B)** Representative quantification of uptake; an average of three experiments. **(C)** Representative FACS plots. Gate indicates double positive cell population; particles that have uptaken a bead (488- x axis) and particles that are positive for UEA-1 (561-y axis). Uptake of control particles is approximately double (x2.25) in organoids cultured in 'ENR+RANKL' media compared to 'ENR' cultured organoids. With UEA-1 modified particles, the entire cell population, for both 'ENR' and 'ENR+RANKL' organoids, shifts leftwards into the double positive gate. There is a significant increase in uptake in both 'ENR' and 'ENR+RANKL' organoids, compared to non-modified particles. Uptake is consistently highest with UEA-1 modified particles in the 'ENR+RANKL' model. Experiment performed in quadruplicate. **(D)** Confocal images of binding of UEA-1 lectin by organoids cultured in 'ENR' media (upper panel) and organoids cultured in 'ENR+RANKL' media (lower panel). UEA-1 binds to organoids in both media conditions. **(E)** Internalisation of microinjected particles co-localised with Gp2.

Gp2+ M cell in RANKL-treated organoids take up nanoparticles at a greater extent than Gp2- cells

To determine whether it was the Gp2+ M cells that were responsible for the increased uptake capacity observed in FAE organoids injected with UEA-1 conjugated particles, we stained the organoids with a Gp2 antibody and imaged whole mount organoids using a confocal microscope. In the FAE model, while some nanoparticles were detected in Gp2- regions, there was also noticeable co-localisation with Gp2+ cells **(see Figure 4, E).** These findings suggest that UEA-1 may not be an exclusive molecular target for M cells, but it can enhance uptake by both M cells and enterocytes in general.

Supplementary Figure 1

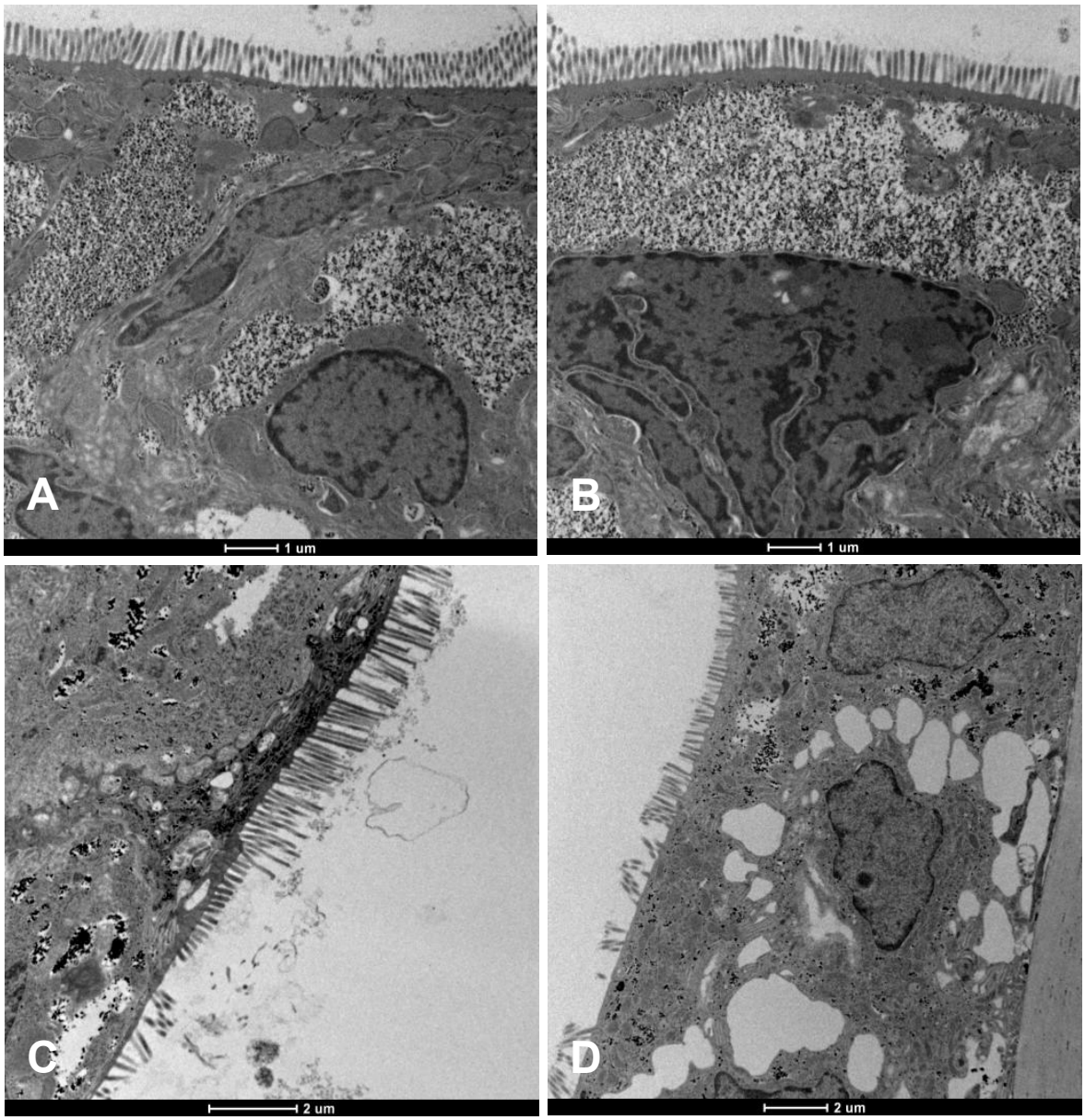

Supplementary Figure 1: Visualization of 'M-like cells' generated by the Caco-2/B cell co-culture by transmission electron microscopy. **(A, B)** Caco-2 cells grown in monolayers present with an organised brush border and a dense cytoplasm. **(C, D)** 'M-like cells' generated from Caco-2 cells through co-culture with Raji B lymphocytes were identified by disrupted brush border, fewer microvilli and cytoplasmic vacuoles. Scale bars; 1 μm **(A, B),** 2 μm **(C, D).**

3.5 Discussion

Due to their propensity for swift and efficient sampling of luminal antigens, M cells have garnered significant attention as possible targets for oral drug delivery. [15] Thus far, studies attempting to recreate M cells *in vitro* to test particle uptake and/or transport have used models that either lack biological relevancy or rely on complex methods and lack reproducibility. These include techniques such as the co-culture of Caco-2 cells with cells of hematopoetic origin and ligated intestinal loops. [13, 14, 22, 24, 32, 33] To date, the Caco-2/B cell co-culture method has served as the gold-standard for *in vitro* models for particle uptake and transport [13, 14, 32], despite an discernible lack of characterization efforts. [15] Conceptually, the co-culture model attempts to replicate the microenvironment in the domal region of the PPs where immune cells secrete factors that act on the follicle-associated epithelium triggering M cell differentiation in a subset of cells. In this paper, we compared the commonly used cell line-based co-culture model to the organoid model of the follicle-associated epithelium first described in 2012. [18] Next, we synthesized nanoparticles targeted to the α-1,2 fucose moiety enriched in M cells and devised a simple method for testing the uptake of these particles.

As reviewed previously [15], despite the widespread use of the Caco-2/B cell co-culture method in the literature, and the general consensus that the technique produces an 'M cell-like' cell type capable of enhanced transcytosis, there is a lack of data characterising these co-culture-derived 'M cell-like' cells'. [16] As such, it has thus far been difficult to gauge how translatable the data gathered from these studies is to the *in vivo* context. Here we show that although Caco-2 cells co-cultured with B cells do induce the differentiation of a subset of cells with an M cell-like phenotype and functional capacity, they do not adhere to traditional M cell differentiation pathways, nor do they express known M cell markers. As discussed in detail previously [34], it appears as though an M cell-like phenotype can be induced independently of the traditional M cell differentiation pathway; this divergent 'M cell'-like population may develop transiently in response to environmental cues and is likely not restricted to the FAE. As these co-culture derived 'M cells' rely neither on RANKL nor on *SpiB*, but can be induced by factors released by hematopoetic cells, it is possible that inflammatory factors secreted by immune cells chemoattracted to the epithelium during inflammation are responsible for the appearance of the transient 'M cell'-like phenotype. This is consistent with observations that compromised epithelial barrier function is a hallmark feature of many mucosal inflammatory diseases. Collectively, these observations

suggest that, though these divergent 'M cells' may mimic the function of true PP M cells, they are induced under adverse conditions and not physiological. Future work in this area should address the epithelial changes that occur under inflammatory conditions, with particular attention given to understanding how phenotypic and functional changes of regular epithelial cells contribute to ongoing inflammation.

As reported previously, treatment of WT murine small intestinal organoids with sRANKL induced the differentiation of intestinal M cells *in vitro.* [18] Organoid-derived M cells expressed all the immature and mature M cell marker genes. A feature of the organoid system that hampers *in vitro* drug testing is that the cells of the organoid polarize rendering the lumen 'closed.' While this mimics the self-organization of the intestinal epithelium *in vivo,* it makes accessing the apical surface of cells difficult. Our simple method for accessing the lumen to inject PSNPs can be achieved easily with relatively common lab equipment and can be extrapolated to other applications, such as the application of microbes and other luminal products. [35]

In this paper, we tested UEA-1 modified PSNPs to gauge whether they would increase uptake in M cells specifically. Though this was achieved, the α-1,2 fucose residues that bind UEA-1 are not specific to M cells. This suggests that UEA-1 PSNP modification might prove a promising method of increasing drug bioavailability generally, not just in the context of M cells. Our ability to visualise M cells and quantify uptake using flourescene-activated cell sorting also presents an opportunity to test other modifications in the future.

3.6 Conclusion

In this study, we utilized the cutting-edge organoid technology to establish a robust and reproducible protocol for the assessment of nanoparticle uptake in the small intestine. This organoid-based model represents a superior alternative to conventional models, providing a more accurate representation of the structural and cellular organization of the small intestinal epithelial barrier. Additionally, the induction of M cells within the organoid system via sRANKL supplementation allows for comparative evaluation of nanoparticle uptake between the normal small intestinal epithelium and the follicle-associated epithelium. This approach represents a significant step forward in the development of oral vaccines specifically targeted towards M cells. To validate the functionality of the model, we targeted M cells by conjugating polystyrene nanoparticles with UEA-1. Our findings demonstrate that UEA-1 modification of the nanoparticles significantly enhances particle uptake, although this effect was not exclusive to M cells, as UEA-1 expression was also observed in wild-type organoids. The *in vitro* model described here provides a reliable and convenient methodology for testing the intestinal uptake of nanocarriers, particularly those targeted towards M cells, without the need for time- and resource-intensive animal models. Further research in this field can explore additional nano-carrier surface modifications to identify and validate novel targets within the intestine.

Contributions

Ana Klisuric, Jotam Bar-Ephraim, Clive Prestidge, Rachel Gibson, Benjamin Thierry and Hans Clevers conceived the study. Ana Klisuric and Jotam Bar-Ephraim performed the experiments. Zhengyang Jia performed the nanoparticle synthesis and characterization. Jotam Bar-Ephraim, Clive Prestidge, Rachel Gibson, Benjamin Thierry and Hans Clevers read the chapter and provided feedback.

Conflict of Interest

The author declares no conflict of interest.

Funding

The work was funded by the Endeavour Leadership Program of Australia, a University of South Australia Student Mobility Grant, the ONCODE Institute and ARC Linkage Grant (LP150100032).

Acknowledgements

The author would like to thank Stefan Van Elst for assistance with FACS experiments and Cayetano Pleguezuelos-Manzano for assistance with microinjections.

3.7 References

1. Homayun, B., X. Lin, and H.J. Choi, *Challenges and Recent Progress in Oral Drug Delivery Systems for Biopharmaceuticals.* Pharmaceutics, 2019. **11**(3).
2. Bolton, D.L., et al., *Comparison of systemic and mucosal vaccination: impact on intravenous and rectal SIV challenge.* Mucosal Immunol, 2012. **5**(1): p. 41-52.
3. Holmgren, J. and C. Czerkinsky, *Mucosal immunity and vaccines.* Nat Med, 2005. **11**(4 Suppl): p. S45-53.
4. Ensign, L.M., R. Cone, and J. Hanes, *Oral drug delivery with polymeric nanoparticles: the gastrointestinal mucus barriers.* Adv Drug Deliv Rev, 2012. **64**(6): p. 557-70.
5. Pridgen, E.M., F. Alexis, and O.C. Farokhzad, *Polymeric nanoparticle technologies for oral drug delivery.* Clin Gastroenterol Hepatol, 2014. **12**(10): p. 1605-10.
6. Kraehenbuhl, J.P. and M.R. Neutra, *Epithelial M cells: differentiation and function.* Annu Rev Cell Dev Biol, 2000. **16**: p. 301-32.
7. Owen, R.L., *Uptake and transport of intestinal macromolecules and microorganisms by M cells in Peyer's patches--a personal and historical perspective.* Semin Immunol, 1999. **11**(3): p. 157-63.
8. Knoop, K.A., et al., *RANKL is necessary and sufficient to initiate development of antigen-sampling M cells in the intestinal epithelium.* J Immunol, 2009. **183**(9): p. 5738-47.
9. Kanaya, T., et al., *Development of intestinal M cells and follicle-associated epithelium is regulated by TRAF6-mediated NF-kappaB signaling.* J Exp Med, 2018. **215**(2): p. 501-519.
10. Bar-Ephraim, Y.E., K. Kretzschmar, and H. Clevers, *Organoids in immunological research.* Nat Rev Immunol, 2020. **20**(5): p. 279-293.
11. Frey, A. and M.R. Neutra, *Targeting of mucosal vaccines to Peyer's patch M cells.* Behring Inst Mitt, 1997(98): p. 376-89.
12. McKenzie, B.S., et al., *Targeting lymphocyte Peyer's patch adhesion molecule-1: a relay approach to gut immunization.* Vaccine, 2005. **23**(28): p. 3668-78.
13. Beloqui, A., et al., *A human intestinal M-cell-like model for investigating particle, antigen and microorganism translocation.* Nat Protoc, 2017. **12**(7): p. 1387-1399.
14. Chaikhumwang, P., et al., *A new cell-to-cell interaction model for epithelial microfold cell formation and the enhancing effect of epidermal growth factor.* Eur J Pharm Sci, 2017. **106**: p. 49-61.

15. Klisuric, A., et al., *Highlight Article: Identifying human and murine M cells in vitro.* Exp Biol Med (Maywood), 2019. **244**(7): p. 554-564.
16. Mabbott, N.A., et al., *Microfold (M) cells: important immunosurveillance posts in the intestinal epithelium.* Mucosal Immunol, 2013. **6**(4): p. 666-77.
17. Sato, T., et al., *Single Lgr5 stem cells build crypt-villus structures in vitro without a mesenchymal niche.* Nature, 2009. **459**(7244): p. 262-5.
18. de Lau, W., et al., *Peyer's patch M cells derived from Lgr5(+) stem cells require SpiB and are induced by RankL in cultured "miniguts".* Mol Cell Biol, 2012. **32**(18): p. 3639-47.
19. Sato, T., et al., *Long-term expansion of epithelial organoids from human colon, adenoma, adenocarcinoma, and Barrett's epithelium.* Gastroenterology, 2011. **141**(5): p. 1762-72.
20. Beumer, J., et al., *Enteroendocrine cells switch hormone expression along the crypt-to-villus BMP signalling gradient.* Nat Cell Biol, 2018. **20**(8): p. 909-916.
21. van der Flier, L.G., et al., *Transcription factor achaete scute-like 2 controls intestinal stem cell fate.* Cell, 2009. **136**(5): p. 903-12.
22. des Rieux, A., et al., *Transport of nanoparticles across an in vitro model of the human intestinal follicle associated epithelium.* Eur J Pharm Sci, 2005. **25**(4-5): p. 455-65.
23. Antunes, F., et al., *Establishment of a triple co-culture in vitro cell models to study intestinal absorption of peptide drugs.* Eur J Pharm Biopharm, 2013. **83**(3): p. 427-35.
24. des Rieux, A., et al., *An improved in vitro model of human intestinal follicle-associated epithelium to study nanoparticle transport by M cells.* Eur J Pharm Sci, 2007. **30**(5): p. 380-91.
25. Sato, S., et al., *Transcription factor Spi-B-dependent and -independent pathways for the development of Peyer's patch M cells.* Mucosal Immunol, 2013. **6**(4): p. 838-46.
26. Wang, X., et al., *Transgene vaccination using Ulex europaeus agglutinin I (UEA-1) for targeted mucosal immunization against HIV-1 envelope.* Vaccine, 2005. **23**(29): p. 3836-42.
27. Lo, D.D., J. Ling, and A.H. Eckelhoefer, *M cell targeting by a Claudin 4 targeting peptide can enhance mucosal IgA responses.* BMC Biotechnol, 2012. **12**: p. 7.
28. Nochi, T., et al., *A novel M cell-specific carbohydrate-targeted mucosal vaccine effectively induces antigen-specific immune responses.* J Exp Med, 2007. **204**(12): p. 2789-96.

29. Mishra, N., et al., *Lectin anchored PLGA nanoparticles for oral mucosal immunization against hepatitis B.* J Drug Target, 2011. **19**(1): p. 67-78.
30. Foster, N., et al., *Ulex europaeus 1 lectin targets microspheres to mouse Peyer's patch M-cells in vivo.* Vaccine, 1998. **16**(5): p. 536-41.
31. Jia, Z., et al., *An ex vivo investigation of the intestinal uptake and translocation of nanoparticles targeted to Peyer's patches microfold cells.* Int J Pharm, 2021. **594**: p. 120167.
32. Beloqui, A., A. des Rieux, and V. Preat, *Mechanisms of transport of polymeric and lipidic nanoparticles across the intestinal barrier.* Adv Drug Deliv Rev, 2016. **106**(Pt B): p. 242-255.
33. Fukuda, S., K. Hase, and H. Ohno, *Application of a mouse ligated Peyer's patch intestinal loop assay to evaluate bacterial uptake by M cells.* J Vis Exp, 2011(58).
34. Lo, D.D., *Vigilance or Subversion? Constitutive and Inducible M Cells in Mucosal Tissues.* Trends Immunol, 2018. **39**(3): p. 185-195.
35. Dutta, D., I. Heo, and R. O'Connor, *Studying Cryptosporidium Infection in 3D Tissue-derived Human Organoid Culture Systems by Microinjection.* J Vis Exp, 2019(151).

Chapter 4 Outstanding questions in intestinal M cell biology

Previous chapters have provided a critical evaluation of the various discrepancies that have been observed between M cell models. This chapter aims to provide a clear and concise overview of the field, with particular emphasis on the phenomenon of multiple M cell lineages. Key challenges and inconsistencies in the field are highlighted, and key areas for investigation are outlined, addressing Aims 1 and 3.

4.1 Abstract

The epithelium directly overlying the lymphoid follicles of the gut harbors a rare cell population termed the M cell. M cells are specialised for the transcytosis of luminal antigens to underlying immune cells, thereby expediting the induction of the mucosal immune response. Despite their importance, the rarity of M cells has presented challenges for their study. The differentiation of M cells within the follicle-associated epithelium is regulated by RANKL-induced and TRAF6-mediated NF-kB signalling. Mature M cells are identified by the apical expression of capture receptor Glycoprotein 2 (Gp2). Recent evidence suggests that, in addition to the traditional Gp2+ M cells found within the follicle-associated epithelium, multiple, distinct M cell lineages may exist, exhibiting divergent developmental pathways but sharing a common morphology that supports their transcytotic function. Unlike traditional M cells, these alternative lineages are not constitutively expressed, but are rather inducible under pathologic conditions. If this notion proves to be accurate, inducible M cells may contribute to the epithelial immune response in yet unbeknown ways. The mechanisms of M cell-mediated transcytosis are not well understood. It is known that cell surface receptors, such as Gp2, play a role in bacterial transcytosis, while the unique morphological features of M cells contribute to non-specific uptake of luminal contents. However, the extent to which each mechanism contributes to overall transcytosis, and whether these mechanisms are comparable across lineages, is unclear. This critical review will summarize the current state of knowledge on M cells, highlighting outstanding questions in intestinal M cell biology that will direct future investigations in this field.

4.2 Introduction

4.2.1 Immunoreactivity in the gut

The intestinal mucosa, comprising a monolayer of epithelial cells conjoined by tight junction proteins, plays a bifunctional role in mediating homeostasis; the selectively permeable barrier permits the absorption of nutrients, electrolytes and water, whilst precluding invasion of harmful microorganisms into the body. [1, 2] The mucosal surfaces of the body, in addition to undergoing continuous exposure to foreign antigens, are colonized by diverse microbial species which comprise the 'microbiota.' [3, 4] The complex and dynamic interaction between the microbiota, luminal antigens and host cells remains improperly understood; in recent years we have come to understand that, in lieu of being a simple physical barrier, the intestinal epithelium acts as an important modulator of the mucosal immune response. Correspondingly, we have acquired a deeper understanding and appreciation of how small differences at the level of the microbial genome can tilt the scales from symbiosis to pathogenesis. [5] In an effort to manage the synergistic relationship between mucosal microbes and host cells, and generate effective immunity against potentially harmful pathogens whilst preserving homeostasis, higher mammals have evolved a robust mucosal immune system. [1] Gut-associated lymphoid tissues (GALT), situated in the sub-epithelial region of the mucosa, are concentrated regions of immunocompetent cells that serve as the primary inductive sites of mucosal immune responses. GALT is the primary site of Immunoglobulin A (IgA) induction, an antibody critical for the maintenance of a diversified and balanced microbiome. [6] The mucosal immune apparatus varies in different regions of the gut, adapting immune-regulatory properties to complement the function of the region. [7] The GALT of the small intestine, the primary site of absorption of nutrients, consists primarily of isolated lymphoid follicles (ILFs) and scattered domal accretions of organised lymphoid follicles harboring immuno-reactive cells termed the Peyer's Patches (PPs). [7] Though the function of the gut as an exceedingly immuno-reactive organ is well recognized, the mechanisms of gut mucosal immune responses are still not fully understood. The mechanisms by which GALT structures such as the PPs adopt oral tolerance against harmless antigens yet generate active immunity against harmful pathogens appears to be a delicate process that underpins the basis of several debilitating gut pathologies. This process is clearly crucial to maintaining homeostatic function of the gut, yet not enough is known about it.

On a cellular level, the villous epithelium is comprised primarily of enterocytes and mucus-secreting goblet cells; the mucus creates a viscous matrix which decreases microbe-epithelial interactions. In addition to mucus, antimicrobial peptides secreted by crypt-dwelling Paneth cells create an antibacterial gradient that prevents microbial species from penetrating into the sub-epithelial space. In contrast, the epithelium that covers the follicular structures of the gut contains a marked decrease in the number of mucus-producing goblet cells, a thinner glyocalyx and no Paneth cells, facilitating the direct interaction of luminal contents with the epithelium. Another distinct feature of the follicle-associated epithelium (FAE) is the presence of a specialised epithelial cell type called the M (microfold or membranous) cells. M cells are few in number, accounting for less than 5-10% of all of the cells of the FAE and are highly specialised for the transcytosis of luminal antigens into the underlying immunocompetent environment. [8, 9]

The first observations of M cells were recorded in 1973 by Bockman and Cooper, who described a unique cell type closely associated with the lymphoid follicles of the gut that were morphologically distinct from neighbouring cells. [10] The newly identified cell type had a denser cytoplasm, numerous cytoplasmic projections, prominent nucleoli and large vacuoles. [10] These morphologically distinct cells exhibited increased pinocytotic activity, as evaluated by the internalization and transcytosis of ferritin and India Ink tracers. [10] The following year, Owen and James conducted an ultrastructural study of the human intestinal lymphoid follicles derived from gastric bypass patients. They described the appearance of these specialised cells using light microscopy and, noting the membranous invaginations that characterized the apical surface of these cells, termed them ‘M’ cells. [11]

Though M cells are thought to be central to mediating mucosal immune responses within the intestine by allowing for the swift transcytosis and sampling of luminal antigens, their functional mechanisms appear to have a paradoxical effect; the same features of M cells that contribute toward bolstering mucosal immunity can also be easily exploited by invading pathogens and can contribute to the onslaught of disease. This incongruity suggests that in order for M cells to contribute beneficially to the immune response, their presence and function requires tight regulation. To fully comprehend the delicate balance required for optimal M cell function, it is imperative to address unresolved questions in M cell biology, such as their scarcity, their yet uncharacterized developmental origins and the functional characteristics that enable their unique role as sentinels in the mucosal immune system.

4.2.2 Developmental pathways of Peyer's Patch M cells

Lineage-tracing studies conducted in transgenic mice expressing a *LacZ* reporter gene under the control of the Lgr5 promoter have shown all epithelial lineage cells of the intestine, including M cells, derive from Lgr5+ stem cells located at the base of the intestinal crypts. [12] Lgr5+ stem cells commit to either the enterocyte or the secretory lineage (Paneth cells, tuft cells, Enteroendocrine cells and goblet cells) in response to well established molecular cues. [13] Briefly, the ligation of Notch 1 and 2 receptors by Notch ligands Delta-like ligand (Dll) 1 and Dll4 induces the expression of transcription factor Hes1, which in turn blocks the expression of Math1; a basic helix loop helix transcription factor required for commitment to the secretory lineage. [13, 14] It is still unclear whether M cells derive from secretory or enterocyte progenitors, although the absence of goblet cells in the FAE may provide some insight. The lack of mucus-producing goblet cells in the FAE is attributed to the high expression of Dll1 by sub-epithelial stromal cells. [14] Dll1-mediated Notch signalling restricts the differentiation of secretory cell types, thus it is known the differentiation of at least one secretory cell lineage (goblet cells) is stifled within the FAE. At first glance, this finding lends credence to the hypothesis that M cells may develop independently of the secretory lineage. However, a separate study found that mice with a conditional deletion of Notch1 in the intestinal epithelium had significantly increased numbers of M cells in the FAE. [15] As well as an increase in the number of M cells, there was also a significant increase in M cell clustering. Conversely, conditional deletion of Notch1 ligand Jagged1 resulted in a similar increase in M cell clustering but a decrease in M cell number. [15] This implicates Notch signalling as playing a critical, likely suppressive, role in the delicate regulation of M cell number and dispersion within the FAE. A similar effect was also observed in a study implicating TRAF6-mediated NfKB signalling as a critical pathway of M cell differentiation. The authors noted that the number of goblet cells increased significantly in the FAE of *Traf6*$^{\text{IEC-KO}}$ mice and, in the absence of M cell lineage commitment, M cells appeared to be replaced by goblet cells. [16] Taken together, it appears as though Notch signalling may play a crucial role in the regulation of M cells. Further, the M cell differentiation pathway likely overlaps significantly with the differentiation pathway of goblet cells. Further studies are required to confirm these observations.

More broadly, commitment to the M cell lineage, from either secretory or enterocyte progenitors, appears to be regulated by several exogenous cytokine signals, of which receptor activator of nuclear factor kappa-B ligand (RANKL) is unequivocally essential. [17,

18] In the intestine, RANKL is produced by numerous cell types. However, M cell differentiation appears to be regulated chiefly by a subset of RANKL-producing, MAdCAM-1^{-} subepithelial mesenchymal cells, often called M cell inducer (MCi) cells, concentrated just beneath the FAE. [17, 19] RANKL produced by T cells and type 3 innate lymphoid cells (ILC3s) appears to be dispensable. Though *RANKL*$^{-/-}$ mice develop visible, albeit smaller, Peyer's Patches, they are almost entirely deficient of M cells and thus their functional uptake capacity is significantly impaired. [18] Subsequent administration of RANKL restores M cell number and function. [18, 20]

RANKL can exert its effects in either a membrane-bound or soluble form. Within the FAE, it appears to function in its membrane-bound state; MCi cells interact directly with the epithelium and their location is polarized toward the FAE. [19] Mice with genetically trimmed RANKL cleavage sites, leading to a complete loss of soluble RANKL, appear to have similar numbers of M cells within the FAE as their WT counterparts. [19] Interestingly, in the intestinal organoid system, M cells are induced via the supplementation of media with soluble RANKL. This suggests that both forms can exert an effect necessary to induce differentiation, though it is still unclear whether the M cells induced in the organoid system via soluble RANKL are identical to *in vivo* M cells, which appear to be primarily regulated by mRANKL on MCi cells. In bone, membrane-bound RANKL was shown to be more effective at modulating osteoclastogenesis than soluble RANKL. [21] A separate study found that lack of sRANKL did not affect overall bone mass or structure, but did lead to a reduction in the number of bone-resorbing osteoclasts. [22] This suggests that mRANKL is more functionally significant than sRANKL, which ought to be considered when extrapolating data obtained from studies where M cells are induced using sRANKL in intestinal organoids.

The ligation of the RANK receptor by RANKL activates the NF-kB pathway which is essential for M cell differentiation. [23] Downstream of canonical NF-kB activation, a regulatory molecule of RANK-mediated NF-kB activation, tumour necrosis receptor-associated factor 6 (TRAF6), is critical for M cell differentiation. [16] The conditional deletion of *TRAF6* in the intestinal epithelium results in a complete loss of PP M cells. [16] Overexpression of NF-kB transcription factors alone is not sufficient for M cell differentiation; RANKL is required. Thus, RANKL-induced and TRAF6-mediated NF-kB signalling is a critical pathway in M cell differentiation. Downstream of this signalling cascade, Ets transcription factor *SpiB* is also essential for M cell differentiation. [24, 25]

Administration of soluble RANKL into media used to culture murine and human small intestinal organoids induces the transcriptional expression of *SpiB* within several hours. [25, 26] Mice deficient in *SpiB* have poorly developed Peyer's Patches with no detectable $Gp2^+$ M cells. [24] Thus *SpiB* is postulated to be the 'master' regulatory gene of M cell development. Despite this, reports suggest an M cell-like phenotype can develop independently of *SpiB*, discussed in a subsequent section.

Finally, mature, terminally differentiated PP M cells are characterized by the expression of cell surface marker Glycoprotein 2 (Gp2). [27] Gp2 functions downstream of *SpiB* and contributes to the receptor-mediated transcytotic function of M cells by interacting with FimH, a component of type I pili on the bacterial outer membrane. [27] Downstream of Gp2 expression, Sox8, a member of the SRY-related HMG box transcription factor family, binds directly to the promoter region of *Gp2*, enhancing its expression. [28] *Sox8* deficient mice exhibit impaired antigen-specific mucosal responses and a marked decrease in the number of mature M cells. Taken together, the current understanding of the steps involved in the differentiation of PP M cells are as follows; RANKL produced by subepithelial mesenchymal cells, alternatively termed M cell inducer (Mci) cells, activates TRAF6-mediated NfKB signaling. This induces the expression of transcription factor *SpiB*. Subsequently, *SpiB* induces the expression of cell surface marker Gp2. Sox8 enhances Gp2 expression by binding directly to the promoter region of *Gp2*. [16, 18, 19, 24, 28]

4.3 Mechanisms of transcytosis

Predating the first-recorded visual identification of M cells in the epithelium overlying the PPs by approximately 50 years, Japanese microbiologist Dr. Kenzaburo Kumagai observed certain mycobacteria can only be taken up by the FAE. [29] Initially, he thought this process was mycobacteria-specific, but later noted the cells of the FAE also preferentially took up carmine pigments and lyophilized red blood cells, indicating the mechanism of uptake was non-specific. As this discovery predated light microscopy, Kumagai did not ascribe this effect to a specific cell type. After M cells were subsequently identified and described [10, 11], the mechanisms underlying their increased transcytotic ability remained improperly understood. To date, mechanisms underpinning M cell-mediated transcytosis remain unclear; the complex process appears to be partly orchestrated and partly indiscriminate.

The induction of mucosal immune responses within the gut is facilitated by the presentation of antigens to the immune cells contained within the submucosal GALT structures. This process is largely mediated by M cells as, in addition to their enhanced transcytotic ability, they are unencumbered by large amounts of mucus and antimicrobial peptides. Despite this, M cells are not regarded as traditional 'antigen-presenting' cells (APCs) as they do not, to our knowledge, have the ability to process antigens in the way that major histocompatibility complex (MHC) molecules can. Instead they act as an efficient delivery shuttle transporting antigens to the APCs underneath the mucosa. Some reports suggest M cells express fewer acid phosphatase-containing structures than regular IECs, indicating less lysosomal activity. [30] This may suggest that transcytosis by M cells preserves the structural integrity of internalized antigens. However, other reports have identified the presence of acid phosphatase-enriched prelysosomal and lysosomal structures, as well as MHC class II determinants, within rat M cells, indicating their potential for enzymatic activity and antigen processing. [30] More studies are required to clarify this. Given the proposed divergent developmental pathways of different M cell subtypes, it is possible both are true, and vary by subtype. A comprehensive characterization of the different M cell subtypes and their internal machinery is required to elucidate this.

4.3.1 Are cell surface receptors the key to transcytosis by M cells?

Despite the limited understanding of the exact molecular mechanisms underlying M cell-mediated transcytosis, it has been established through various studies that M cells exhibit increased efficiency in transcytosing luminal antigens compared to conventional absorptive enterocytes. The extent to which this process is regulated by cell-surface receptors is still an area of ongoing investigation. Glycoprotein 2 (Gp2) is a glycosylphosphatidylinositol (GPI)-linked protein that recognizes a component of type I pili on the outer membrane of certain pathogenic and commensal bacteria, such as *Escherichia coli* and *Salmonella* Typhimurium. [31] Studies have shown that both *Escherichia coli* and *Salmonella* Typhimurium co-localise with endogenous Gp2 and that subsequent loss of Gp2 results in impaired bacterial transcytosis and a concomitant reduction of antigen-specific immune response in the PPs. [27] Receptor-mediated recognition of specific bacterial strains has been suggested based on the observation that live, but not killed or inactivated, *Vibrio cholerae* are taken up efficiently by M cells in rabbit. [32] Furthermore, uptake efficiency by M cells varies among different strains of *Escherichia coli.* [33]

Another GPI-linked protein, cellular prion protein (PrPC) is highly, though not exclusively, expressed on the apical surface of M cells. [34] Upon exposure to oral prions, PrPC can refold into an amyloidogenic conformation, scrapie prion protein (PrPSc), which is known to cause a number of debilitating neurodegenerative disorders collectively termed transmissible spongiform encephalopathies. [34] Under normal physiological conditions, the binding partners of PrPC remain ill-defined. It is known that in both macrophages and M cells, PrPC can recognize Hsp60 on *Brucella abortus*, an intracellular pathogen that causes brucellosis. [35, 36] Bacterial Hsp60 is secreted by a Type IV secretion system (T4SS) and is conserved among many different species of bacteria, suggesting PrPC could serve as an uptake receptor for numerous microbial species with this feature. Strikingly, M cells have been implicated as being central to oral prion disease pathogenesis with M cell depletion through RANKL neutralization blocking the uptake of PrPSc. [37]

Another transcytotic pathway postulated to be unique to M cells involves the redistribution of membrane proteins to serve as apical capture receptors. One example is β1-integrin, a cell surface receptor that binds to invasin protein expressed by enteropathogenic species of *Yersinia*. β1-integrin is usually expressed on the basolateral surface of enterocytes, but is apically expressed on M cells. [38] Reports suggest the primary site for invasion of enteropathogenic *Yersinia* is the FAE and translocation of *Yersinia* is mediated by interaction of invasin expressed by *Yersinia* and β1-integrin expressed on the apical surface of M cells. [38-40] These examples, among others, suggest M cell-mediated transcytosis is at least partially mediated by specific cell surface receptors.

4.3.2 To what extent do the unique morphological features of M cells contribute to transcytosis?

In addition to receptor-mediated transcytosis, non-specific uptake of luminal contents is a distinctive feature of PP M cells. M cells have been shown to be able to take up inert particles, such as latex beads, at a greater rate than surrounding enterocytes. [25] However, it is unclear which mechanism, receptor-mediated or non-specific, contributes to transcytosis more significantly. It is likely that non-specific uptake of antigens is the inadvertent consequence of the relative accessibility of M cells, by virtue of the blunted apical microvilli of M cells and lack of a protective mucus layer, but that M cell mediated transcytosis is inherently receptor-mediated. Regardless, in the context of both specific and non-specific

uptake, it appears M cells have additional screening mechanisms, or perhaps limiting physicochemical characteristics, for acquiring antigens and other particles.

Multiple physical and chemical features, including antigen/particle size, shape, and charge, have been shown to impact transcytosis, though the relative significance of each remains uncertain. One study postulates that the "naked" M cell surface, void of microvilli, has a lower electrostatic charge and resulting in reduced repulsion of luminal microbial particles, which generally also exhibit a net negative surface charge. [41] To test the contribution of surface charge in the maintenance of an electrostatic barrier, the study utilized Caco-2 cells modified to express impaired microvilli formation. Cells with disrupted formation of apical microvilli showed a statistically significant increase in bacterial adhesion. [41] Another study used M cells generated through the co-culture of Caco-2 cells with Raji cells to show the transcytosis of fluorescent nanoparticles was temperature, size and concentration dependent; transcytosis was optimal for smaller nanoparticles at 37 ^{o}C in a certain concentration range. [42] The impact of particle concentration and size in M cell-mediated transcytosis was also observed in rabbit PPs. [43] The extent to which these results translate to the human *in vivo* system is unclear, however the data may give some indication of the general factors contributing to M cell mediated transcytosis. It is important to note that while cell line-based co-culture systems have been widely utilized in the literature to study M cell-like behaviours, data suggests that these M cells have a different genetic and proteomic profile compared to Peyer's Patch M cells and the translatability of this data to the in vivo system is currently unknown. [44-46] These cells may be more indicative of an immature or 'inducible' M cell, as opposed to the traditional PP M cells.

Another pertinent feature contributing to both the specific and indiscriminate increased antigen capture by PP M cells is the reduced mucus covering of the FAE. Gastrointestinal mucus, predominantly secreted by goblet cells, creates a viscous barrier extending the length of the GI tract and protecting the mucosal surface. The dynamic structure and function of the GI mucus varies in different regions of the gut; within the small intestine the mucus comprises a single, porous layer of mucins that is easily dislodged and complements the predominantly absorptive function of this region of the GI tract. [47] In order to prevent bacterial penetration through this porous, loose mucus, antimicrobial peptides (AMPs), secreted primarily by Paneth cells, create a diffusion gradient. [48, 49] This effect is almost entirely absent in the PP region due to the significant decrease in both mucus producing goblet cells and AMP secretion. Interleukin-22 (IL-22) signalling promotes

AMP secretion; in the sub-epithelial region of the PPs, immature dendritic cells constitutively express IL-22 decoy receptor IL-22-binding-protein (IL-22BP), effectively inhibiting IL-22 mediated AMP secretion. [50] Collectively, these features contribute to the specialised function of the region; they facilitate efficient antigen sampling and the induction of effective local immune responses by attenuating the protective mechanisms of the gut.

The precise underlying mechanisms regulating antigen uptake by M cells have remained elusive, mainly because the low frequency of M cells and the lack of cell surface markers make it difficult to purify M cells in sufficient quantities required for molecular and biochemical analyses. A better understanding of the exact mechanisms of transcytosis could provide more insight into the potential of M cell targeting for improving oral vaccine development. Additionally, it is plausible that different subtypes of M cells, if the presence of multiple lineages is confirmed, may have distinct mechanisms of transcytosis. This seems probable, as only true Peyer's Patch M cells have been shown to express Gp2.

Whether receptor-specific capture or non-discriminant uptake contributes more to M cell-mediated transcytosis is unclear. This requires further investigation, perhaps in the form of large scale proteomics studies to identify high affinity targets, especially as preliminary animal studies have postulated targeting vaccines to M cells via cell surface receptors may have positive implications for bioavailability of oral vaccines. [51]

4.4 M cell subtypes

Sequencing studies have identified subsets of genes that are upregulated specifically in the FAE. Among them, *SpiB* and *Gp2* have emerged as the transcription factor responsible for the regulation of M cell differentiation and the terminal differentiation marker of mature M cells, respectively. [24, 31] Alongside these two critical genes indicative of mature, terminally differentiated M cells, several other genes are upregulated in the FAE at various stages of M cell development. Independent data sets have implicated genes such *Anxa5* and *Marcskl1*, encoding for annexin A5 and MARCKS-like protein 1 respectively, as being expressed by differentiating, or ‘immature’ M cells. [24, 52, 53]

In the literature to date, the term ‘M cells’ has referred to highly transcytotic, Gp2+ cells constitutively expressed within the FAE of mucosal tissues. [24, 31] However, the notion of a single M cell developmental pathway is challenged by the existance of ‘inducible’ or

'villous' M cells that appear to function independently of *SpiB* and the PP microenvironment. In recent years, the theory that 'inducible' M cells are a yet unrecognized, distinct lineage of the traditional M cell has persisted. [45]

Multiple studies have observed that certain stimuli, such as exposure to *Salmonella* Typhimirium and cholera toxin, can trigger the development of an M cell-like phenotype within the villous epithelium. [54, 55] These inducible "villous" M cells exhibit morphological and functional similarities to Peyer's Patch M cells, but have different proteomic and transcriptional profiles. 'Villous' M cells retain expression of some M cell marker genes generally attributed to 'immature' M cells, such as *Fut1, Marcskl1* and *Pglyrp1,* but lack expression of others, such as of *Gp2* and *SpiB.* [52] Though this transient population of 'inducible' M cells appears to be less functional compared to constitutively expressed M cells, the extent of convergence between the developmental pathways and functional capacities of the two M cell subtypes remains unclear. [56]

A similar phenomenon can be observed in other mucosal areas of the body. For example, in the colon, inflammation caused by *Citrobacter rodentium* triggers the development of 'villous' M cells. [57] Unlike their constitutively expressed counterparts, inducible M cells appear to develop primarily in response to pathogenic stimuli and may be a form of inducible epithelial immunity; a protective reaction during which normal epithelial cells transiently adopt a partial M cell-like phenotype to allow for more efficient sampling of luminal antigens.

Numerous questions regarding the phenomenon of villous M cells remain unresolved, with conflicting reports claiming villous M cells are indeed constitutively expressed [58] and claims that increased transcytotic uptake in response to pathologic stimuli is due to increased activity of M cells that are already present, and not as a result of *de novo* M cell formation. [59] The complex *in vivo* dynamics of this process are yet to be fully elucidated. If a subpopulation of M cells can be 'induced' but their developmental origins and genetic profile differs significantly from their constitutively expressed counterparts, can they be deemed M cells at all? It is evident that the unique microenvironment of the Peyer's Patches influences the functional phenotype of all cells within the FAE, and not just M cells. The extent to which this functional adaptation to environmental cues can constitute a separate cell type altogether requires further investigation. Given the implication of M cells in the pathogenesis of several debilitating gut pathologies, understanding how regular enterocytes respond to

stress and how inducible M cells arise may be central to understanding the mechanisms of mucosal immunity. [37, 60]

4.4.1 Distinct M cell lineage or inevitable consequence of bacterial invasion?

The current theory that Peyer's Patch M cells represent a single lineage within a larger family of related phenotypes suggests that our understanding of intestinal mucosal immunity is not yet complete. Whether villous M cells are indeed a distinct M cell lineage or whether they represent a reaction to a pathogenic challenge remains unclear. Further investigation into the mechanisms of bacterial invasion in both M cells and regular enterocytes may offer important insights into this matter.

Bacterial invasion of M cells appears to be mediated partially by M cell surface marker Gp2. Gp2 interacts directly with FimH, a component of type I pili on the outer membrane of bacteria such as *Salmonella* and *Escherichia coli*. [27] M cells take up FimH-expressing bacteria at a significantly greater rate than *FimH*-deficient mutants. Furthermore, FimH+ bacteria consistently colocalise with endogenous Gp2. The impaired transcytosis of *FimH*-deficient bacteria by M cells is complemented by a reduced antigen-specific helper T cell response in the Peyer's Patches. [27]

Despite the well-documented role of M cells in bacterial translocation, opportunistic pathogens, such as *Salmonella,* utilize a multitude of strategies to invade host cells. Further away from the FAE, bacterial pathogens can efficiently invade regular villous enterocytes by interacting directly with the brush border protein villin, triggering rapid cytoskeletal remodeling at the apical surface of the cell. [61] The resulting morphology of the infected cell features a disrupted apical brush border, reminiscent of the M cell, and is more amenable to invasion.

Bacterial invasion triggers the rapid and transient rearrangement of the actin cytoskeleton of enterocytes, resulting in a phenotype that is reminiscent of the M cell. At the site of bacterial entry, the invasion of pathogens such as *Salmonella* triggers a rapid, transient rearrangement of actin filaments, mediated primarily by actin-modifying filament villin present in the brush border. [61] In its role as an actin-modifying protein, villin is able to sever, nucleate or bundle actin filaments. This severing ability aids in the disruption of the organised brush border, enabling more efficient interaction of bacteria and membrane. Actin-rich protrusions,

termed ‘ruffles’, form on the apical surface of the cell. [62-64] Interestingly, villin knockout mice display a normal brush border under homeostatic conditions. However, DSS treatment causes significant disruption of the brush border in WT mice, but not in their villin-deficient counterparts. [65] This finding suggests that villin is crucial for cellular reorganization in response to non-physiological signals.

It is difficult to ascertain, without further investigation, whether villous M cells are indeed a distinct lineage or an adaptive cellular mechanism triggered by bacterial invasion. Given recent reports proposing the existence of various, distinct lineages of M cells, it is important to consider all the physiological reasons why epithelial cells may adopt a different phenotype in response to stimuli.

Reports suggest that ‘inducible’ M cells are functionally more transcytotic than regular enterocytes. Membrane ruffling involves the structural rearrangement of membranous actin filaments that contribute to cell motility, invasiveness and endocytosis. [61] This process not only exposes the membrane, promoting engagement with bacteria, but may also facilitate actin-mediated transcytosis spatially. Cytoskeletal actin rearrangement controls all forms of phagocytosis and contributes significantly to a more motile and invasive cell phenotype. [66, 67] This multifunctional process is largely controlled by a family of small G signalling molecules called Rho GTPases. The three most studied members of the Rho GTPase family, Rho, Rac and Cdc42, are known to be responsible for the polymerization of specific actin structures. The highly homologous Rac subfamily, consisting of Rac1, Rac2 and Rac3, is involved in the regulation of the actin cytoskeleton, involving ruffling. In 2012, the Clevers group reported M cells could be induced in mouse intestinal organoids through stimulation with soluble RANKL. [25] Microarray data of RANKL-stimulated organoids revealed an upregulation of 164 genes. Interestingly, the ninth highest expressed gene, with an approximate five-fold upregulation in both the RANKL-treated organoids and in *in vivo* M cells, was *Rac2*. The elevated expression of Rac2 in M cells was also reported by other sources. [68] It is highly likely that *Rac2*, which upregulates at similar levels as *SpiB* and *Gp2*, is involved in the cytoskeletal rearrangement of actin filaments in a manner that facilitates bacterial invasion. Dendritic cells defective in Rac-activator Dedicator of cytokinesis 2 (DOCK2) display an impaired ability to endocytose soluble antigens and phagocytose insoluble antigens, suggesting DOCK2 may be essential for engulfment. [69]

Taken together, it is evident that the entirety of mechanisms that regulate transcytosis by enterocytes and M cells is still not completely understood. Nonetheless, transcytosis facilitated by M cells appears to be largely driven by receptor interactions. The ability of regular epithelial cells to acquire a transiently different phenotype does not necessarily indicate the emergence of a new cell type. The similarities in the morphology and function of true M cells and enterocytes that display M cell-like properties may suggest that the epithelium can undergo transient changes that mimic the role of immune sentinels, the M cells, when faced with pathogenic challenges.

Roadmap For Future Work		
Areas of Investigation		**Scope of Work**
1	**Differentiation Pathways**	Investigate the molecular cues and pathways leading to commitment to the M cell lineage. Conduct experiments to identify key regulators.
2	**Transcytosis Mechanisms**	Explore the receptor-mediated and indiscriminate aspects of transcytosis. Examine the role of specific capture receptors and repurposed proteins.
3	**Villous M Cells**	Study the inducible M cells in more detail. Investigate their development, functions, and how they respond to pathogenic challenges.
4	**Mucosal Challenges**	Assess the roles of true M cells and inducible M cells when the mucosa is directly challenged, particularly in the context of immune responses to pathogens.

4.5 Conclusion

Intestinal M cells, a specialised epithelial cell type contained within the follicle-associated epithelium, play a crucial role in the induction of mucosal immune responses. Though several key signalling pathways have been implicated in M cell differentiation, early molecular cues leading to commitment to the M cell lineage remain undefined. M cells are strategically located directly overlying organised lymphoid follicles of the gut, indicating a key role in mediating mucosal immune responses. Numerous studies have demonstrated that M cells are not capable of antigen processing; rather they serve as an efficient shuttle presenting antigens to APCs located in the lymphoid tissues subepithelially. Transcytosis by M cells appears to be a partly receptor mediated and partly indiscriminate process. The unique morphological features of M cells facilitate transcytosis. Additionally, specific capture receptors and repurposed proteins also contribute to M cell-mediated transcytosis.

Challenging the notion of a single M cell developmental pathway is the presence of an inducible M cell population termed the ‘villous’ M cells. These M cells can be induced by a pathogenic challenge, they appear to develop independently of *SpiB* and lack the expression of M cell-specific capture receptors. Despite this, they exhibit the characteristic M cell morphology and are capable of increased transcytosis. Despite their divergent developmental pathways, they retain a similar functional profile to true M cells. The role of both true M cells and inducible M cells when the mucosa is directly challenged remains unclear.

Contributions

Ana Klisuric and Hans Clevers conceived the ideas presented in this chapter.

Conflict of Interest

The author declares no conflict of interest.

Funding

The work was funded by the Endeavour Leadership Program of Australia, a University of South Australia Student Mobility Grant, the ONCODE Institute and ARC Linkage Grant (LP150100032).

4.6 References

1. McGhee, J.R. and K. Fujihashi, *Inside the mucosal immune system.* PLoS Biol, 2012. **10**(9): p. e1001397.
2. Groschwitz, K.R. and S.P. Hogan, *Intestinal barrier function: molecular regulation and disease pathogenesis.* J Allergy Clin Immunol, 2009. **124**(1): p. 3-20; quiz 21-2.
3. Gilbert, J.A., et al., *Current understanding of the human microbiome.* Nat Med, 2018. **24**(4): p. 392-400.
4. Cani, P.D., *Human gut microbiome: hopes, threats and promises.* Gut, 2018. **67**(9): p. 1716-1725.
5. Zeevi, D., et al., *Structural variation in the gut microbiome associates with host health.* Nature, 2019. **568**(7750): p. 43-48.
6. Holmgren, J. and C. Czerkinsky, *Mucosal immunity and vaccines.* Nat Med, 2005. **11**(4 Suppl): p. S45-53.
7. Mowat, A.M. and W.W. Agace, *Regional specialization within the intestinal immune system.* Nat Rev Immunol, 2014. **14**(10): p. 667-85.
8. Kobayashi, A., et al., *The functional maturation of M cells is dramatically reduced in the Peyer's patches of aged mice.* Mucosal Immunol, 2013. **6**(5): p. 1027-37.
9. Kraehenbuhl, J.P. and M.R. Neutra, *Epithelial M cells: differentiation and function.* Annu Rev Cell Dev Biol, 2000. **16**: p. 301-32.
10. Bockman, D.E. and M.D. Cooper, *Pinocytosis by epithelium associated with lymphoid follicles in the bursa of Fabricius, appendix, and Peyer's patches. An electron microscopic study.* Am J Anat, 1973. **136**(4): p. 455-77.
11. Owen, R.L. and A.L. Jones, *Epithelial cell specialization within human Peyer's patches: an ultrastructural study of intestinal lymphoid follicles.* Gastroenterology, 1974. **66**(2): p. 189-203.
12. Barker, N., et al., *Identification of stem cells in small intestine and colon by marker gene Lgr5.* Nature, 2007. **449**(7165): p. 1003-7.
13. Yang, Q., et al., *Requirement of Math1 for secretory cell lineage commitment in the mouse intestine.* Science, 2001. **294**(5549): p. 2155-8.
14. Obata, Y., et al., *Epithelial-stromal interaction via Notch signaling is essential for the full maturation of gut-associated lymphoid tissues.* EMBO Rep, 2014. **15**(12): p. 1297-304.
15. Hsieh, E.H. and D.D. Lo, *Jagged1 and Notch1 help edit M cell patterning in Peyer's patch follicle epithelium.* Dev Comp Immunol, 2012. **37**(2): p. 306-12.
16. Kanaya, T., et al., *Development of intestinal M cells and follicle-associated epithelium is regulated by TRAF6-mediated NF-kappaB signaling.* J Exp Med, 2018. **215**(2): p. 501-519.

17. Taylor, R.T., et al., *Lymphotoxin-independent expression of TNF-related activation-induced cytokine by stromal cells in cryptopatches, isolated lymphoid follicles, and Peyer's patches.* J Immunol, 2007. **178**(9): p. 5659-67.
18. Knoop, K.A., et al., *RANKL is necessary and sufficient to initiate development of antigen-sampling M cells in the intestinal epithelium.* J Immunol, 2009. **183**(9): p. 5738-47.
19. Nagashima, K., et al., *Targeted deletion of RANKL in M cell inducer cells by the Col6a1-Cre driver.* Biochem Biophys Res Commun, 2017. **493**(1): p. 437-443.
20. Donaldson, D.S., et al., *Increased Abundance of M Cells in the Gut Epithelium Dramatically Enhances Oral Prion Disease Susceptibility.* PLoS Pathog, 2016. **12**(12): p. e1006075.
21. Nakashima, T., et al., *Protein expression and functional difference of membrane-bound and soluble receptor activator of NF-kappaB ligand: modulation of the expression by osteotropic factors and cytokines.* Biochem Biophys Res Commun, 2000. **275**(3): p. 768-75.
22. Xiong, J., et al., *Soluble RANKL contributes to osteoclast formation in adult mice but not ovariectomy-induced bone loss.* Nat Commun, 2018. **9**(1): p. 2909.
23. Kimura, S., et al., *Visualization of the entire differentiation process of murine M cells: suppression of their maturation in cecal patches.* Mucosal Immunol, 2015. **8**(3): p. 650-60.
24. Kanaya, T., et al., *The Ets transcription factor Spi-B is essential for the differentiation of intestinal microfold cells.* Nat Immunol, 2012. **13**(8): p. 729-36.
25. de Lau, W., et al., *Peyer's patch M cells derived from Lgr5(+) stem cells require SpiB and are induced by RankL in cultured "miniguts".* Mol Cell Biol, 2012. **32**(18): p. 3639-47.
26. Rouch, J.D., et al., *Development of Functional Microfold (M) Cells from Intestinal Stem Cells in Primary Human Enteroids.* PLoS One, 2016. **11**(1): p. e0148216.
27. Hase, K., et al., *Uptake through glycoprotein 2 of FimH(+) bacteria by M cells initiates mucosal immune response.* Nature, 2009. **462**(7270): p. 226-30.
28. Kimura, S., et al., *Sox8 is essential for M cell maturation to accelerate IgA response at the early stage after weaning in mice.* J Exp Med, 2019.
29. Kumagai, K., *Über den Resorptionsvergang der corpusculären Bestandteile im Darm.* Kekkaku-Zassi, 1922. **4**: p. 429-431.
30. Allan, C.H., D.L. Mendrick, and J.S. Trier, *Rat intestinal M cells contain acidic endosomal-lysosomal compartments and express class II major histocompatibility complex determinants.* Gastroenterology, 1993. **104**(3): p. 698-708.
31. Ohno, H. and K. Hase, *Glycoprotein 2 (GP2): grabbing the FimH bacteria into M cells for mucosal immunity.* Gut Microbes, 2010. **1**(6): p. 407-10.
32. Owen, R.L., et al., *M cell transport of Vibrio cholerae from the intestinal lumen into Peyer's patches: a mechanism for antigen sampling and for microbial transepithelial migration.* J Infect Dis, 1986. **153**(6): p. 1108-18.

33. Von Moll, L.K. and J.R. Cantey, *Peyer's patch adherence of enteropathogenic Escherichia coli strains in rabbits.* Infect Immun, 1997. **65**(9): p. 3788-93.
34. Wille, H. and J.R. Requena, *The Structure of PrP(Sc) Prions.* Pathogens, 2018. **7**(1).
35. Watarai, M., et al., *Cellular prion protein promotes Brucella infection into macrophages.* J Exp Med, 2003. **198**(1): p. 5-17.
36. Nakato, G., et al., *Cutting Edge: Brucella abortus exploits a cellular prion protein on intestinal M cells as an invasive receptor.* J Immunol, 2012. **189**(4): p. 1540-4.
37. Donaldson, D.S., et al., *M cell-depletion blocks oral prion disease pathogenesis.* Mucosal Immunol, 2012. **5**(2): p. 216-25.
38. Clark, M.A., B.H. Hirst, and M.A. Jepson, *M-cell surface beta1 integrin expression and invasin-mediated targeting of Yersinia pseudotuberculosis to mouse Peyer's patch M cells.* Infect Immun, 1998. **66**(3): p. 1237-43.
39. Marra, A. and R.R. Isberg, *Invasin-dependent and invasin-independent pathways for translocation of Yersinia pseudotuberculosis across the Peyer's patch intestinal epithelium.* Infect Immun, 1997. **65**(8): p. 3412-21.
40. Grutzkau, A., et al., *Involvement of M cells in the bacterial invasion of Peyer's patches: a common mechanism shared by Yersinia enterocolitica and other enteroinvasive bacteria.* Gut, 1990. **31**(9): p. 1011-5.
41. Bennett, K.M., S.L. Walker, and D.D. Lo, *Epithelial microvilli establish an electrostatic barrier to microbial adhesion.* Infect Immun, 2014. **82**(7): p. 2860-71.
42. des Rieux, A., et al., *Transport of nanoparticles across an in vitro model of the human intestinal follicle associated epithelium.* Eur J Pharm Sci, 2005. **25**(4-5): p. 455-65.
43. Frey, A., et al., *Role of the glycocalyx in regulating access of microparticles to apical plasma membranes of intestinal epithelial cells: implications for microbial attachment and oral vaccine targeting.* J Exp Med, 1996. **184**(3): p. 1045-59.
44. Mabbott, N.A., et al., *Microfold (M) cells: important immunosurveillance posts in the intestinal epithelium.* Mucosal Immunol, 2013. **6**(4): p. 666-77.
45. Lo, D.D., *Vigilance or Subversion? Constitutive and Inducible M Cells in Mucosal Tissues.* Trends Immunol, 2018. **39**(3): p. 185-195.
46. Klisuric, A., et al., *Highlight Article: Identifying human and murine M cells in vitro.* Exp Biol Med (Maywood), 2019. **244**(7): p. 554-564.
47. Johansson, M.E. and G.C. Hansson, *Immunological aspects of intestinal mucus and mucins.* Nat Rev Immunol, 2016. **16**(10): p. 639-49.
48. van Es, J.H. and H. Clevers, *Paneth cells.* Curr Biol, 2014. **24**(12): p. R547-R548.
49. Clevers, H.C. and C.L. Bevins, *Paneth cells: maestros of the small intestinal crypts.* Annu Rev Physiol, 2013. **75**: p. 289-311.
50. Jinnohara, T., et al., *IL-22BP dictates characteristics of Peyer's patch follicle-associated epithelium for antigen uptake.* J Exp Med, 2017. **214**(6): p. 1607-1618.

51. Kim, S.H. and Y.S. Jang, *Antigen targeting to M cells for enhancing the efficacy of mucosal vaccines.* Exp Mol Med, 2014. **46**: p. e85.
52. Sato, S., et al., *Transcription factor Spi-B-dependent and -independent pathways for the development of Peyer's patch M cells.* Mucosal Immunol, 2013. **6**(4): p. 838-46.
53. Verbrugghe, P., et al., *Murine M cells express annexin V specifically.* J Pathol, 2006. **209**(2): p. 240-9.
54. Etienne-Mesmin, L., et al., *Interactions with M Cells and Macrophages as Key Steps in the Pathogenesis of Enterohemorragic Escherichia coli Infections.* Plos One, 2011. **6**(8).
55. Verbrugghe, P., et al., *Clusterin in human gut-associated lymphoid tissue, tonsils, and adenoids: localization to M cells and follicular dendritic cells.* Histochem Cell Biol, 2008. **129**(3): p. 311-20.
56. Wang, J., et al., *Convergent and divergent development among M cell lineages in mouse mucosal epithelium.* J Immunol, 2011. **187**(10): p. 5277-85.
57. Bennett, K.M., et al., *Induction of Colonic M Cells during Intestinal Inflammation.* Am J Pathol, 2016. **186**(5): p. 1166-79.
58. Jang, M.H., et al., *Intestinal villous M cells: an antigen entry site in the mucosal epithelium.* Proc Natl Acad Sci U S A, 2004. **101**(16): p. 6110-5.
59. Gebert, A., et al., *Antigen transport into Peyer's patches: increased uptake by constant numbers of M cells.* Am J Pathol, 2004. **164**(1): p. 65-72.
60. Gullberg, E. and J.D. Soderholm, *Peyer's patches and M cells as potential sites of the inflammatory onset in Crohn's disease.* Ann N Y Acad Sci, 2006. **1072**: p. 218-32.
61. Lhocine, N., et al., *Apical invasion of intestinal epithelial cells by Salmonella typhimurium requires villin to remodel the brush border actin cytoskeleton.* Cell Host Microbe, 2015. **17**(2): p. 164-77.
62. Jones, B.D., N. Ghori, and S. Falkow, *Salmonella typhimurium initiates murine infection by penetrating and destroying the specialized epithelial M cells of the Peyer's patches.* J Exp Med, 1994. **180**(1): p. 15-23.
63. Clark, M.A., et al., *Preferential interaction of Salmonella typhimurium with mouse Peyer's patch M cells.* Res Microbiol, 1994. **145**(7): p. 543-52.
64. Borghesi, C., et al., *Modifications of the follicle-associated epithelium by short-term exposure to a non-intestinal bacterium.* J Pathol, 1996. **180**(3): p. 326-32.
65. Ferrary, E., et al., *In vivo, villin is required for Ca(2+)-dependent F-actin disruption in intestinal brush borders.* J Cell Biol, 1999. **146**(4): p. 819-30.
66. Patel, J.C. and J.E. Galan, *Investigating the function of Rho family GTPases during Salmonella/host cell interactions.* Methods Enzymol, 2008. **439**: p. 145-58.
67. Stradal, T.E., et al., *Regulation of actin dynamics by WASP and WAVE family proteins.* Trends Cell Biol, 2004. **14**(6): p. 303-11.

68. Terahara, K., et al., *Comprehensive gene expression profiling of Peyer's patch M cells, villous M-like cells, and intestinal epithelial cells.* J Immunol, 2008. **180**(12): p. 7840-6.

69. Ippagunta, S.K., et al., *The inflammasome adaptor ASC regulates the function of adaptive immune cells by controlling Dock2-mediated Rac activation and actin polymerization.* Nat Immunol, 2011. **12**(10): p. 1010-6.

Chapter 5 Osteoprotegerin negatively regulates M cell differentiation

The following research chapter utilizes the advanced *in vitro* model of the follicle-associated epithelium developed in **Chapter 3** to investigate the M cell differentiation pathway, implicating a novel molecule, osteoprotegerin, as a key negative regulator of M cell differentiation, thus addressing Aims 2 and 3.

5.1 Abstract

M cells, a population of antigen-sampling epithelial cells highly specialised for transcytosis, are strategically localised within the epithelium overlying intestinal lymphoid follicles. M cells continuously sample luminal antigens, presenting them to immune cells in the subepithelial dome, thereby facilitating the induction of mucosal immune responses. Despite their critical role, M cells constitute only a minor fraction of the cells of the follicle-associated epithelium, which has hindered efforts to achieve a comprehensive understanding of their differentiation pathway and functional mechanisms. Within the intestine, the differentiation of M cells is regulated by RANK/RANKL-mediated NF-kB signalling. It is well established that the RANKL/OPG ratio within an organ system can modulate NF-kB signalling. Osteoprotegerin (OPG) acts as a soluble decoy receptor that shows high binding affinity for RANKL. The antagonistic endogenous receptor thereby attenuates the biological effects of RANK/RANKL-activated NF-kB signalling. Given the established role of RANK/RANKL-mediated NF-kB signalling in M cell differentiation, we sought to investigate whether OPG is involved in the M cell differentiation pathway. In this study, we utilized small intestinal organoids to explore the potential role of OPG in M cell differentiation. Utilising wild-type and OPG-null organoids, we induced M cell differentiation with soluble RANKL, determining that in the absence of OPG, M cell differentiation is significantly enhanced.

5.2 Introduction

The gastrointestinal mucosa undergoes continuous exposure to ingested antigens and commensal microbes. Interspersed along the length of the gastrointestinal tract are domal accretions of organised lymphoid follicles termed the Peyer's Patches (PPs). [1] PPs constitute the first line of defense against mucosal antigens. The epithelium overlying the PPs differs from the regular villous epithelium in that it has a reduced mucus layer and the presence of a specialised cell type termed the M cell. [2-4] M cells represent a subpopulation of rare epithelial cells specialised for antigen sampling at the interface of gut-associated lymphoid tissues and the external environment. [5, 6] The unique transcytotic ability of M cells allows for the swift and efficient capture of luminal antigens and subsequent presentation to the various populations of immune cells residing beneath the follicle-associated epithelium. M cell-mediated transcytosis appears to be mediated partly by apically-expressed capture receptors and partly by the unique cellular morphology that facilitates uptake. Transcytosis of luminal antigens by M cells is considered a key step in the induction of an effective mucosal immune response with mice deficient in M cells exhibiting profound delays in mucosal immune maturity. [3, 7, 8] Owing to their increased transcytotic ability, M cells can be exploited by numerous pathogens as an entry portal to systemic circulation. [9-13] Numerous studies report that M cells increase in abundance in response to pathogenic challenge. [10, 12, 14, 15] This may contribute to ongoing inflammation. As such, it is evident that regulation of M cell number and dispersion is critical for maintaining homeostasis.

Lineage tracing experiments have revealed that M cells derive from Lgr5+ stem cells. [16] Cytokines released by sub-epithelial stromal cells direct cellular differentiation along the M cell lineage. Most notably, subepithelial stromal cells secrete tumour necrosis factor (TNF) superfamily member receptor activator of the nuclear factor kappa-B ligand (RANKL) which binds to the RANK receptor expressed by epithelial cells; RANK/RANKL interaction is a critical step in the differentiation of M cells. [17] Mice with antibody-mediated neutralization of RANKL exhibit less than 2% of wildtype levels of PP M cells. [18] Upstream of RANK/RANKL signaling, the activation of the TNF receptor associated factor (TRAF) 6-mediated NF-kB signalling leads to the induction of Ets transcription factor *SpiB,* the gene postulated to act as a 'master' regulator of M cell differentiation. [19] The activation of NF-kB signalling by TRAF-6-mediated RANK/RANKL interaction results in mature M cells

characterized by a unique morphology, enhanced trancytotic ability and the expression of cell surface capture receptors such as Gp2. [18-20]

Osteoprotegerin (OPG) is a critical component of the RANK/RANKL/OPG signalling pathway, acting as a soluble decoy receptor preventing the biological effects of RANKL. [21] Encoded by the *TNFRSF11B* gene, the functional OPG protein is comprised of 380 amino acids and plays a vital role in numerous physiological functions. [22] Under homeostatic conditions, the ratio of RANKL to OPG regulates numerous processes in different organ systems (organogenesis, lactation and proliferation, among others), however its function is best characterized in bone. [23] Homeostatic bone remodeling requires the ligation of the RANK receptor on osteoclast precursors by RANKL, expressed by osteoblasts, leading to the TRAF6-mediated activation of the NF-kB pathway and, ultimately, the transcription of osteoclastogenic genes. [24] OPG, secreted by osteoblasts, binds to RANKL, preventing the RANK/RANKL interaction and limiting osteoclastogenesis. Thus OPG plays a crucial role in regulating RANK/RANKL interactions by functioning as a decoy receptor for RANKL, effectively reducing its ability to activate the RANK/NF-kB signalling pathway.

RANKL is the highest affinity binding partner for OPG known to date, although multiple other binding partners for OPG have been identified. [25, 26] These include TRAIL [27], syndecan-1 [28], glycosaminoglycans (GAGs) [29, 30], von Willebrand Factor [31] and Factor VIII-von Willebrand Factor complex. [32] OPG expression is influenced both positively (TGF-B, IL-1, TNF, estrogen) and negatively (prostaglandin E2, PTH) by numerous factors, with dysregulation having marked effects on a range of biological functions. [33-38]

The following study utilized organoids cultured from ISCs harvested from WT or *TNFRSF11B*$^{-/-}$ mice to investigate the regulatory role of the RANK/RANKL/OPG axis in M cell number and function. We demonstrate, using organoids harvested from said genotypes, that *TNFRSF11B* plays an inhibitory role in M cell differentiation.

5.3 Materials and Methods

Organoid Culture

Organoids were derived from excised small intestinal segments of WT and *TNFRSF11B* $^{-/-}$ mice, as described previously. [39] Briefly, crypts were isolated by digestion in a chelation buffer for 30 minutes at 4°C. Organoids were plated in Basal Membrane Extract (RGF Type 2, Amsbio) and cultured in 'ENR' medium comprised of Dulbecco's Modified Eagle's medium/F12 supplemented with penicillin/streptomycin, 10 mM HEPES, Glutamax, B27 (Life Technologies, Carlsbad, CA), 1 mM N-acetylcysteine (Sigma), 50 ng/ml murine recombinant epidermal growth factor (Peprotech, Hamburg, Germany), R-spondin1 (conditioned medium, 5% of final volume) and Noggin (conditioned medium, 5% of final volume). Organoids were cultured for 5-7 days after passaging. To induce the differentiation of M cells in organoids, ENR medium was supplemented with 200ng/ml of murine sRANK ligand (315-11-50UG, Peprotech, Hamburg, Germany).

Immunostaining

Immunostaining of organoids was performed as described previously. [40] Briefly, whole organoids were collected by dissolving the BME with cold PBS and fixed overnight in 4% paraformaldehyde at 4°C. Then, organoids were washed in ice-cold PBS and blocked for 1h at RT in PBS with 2% normal donkey serum (Jackson ImmunoResearch). After blocking, organoids were washed again and then permeabilized using PBS contaning 1% Triton X-100 (Sigma) for 30 minutes at RT. Then, organoids were resuspended in blocking buffer containing primary antibodies overnight at 4°C. Primary antibody used to detect Gp2 was mouse anti rat Gp2 (D278-3, MBL). The primary antibody was combined with Phalloidin-488 (A12379, Life Technologies) and UEA-1. The next day, organoids were again washed twice and subsequently incubated with the corresponding secondary antibodies in blocking buffer containing DAPI (1:1000; Invitrogen). Secondary antibodies used were donkey anti rat Alexa Flour 488 (LN0803245, LabNed) to visualize Gp2 and donkey anti goat streptavidin Alexa Flour 568 (INSERT) to visualize UEA-1. Sections were embedded in Vectashield (Vector Labs) and imaged using Sp8 confocal microscope (Leica). Image analysis was performed using ImageJ/Fiji software.

Reverse Transcriptase (RT) quantitative PCR

RNA was isolated using the RNAeasy Mini Kit (Qiagen) according to the manufacturer's instructions. RNA (1 μg) was subjected to reverse transcription using Oligo dT primer and Superscript IV reverse transcriptase (18090050, Thermo Fisher Scientific), as per the manufacturer's instructions. cDNA was used for the RT-qPCR, performed with SYBR Green PCR Master Mix (A25742, Thermo Fisher Scientific). Gene analysis was conducted using a Bio-Rad RT-qPCR machine as previously described, with reactions performed in triplicate. Primers used in this study are listed in *Table 1*. Levels of mRNA expression were normalized to the expression of a reference gene, as calculated using the $2^{-}\Delta\Delta CT$ method.

Statistical Analysis

The GraphPad Prism 5 software (La Jolla, CA, USA, http://graphpad.com) was used for statistical analysis of data. Student *t*-tests or one-way ANOVAs were used throughout the study, where indicated, to evaluate statistical significance. Statistical significance is represented as * $p<0.05$.

5.4 Results

OPG negatively regulates M cell differentiation

As RANKL is a high affinity binding partner for OPG, we compared expression of M cell specific genes between WT organoids and *TNFRSF11B* $^{-/-}$ organoids cultured in control and RANKL-supplemented media. Morphologically, WT and *TNFRSF11B* $^{-/-}$ organoids retained a similar morphology during culture, with well-formed crypts and villi **(Figure 1, A).** Next, we examined the RNA expression of commonly known M cell specific genes among four groups; **(1)** WT mouse small intestinal (MsSI) organoids, **(2)** WT MsSI organoids treated with 200ng/ml of RANKL for 7 days, **(3)** *TNFRSF11B* $^{-/-}$ MsSI organoids and **(4)** *TNFRSF11B* $^{-/-}$ MsSI organoids treated with 200ng/ml of RANKL for 7 days **(Figure 1, B).** An ANOVA test with Tukey's multiple comparisons revealed a statistically significant increase in the level of *Gp2* and *SpiB* mRNA transcripts between control and RANKL-treated *TNFRSF11B* $^{-/-}$ organoids. The expression of *Gp2*, a mature M cell marker, increased significantly between control and RANKL-treated *TNFRSF11B* $^{-/-}$ organoids; the average mean across samples rose from 0.000009516 to 3.636, respectively (p=0.0171). *Gp2* was also elevated in the RANKL-treated WT organoids compared to the untreated WT control (p=0.7660), albeit in a non-statistically significant manner. *Gp2* transcripts were correspondingly significantly elevated between RANKL-treated WT organoids and RANKL-treated *TNFRSF11B*$^{-/-}$ organoids (p=0.0222). Next, the expression of *SpiB,* the master regulator gene of M cell differentiation, rose significantly in RANKL-treated WT organoids compared to untreated control organoids (p=0.0376) and in RANKL-treated *TNFRSF11B* $^{-/-}$ organoids compared to the untreated *TNFRSF11B* $^{-/-}$ control organoids (p=0.0130). The difference in expression was not significantly different between the control groups (Group 1 and Group 3) nor between the RANKL-treated groups of both genotypes (Group 2 and Group 4). These results suggest that OPG, a high affinity RANKL ligand, negatively influences M cell differentiation and that ablation of the *TNFRSF11B* gene encoding for OPG leads to an increase in the expression of M cell specific genes.

Figure 1

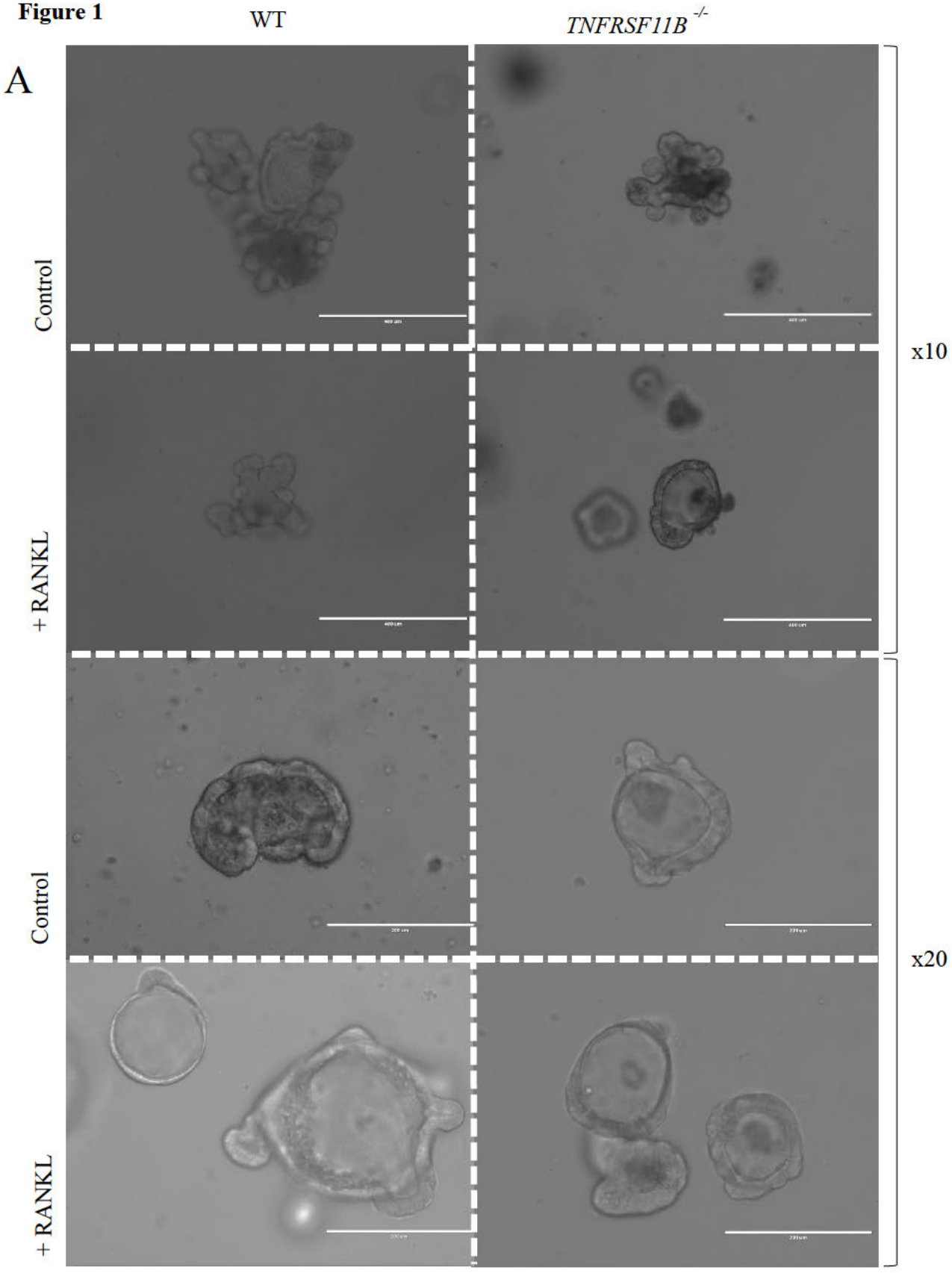

B

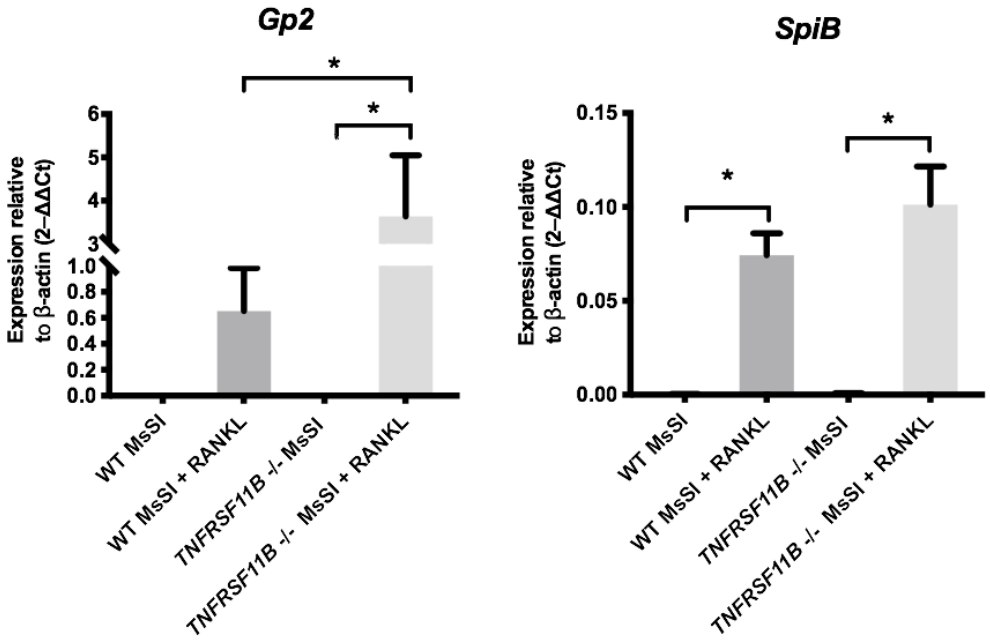
Gp2
Expression relative to β-actin (2−ΔΔCt)
6
5
4
3
1.0
0.8
0.6
0.4
0.2
0.0
*
*
WT MsSI
WT MsSI + RANKL
TNFRSF11B -/- MsSI
TNFRSF11B -/- MsSI + RANKL
SpiB
Expression relative to β-actin (2−ΔΔCt)
0.15
0.10
0.05
0.00
*
*
WT MsSI
WT MsSI + RANKL
TNFRSF11B -/- MsSI
TNFRSF11B -/- MsSI + RANKL

C

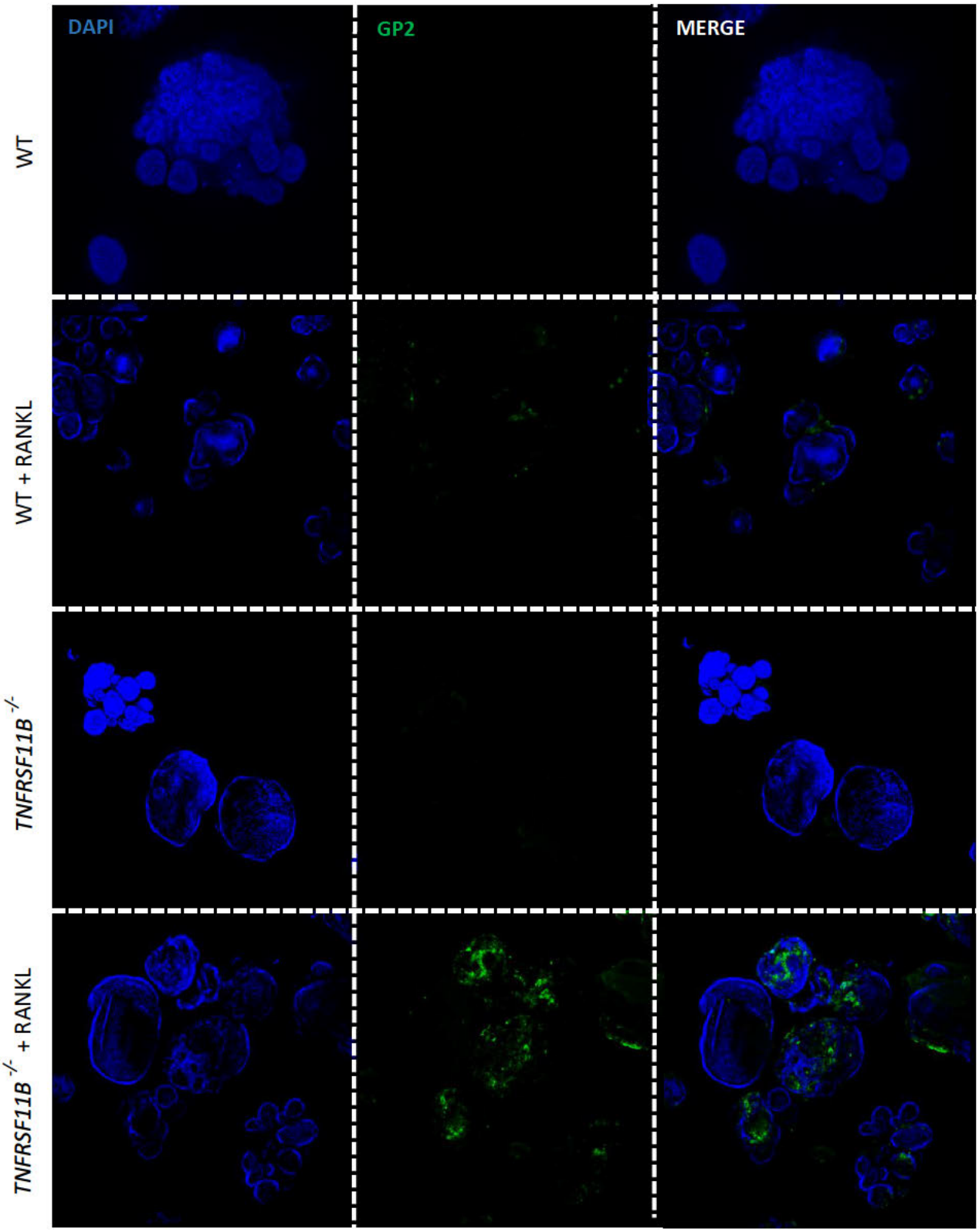

Figure 1: OPG negatively regulates the M cell differentiation. **(A)** WT and *TNFRSF11B* $^{-/-}$ mouse small intestinal organoids were cultured with and without RANKL for 7 days. **(B)** The transcriptional expression of M cell specific genes, *Gp2* and *SpiB*, was evaluated; *Gp2* was elevated in a statistically significant manner between control and RANKL-treated *TNFRSF11B* $^{-/-}$ organoids (p=0.0171) and between RANKL-treated WT organoids and RANKL-treated *TNFRSF11B* $^{-/-}$ organoids (p=0.0222). *SpiB* was elevated in a statistically significant manner between control and RANKL-treated WT organoids (p=0.0376) and between control and RANKL-treated *TNFRSF11B* $^{-/-}$ organoids (p=0.0130). **(C)** The difference in protein expression of mature M cell marker Gp2 was assessed between the four groups; untreated WT and *TNFRSF11B* $^{-/-}$ organoids showed no Gp2 expression, RANKL-treated WT organoids showed some Gp2 expression and RANKL-treated *TNFRSF11B* $^{-/-}$ organoids showed a high level of Gp2 positivity.

Epithelial cells secrete OPG in response to RANKL stimulation

Next, we investigated whether transcripts of *TNFRSF11B* rose in response to RANKL-stimulation. Indeed, transcriptional expression of *TNFRSF11B* rose non-significantly between the RANKL-treated WT organoids and untreated WT control organoids at 200ng/ml of RANKL (p=0.3210) **(Figure 2, A).** Some transcriptional expression of *TNFRSF11B* was observed in the untreated control organoids, however this rose almost three-fold once 200ng/ml of RANKL was supplemented into the media. The transcriptional expression of *TNFRSF11B* also rose in a RANKL-dependent manner **(Figure 2, B),** in accordance with the expression of *Gp2* and *SpiB*, with the highest expression observed at 1ug/ml. No *TNFRSF11B* expression was observed in the *TNFRSF11B* $^{-/-}$ organoids. Collectively, these results suggest that RANKL regulates the expression of M cell specific genes in a dose dependent manner. Also, RANKL stimulation of organoids leads to an increase in the transcriptional expression of *TNFRSF11B*, encoding for OPG. This indicates that small intestinal organoids secrete OPG as a method of inhibiting the biological effects of RANK/RANKL interaction. Next we investigated whether a specific type of epithelial cell is responsible for the upregulation in *TNFRSF11B* expression, or whether M cells secreted OPG themselves as a method of self-regulation. Representative confocal images of suggest that, as OPG and Gp2 expression do not co-localise, OPG may be secreted more generally by epithelial cells rather than by M cells alone.

Figure 2

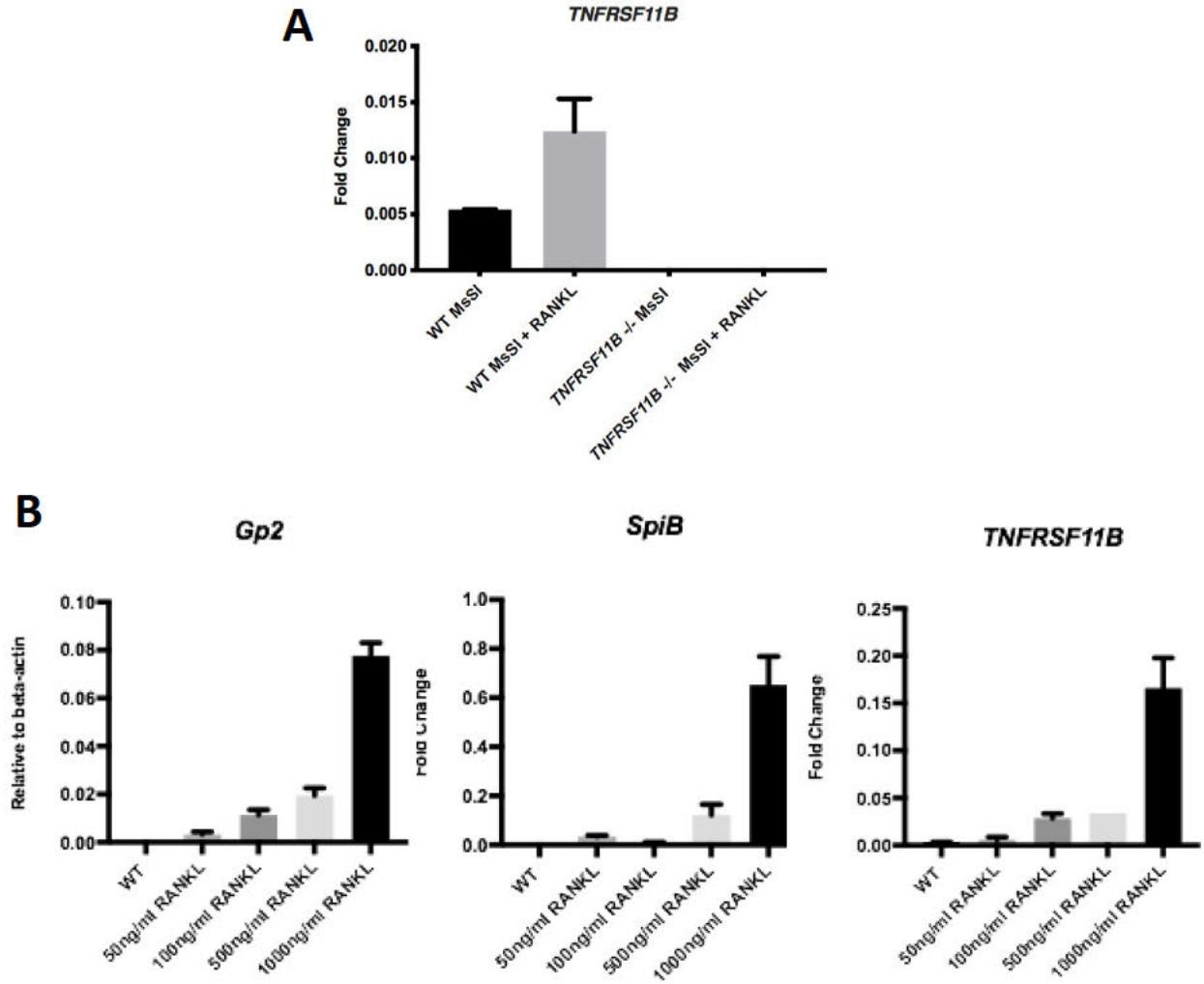
A
TNFRSF11B
Fold Change
0.020
0.015
0.010
0.005
0.000
WT MsSI
WT MsSI + RANKL
TNFRSF11B -/- MsSI
TNFRSF11B -/- MsSI + RANKL
B
Gp2
SpiB
TNFRSF11B
Relative to beta-actin
Fold Change
0.10
0.08
0.06
0.04
0.02
0.00
1.0
0.8
0.6
0.4
0.2
0.0
0.25
0.20
0.15
0.10
0.05
0.00
WT
50ng/ml RANKL
100ng/ml RANKL
500ng/ml RANKL
1000ng/ml RANKL

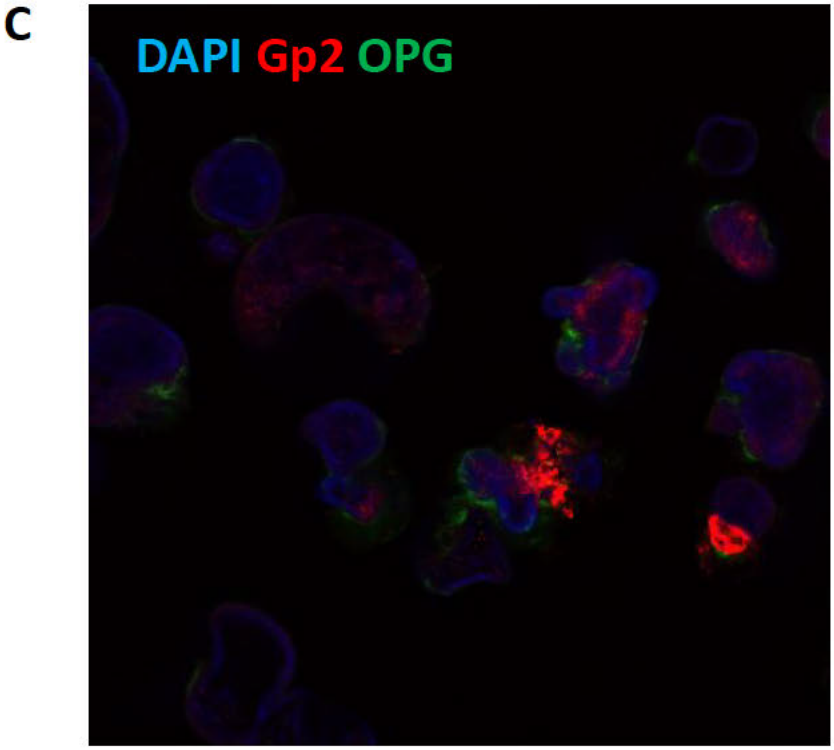
C
DAPI Gp2 OPG

Figure 2: Small intestinal organoids secrete OPG in response to exogenous RANKL.
(A) Transcriptional expression of *TNFRSF11B* is elevated in small intestinal organoids derived from WT mice treated with 200ng/ml of soluble RANKL, compared to untreated control organoids (p=0.3210). No transcriptional expression of *TNFRSF11B* was observed in *TNFRSF11B* $^{-/-}$ organoids. **(B)** The transcriptional expression of mature M cells marker *Gp2* and *SpiB* rose in a RANKL dependent manner, peaking at 1ug/ml. The expression of *TNFRSF11B* also rose in a RANKL dose dependent manner. **(C)** Representative confocal images suggest that OPG secretion is not strictly restricted to Gp2+ M cells.

5.5 Discussion

M cells, a specialised subpopulation of epithelial cells present within the follicle-associated epithelium, play a key role in the initiation of mucosal immune responses by transporting luminal antigens to subepithelial lymphoid tissue. [6] M cells are highly specialised for transcytosis; this feature enables them to act as competent sentinels of luminal contents but also renders them vulnerable to exploitation by invading pathogens seeking to gain access to systemic circulation. [14] As a result, M cell differentiation and function appear to be a tightly regulated process. Constitutively expressed M cells differentiate from Lgr5+ stem cells in response to a series of cytokine signals. RANKL-activated, TRAF6-mediated activation of the NFkB pathway is crucial for M cell development; RANKL neutralization leads to depletion of M cells and *RANKL*$^{-/-}$ mice are almost entirely deficient of M cells. M cell number and function can be restored by subsequent administration of RANKL. [16, 18, 45]

RANKL is a type II transmembrane protein belonging to the tumour necrosis factor (TNF) family of cytokines. In the Peyer's Patches, stromal cells secrete RANKL which exerts its effect by binding to the receptor activator of nuclear factor kappa B (RANK) on enterocytes, triggering the activation of the NFkB signalling pathway. It is well established that in bone, RANK/RANKL binding can be prevented by a soluble decoy molecule termed osteoprotegerin (OPG). OPG, encoded by the *TNFRSF11B* gene, binds to RANKL, preventing RANK/RANKL interaction and thereby limiting the activation of the downstream pathways. Under homeostatic conditions, the OPG/RANKL complex acts to counteract the biological effects of RANK/RANKL binding.

In this study, we harvested stem cells and cultured organoids from WT and *TNFRSF11B* $^{-/-}$ mice in order to investigate whether OPG plays a role in M cell differentiation. We induced M cell differentiation in both organoid models through stimulation with soluble RANKL, determining that depletion of OPG through genetic nullification greatly enhances the number of M cells present, as determined by the transcriptional expression of M cell markers and immunofluorescent staining. The expression of Gp2 at both the gene and protein level was significantly elevated in OPG-null organoids, as compared to WT organoids. The expression of M cell marker genes is RANKL-dependent, with expression peaking at the highest dose tested. Furthermore, we determined that transcriptional expression of *TNFRSF11B* is significantly increased in response to RANKL supplementation, likely as a self-regulating

mechanism of the epithelium. Enhanced expression of *TNFRSF11B* does not appear to be restricted to M cells. Collectively, these results implicate OPG as an important regulatory factor of M cell differentiation. Our data shows that in the absence of OPG, M cell number is significantly increased. As M cells are known to be vulnerable to exploitation by pathogens, the role of OPG as an inhibitory molecule in M cell differentiation is crucial.

5.6 Conclusion

In this study, we utilized organoid technology to demonstrate the inhibitory effects of osteoprotegerin on M cell differentiation. The findings indicate that OPG acts as an inhibitory factor in M cell differentiation, regulating the process through its ability to bind RANKL and attenuate RANK/RANKL-activated NFkB signalling. Additionally, our results show that the administration of RANKL leads to an increase in the secretion of OPG in small intestinal organoids, indicating a potential self-regulating mechanism of the epithelium. However, this effect is not restricted solely to Gp2+ M cells. Collectively, these observations provide novel insight into how M cell differentiation is regulated in the small intestine, implicating OPG as an inhibitory molecule in M cell differentiation.

Contributions

Ana Klisuric, Jotam Bar-Ephraim, Benjamin Thierry and Hans Clevers conceived the study. Ana Klisuric and Jotam Bar-Ephraim performed the experiments.

Conflict of Interest

The author declares no conflict of interest.

Funding

The work was funded by the Endeavour Leadership Program of Australia, a University of South Australia Student Mobility Grant, the ONCODE Institute and an ERC Grant.

Acknowledgements

The author would like to thank Kai Kretzschmer for assistance with bulk cell sequencing.

5.7 References

1. Jung, C., J.P. Hugot, and F. Barreau, *Peyer's Patches: The Immune Sensors of the Intestine.* Int J Inflam, 2010. **2010**: p. 823710.
2. Gebert, A., et al., *Antigen transport into Peyer's patches: increased uptake by constant numbers of M cells.* Am J Pathol, 2004. **164**(1): p. 65-72.
3. Jang, M.H., et al., *Intestinal villous M cells: an antigen entry site in the mucosal epithelium.* Proc Natl Acad Sci U S A, 2004. **101**(16): p. 6110-5.
4. Mabbott, N.A., et al., *Microfold (M) cells: important immunosurveillance posts in the intestinal epithelium.* Mucosal Immunol, 2013. **6**(4): p. 666-77.
5. Kanaya, T., et al., *The Ets transcription factor Spi-B is essential for the differentiation of intestinal microfold cells.* Nat Immunol, 2012. **13**(8): p. 729-36.
6. Lo, D.D., *Vigilance or Subversion? Constitutive and Inducible M Cells in Mucosal Tissues.* Trends Immunol, 2018. **39**(3): p. 185-195.
7. Rios, D., et al., *Antigen sampling by intestinal M cells is the principal pathway initiating mucosal IgA production to commensal enteric bacteria.* Mucosal Immunol, 2016. **9**(4): p. 907-16.
8. Nakamura, Y., S. Kimura, and K. Hase, *M cell-dependent antigen uptake on follicle-associated epithelium for mucosal immune surveillance.* Inflamm Regen, 2018. **38**: p. 15.
9. Blanco, L.P. and V.J. DiRita, *Bacterial-associated cholera toxin and GM1 binding are required for transcytosis of classical biotype Vibrio cholerae through an in vitro M cell model system.* Cell Microbiol, 2006. **8**(6): p. 982-98.
10. Jones, B.D., N. Ghori, and S. Falkow, *Salmonella typhimurium initiates murine infection by penetrating and destroying the specialized epithelial M cells of the Peyer's patches.* J Exp Med, 1994. **180**(1): p. 15-23.
11. Sansonetti, P.J. and A. Phalipon, *M cells as ports of entry for enteroinvasive pathogens: mechanisms of interaction, consequences for the disease process.* Semin Immunol, 1999. **11**(3): p. 193-203.
12. Tahoun, A., et al., *Salmonella transforms follicle-associated epithelial cells into M cells to promote intestinal invasion.* Cell Host Microbe, 2012. **12**(5): p. 645-56.
13. Nakato, G., et al., *Cutting Edge: Brucella abortus exploits a cellular prion protein on intestinal M cells as an invasive receptor.* J Immunol, 2012. **189**(4): p. 1540-4.

14. Donaldson, D.S., et al., *Increased Abundance of M Cells in the Gut Epithelium Dramatically Enhances Oral Prion Disease Susceptibility.* PLoS Pathog, 2016. **12**(12): p. e1006075.
15. Owen, R.L., et al., *M cell transport of Vibrio cholerae from the intestinal lumen into Peyer's patches: a mechanism for antigen sampling and for microbial transepithelial migration.* J Infect Dis, 1986. **153**(6): p. 1108-18.
16. de Lau, W., et al., *Peyer's patch M cells derived from Lgr5(+) stem cells require SpiB and are induced by RankL in cultured "miniguts".* Mol Cell Biol, 2012. **32**(18): p. 3639-47.
17. Taylor, R.T., et al., *Lymphotoxin-independent expression of TNF-related activation-induced cytokine by stromal cells in cryptopatches, isolated lymphoid follicles, and Peyer's patches.* J Immunol, 2007. **178**(9): p. 5659-67.
18. Knoop, K.A., et al., *RANKL is necessary and sufficient to initiate development of antigen-sampling M cells in the intestinal epithelium.* J Immunol, 2009. **183**(9): p. 5738-47.
19. Kanaya, T., et al., *Development of intestinal M cells and follicle-associated epithelium is regulated by TRAF6-mediated NF-kappaB signaling.* J Exp Med, 2018. **215**(2): p. 501-519.
20. Hase, K., et al., *Uptake through glycoprotein 2 of FimH(+) bacteria by M cells initiates mucosal immune response.* Nature, 2009. **462**(7270): p. 226-30.
21. Silva, I. and J.C. Branco, *Rank/Rankl/opg: literature review.* Acta Reumatol Port, 2011. **36**(3): p. 209-18.
22. Liu, J.Z., et al., *[Expression of human osteoprotegerin gene in E. Coli and bioactivity analysis of expression product].* Zhonghua Wai Ke Za Zhi, 2003. **41**(9): p. 641-5.
23. Boyce, B.F., et al., *Regulation of bone remodeling and emerging breakthrough drugs for osteoporosis and osteolytic bone metastases.* Kidney Int Suppl, 2003(85): p. S2-5.
24. Arthur, A., et al., *The osteoprogenitor-specific loss of ephrinB1 results in an osteoporotic phenotype affecting the balance between bone formation and resorption.* Sci Rep, 2018. **8**(1): p. 12756.
25. Lacey, D.L., et al., *Osteoprotegerin ligand is a cytokine that regulates osteoclast differentiation and activation.* Cell, 1998. **93**(2): p. 165-76.
26. Yasuda, H., et al., *Osteoclast differentiation factor is a ligand for osteoprotegerin/osteoclastogenesis-inhibitory factor and is identical to TRANCE/RANKL.* Proc Natl Acad Sci U S A, 1998. **95**(7): p. 3597-602.

27. Emery, J.G., et al., *Osteoprotegerin is a receptor for the cytotoxic ligand TRAIL.* J Biol Chem, 1998. **273**(23): p. 14363-7.
28. Standal, T., et al., *Osteoprotegerin is bound, internalized, and degraded by multiple myeloma cells.* Blood, 2002. **100**(8): p. 3002-7.
29. Theoleyre, S., et al., *Characterization of osteoprotegerin binding to glycosaminoglycans by surface plasmon resonance: role in the interactions with receptor activator of nuclear factor kappaB ligand (RANKL) and RANK.* Biochem Biophys Res Commun, 2006. **347**(2): p. 460-7.
30. Lamoureux, F., et al., *Regulation of osteoprotegerin pro- or anti-tumoral activity by bone tumor microenvironment.* Biochim Biophys Acta, 2010. **1805**(1): p. 17-24.
31. Zannettino, A.C., et al., *Osteoprotegerin (OPG) is localized to the Weibel-Palade bodies of human vascular endothelial cells and is physically associated with von Willebrand factor.* J Cell Physiol, 2005. **204**(2): p. 714-23.
32. Baud'huin, M., et al., *Factor VIII-von Willebrand factor complex inhibits osteoclastogenesis and controls cell survival.* J Biol Chem, 2009. **284**(46): p. 31704-13.
33. Kanematsu, M., et al., *Prostaglandin E2 induces expression of receptor activator of nuclear factor-kappa B ligand/osteoprotegerin ligand on pre-B cells: implications for accelerated osteoclastogenesis in estrogen deficiency.* J Bone Miner Res, 2000. **15**(7): p. 1321-9.
34. Lee, S.K. and J.A. Lorenzo, *Parathyroid hormone stimulates TRANCE and inhibits osteoprotegerin messenger ribonucleic acid expression in murine bone marrow cultures: correlation with osteoclast-like cell formation.* Endocrinology, 1999. **140**(8): p. 3552-61.
35. Lindberg, M.K., et al., *Estrogen receptor alpha, but not estrogen receptor beta, is involved in the regulation of the OPG/RANKL (osteoprotegerin/receptor activator of NF-kappa B ligand) ratio and serum interleukin-6 in male mice.* J Endocrinol, 2001. **171**(3): p. 425-33.
36. Piri, F., et al., *The Effects of Dietary Supplements of Calcium, Vitamin D and Estrogen Hormone on Serum Levels of OPG and RANKL Cytokines and their Relationship with Increased Bone Density in Rats.* J Clin Diagn Res, 2016. **10**(9): p. AF01-AF04.
37. Takai, H., et al., *Transforming growth factor-beta stimulates the production of osteoprotegerin/osteoclastogenesis inhibitory factor by bone marrow stromal cells.* J Biol Chem, 1998. **273**(42): p. 27091-6.

38. Jurado, S., et al., *Effect of IL-1beta, PGE(2), and TGF-beta1 on the expression of OPG and RANKL in normal and osteoporotic primary human osteoblasts.* J Cell Biochem, 2010. **110**(2): p. 304-10.
39. Sato, T., et al., *Long-term expansion of epithelial organoids from human colon, adenoma, adenocarcinoma, and Barrett's epithelium.* Gastroenterology, 2011. **141**(5): p. 1762-72.
40. Beumer, J., et al., *Enteroendocrine cells switch hormone expression along the crypt-to-villus BMP signalling gradient.* Nat Cell Biol, 2018. **20**(8): p. 909-916.
41. Grun, D., et al., *De Novo Prediction of Stem Cell Identity using Single-Cell Transcriptome Data.* Cell Stem Cell, 2016. **19**(2): p. 266-277.
42. Muraro, M.J., et al., *A Single-Cell Transcriptome Atlas of the Human Pancreas.* Cell Syst, 2016. **3**(4): p. 385-394 e3.
43. Hashimshony, T., et al., *CEL-Seq2: sensitive highly-multiplexed single-cell RNA-Seq.* Genome Biol, 2016. **17**: p. 77.
44. Love, M.I., W. Huber, and S. Anders, *Moderated estimation of fold change and dispersion for RNA-seq data with DESeq2.* Genome Biol, 2014. **15**(12): p. 550.
45. Donaldson, D.S., et al., *M cell-depletion blocks oral prion disease pathogenesis.* Mucosal Immunol, 2012. **5**(2): p. 216-25.

Chapter 6 Stem cells, signalling gradients and cellular differentiation

Previous chapters have highlighted the various gaps in our understanding of M cell differentiation whilst also contributing to the current knowledge of the pathways that drive this differentiation. Given the biological significance of epithelial-stromal interactions on gene expression in the follicle-associated epithelium, it is crucial to convey that the unique microenvironment of the Peyer's Patches influences regional epithelial physiology significantly.

Numerous pathways that regulate cellular differentiation and function within the regular epithelium have been well characterized. This chapter will address Aim 3 by covering the following topics;

1. The signalling mechanisms regulating cellular differentiation and function of cells of the regular epithelium.
2. The signalling mechanisms prevalent in the dome of the Peyer's Patches and the current state of knowledge on how these mechanisms influence the follicle-associated epithelium.

6.1 Intestinal stem cell niche

The surface of the small intestine (SI) consists of a monolayer of polarized epithelial cells, conjoined by laterally interacting proteins, organised into distinct crypt-villus subunits. The SI epithelium is one of the most rapidly renewing tissues in the human body. Continuous cell proliferation is supported by a continuously dividing pool of Lgr5+ intestinal stem cells (ISCs) residing at the base of the crypts. [1, 2] The ISC pool is contained within a stem cell 'niche.' The niche represents a protective milieu in which secretions from neighbouring Paneth cells, growth factors from the surrounding mesenchyme and a specialised microenvironment all contribute to the maintenance of a conducive environment for ISC proliferation. A number of signalling cascades (Wnt, Notch, EGF, BMP and Hippo) regulate not only the maintenance of the niche, but also guide cellular differentiation within the entire crypt-villus subunit.

Though Lgr5+ stem cells have long been believed to be the sole source of cellular proliferation within the SI, over the last several years it has become evident that the stem cell niche exhibits significant plasticity. Injury to the ISC niche (e.g. irradiation, doxorubicin administration) resulting in the complete depletion of Lgr5+ ISCs is not irreversible. In fact, within several days Lgr5+ ISCs reappear and intestinal regeneration continues. [3-5] A number of possible explanations exist; mature cell types may be able to de-differentiate in events of injury and adopt the function of lost ISCs. Another theory stipulates that a stem cell-like population exists in the +4 position of the epithelium, relative to the crypt bottom. Whilst bona fide, Lgr5+ stem cells are located in the stem cell compartment within the crypts, directly beneath the +4 position, these proliferative, uncharacterized +4 'stem-like' cells appear to be able to reconstitute the epithelium almost entirely after injury. Whichever mechanism is dominant post-injury, it is clear that homeostatic maintenance of the ISC niche is not the sole mechanism of regeneration.

Within the human body, most stem cell populations exhibit quiescence in an attempt to attenuate possible DNA mutagenic events. In contrast, Lgr5+ ISCs divide almost daily. The relatively non-quiescent nature of ISCs may suggest a greater risk of mutations, especially in the acidic environment of the intestine. However, this does not seem to be the case. In fact, the rate at which the intestinal epithelium acquires mutations is comparable to far less proliferative tissues. This may be in large part due to the protective physiological and molecular environment that prevails in the intestine.

Stem cells are located at the bottom of the SI crypts, spatially as far away from the luminal environment as possible. Paneth cells are interspersed between the ISCs where, in addition to secreting products that maintain the stem cell niche, they also secrete anti-microbial peptides that repel invading bacterial species. [6] Mechano-sensory tuft cells continuously monitor luminal contents for potential adverse stimuli; enteroendocrine cells perform a similar function, secreting metabolic products in response to stimuli. Lastly, mucus-secreting goblet cells secrete a viscous physical barrier that protects the epithelium and restricts access to the crypts. [7] As such, the ISC population is relatively protected from adverse effects as it undergoes continuous division to keep up with the high cell turnover demand in the SI.

Though ISCs are more proliferative than other stem cell populations elsewhere within the body, they still cannot divide rapidly enough to give rise to all the cells within the epithelium. Thus an intermediary cell population, the transit-amplifying cells (TACs) exists. ISCs likely divide asymmetrically, producing one stem cell and one TAC. [8] The TACs are highly proliferative and undergo four to five rounds of rapid cell division prior to committing to a specific lineage.

On a more localised level, ISC proliferation is highly influenced by Paneth cells. Upon reaching the crypt-villus junction, Paneth cells migrate downward into the crypt and settle between individual ISCs. Once differentiated, Paneth cells secrete a variety of products that both protect and nurture the stem cell population. [9] Paneth cell-secreted products promote proliferation of ISCs and maintain the signalling pathways dominant in the crypt base.

6.2 Signalling gradients along the crypt-villus axis

Several well characterized signalling pathways regulate homeostatic maintenance of the stem cell niche and subsequent fate determination of ISCs. The key pathways providing directional signalling to regulate cellular fate determination in the intestine are **1)** the Wnt pathway, **2)** the Notch pathway, **3)** the EGF pathway and **4)** BMP signalling. [10] The ligands activating these pathways are produced by both cells of the epithelium and cells of the subepithelial mesenchyme. They are also differentially expressed along the crypt-villus subunit, creating crucial signalling gradients that serve as directional signals for progenitor cells as they migrate out of the crypt-based stem cell niche.

The most critical pathway regulating stem cell proliferation and fate determination is unequivocally Wnt. The Wnt pathway is tightly regulated at the crypt base, and dysregulation of this pathway is closely associated with aberrant cell proliferation and cancer. Briefly, the Wnt pathway involves the activation of the Frizzled-LRP5-LRP6 receptor complex by Wnt ligands. This inhibits the continuous destruction of **β**-catenin by the adenomatous polyposis coli (APC) destruction complex. [11, 12]

Within the crypt, active Wnt and Notch signalling maintain the stem cell population and keep the transit-amplifying cells in an undifferentiated state, respectively. Wnt and Notch ligands are actively secreted by Paneth cells and, until recently, it was widely accepted that Wnt and Notch ligands produced by Paneth cells are essential to maintaining the stem cell niche. Recent reports have challenged this notion, as the genetic ablation of Paneth cells through the knockout of *Atoh1* does not appear to influence stem cell proliferation. [13, 14] This suggests alternative sources of Wnt ligands, particularly Wnt3 and EGF, are likely available to maintain the stem cell population. Interestingly, Notch signalling requires the repression of transcription factor *Atoh1* through the stimulation of transcription factor *Hes1*. Thus, these observations bring into question the requirement for Notch ligands (e.g. Dll1 and Dll1) in intestinal stem cell maintenance. The repression of *Atoh1*, through *Hes1* activation or an *Atoh1* knockout, maintain the stem cells in a state of continuous Notch activation even in the absence of Notch ligands. [15] This phenomenon requires further studies.

Sub-epithelially, the mesenchyme plays an important role in stem cell maintenance. At least two different cell populations located in the sub-epithelial space, *GLI1*$^{+}$ mesenchymal cells and CD34^{+}GP38+aSMA^{-} mesenchymal cells, produce Wnt2B. [16] Additionally, CD34^{+}GP38+aSMA^{-} mesenchymal cells also produce the Lgr5 ligand RSPO1 and BMP inhibitor Gremlin1. [16, 17] The ablation of FOXL1+ mesenchymal cells in mice disrupts stem cell and TAC proliferation due to lack of sufficient Wnt signalling. [18] Collectively, these observations suggest that the mesenchyme is vital in maintaining the structural and cellular integrity of the epithelium. However, the epithelium is also important for the maintenance of the mesenchyme. Epithelial cells secrete ligands that stimulate Hedgehog signalling; this signalling pathway is essential for the development of the mesenchyme and the maintenance of smooth muscle cells. [19]

At the crypt-villus junction, Wnt and Notch signalling subsides in favour of active bone morphogenic protein (BMP) signalling. Here, the cells migrate up the crypt-villus subunit, terminally differentiating into either enterocytes or one of the secretory cell lineages; goblet cells Enteroendocrine cells or tuft cells. Conversely, Paneth cells are the only secretory cell type that, upon reaching the crypt-villus junction, migrate downward to settle at the base of the crypts. The developmental origins of M cells remain undefined.

6.3 Lineage commitment

Lineage commitment begins when the progenitor cell migrates out of the stem cell niche upward, toward the crypt villus junction. Three main signalling pathways provide directional cues for fate determination in the small intestine; the Notch pathway, the Wnt pathway and BMP signalling. Cells leaving the crypt-base experience Wnt and BMP signalling sequentially and conversely. Wnt signals are produced predominantly by crypt-dwelling Paneth cells and subepithelial mesenchymal cells, making the concentration of active Wnt highest at the crypt base. Poorly soluble Wnt ligands taper off along the crypt villus axis. In contrast, the concentration of BMP ligands and active BMP signalling increases. BMP ligands are secreted by mesenchymal cells that are contained within the villus. To attenuate this effect in the vicinity of the stem cell niche, myofibroblasts and smooth muscle cells actively secrete BMP inhibitors (Gremlin 1, Gremlin 2, Chordin-like 1). [16]

Within the niche, Paneth cells and surrounding mesenchymal cells produce epidermal growth factor (EGF) and transforming growth factor α (TGF α) which bind to EphrinB1 (ERBB1) receptors on ISCs to induce proliferation. Paneth cells also secrete essential Notch ligands, Dll1 and Dl4, that act on ISCs. [20] Notch signalling not only maintain the ‘stemness’ of the niche, but is also a crucial determinant of whether progenitor cells commit to the secretory or the absorptive lineage. [20] Notch signalling requires cell-to-cell contact. When the receptor and ligand interact, the outcome is the expression of the basic helix-loop-helix transcription factor *Hes1*. *Hes1* has an inhibitory effect on another basic helix-loop-helix transcription factor called *Math1*. When *Math1* is repressed in a cell, the cell becomes unable to express Notch ligands. When Notch is repressed, the cell by default commits to the secretory lineage. Thus, Notch signalling determines lineage commitment through the principle of lateral inhibition using a signalling feedback loop.

Once secretory progenitors commit to the secretory lineage, additional transcription factor activation, plus other external stimuli, drive the differentiation of different subsets of secretory cells. [4] Enteroendocrine cell differentiation is controlled by the basic helix-loop-helix transcription factor *Neurogenin-2 (neurog3)* that is transiently expressed in all EE progenitors of the small intestine. [21] Goblet cell differentiation is influenced by interleukins, particularly IL4 and IL13, where both can induce goblet cell hyperplasia. The mechanism behind this is unclear. Paneth cell differentiation is highly dependent on Wnt signalling and expression of the the Wnt target gene *Sox9.* [22] The transcription factor *Pou2f3* has been reported to be specific to tuft cells.

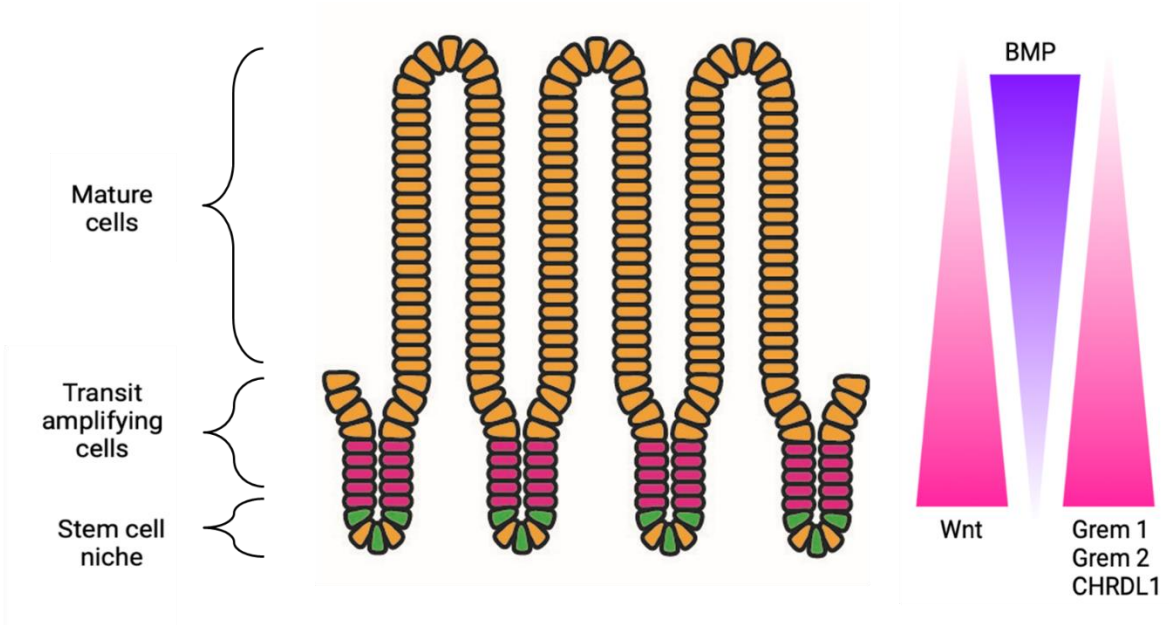

Figure 1: Signalling gradients along the crypt villus axis. The base of the intestinal crypts experiences high levels of Wnt signalling. Wnt, and its potentiator R-spondin, are secreted by mesenchymal cells and Paneth cells. Wnt signalling helps maintain active stem cell proliferation. As Wnt ligands are poorly soluble, their exerted effect tapers off with increasing distance from the crypt bottom. In contrast, BMP signalling is highest at the base of the villous tips. Mesenchymal cells above the crypt-villus junction secrete BMP proteins that allow for the induction of differentiated cell types. To attenuate this effect at the crypt base, several cell types secrete BMP inhibitors such as Gremlin 1 (Grem 1), Gremlin 2 (Grem 2) and Chordin-like 1 (CHRDL1) protein.

6.4 Signalling gradients in the Peyer's Patches

The gut-associated lymphoid tissues (GALTs) constitute one of the largest immune-inductive sites in the body. Within the small intestine, GALT encompasses domal accretions of lymph tissue termed the Peyer's Patches (PPs) and isolated lymphoid follicles (ILFs). The function of GALT structures is to sample luminal antigens and induce adaptive immunity against harmful pathogens. The presence of transcytotically-active M cells in the follicle-associated epithelium (FAE) contributes to the continuous antigen sampling required for efficient mucosal immunity. However, due to their rarity, their mechanisms of function and developmental origins remain unclear.

Transcriptome analyses reveal a large difference in the gene expression profile of cells of the FAE versus cells of the villous epithelium. [23] Sub-epithelially, the Peyer's Patches harbour a concentrated population of immune cells that influences the genetic profile of the overlying epithelium significantly. The mesenchyme-epithelial relationship is symbiotic; mesenchymal cells beneath the epithelial barrier secrete several substances important for epithelial cell survival and differentiation. Concomitantly, the epithelial cells secrete factors that also influence the mesenchyme. Recently, a new aspect has emerged as transcriptomic data suggests that there is a marked difference in gene expression between distal and proximal Peyer's Patches, indicating that the complex microenvironment of the Peyer's Patches varies according to location. [24] This further confirms the necessity for the characterization of the molecular signalling pathways that regulate cellular differentiation and function within the PPs.

The primordial formation of the PPs requires the early clustering of lymphoid tissue (LTi) cells. LTi cells express lymphotoxin $\alpha_1\beta_2$ ($LT\alpha_1\beta_2$) which stimulates lymphoid tissue organiser (LTo) cells to produce chemokines and adhesion molecules that recruit and organise lymphocytes. [25] Once the lymphocytes are clustered in large numbers and the dome-like shape of the PPs and its FAE has formed, the cells of the FAE secrete CCL20 to attract CCR6-expressing B cells and immature $CD11b^+$ dendritic cells into the region. [26, 27]

As discussed, active Notch signalling within the epithelium restricts secretory cell differentiation. It has been reported that stromal cells located beneath the FAE express abundant Dll1, a potent Notch ligand. [28] In the presence of active Notch signalling, secretory cell differentiation is supressed, resulting in a complete lack of secretory cells (enteroendocrine

cells, goblet cells, tuft cells) within the FAE. Mice lacking *Rbpj*, a gene encoding for a protein that in crucial in the Notch signalling cascade, exhibit defective GALT formation. [28] The suppression of secretory cell differentiation, particularly that of goblet cells, helps facilitate M cell-mediated antigen uptake by reducing the mucus layer that spatially segregates the epithelium from the lumen.

As active Notch signalling is known to result in repression of secretory cell differentiation, the presence of Dll1, a Notch ligand, beneath the FAE suggests M cells develop independently of the secretory cell lineage. This theory is challenged by the observation that genetic ablation of the Notch1 receptor in the intestinal epithelium leads to an increase in M cell density by approximately 25%, in addition to an increase in M cell clustering. [28] This suggests that *in vivo* Notch signalling has an inhibitory effect on M cell numbers and clustering. Conversely, conditional deletion of Jagged1, a Notch ligand, in the intestinal epithelium caused a decrease in M cell density (~25%), whilst increasing M cell clustering. [28] This evidence suggests that Jagged-1/Notch signalling is involved in maintaining M cell number and patterning across the FAE.

The lymphocytes contained within the Peyer Patch dome comprise of approximately 60% B cells, 25% T cells, 10% dendritic cells and 5% macrophages and neutrophils. [29] In addition to lymphocytes, the follicular region is rich with stromal cells. Stromal cells selectively express the receptor activator of NF-κB ligand (RANKL). [30] RANKL binds to the receptor activator of NF-κB (RANK) receptor, initiating a signalling cascade that involves downstream co-regulator TRAF6. RANK/RANKL interaction appears to be crucial for the latter stages of PP development; mice deficient in *TNFRSF11* encoding for RANKL do form PPs, albeit they are significantly reduced in size. [31] Though not strictly necessary for primordial PP formation, RANKL is crucial for M cell development, with RANKL-deficient mice displaying a significant depletion of M cells. [32] The RANK/RANKL pathway as pertaining to M cell development depends on downstream co-regulator TRAF6; conditional deletion of TRAF6 in the intestinal epithelium causes a complete loss of PP M cells. [33] In this thesis we implicate OPG expression by cells of the epithelium as a critical inhibitor of RANK/RANKL-mediated M cell differentiation.

Given the novel role of OPG in M cell differentiation, further studies can explore how other factors known to interact with the RANK/RANKL/OPG pathway influence M cell

development and function in the PPs. As an example, it is known that multiple OPG binding partners are expressed within the PPs. The PP microenvironment is highly dependent on chemokines and glycosaminoglycans (GAGs); chemokines control the migration of leukocytes during inflammation by binding to GAGs. [34] GAGs significantly diminish the biological effects of OPG *in vivo.* [35] It is also known that pathogenic challenge and subsequent inflammation induces development of new M cells. The inhibition of M cell differentiation by OPG has been established previously in this thesis, prompting the question of whether the suppression of OPG by GAGs is involved in the development of new M cells during pathogenic challenges and inflammation. [36, 37]

The function of the RANK/RANKL/OPG signalling pathway has been well characterized in bone; dysregulation in the ratio of three molecules can have significant implications on homeostasis. Studies using chemically induced models of intestinal inflammation in rats show that there is increased M cell formation under inflammatory conditions. [38] In mice, dextran sodium sulfate (DSS) and *Citrobacter rodentium*-induced colitis significantly increased the number of PP M cells. [39] Interestingly, another hallmark feature of intestinal inflammation, specifically in inflammatory bowel diseases, is the presence of OPG. OPG serves as a biomarker for both Crohn's disease and ulcerative colitis. [40] Dysregulation of the homeostatic ratio of OPG/RANKL may be involved in the pathogenesis of inflammatory bowel disease. Further study of the RANK/RANKL/OPG pathway could provide crucial insight into M cell differentiation in homeostasis and disease.

6.5 References

1. Barker, N., et al., *Identification of stem cells in small intestine and colon by marker gene Lgr5.* Nature, 2007. **449**(7165): p. 1003-7.
2. Sato, T., et al., *Single Lgr5 stem cells build crypt-villus structures in vitro without a mesenchymal niche.* Nature, 2009. **459**(7244): p. 262-5.
3. Dekaney, C.M., et al., *Regeneration of intestinal stem/progenitor cells following doxorubicin treatment of mice.* Am J Physiol Gastrointest Liver Physiol, 2009. **297**(3): p. G461-70.
4. van Es, J.H., et al., *Dll1+ secretory progenitor cells revert to stem cells upon crypt damage.* Nat Cell Biol, 2012. **14**(10): p. 1099-1104.
5. Tian, H., et al., *A reserve stem cell population in small intestine renders Lgr5-positive cells dispensable.* Nature, 2011. **478**(7368): p. 255-9.
6. Sato, T., et al., *Paneth cells constitute the niche for Lgr5 stem cells in intestinal crypts.* Nature, 2011. **469**(7330): p. 415-8.
7. Johansson, M.E., J.M. Larsson, and G.C. Hansson, *The two mucus layers of colon are organized by the MUC2 mucin, whereas the outer layer is a legislator of host-microbial interactions.* Proc Natl Acad Sci U S A, 2011. **108 Suppl 1**: p. 4659-65.
8. Darwich, A.S., et al., *Meta-analysis of the turnover of intestinal epithelia in preclinical animal species and humans.* Drug Metab Dispos, 2014. **42**(12): p. 2016-22.
9. Bevins, C.L. and N.H. Salzman, *Paneth cells, antimicrobial peptides and maintenance of intestinal homeostasis.* Nat Rev Microbiol, 2011. **9**(5): p. 356-68.
10. Gehart, H., et al., *Identification of Enteroendocrine Regulators by Real-Time Single-Cell Differentiation Mapping.* Cell, 2019. **176**(5): p. 1158-1173 e16.
11. Nusse, R. and H. Clevers, *Wnt/beta-Catenin Signaling, Disease, and Emerging Therapeutic Modalities.* Cell, 2017. **169**(6): p. 985-999.
12. Flanagan, D.J., et al., *Frizzled7 functions as a Wnt receptor in intestinal epithelial Lgr5(+) stem cells.* Stem Cell Reports, 2015. **4**(5): p. 759-67.
13. Durand, A., et al., *Functional intestinal stem cells after Paneth cell ablation induced by the loss of transcription factor Math1 (Atoh1).* Proc Natl Acad Sci U S A, 2012. **109**(23): p. 8965-70.
14. Kim, T.H., S. Escudero, and R.A. Shivdasani, *Intact function of Lgr5 receptor-expressing intestinal stem cells in the absence of Paneth cells.* Proc Natl Acad Sci U S A, 2012. **109**(10): p. 3932-7.

15. Sancho, R., C.A. Cremona, and A. Behrens, *Stem cell and progenitor fate in the mammalian intestine: Notch and lateral inhibition in homeostasis and disease.* EMBO Rep, 2015. **16**(5): p. 571-81.
16. Stzepourginski, I., et al., *CD34+ mesenchymal cells are a major component of the intestinal stem cells niche at homeostasis and after injury.* Proc Natl Acad Sci U S A, 2017. **114**(4): p. E506-E513.
17. Valenta, T., et al., *Wnt Ligands Secreted by Subepithelial Mesenchymal Cells Are Essential for the Survival of Intestinal Stem Cells and Gut Homeostasis.* Cell Rep, 2016. **15**(5): p. 911-918.
18. Aoki, R., et al., *Foxl1-expressing mesenchymal cells constitute the intestinal stem cell niche.* Cell Mol Gastroenterol Hepatol, 2016. **2**(2): p. 175-188.
19. Mao, J., et al., *Hedgehog signaling controls mesenchymal growth in the developing mammalian digestive tract.* Development, 2010. **137**(10): p. 1721-9.
20. Clevers, H.C. and C.L. Bevins, *Paneth cells: maestros of the small intestinal crypts.* Annu Rev Physiol, 2013. **75**: p. 289-311.
21. Bjerknes, M. and H. Cheng, *Neurogenin 3 and the enteroendocrine cell lineage in the adult mouse small intestinal epithelium.* Dev Biol, 2006. **300**(2): p. 722-35.
22. Bastide, P., et al., *Sox9 regulates cell proliferation and is required for Paneth cell differentiation in the intestinal epithelium.* J Cell Biol, 2007. **178**(4): p. 635-48.
23. Hase, K., et al., *Distinct gene expression profiles characterize cellular phenotypes of follicle-associated epithelium and M cells.* DNA Res, 2005. **12**(2): p. 127-37.
24. Phillips, C.L., et al., *Regional heterogeneity in rat Peyer's patches through whole transcriptome analysis.* Exp Biol Med (Maywood), 2021. **246**(5): p. 513-522.
25. Luther, S.A., K.M. Ansel, and J.G. Cyster, *Overlapping roles of CXCL13, interleukin 7 receptor alpha, and CCR7 ligands in lymph node development.* J Exp Med, 2003. **197**(9): p. 1191-8.
26. McDonald, K.G., et al., *CC chemokine receptor 6 expression by B lymphocytes is essential for the development of isolated lymphoid follicles.* Am J Pathol, 2007. **170**(4): p. 1229-40.
27. Rumbo, M., et al., *Lymphotoxin beta receptor signaling induces the chemokine CCL20 in intestinal epithelium.* Gastroenterology, 2004. **127**(1): p. 213-23.
28. Obata, Y., et al., *Epithelial-stromal interaction via Notch signaling is essential for the full maturation of gut-associated lymphoid tissues.* EMBO Rep, 2014. **15**(12): p. 1297-304.

29. Jung, C., J.P. Hugot, and F. Barreau, *Peyer's Patches: The Immune Sensors of the Intestine.* Int J Inflam, 2010. **2010**: p. 823710.
30. Taylor, R.T., et al., *Lymphotoxin-independent expression of TNF-related activation-induced cytokine by stromal cells in cryptopatches, isolated lymphoid follicles, and Peyer's patches.* J Immunol, 2007. **178**(9): p. 5659-67.
31. Kong, Y.Y., et al., *OPGL is a key regulator of osteoclastogenesis, lymphocyte development and lymph-node organogenesis.* Nature, 1999. **397**(6717): p. 315-23.
32. Knoop, K.A., et al., *RANKL is necessary and sufficient to initiate development of antigen-sampling M cells in the intestinal epithelium.* J Immunol, 2009. **183**(9): p. 5738-47.
33. Kanaya, T., et al., *Development of intestinal M cells and follicle-associated epithelium is regulated by TRAF6-mediated NF-kappaB signaling.* J Exp Med, 2018. **215**(2): p. 501-519.
34. Verkaar, F., et al., *Chemokine cooperativity is caused by competitive glycosaminoglycan binding.* J Immunol, 2014. **192**(8): p. 3908-3914.
35. Lamoureux, F., et al., *Glycosaminoglycans as potential regulators of osteoprotegerin therapeutic activity in osteosarcoma.* Cancer Res, 2009. **69**(2): p. 526-36.
36. Pilarowski, G.O., et al., *Abnormal Peyer patch development and B-cell gut homing drive IgA deficiency in Kabuki syndrome.* J Allergy Clin Immunol, 2020. **145**(3): p. 982-992.
37. Pan, J., et al., *Patterns of expression of factor VIII and von Willebrand factor by endothelial cell subsets in vivo.* Blood, 2016. **128**(1): p. 104-9.
38. Kucharzik, T., et al., *Characterization of M cell development during indomethacin-induced ileitis in rats.* Aliment Pharmacol Ther, 2000. **14**(2): p. 247-56.
39. Bennett, K.M., et al., *Induction of Colonic M Cells during Intestinal Inflammation.* Am J Pathol, 2016. **186**(5): p. 1166-79.
40. Franchimont, N., et al., *Increased expression of receptor activator of NF-kappaB ligand (RANKL), its receptor RANK and its decoy receptor osteoprotegerin in the colon of Crohn's disease patients.* Clin Exp Immunol, 2004. **138**(3): p. 491-8.

Chapter 7 Gastrointestinal mucus regulates particulate uptake in human *in vitro* models of the small intestinal epithelium

This thesis has examined the mechanisms of nanoparticle uptake for enhanced oral drug delivery as pertaining to M cells. Mucus as an important physiological barrier to drug delivery has largely been unexplored. This chapter will focus on;

1. Investigating the role of mucus in nanoparticle uptake using cell lines in lieu of organoids.
2. Discussing the practical considerations pertaining to the study of mucus *in vitro*.

7.1 Abstract

Oral drug delivery is significantly hampered by the presence of physiological barriers to absorption within the gastrointestinal tract. Gastrointestinal mucus, a viscoelastic layer of highly glycosylated proteins, lines the mucosal surface of the small intestinal epithelial barrier, precluding the efficient absorption of orally delivered biologics. Mucus, amongst other physiological factors, plays a key role in the suboptimal bioavailability of orally administered compounds. To better understand the interaction of orally administered compounds with small intestinal mucus, we constructed and characterized a robust, cell line- based protocol for testing the absorption of particles in cell models with varying levels of mucus. Then, we tested the effectiveness of the mucus-containing model with either control particles or particles conjugated to the mucopenetrative substance polyethylglycene. We demonstrate that particles modified with polyethylglycene exhibit a higher mucopenetrative ability and are uptaken by the cells at a greater rate. We also tested the mucopenetrative effects of a novel compound, 6-phosphogluconic acid and show, for the first time, the mucopenetrative effects of 6-phosphogluconic acid modified particles, in a model characterized by high levels of mucus.

7.2 Introduction

Given that a significant number of pathogens enter the body via mucosal routes (i.e. respiratory, intestinal and urogenital mucosae), mucosal immunization presents an opportunity to generate a robust immune response at the prominent site of pathogen infection. [1-3] However, this effort is impeded by several physiological protective mechanisms the mucosa has evolved to protect the epithelium from the harsh gastrointestinal environment. Perhaps the most significant protective barrier preventing drug permeation across intestinal membranes is the gastrointestinal mucus. [4] The gastrointestinal tract (GIT) is lined by a viscoelastic layer of glycosylated proteins that form a mucus. The dynamic structure and function of the GIT mucus varies by location; within the small intestine, the mucus comprises a single, porous layer of mucins that is easily dislodged and complements the predominantly absorptive function of this region of the GIT. [5] Conversely, the mucus lining the mucosa of the large intestine and colon consists of two layers; an inner adherent layer and less adherent outer layer. Here, the mucus is less adapted to absorption and primarily serves a lubricative function. [6]

GIT mucus is composed of several different highly O-glycosylated glycoproteins with gel-like properties collectively termed mucins. [5] In humans, 22 subtypes of mucins have been identified. [7] The distribution of different mucins varies by region. Mucins can be subdivided into two main classes; transmembrane and gel-forming mucins. Transmembrane mucins are formed by a single, membrane-spanning domain located near the carboxyl terminus. [8] Transmembrane mucins MUC3, MUC4, MUC12, MUC13 and MUC17 are always expressed within the gut, [8] whereas the expression of MUC1 and MUC16 is upregulated during infection and cancer. [5] Gel-forming mucins are secreted by goblet cells and have cysteine-rich N- and C-terminal parts. MUC2 is the primary gel-forming mucin, whereas MUC6 is expressed by glandular structures within the stomach and the duodenum and MUC5AC is expressed on the surface of the stomach. [5, 9, 10]

Within the small intestine, absorptive enterocytes express transmembrane mucins that protrude from the apical cell surface into the gut lumen creating a local diffusion barrier called the glycocalyx. [8, 11] Specialised, secretory cells called goblet cells produce gel-forming mucins. [12] Small intestinal mucins are almost immediately cleaved by the activated protease meprin- β, allowing the porous mucus to be dislodged easily and thus accommodating the specialised absorptive function of small intestinal epithelial cells. [13]

In order to prevent bacterial penetration through the porous, small intestinal mucus, Paneth cell-derived antimicrobial peptides (AMPs) create a diffusion gradient. [14]

Mucus poses a significant barrier limiting the diffusion of particles into the subepithelial space; in the context of oral biologics, mucus restricts the efficient uptake of biologics by cells of the epithelial layer. Cell line-based *in vitro* models are frequently used tools for studying drug development. Despite this, mucus-containing models are seldom used, even though mucus is an important parameter to address in drug development.

The challenges associated with oral drug delivery are primarily related to navigating the numerous physiological protective mechanisms of the mucosa, including traversing the mucus barrier. This is especially true for large, hydrophilic molecules such as peptides and proteins. [15, 16] In recent years, the importance of overcoming the mucus barrier as a means of increasing bioavailability of orally delivered compounds has become evident. Consequently, this has prompted renewed interest in mucus containing *in vitro* models. [7] Furthermore, it is unclear how oral formulations may be modified to diffuse through mucus more effectively. In this study we describe a novel *in vitro*, cell line-based model that can be used to study drug-mucus interactions. Furthermore, in this model we demonstrate the effect of two particle-modification methods on the rate of uptake of fluorescent microspheres into cells. The outcome of this work is a convenient, reproducible model for the study of drug-mucus interactions that can be applied to study the behaviour of particles when exposed to different layers of mucus.

7.3 Materials and Methods

Cell Lines

The human colorectal adenocarcinoma Caco-2 cell line (C2BBe1 clone) was purchased from American Type Culture Collection (ATCC, USA). The colonic HT29-MTX cell line and its methotrexate treated mucus-producing sub-clone, HT29-MTX-E12, were purchased from Sigma Aldrich (Sigma Aldrich, St. Louis, MO., USA). All cell lines were used between 10-30 passages. All cell culture reagents were purchased from Sigma Aldrich (Sigma Aldrich, St. Louis, MO., USA).

Cell Culture

Cells were maintained in 25cm^2 or 75cm^2 sterile cell culture flasks (Corning Life Sciences, MA, USA) in a humid environment at 37 °C with 5% CO_2. All cell lines were maintained in Dulbecco's Modified Eagle Medium/Nutrient Mixture F12 Ham (DMEM/F12, Sigma Aldrich, Cat: D8427) containing 15mM HEPES and sodium bicarbonate, supplemented with 1% L-glutamine, 1% penicillin/streptomycin, 10% FBS and 1% non-essential amino acids. Culture medium was replenished every 2-3 days. Cells were passaged routinely when monolayers reached approximately 80% confluence. Cells were sub-cultured with ratios between 1:3 and 1:6 in fresh, complete growth medium. Briefly, the growth medium was *aspirated,* the monolayer was washed twice with 1X phosphate buffered saline (PBS) *(Sigma)* followed by the addition of 4ml of trypsin-ethylenediaminetetraacetic acid (EDTA) (Sigma Aldrich, St. Louis, MO., USA). Flasks were incubated for 15 min at 37 °C with 5% CO_2 (ThermoFisher Scientific). Trypsin was neutralized with complete, FBS-containing growth medium. Cells were centrifuged at 300 g for 7 min, the supernatant was aspirated and the cell pellet was resuspended in fresh complete growth media.

Conjugation of FluoSpheres to polyethylglycene

The PEGylation of polystyrene particles was performed according to the amide condensation reaction protocol. Briefly, carboxylated PEG (60 mg), EDC (20 mg) and NHS (16 mg) were dissolved in 3 ml of 70% ethanol. The solution was stirred for 20 min at 35 °C to activate the –COOH group. Next, aminated polystyrene particles (4 mg) were added into the solution and

continously stirred for a further 2 h at the 35 °C. After the reaction, the residual PEG chains and other salts were washed off by adding 1 ml of Milli Q, centrifuging, removing supernatant and resuspending in PBS. PEGylated particels were stored at 4 °C for the subsequent analyses and experiments.

Conjugation of FluoSpheres to 6- phosphogluconic acid

The conjugation process was performed according to the amide condensation reaction protocol. Briefly, 6-PGA (3 mg), EDC (10 mg) and NHS (20 mg) were dissolved in 3 ml of distilled water. The solution was stirred for 15 min to activate the carboxy groups at the end of 6-PGA chains. Subsequently, aminated polystyrene particles were added and the mixed solution was stirred for a further 2 h at RT. After the reaction, residual, free-floating 6-PGA and other salts were washed off by adding 1 ml of Milli Q water, centrifuging, removing supernatant and resuspending in PBS (Sigma). 6-PGA modified particles were stored at 4 °C for subsequent analyses and experiments.

Transmission Electron Microscopy for Particle Analysis

Transmission electron microscopy analysis was utilised to establish average size, surface morphology and dispersion of particles. A drop of undiluted particle product was placed onto ultrathin Formvar-coated 200-mesh copper grids and allowed to air dry. Particles were visualized using a TEM (JEOL JEM-2100F-HR, Transmission Electron Microscope, Japan) at an accelerating voltage of 200kV.

Dynamic Light Scattering, XPS Analysis and Zeta Potential Measurements

Dynamic light scattering (DLS) (Zetasizer Nano-ZS instrument, Malvern Instruments Ltd, UK) was used to assess the size distribution of the control and modified particles in aqueous media. Zeta potential was measured using a Zetasizer Nano-ZS instrument (Malvern Instruments Ltd, UK) and recorded in a plastic cuvette with an equilibration time of 120 s. X-ray photoelectron spectroscopy (XPS) elemental analysis was conducted to investigate the surface chemical properties of different particles and to quantify the amounts of PEG and 6-PGA after the

conjugation process. XPS was gathered on a Kratos AXIS Ultra DLD X-ray photoelectron spectrometer and the data was analyzed using the CasaXPS software (Version 2.3.12).

Uptake Studies

For uptake studies, all cells (Caco-2; HT29 and HT29-MTX) were seeded at a density of 1 x 10^6 cells/3.8 cm^2 in 12 well plates (Sigma Aldrich, Cat: CLS3512). Cells were cultured for 10-12 days, with media changes every 48 hours. Cell medium was aspirated, monolayers were washed once with 1 x PBS and 1 ml of Hanks Buffered Salt Solution (HBSS, Sigma Aldrich, St. Louis, MO., USA, Cat: H6648) buffered with 10 mM of HEPES containing a suspension of 9 x 10^9/ml particles was added to the cells. For uptake studies that involved the removal of mucus from the cell surface, 1ml of Ca2+/Mg2+- free PBS (Sigma Aldrich, St. Louis, MO., USA, Cat: D1408) was added to each well and left to incubate for 15 min, before, the PBS was pipetted vigorously up and down for 60 sec to dislodge apical mucus. This was repeated twice prior to the addition of the particle suspension in HEPES-buffered HBSS. All cells were incubated with the particle suspension for 1 h at 37 °C with 5% $CO_{2,}$ before the particle suspension was aspirated and monolayers were washed twice with 1 x PBS. Cells were trypsinized with 400 µl of trypsin-EDTA, washed in 1 x PBS and then fixed with 10% formalin (4% formaldehyde, Sigma Aldrich, St. Louis, MO., USA). Cells were incubated with formalin solution for 15 minutes at room temperature (RT), washed again and resuspended in 200µl of PBS prior to analysis with an Imaging Flow Cytometer.

Imaging Flow Cytometry

To evaluate degree of uptake of yellow-green fluorescent particles by the cells, they were analysed with the Imaging Flow Cytometer (IFC) Image Stream X Mark II (AMNIS, Seattle, USA) and data was acquired using the INSPIRE acquisition software (AMNIS). A cell classifier was applied to the brightfield channel to exclude events smaller than 15 µm. This excluded background calibration beads and debris. Cells were excited with the 488 laser with a laser intensity of 50 mW. Channel 2 captured yellow-green fluorescent positive events, channel 4 recorded brightfield images and channel 6 recorded darkfield (side scatter) images. Images were compensated based on a matrix generated by single-stained samples. For each

sample at least 10,000 events were recorded. IFC data analysis was performed with IDEAS software (version 6.0, AMNIS).

Immunofluorescence

For immunocytochemistry, cells were plated on chambered coverslips (Ibidi, Cat: 80826) at a concentration of 3 x 10^5/1.0cm^2. Cells were cultured for 10-12 days with media changed every 48 hours. Media was aspirated and cells were gently washed twice with 1 x PBS. Cells were fixed by adding 200 µl of 10% formalin to each well for 15 min. Cells were rinsed with 1 x PBS, permeabilized using 0.1% (v/v) Triton X-100/PBS for 3 min, washed 2 x 5 min in 1 x PBS and blocked for 1 h in 3% (w/v) bovine serum albumin (BSA)/PBS at RT (Sigma Aldrich, St. Louis, MO., USA, Cat: 9048-46-8). The blocking solution was aspirated and 200 µl of primary antibody was applied to cells (5 mg/ml mouse mAb occludin, Invitrogen 33–1500; 2.5 mg/ml rabbit pAb ZO-1, Invitrogen 61–7300; 2mg/ml rabbit pAb claudin-1, Abcam ab15098). The primary antibodies were diluted in 1% (w/v) BSA/PBS and incubated for 1 h at RT. Cells were washed 4 x (5 min in 1 x PBS. For unconjugated primary antibodies, 200 µl of fluorescent-conjugated secondary antibody was added to the cells. The secondary antibodies were diluted in 1% (w/v) BSA/PBS and incubated for 1 h at RT. To visualize the cell nuclei, cells were incubated with 1 µg/ml Hoecsht for 10 min at RT. Cells were washed 3 x 5 mins in 1 x PBS , before the chambers were removed gently and cells were mounted using FluoroShield mounting medium (Sigma Aldrich, St. Louis, MO., USA, Cat: F6182). Cells were imaged using a Zeiss Confocal Microscope (Zeiss, Lonsdale, South Australia, Australia). Results represent average values from three separate experiments, (n=3).

Alcian Blue Staining

The alcian blue stain is used for histological visualization of acidic sulfated mucosubstances. To ensure efficient removal of mucus after washing, HT29 and HT29-MTX cells were stained with alcian blue with **i)** an intact mucus layer and **ii)** after the dislodgement of the mucus through physical agitation and washing. To assess for the presence of acidic sulfated

mucosubstances, a staining kit was used as per manufacturers instructions (Sigma Aldrich, 1.32647). The stained slides were imaged using a light microscope.

Statistical Analysis

The GraphPad Prism 5 software (La Jolla, CA, USA, http://graphpad.com) was used for statistical analysis of data. Student t-tests were used throughout the study, where indicated, to evaluate statistical significance. Statistical significance is represented as * $p<0.05$.

7.4 Results

The absorptive capacity of cell lines of epithelial origin

The absorptive capacity of three cell lines with an epithelial phenotype, Caco-2 cells, HT29 cells and HT29-MTX cells, was assessed. Cells were cultured for 10-12 days and then exposed to a solution of 0.02mg/ml yellow-green microspheres for 1 hour and the uptake of microspheres was assessed by IFC. Caco-2 cells had the highest absorptive capacity, followed by HT29 cells and then HT29-MTX **(Figure 1, A-B).** Caco-2 cells had a significantly increased absorptive capacity when compared to HT29 cells ($p=0.0079$) and HT29-MTX cells ($p=0.0011$).

Figure 1

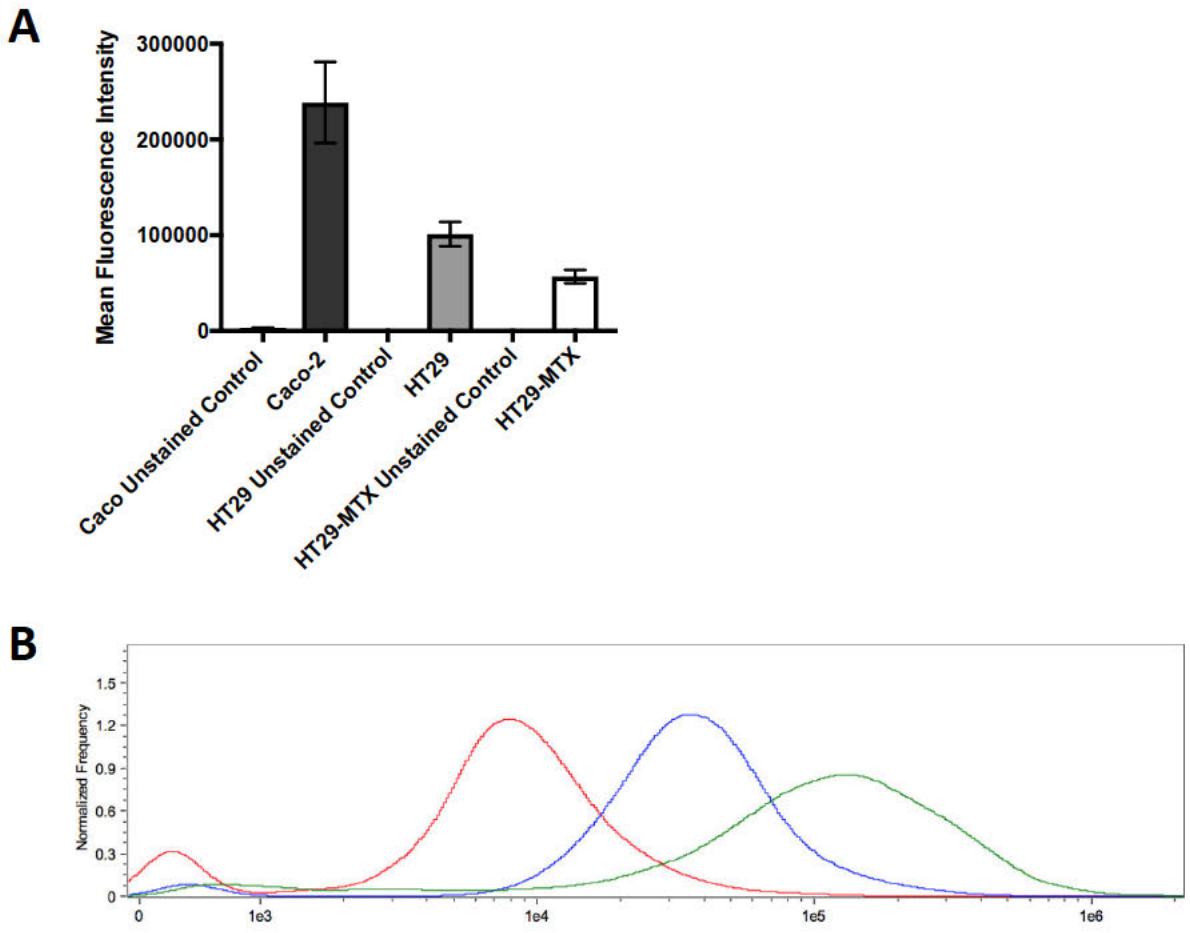

Figure 1: The absorptive capacity of Caco-2 cells, HT29 cells and HT29-MTX cells, represented as a mean fluorescence intensity value, as assessed using IFC. **(A)** Caco-2 cells display the highest uptake of 200nm amine-modified FluoSpheres, followed by HT29 cells, and then HT29-MTX cells. A one-way ANOVA analysis of the three groups determined the difference in absorptive capacity between the three cell types was statistically significant, p=0.0003. Results represent average values from three separate experiments, (n=3). **(B)** An IFC representative image of the fluorescence curve of the three cell populations; Caco-2 (green), HT29 (blue) and HT29-MTX (red).

The presence of mucus decreases the absorptive capacity of the cell

To assess whether the presence of mucus played a role in altering the absorptive capacity of the cells, cell uptake capacity was assessed with either **i)** an intact mucin layer or **ii)** cells with the mucin layer dislodged through physical agitation and washing. Despite their widespread use in studies involving epithelial barrier function, Caco-2 cells are known to express low/no mucin-related genes. [17-19] In contrast, HT29 and HT29-MTX cells are known to produce high levels of mucus. Both HT29 and HT29-MTX cell monocultures displayed significantly increased absorptive capacity after the mucus layer was removed, $p=0.0123$ and 0.0287 respectively. This indicates that, though the innate absorptive capacity of each cell line is inherently different, the presence of mucus inhibits the absorptive capacity of cells, which can be restored, to some degree, through the removal of mucus.

HT29-MTX cells produce a thicker mucus layer than HT29 cells

The staining of the cell monolayers prior to the washing of the mucus shows a deep blue stain for the HT29-MTX cells, and a slightly lighter blue for the HT29 cells. This indicates the presence of more mucosubstances in the HT29-MTX cell cultures, as compared to HT29 cells. After the dislodgement and removal of the mucus through washing, the HT29-MTX cells still retain some mucosubstances on the apical cell surface. The HT29 cells are void of any staining, indicating complete mucus removal. This may suggest that the mucus produced by the HT29-MTX cells is more firmly attached to the apical cell surface cell surface.

Figure 2

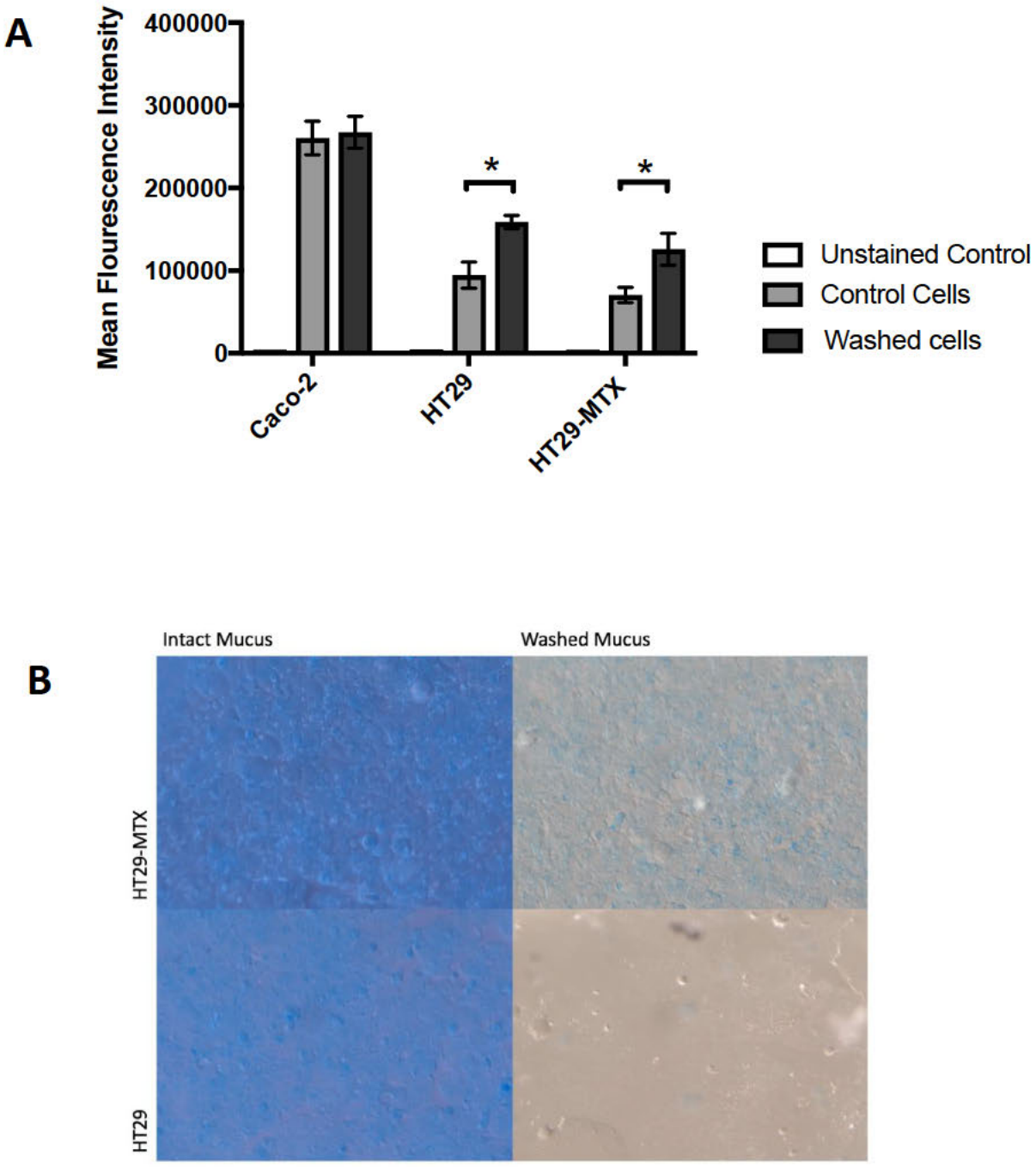
A
Mean Flourescence Intensity
400000
300000
200000
100000
0
*
*
Caco-2
HT29
HT29-MTX
Unstained Control
Control Cells
Washed cells
B
Intact Mucus
Washed Mucus
HT29-MTX
HT29

Figure 2: The absorptive capacity of Caco-2 cells, HT29 cells and HT29-MTX cells before and after the dislodgement of the mucus from the cell surface through physical agitation and washing, represented as a mean fluorescence intensity value as assessed using IFC. **(A)** The washing of the Caco-2 cells did not result in a difference in uptake capacity. The washing of the HT29 cells and the HT29-MTX cells resulted in a statistically significant increase in the uptake capacity of the cells (p=0.0123 and p=0.0287, respectively). Results represent average values from three separate experiments, (n=3). **(B)** Alcian blue staining of HT29 and HT29-MTX monolayers before and after washing. Before washing, HT29-MTX cells display a higher level of mucus staining. After washing, HT29-MTX cells retain staining, whereas HT29 cells are completely void of mucus.

Characterising Particles

Prior to use in functional experiments, the morphology and distribution of control and modified particles was assessed using TEM. TEM images showed a monodispersed particle population; no formation of aggregates was observed **(Figure 3, A-C).** The DLS analysis revealed that all particles fell within a narrow size range; 235 nm, 251 nm and 270 nm for the control particles, PEGylated particles and 6-PGA modified particles, respectively. This indicates the conjugation process was controlled and formation of aggregates was prevented under the current conjugation methods **(Figure 3, D-E).**

To determine whether the attachment of PEG (PEGylation) of particles would leads to a mucopenetrative effect, 200nm amine-modified FluoSphere particles were modified with PEG attached to the amine-chain. The successful PEGylation of 200nm FluoSpheres was confirmed with zeta potential measurements and XPS elemental analysis **(Figure 4, A-C).** A significant increase in oxygen (O) (from 9.1% to 25.6%) and decrease in nitrogen (N) (from 6.3% to 1.6%) signal was measured for the PEGylated particles compared to the aminated control particles. C 1s high resolution spectra also showed a significant increase in the CO component (286.5 eV), which can be attributed to the PEG chains. As expected, the ratio of CO to CC/CH (285 eV) carbon in the C 1s signal was higher for PEG coated particles compared to the aminated control particles (2.5 vs 0.1), indicating a successful PEGylation protocol. For 6-PGA modified particles, a higher O component, was observed for 6-PGA in comparison with the original aminated particles (from 9.1% to 17.8%). Meanwhile, C 1s high resolution also confirmed the presence of 6-PGA, associated with increase in the ratio of CO to CC/CH component (from 0.1 to 0.6). The zeta potentials of the differently modified particles were measured in 15 mM PBS solution. As summarized in **Figure 4 (C),** the aminated control particles had a positive zeta potential of 18 mV, likely due to the ionization of free $–NH_2$ groups. The charge of the PEGylated particles decreased to -5 mV, likely due to the absence of free $–NH_2$ groups that formed amide bonds during the conjugation process. The 6-PGA modified particles also displayed a negative net zeta potential, -20 mV, also likely caused by the absence of free $–NH_2$ and the ionzation of free phosphate groups at the end of 6-PGA chains coating the particles.

Figure 3

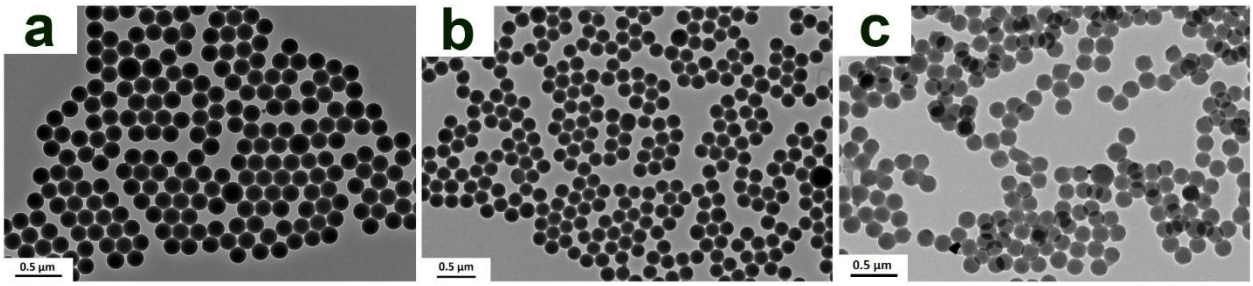

D

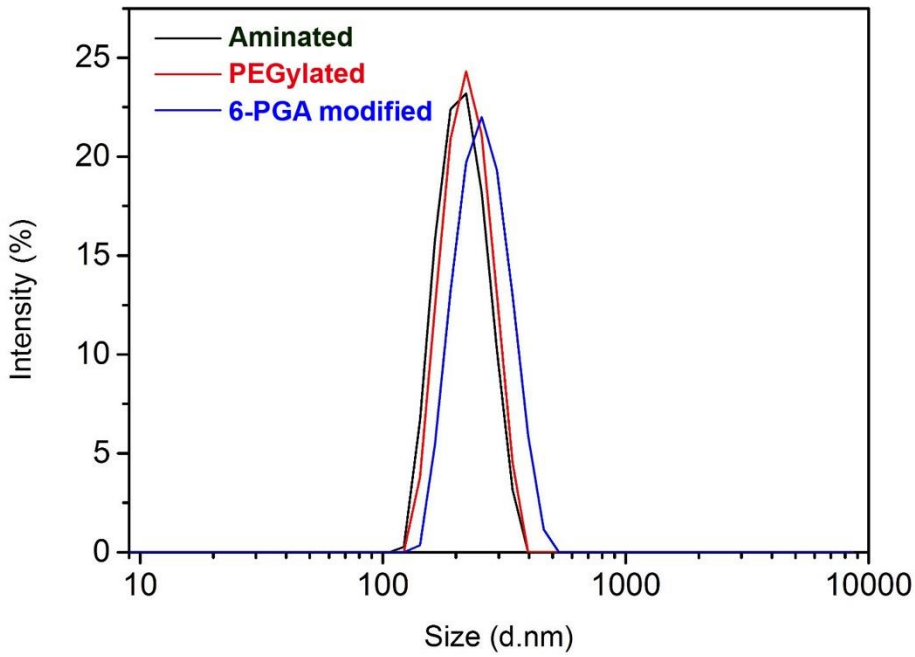

E

Modification	**Size (hydrodynamic, nm)**
Aminated FluoSpheres	235 ± 5
PEG	251 ± 7
6-PGA	270 ± 10

Figure 3: Transmission electron microscope (TEM) images of **(A)** aminated polystyrene FluoSpheres prior to any surface modification, **(B)** PEGylated, aminated polystyrene FluoSpheres and **(C)** 6-PGA modified, aminated polystyrene FluoSpheres. TEM analysis revealed no significant differences in the morphology, size and distribution of the particles before and after modification. The TEM images reveal a monodispersed particle population before and after modification, with no visible aggregation. Size distribution measurement of particles before and after modification in aqueous media was measured by dynamic light scattering and revealed that the particles maintained a narrow size range and did not aggregate. **(D)** The results show that the aminated polystyrene particles had a narrow size distribution with an average diameter of 235 nm (intensity distribution). Coating the particles with PEG polymers or 6-PGA molecules resulted in a slight increase in their average hydrodynamic diameter (251 nm for PEGylation and 270 nm for 6-PGA modification, respectively), as summarised in Table E **(E)**.

Figure 4

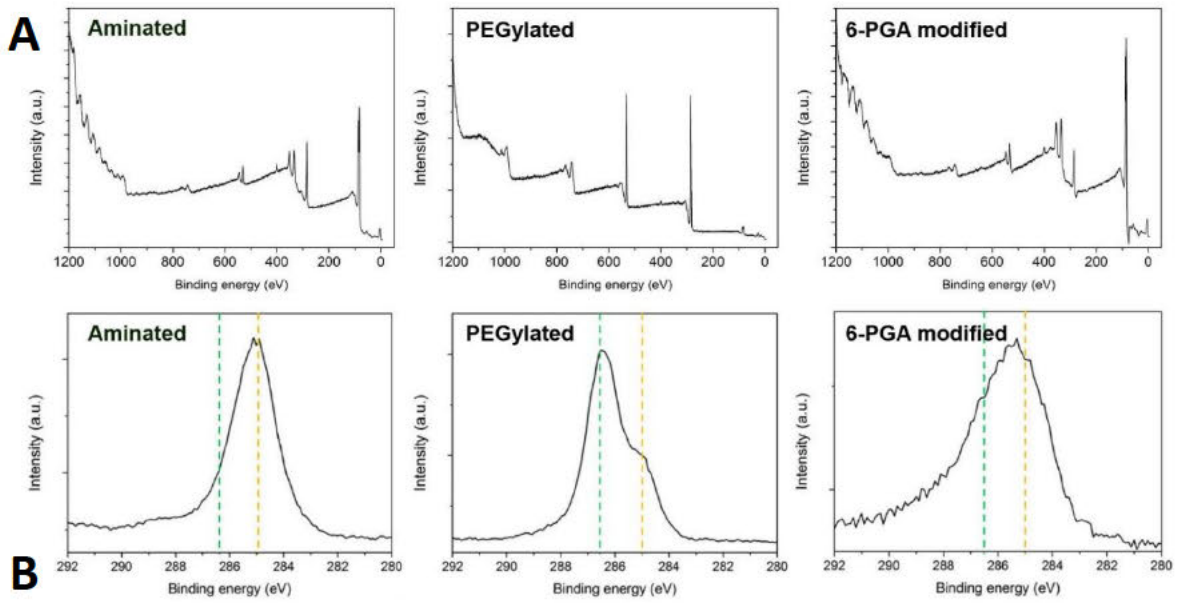

	Amino	**PEG**	**6-PGA**
Zeta potential	18 ± 1 mV	-5 ± 2 mV	-20 ± 2 mV

C

Sample	XPS elemental composition (%)			% contribution in the C 1s simulation				
	C	N	O	CC/CH	CN	CO	C=O	O-C=O
Aminated	84.6	6.3	9.1	62.6	23	8.9	2.9	2.6
PEGylated	72.8	1.6	25.6	27.3	/	68	2.7	2
6-PGA modified	77.3	4.9	17.8	51.3	7.8	32.4	2.2	6.3

Figure 4: XPS analysis was used to confirm the successful modification of the particles and quantify the amounts of PEG and 6-PGA present after the conjugation process. **(A-B)** XPS elemental composition analysis and C 1s high resolution spectra of polystyrene particles with different surface modifications. The dash lines in the C 1s spectra indicate the CC/CH (285 eV, yellow) and CO (286.5 eV, green) components. A significant increase in the oxygen (O) and decrease in nitrogen (N) signals were detected for the PEGylated particles in comparison with the aminated particles. C 1s high resolution spectra also show an increase in the CO component, which can be attributed to the PEG chains. The ratio of CO to CC/CH in the C 1s signal was higher for PEGylated particles compared to the aminated control particles, suggesting successful PEGylation. For 6-PGA modified particles, an increase in the O component, from the GA molecule, was observed for the 6-PGA modified particles compared to control particles. C 1s high resolution spectra also confirmed the presence of 6-PGA, as shown by the increase in the ratio of CO to CC/CH component. **(C)** Zeta potential values of different polystyrene particles in PBS buffer (0.1×, the concentration of electrolytes is 15 mM).

PEGylation of particles leads to increased uptake in a mucus-containing cell model

To verify the mucopenetrative effects of PEG, the absorption of characterized PEGylated and control particles was assessed through IFC in models with moderate mucus production; Caco-2/HT29 and Caco-2/HT29-MTX (1:1) co-cultures, and in models with high mucus production, HT29 and HT29-MTX monocultures. In the co-cultures marked by moderate mucus production, PEGylation of particles either resulted in a diminished absorptive capacity or in no change in absorptive capacity **(Figure 5, A).** In HT29 and HT29-MTX monocultures, marked by higher mucus production, the PEGylation of particles led to a statistically significant increase in absorption, despite the negative charge. This suggests that in *in vitro* systems marked by low mucus production and a thin mucus layer, PEGylation of particles does not necessarily exhibit muco-penetrative properties, but instead the negatively charged PEG layer decreases absorption of particles. However, in models marked by higher mucus production and a thick mucus layer covering the cells, PEGylation may be useful to increase the muco-penetrative ability of the particle.

6- phosphogluconic acid modified particles exhibit increased uptake in a mucus-containing cell model

To test whether 6-PGA modified particles have mucopenetrative properties, a solution of 6-PGA particles and control aminated particles was exposed to HT29-MTX monolayers, characterized by high levels of mucus. Uptake was assessed using IFC. Compared to aminated control particles, 6-PGA modified particles were uptaken at a higher rate ($p=0.0198$).

Figure 5

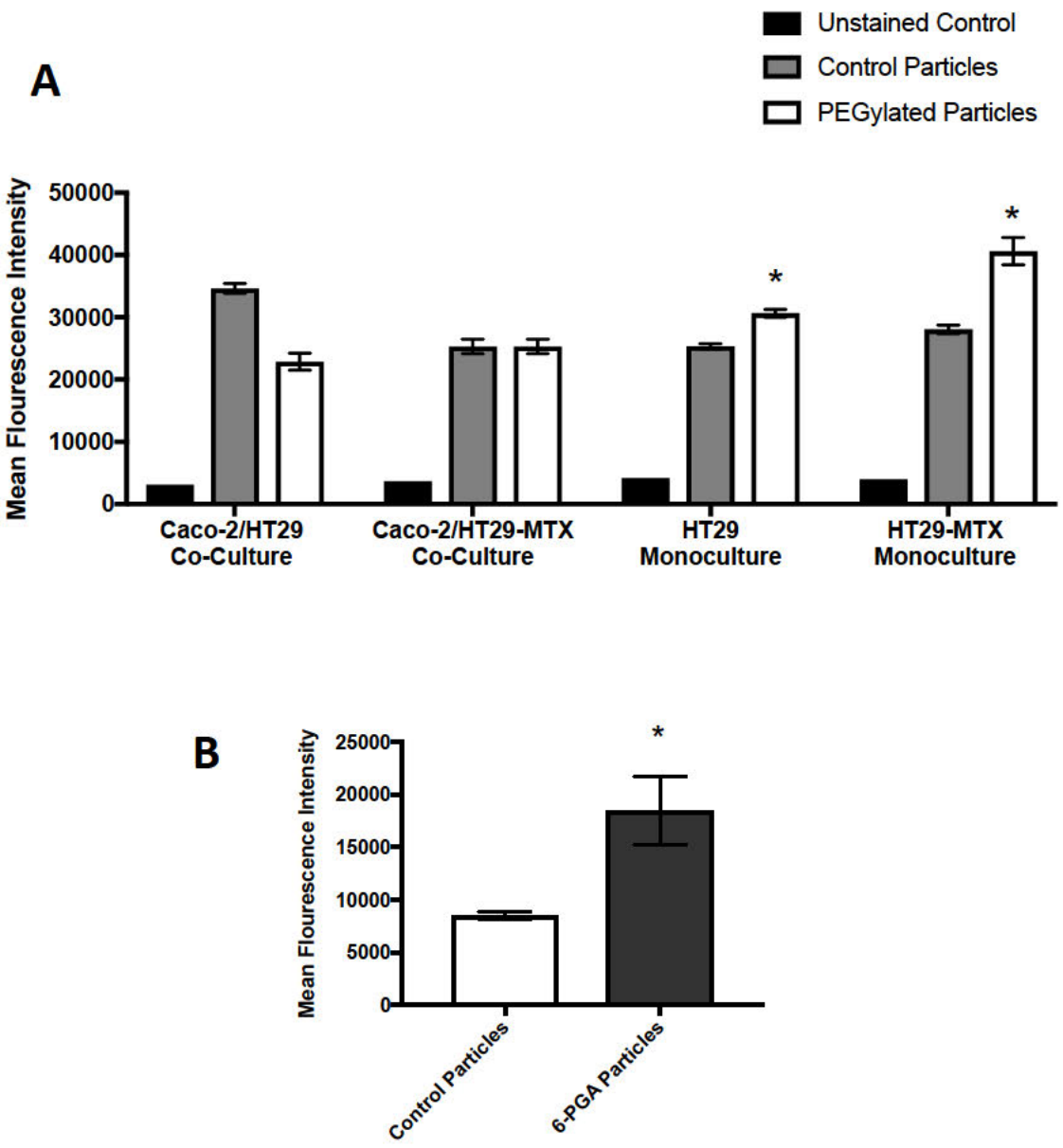
A
Unstained Control
Control Particles
PEGylated Particles
Mean Flourescence Intensity
50000
40000
30000
20000
10000
0
*
*
Caco-2/HT29 Co-Culture
Caco-2/HT29-MTX Co-Culture
HT29 Monoculture
HT29-MTX Monoculture
B
Mean Flourescence Intensity
25000
20000
15000
10000
5000
0
*
Control Particles
6-PGA Particles

Figure 5: The PEGylation of polystyrene FluoSpheres increases uptake in a statistically significant manner in all mucus models, compared to the non-PEGylated controls. **(A)** The four models with varying amounts of mucus were cultured for 10-12 days and exposed to a solution of control, non-PEGylated particles or PEGylated particles for 1 hour. PEGylated particles were uptaken by the cells at a higher rate in models characterised by higher levels of mucus, as determined by a Student t-test (*p>0.05). **(B)** Control particles or 6-PGA modified particles were exposed to HT29-MTX monolayers, the highest mucus containing model, for 1 hour. Uptake, assessed using IFC, was significantly higher with 6-PGA modified particles compared to the control particles (*p>0.05). Results represent the average of three separate experiments, n=3.

7.5 Discussion

Currently, intravenous (IV) administration of biopharmaceuticals is the preferred delivery route as it offers high bioavailability and triggers a robust and rapid systemic immune response. However, IV administration is associated with numerous supply and administration difficulties. [20] In contrast, oral drug delivery methods are considered more convenient and cost-effective and may provide a rapid immune response directly at the mucosal surfaces, directly at the site of pathogen entry. Despite this, bioavailability of oral drug delivery systems remains low as there are numerous challenges associated with absorption of compounds at mucosal surfaces.

Recently, nanocarriers have emerged as a promising vehicle for orally delivered compounds. Nanocarriers encapsulate their biological payload, protecting it from the harsh GIT environment, and their polymer surface is amenable to chemical modification. Surface modifications (e.g. PEG) may help overcome challenges associated with cell receptor-mediated uptake and traversing the mucus barrier.

Previous research has established that Caco-2 cells have a relatively absorptive phenotype but a negligible expression of mucin-related genes, despite being frequently used as an appropriate *in vitro* model of the epithelial barrier. [15, 19] Compared to Caco-2 cells, HT29 and HT29-MTX cells are characterized by a relatively high level of mucin expression. [21-23] In this study, we utilize three cell lines (Caco-2, HT29 and HT29-MTX cells) to evaluate how varying levels of mucus impact uptake of nanoparticles. We demonstrate that Caco-2 cells have the highest absorptive capacity, then HT29 cells, and finally HT29-MTX cells.

The role of gastrointestinal mucus as a physiological barrier to oral drug delivery is well established. [24, 25] Gel-forming mucins, secreted primarily by goblet cells, form a protective layer on the apical surface of the epithelial cellular barrier preventing luminal pathogens, as well as potentially beneficial orally administered biologics, from being absorbed by the cells. Much effort has been channelled into investigating the interactions of orally administered particles with GI mucus in order to formulate better methods for particle synthesis with enhanced bioavailability. To better understand how mucus impacts the absorptive capacity of the cells utilised in this study, we measured absorptive capacity of the cell lines with and without mucus. The absorptive capacity of Caco-2 cells, which are known not to produce mucus [17], was not affected by washing. In contrast, the HT29 and HT29-MTX cells, which

are known to produce mucus, displayed significantly higher absorptive capacity of 200nm particles after the mucus was removed via vigorous washing.

Next, we investigated whether absorption of the particles can be improved by chemical modification. The polyether compound polyethylene glycol (PEG) has been shown to exhibit mucopenetrative properties in oral drug delivery studies. To investigate the effects of PEG-modification on absorption, we tested absorption of particles in the HT29 and HT29 monocultures, which are known to produce mucus. To better mimic the molecular architecture of the small intestinal barrier *in vivo,* we also tested the particles in co-cultures (1:1) of Caco-2 cells and HT29 cells and in co-cultures (1:1) of Caco-2 cells and HT29-MTX cells. This was done as initially we determined that the Caco-2 cells had the highest absorptive capacity of the cell types studied but no mucus. In contrast, HT29 and HT29-MTX cells produced mucus but were less absorptive. The absorptive capacity of the cells in co-cultures was not significantly affected by PEGylation of particles. This may be since the control particles displayed a positive zeta potential and cationic particles are generally more easily uptaken by the anionic phospho-lipid plasma membrane when no/thin mucus barrier is present. This is likely because a thin mucus layer is not a sufficient barrier to impede absorption of control cationic particles. The mucus producing models, the HT29 and HT29-MTX monocultures, showed a significant increase in absorptive capacity with PEGylated particles as opposed to control particles.

Cellular mucus-containing models are often based on Caco-2/HT29-MTX co-cultures in an effort to cellularly represent both the absorptive enterocytes of the barrier, as well as the mucus secreting goblet cells [19, 21, 26-28]. The most prominent issue with the current Caco-2/HT29-MTX co-culture model is that the obtained result does not necessarily indicate an effect mediated by mucus. The advantage of having several models concurrently with varying levels of mucus is that any result that is mediated by mucus interaction will show a proportional effect in each model. As such, the mono and co-cultures presented in this study are useful indicators of how much a modified particle is interacting with the mucus directly. The models are robust, easily reproducible and simple.

Finally, the mucopenetrative potential of a novel molecule, 6-PGA, was demonstrated. 6-PGA was hypothesized to have mucopenetrative effects as 6-PGA modification reduces the charge of the particle. The temporarily negative charge of the particle allows for easier diffusion through the mucus, as both mucus and the particle are negatively charged. Here we

hypothesized that upon traversing the mucus and reaching the epithelial cell layer, alkaline phosphatase, a phosphate-cleaving enzyme continuously secreted by epithelial cells, will cleave the 6-PGA off the particle, restoring the previously positive charge and allowing for enhanced uptake. Though we observe the intended effect in the model characterized by the highest mucus production, we have not demonstrated the mechanisms behind this effect. Future work in this area could concentrate on further studying how 6-PGA interacts with mucus and translating the suggested 6-PGA modification into *in vivo* systems.

7.6 Conclusion

Oral drug delivery is a convenient and cost-effective means of administering biopharmaceuticals. However, this route of administration has reduced bioavailability compared to other methods, largely because of significant physiological obstacles to absorption, such as gastrointestinal mucus. Nanocarriers have emerged as a promising vehicle for orally delivered compounds, and their surface modification with PEG may help overcome the mucus barrier . In this study, we used three different cell lines to produce several *in vitro* cell models with varying levels of mucus. This was done to evaluate the impact of mucus on nanoparticle uptake and investigate whether absorption can be improved by chemical modification. The protocol developed in this study allows for the simple and reproducible analysis of the interactions of differently modified particles with gastrointestinal mucus. In contrast to other mucus-containing epithelial cell models, the protocol described in this chapter allows for the observations of particle interaction with different amounts of mucus in a well-characterized, simple and efficient model. Furthermore, the mucopenetrative potential of a novel molecule, 6-PGA, was demonstrated. The models used in this study are useful indicators of how much a modified particle is interacting with the mucus directly, and the obtained results could contribute to the development of oral drug delivery systems with enhanced bioavailability.

Contributions

Ana Klisuric and Benjamin Thierry conceived the study. Ana Klisuric conducted the experiments. Zhengyang Jia performed the conjugation and characterization of particles. Marnie Winter assisted with analysis of IFC data.

Conflict of interest

The author declares no conflict of interest.

Funding

This was funded by an ARC Linkage Grant LP150100032. This work was supported by a University of South Australia Postgraduate Award and an Endeavour Research Fellowship.

7.7 References

1. Lavelle, E.C., *Generation of improved mucosal vaccines by induction of innate immunity.* Cell Mol Life Sci, 2005. **62**(23): p. 2750-70.
2. Lavelle, E.C. and D.T. O'Hagan, *Delivery systems and adjuvants for oral vaccines.* Expert Opin Drug Deliv, 2006. **3**(6): p. 747-62.
3. Lavelle, E.C. and R.W. Ward, *Mucosal vaccines - fortifying the frontiers.* Nat Rev Immunol, 2022. **22**(4): p. 236-250.
4. Boegh, M. and H.M. Nielsen, *Mucus as a barrier to drug delivery - understanding and mimicking the barrier properties.* Basic Clin Pharmacol Toxicol, 2015. **116**(3): p. 179-86.
5. Corfield, A.P., et al., *Mucins in the gastrointestinal tract in health and disease.* Front Biosci, 2001. **6**: p. D1321-57.
6. Herath, M., et al., *The Role of the Gastrointestinal Mucus System in Intestinal Homeostasis: Implications for Neurological Disorders.* Front Cell Infect Microbiol, 2020. **10**: p. 248.
7. Chatterjee, M., J.P.M. van Putten, and K. Strijbis, *Defensive Properties of Mucin Glycoproteins during Respiratory Infections-Relevance for SARS-CoV-2.* mBio, 2020. **11**(6).
8. Johansson, M.E. and G.C. Hansson, *Immunological aspects of intestinal mucus and mucins.* Nat Rev Immunol, 2016. **16**(10): p. 639-49.
9. Bajka, B.H., et al., *The influence of small intestinal mucus structure on particle transport ex vivo.* Colloids Surf B Biointerfaces, 2015. **135**: p. 73-80.
10. Volynets, V., et al., *Intestinal barrier analysis by assessment of mucins, tight junctions, and alpha-defensins in healthy C57BL/6J and BALB/cJ mice.* Tissue Barriers, 2016. **4**(3): p. e1208468.
11. Kararli, T.T., *Comparison of the gastrointestinal anatomy, physiology, and biochemistry of humans and commonly used laboratory animals.* Biopharm Drug Dispos, 1995. **16**(5): p. 351-80.
12. Haber, A.L., et al., *A single-cell survey of the small intestinal epithelium.* Nature, 2017. **551**(7680): p. 333-339.
13. Schutte, A., et al., *Microbial-induced meprin beta cleavage in MUC2 mucin and a functional CFTR channel are required to release anchored small intestinal mucus.* Proc Natl Acad Sci U S A, 2014. **111**(34): p. 12396-401.
14. Bevins, C.L. and N.H. Salzman, *Paneth cells, antimicrobial peptides and maintenance of intestinal homeostasis.* Nat Rev Microbiol, 2011. **9**(5): p. 356-68.
15. Frokjaer, S. and D.E. Otzen, *Protein drug stability: a formulation challenge.* Nat Rev Drug Discov, 2005. **4**(4): p. 298-306.
16. Goldberg, M. and I. Gomez-Orellana, *Challenges for the oral delivery of macromolecules.* Nat Rev Drug Discov, 2003. **2**(4): p. 289-95.

17. Van Klinken, B.J., et al., *The human intestinal cell lines Caco-2 and LS174T as models to study cell-type specific mucin expression.* Glycoconjugate Journal, 1996. **13**(5): p. 757-768.
18. Lian, P., et al., *Hypoxia and heat stress affect epithelial integrity in a Caco-2/HT-29 co-culture.* Sci Rep, 2021. **11**(1): p. 13186.
19. Gagnon, M., et al., *Comparison of the Caco-2, HT-29 and the mucus-secreting HT29-MTX intestinal cell models to investigate Salmonella adhesion and invasion.* J Microbiol Methods, 2013. **94**(3): p. 274-9.
20. Azegami, T., Y. Yuki, and H. Kiyono, *Challenges in mucosal vaccines for the control of infectious diseases.* Int Immunol, 2014. **26**(9): p. 517-28.
21. Beduneau, A., et al., *A tunable Caco-2/HT29-MTX co-culture model mimicking variable permeabilities of the human intestine obtained by an original seeding procedure.* Eur J Pharm Biopharm, 2014. **87**(2): p. 290-8.
22. Mahler, G.J., M.L. Shuler, and R.P. Glahn, *Characterization of Caco-2 and HT29-MTX cocultures in an in vitro digestion/cell culture model used to predict iron bioavailability.* J Nutr Biochem, 2009. **20**(7): p. 494-502.
23. Walter, E., et al., *HT29-MTX/Caco-2 cocultures as an in vitro model for the intestinal epithelium: in vitro-in vivo correlation with permeability data from rats and humans.* J Pharm Sci, 1996. **85**(10): p. 1070-6.
24. Lundquist, P. and P. Artursson, *Oral absorption of peptides and nanoparticles across the human intestine: Opportunities, limitations and studies in human tissues.* Adv Drug Deliv Rev, 2016. **106**(Pt B): p. 256-276.
25. Ensign, L.M., R. Cone, and J. Hanes, *Oral drug delivery with polymeric nanoparticles: the gastrointestinal mucus barriers.* Adv Drug Deliv Rev, 2012. **64**(6): p. 557-70.
26. Lozoya-Agullo, I., et al., *Usefulness of Caco-2/HT29-MTX and Caco-2/HT29-MTX/Raji B Coculture Models To Predict Intestinal and Colonic Permeability Compared to Caco-2 Monoculture.* Mol Pharm, 2017. **14**(4): p. 1264-1270.
27. Wen, Z., et al., *[Transport of PLGA nanoparticles across Caco-2/HT29-MTX co-cultured cells].* Yao Xue Xue Bao, 2013. **48**(12): p. 1829-35.
28. Pontier, C., et al., *HT29-MTX and Caco-2/TC7 monolayers as predictive models for human intestinal absorption: role of the mucus layer.* J Pharm Sci, 2001. **90**(10): p. 1608-19.

Chapter 8 Discussion and conclusion

8.1 Discussion

The mucosal immune system is comprised of a network of integrated tissues and cells that coordinate localised immune responses at the predominant site of pathogen entry. [1] Infectious diseases caused by mucosal pathogens are associated with significant mortality and morbidity; most recently, the coronavirus 2 (SARS-CoV-2) pandemic served as an important reminder of the challenges associated with treatment of mucosal infections. [2] Despite the significant burden on public health associated with mucosal pathogens, mucosal immunisation remains a promising yet poorly understood field.

From a public health perspective, mucosal vaccines can be leveraged to combat numerous pathogens that replicate in mucosal tissues, significantly reducing the immense global burden of mortality and morbidity associated with infectious diseases. [3, 4] [5] Though most vaccines are currently administered parenterally, mucosal vaccines are more efficient at eliciting mucosal immune responses directly at the site of pathogen entry. [6] As such, mucosal vaccines present a great opportunity to leverage the unique features of the mucosal immune system to swiftly prevent the spread of infection. Despite this, several challenges limit advancement of mucosal vaccine development. The most prominent limitation is our incomplete understanding of the mucosal immune response and the challenges associated with delivering a vaccine mucosally. In the context of the GIT, an effective mucosal vaccine must traverse the hostile GIT environment to its destination, navigate the numerous protective mechanisms that protect the epithelium and, finally, gain access to the rich lymphoid network of cells located in subepithelial tissues. As discussed throughout this thesis, the small intestinal mucosa is exposed to the harsh environment of intestinal digestion and has therefore evolved several necessary protective mechanisms that limit the uptake of biomacromolecules and pathogens. [7-9] These mechanisms are vital for protecting the stem cell niche and preserving the integrity of the epithelial barrier, but also pose a challenge to mucosal immunisation attempts. [10, 11]

M cells, located in the follicle-associated epithelium (FAE) overlying lymphoid tissues of the gut, are uniquely adapted for the transcytosis of luminal antigens to the immune-competent environment of the Peyer's Patches (PPs). [12, 13] The FAE is distinct from the villous

epithelium in several keys ways that may facilitate intestinal absorption. Antimicrobial peptide (AMP) secretion is diminished in the FAE as sub-epithelial dendritic cells secrete interleukin-22 binding protein (ILL-22BP) that inhibits IL-22BP-mediated secretions of AMPs. [13] Stromal cells in the subepithelial region secrete Dll1, a Notch signalling pathway inhibitor, which restricts secretory cell differentiation. As a result, goblet cells are virtually absent in the FAE and the mucus layer is significantly reduced. [14] Finally, subepithelial stromal cells secrete receptor activator of nuclear factor kappa B ligand (RANKL) triggering the differentiation of M cells. [15] M cells act as an efficient shuttle transporting luminal antigens to the antigen-presenting cells located subepithelially and thereby initiating antigen-specific mucosal immune responses. [13] Taken together, these features of the FAE and M cells specifically, make them an attractive target for developing strategies for mucosal immunisation.

A substantial body of research suggests that targeting intestinal M cells presents a significant opportunity to enhance the efficacy of oral vaccines. Despite this, the field of M cell biology remains in relative flux, as divergent theories regarding multiple M cell lineages and a lack of clarity regarding the molecular pathways influencing M cell differentiation lead to ambiguity within the field. A significant factor contributing to the ongoing ambiguity in the field is the lack of a standardized *in vitro* model containing true M cells, which would facilitate research efforts. Much of the research generated in the field of M cell-mediated transcytosis has relied on models that fail to recapitulate the complexity of the corresponding *in vivo* environment.

Accordingly, this thesis sought to advance the field by adressing three main research areas;

1. The establishment of an *in vitro* model of the follicle-associated epithelium, containing M cells, that recapitulates the physiological and molecular complexity of the *in vivo* tissue.
2. Utilization of the established model to develop a methodology for the assesment of nanoparticle uptake by M cells and enterocytes.
3. Advance understanding of M cell differentiation pathways.

The initial introductory chapter, **Chapter 1**, provided a comprehensive overview of the anatomy and physiology of the gastrointestinal tract. The molecular composition of the

epithelial barrier was analysed in detail, with a particular focus on highlighting the differences between the follicle-associated epithelium and the regular epithelium. This distinction is important as an extensive body of research suggests that targeting M cells may enhance the efficacy of orally delievered vaccines. By clarifying the physiological and molecular differences between these two types of epithelium, this chapter provided a clear rationale for the significance of establishing an *in vitro* model of the follicle-associated epithelium that is both molecularly and physiologically accurate.

Numerous attempts have been made to study the functional mechanisms of M cell-mediated transcytosis *in vitro.* [16-23] These attempts have been hampered by a significant discrepancy in the *in vitro* models used. [24] This is discussed in **Chapter 2**. The article "Identifying human and murine M cells *in vitro"* sought to convey that the current models lack reproducibility and may not be applicable to the *in vivo* context. *In vitro* studies of M cell differentiation and function have mostly relied on cell line-based assays that do not accurately represent the transcriptional and proteomic profile of traditional PP M cells. [24] Cell line-based assays usually require the co-culturing of an epithelial cell type, such as the Caco-2 cells, with cell lines of lymphocytic origin. [20] The exogenous factors secreted by the lymphocytic cells trigger a subset of epithelial cells to develop an M cell-like phenotype. These induced 'M cells' are reported to exhibit significantly increased uptake capacity of nanoparticles compared to cultures of pure enterocytes, with uptake by these 'M cells' reported to be up to 50 times higher. [20, 25, 26] However, as these inducible 'M cells' do not express the markers of terminally differentiation *in vivo* M cells, it cannot be definitively ascertained how translatable these results are. This further underscores the necessity for the establishment of a molecularly and physiologically more accurate model of the follicle-associated epithelium. In the initial stages of this thesis, this research was pivotal to determine whether existing models were suitable for studying nanoparticle uptake or whether this work necessitated the development of an advanced model.

In **Chapter 3**, we utilise the cutting-edge organoid technology to produce M cells that express *SpiB* and Gp2, employing the resulting model to test the uptake of control and modified nanoparticles via a newly described method. Organoid technology represents an improvement over the commonly used cell line-based assays for studying M cells. [27] Derived from Lgr5+

stem cells excised from *in vivo* tissue, organoids are microscopic, three-dimensional tissue cultures that recapitulate the physiological, cellular and genomic complexity of the organ of origin. [28] Intestinal organoids develop M cells in response to media supplementation with soluble RANKL. [16] Organoid-derived M cells express terminal markers of M cell differentiation. Despite the superiority of organoids over cell lines in terms of physiological relevance, the use of organoids for drug screening and assessment of nanoparticle uptake has been limited. This is largely attributed to the inherent differentiation of organoids *in vitro,* where the surrounding epithelial layer becomes polarized, forming a closed central lumen that limits access to the apical membrane. In this chapter, we overcome this limitation by employing a method where a microinjector is used to 'inject' the particle solution into the lumen. After a period of time has elapsed, the cells are disassociated and analysed using fluorescence-activated cell sorting to determine the rate of uptake. To our knowledge, this method presents the most convenient way to access the apical membrane without disrupting the formation of the organoid. However, due to the discrepancy in size of organoids and the difficulty in determining the number of cells contained within each organoids, a high level of repetitions across a large number of organoids is necessary to obtain a reliable average rate of uptake. Ultimately, the M cells generated via this method are a more accurate representation of the M cells constitutively expressed *in vivo.* As such, the results generated from this study may be more translatable to the *in vivo* context. We anticipate that this model, and the associated method for testing M cell-mediated transcytosis, present a significant improvement over the cell line-based co-cultures currently used.

M cell differentiation remains an improperly understood process. M cell number and patterning within the FAE appear to be strictly regulated via several signalling pathways. Tight regulation of M cells is necessary as the same features that contribute to efficient antigen sampling can also be exploited by invading pathogens to gain access to systemic circulation. Correspondingly, M cell expansion is frequently observed under pathologic conditions. Inflammatory bowel disease patients present with increased number of M cells that likely contribute to the inflammatory process. [29, 30] Bacterial infection also appears to rapidly induce production of new M cells. [31, 32] As such, it is important to gain a deeper understanding of the molecular processes and signalling pathways that regulate M cell differentiation and function. In **Chapter 4**, we provide an outline of the important outstanding questions in M cell biology. This chapter explores the key outstanding questions in the current

knowledge of the numerous M cell developmental pathways and the still unknown signalling mechanisms that may regulate M cell development.

Due to the crucial role of M cells in mucosal immunity and with M cell expansion being a key feature of inflammatory diseases and infections, it is imperative to gain a better understanding of the mechanisms that regulate the induction of M cells. **Chapter 5** investigates the RANK/RANKL signalling pathway in regulating M cell number. Specifically, osteoprotegerin (OPG) is known to act as a decoy receptor for RANKL, inhibiting the biological effects of RANK/RANKL coupling. Here, we utilised the organoid technology to demonstrate that OPG plays an inhibitory role in M cell differentiation. OPG-null organoids generate much higher numbers of M cells compared to wildtype organoids. In addition to the data presented in this chapter, we performed single-cell gene sequencing of wildtype and OPG-null organoids with and without RANKL stimulation. Though this data could not be included in the results, understanding the epithelial changes that occur in response to RANKL at the genome level may provide further insight into other molecular partner for this signalling cascade.

Chapter 6 explores the signalling mechanisms regulating cellular differentiation within the small intestine and the PPs. Numerous signalling pathways regulate cellular fate determination and function within the small intestine and the PPs. While some of these molecular pathways have been well described, the signalling mechanisms prevalent in the subepithelial region of the PPs remain largely uncharacterized. [16, 33-35] Previous research indicates that epithelial cells overlying the PPs exhibit significantly different gene expression than cells of the regular epithelium. [36] Additionally, transcriptomic data suggests that there is significant discrepancy in gene expression between distally and proximally located PPs, suggesting that the complex microenvironment of the PPs varies with location. [37] As such, it is necessary to convey that despite the significance of the work conducted in Chapter 5, the unique microenvironment of the PPs influences the overlying epithelium significantly and our understanding of these mechanisms is incomplete.

Chapter 7 explores the role of mucus in nanoparticle uptake. Utilising cell lines with varying levels of mucus production, this chapter shows the limiting role of mucus in nanoparticle uptake. Although this thesis has established organoids as an advanced model for the study of M cells as potential targets for modified nanocarriers in **Chapter 3**, the experiments conducted

in **Chapter 7** utilized cell lines in lieu of organoids. There are several reasons why organoids are not ideal for studying the function of mucus in nanoparticle uptake. Firstly, though organoids contain goblet cells, the spherical shape of the organoid renders the lumen closed. This causes mucus to be secreted into the lumen where it accumulates in the enclosed structure, making it challenging to quantify and evaluate mucus. Secondly, organoids are cultured in a specific growth factor cocktail that consists of epidermal growth factor (EGF), the BMP antagonist Noggin and Wnt activator R-spondin. [28] The resulting cellular media, termed 'ENR', can be modified via the addition/withdrawal of certain growth factors to direct cellular differentiation to a specific lineage. As an example, although enteroendocrine cells (EECs) are present in the regular 'ENR' cultured organoid system, EEC enrichment for the specific study of EEC function requires the withdrawal of BMP antagonist Noggin and the addition of Notch inhibitor DAPT and BMP agonist BMP4. [28, 38] Enrichment for goblet cells requires the addition of Notch inhibitor DAPT and Wnt pathway inhibitor IWP2. [39] As a result of these modifications, extraneous variables are introduced into the culture protocol that may influence the transcriptomic profile of the system in unknown ways. As a result of these factors, enriching organoids for goblet cells to study particle uptake in the context of mucus may prove practically difficult. As such, the cell line-based model used in **Chapter 7** provides a more reproducible and practical approach to studying mucus interactions with modified nanocarriers. Though the cellular models presented in this chapter provide a convenient and reproducible set of well-characterized models for studying mucus, mucus-containing organoids merit further exploration in the future. Characterising the transcriptomic profile of goblet cell-enriched organoids can provide insight into the epithelial changes that may occur pertaining to other cell types, including M cells. Future work in this area should also focus on overcoming the practical limitations associated with the continuous accumulation of mucus within the enclosed lumen. Establishing and characterising a goblet cell-enriched organoid model and an associated method for testing nanoparticle uptake can significantly further our understanding of mucus as a barrier to drug delivery.

Though the work presented in this thesis will help facilitate future attempts to study the function of M cells pertaining to drug uptake *in vitro*, our knowledge of the precise mechanisms of transcytosis remains incomplete. Utilising the model established here, we suggest that future work in this field may benefit from investigating the outstanding questions in M cell biology as outlined in **Chapter 4**; whether M cell-mediated uptake is receptor mediated or

indiscriminate and the optimal particle size and surface modifications that will facilitate the greatest uptake.

8.2 Conclusion

Mucosal immunization holds great potential as a strategy for generating a potent and robust immune response at the primary site of infection. M cell targeting has been implicated as a strategy with significant potential to increase the bioavailability of orally delivered biopharmaceuticals. Enhancing the potency of oral vaccines through M cell targeting requires a comprehensive understanding of M cell biology. Despite a perfunctory understanding of the M cell's exceptional ability to swiftly transcytose luminal antigens, the field lacks a comprehensive understanding of the mechanisms by which M cells orchestrate mucosal immune responses. This can be attributed to numerous factors that impede the large-scale study of M cells; their scarcity, the lack of a universal M cell markers across different purported lineages and the variance in relevancy among the *in vitro* models used within the literature. The research conducted in this thesis demonstrated that targeting M cells poses several challenges. It highlighted the need for reliable and physiologically relevant models to study M cell-mediated nanoparticle uptake. Accordingly, it presented an advanced model for studying M cells and a reproducible method for evaluating M cell-mediated particle uptake. The thesis further explored the mechanisms that govern M cell differentiation, with OPG being implicated as a regulatory molecule in suppressing M cell development. The knowledge gained from this research can inform future efforts to target specific cells within the gastrointestinal tract and advance the study of signalling pathways that regulate the function of specific cells.

8.4 References

1. Kiyono, H., et al., *Mucosal vaccines: wisdom from now and then.* Int Immunol, 2021. **33**(12): p. 767-774.
2. Lamers, M.M., et al., *SARS-CoV-2 productively infects human gut enterocytes.* Science, 2020. **369**(6499): p. 50-54.
3. Lavelle, E.C. and R.W. Ward, *Mucosal vaccines - fortifying the frontiers.* Nat Rev Immunol, 2022. **22**(4): p. 236-250.
4. Organisation, W.H. *The top 10 causes of death*. 2020; Available from: https://www.who.int/news-room/fact-sheets/detail/the-top-10-causes-of-death.
5. Organisation, W.H. *Coronavirus (COVID19) Dashboard*. 2022; Available from: https://covid19.who.int.
6. Lycke, N., *Recent progress in mucosal vaccine development: potential and limitations.* Nat Rev Immunol, 2012. **12**(8): p. 592-605.
7. Boegh, M. and H.M. Nielsen, *Mucus as a barrier to drug delivery - understanding and mimicking the barrier properties.* Basic Clin Pharmacol Toxicol, 2015. **116**(3): p. 179-86.
8. Vancamelbeke, M. and S. Vermeire, *The intestinal barrier: a fundamental role in health and disease.* Expert Rev Gastroenterol Hepatol, 2017. **11**(9): p. 821-834.
9. Clevers, H.C. and C.L. Bevins, *Paneth cells: maestros of the small intestinal crypts.* Annu Rev Physiol, 2013. **75**: p. 289-311.
10. Holmgren, J. and C. Czerkinsky, *Mucosal immunity and vaccines.* Nat Med, 2005. **11**(4 Suppl): p. S45-53.
11. Azegami, T., Y. Yuki, and H. Kiyono, *Challenges in mucosal vaccines for the control of infectious diseases.* Int Immunol, 2014. **26**(9): p. 517-28.
12. Azizi, A., et al., *Enhancing oral vaccine potency by targeting intestinal M cells.* PLoS Pathog, 2010. **6**(11): p. e1001147.
13. Nakamura, Y., S. Kimura, and K. Hase, *M cell-dependent antigen uptake on follicle-associated epithelium for mucosal immune surveillance.* Inflamm Regen, 2018. **38**: p. 15.
14. Obata, Y., et al., *Epithelial-stromal interaction via Notch signaling is essential for the full maturation of gut-associated lymphoid tissues.* EMBO Rep, 2014. **15**(12): p. 1297-304.

15. Knoop, K.A., et al., *Distinct developmental requirements for isolated lymphoid follicle formation in the small and large intestine: RANKL is essential only in the small intestine.* Am J Pathol, 2011. **179**(4): p. 1861-71.
16. de Lau, W., et al., *Peyer's patch M cells derived from Lgr5(+) stem cells require SpiB and are induced by RankL in cultured "miniguts".* Mol Cell Biol, 2012. **32**(18): p. 3639-47.
17. Antunes, F., et al., *Establishment of a triple co-culture in vitro cell models to study intestinal absorption of peptide drugs.* Eur J Pharm Biopharm, 2013. **83**(3): p. 427-35.
18. Amerongen, H.M., et al., *Transepithelial transport of HIV-1 by intestinal M cells: a mechanism for transmission of AIDS.* J Acquir Immune Defic Syndr, 1991. **4**(8): p. 760-5.
19. Beduneau, A., et al., *A tunable Caco-2/HT29-MTX co-culture model mimicking variable permeabilities of the human intestine obtained by an original seeding procedure.* Eur J Pharm Biopharm, 2014. **87**(2): p. 290-8.
20. Beloqui, A., et al., *A human intestinal M-cell-like model for investigating particle, antigen and microorganism translocation.* Nat Protoc, 2017. **12**(7): p. 1387-1399.
21. Beloqui, A., A. des Rieux, and V. Preat, *Mechanisms of transport of polymeric and lipidic nanoparticles across the intestinal barrier.* Adv Drug Deliv Rev, 2016. **106**(Pt B): p. 242-255.
22. Chaikhumwang, P., et al., *A new cell-to-cell interaction model for epithelial microfold cell formation and the enhancing effect of epidermal growth factor.* Eur J Pharm Sci, 2017. **106**: p. 49-61.
23. Jia, Z., et al., *An ex Vivo Model Enables Systematic Investigation of the Intestinal Absorption and Transcytosis of Oral Particulate Nanocarriers.* ACS Biomater Sci Eng, 2021.
24. Klisuric, A., et al., *Highlight Article: Identifying human and murine M cells in vitro.* Exp Biol Med (Maywood), 2019. **244**(7): p. 554-564.
25. des Rieux, A., et al., *An improved in vitro model of human intestinal follicle-associated epithelium to study nanoparticle transport by M cells.* Eur J Pharm Sci, 2007. **30**(5): p. 380-91.
26. des Rieux, A., et al., *Transport of nanoparticles across an in vitro model of the human intestinal follicle associated epithelium.* Eur J Pharm Sci, 2005. **25**(4-5): p. 455-65.
27. Bar-Ephraim, Y.E., K. Kretzschmar, and H. Clevers, *Organoids in immunological research.* Nat Rev Immunol, 2020. **20**(5): p. 279-293.

28. Sato, T., et al., *Single Lgr5 stem cells build crypt-villus structures in vitro without a mesenchymal niche.* Nature, 2009. **459**(7244): p. 262-5.
29. Fujimura, Y., R. Kamoi, and M. Iida, *Pathogenesis of aphthoid ulcers in Crohn's disease: correlative findings by magnifying colonoscopy, electron microscopy, and immunohistochemistry.* Gut, 1996. **38**(5): p. 724-32.
30. Smillie, C.S., et al., *Intra- and Inter-cellular Rewiring of the Human Colon during Ulcerative Colitis.* Cell, 2019. **178**(3): p. 714-730 e22.
31. Borghesi, C., M.J. Taussig, and C. Nicoletti, *Rapid appearance of M cells after microbial challenge is restricted at the periphery of the follicle-associated epithelium of Peyer's patch.* Lab Invest, 1999. **79**(11): p. 1393-401.
32. Grutzkau, A., et al., *Involvement of M cells in the bacterial invasion of Peyer's patches: a common mechanism shared by Yersinia enterocolitica and other enteroinvasive bacteria.* Gut, 1990. **31**(9): p. 1011-5.
33. Gregorieff, A., et al., *Expression pattern of Wnt signaling components in the adult intestine.* Gastroenterology, 2005. **129**(2): p. 626-38.
34. Demitrack, E.S. and L.C. Samuelson, *Notch regulation of gastrointestinal stem cells.* J Physiol, 2016. **594**(17): p. 4791-803.
35. Lo, D.D., *Vigilance or Subversion? Constitutive and Inducible M Cells in Mucosal Tissues.* Trends Immunol, 2018. **39**(3): p. 185-195.
36. Hase, K., et al., *Distinct gene expression profiles characterize cellular phenotypes of follicle-associated epithelium and M cells.* DNA Res, 2005. **12**(2): p. 127-37.
37. Phillips, C.L., et al., *Regional heterogeneity in rat Peyer's patches through whole transcriptome analysis.* Exp Biol Med (Maywood), 2021. **246**(5): p. 513-522.
38. Gehart, H., et al., *Identification of Enteroendocrine Regulators by Real-Time Single-Cell Differentiation Mapping.* Cell, 2019. **176**(5): p. 1158-1173 e16.
39. Yin, X., et al., *Niche-independent high-purity cultures of Lgr5+ intestinal stem cells and their progeny.* Nat Methods, 2014. **11**(1): p. 106-12.

.

Appendix I: Publication Contributions and Permissions

Chapter 1

Figure 3, adapted from Barker and Clevers (2007), is reproduced with permission.

SPRINGER NATURE LICENSE TERMS AND CONDITIONS Jul 07, 2022	
This Agreement between Ms. Ana Klisuric ("You") and Springer Nature ("Springer Nature") consists of your license details and the terms and conditions provided by Springer Nature and Copyright Clearance Center.	
License Number	5343770736134
License date	Jul 07, 2022
Licensed Content Publisher	Springer Nature
Licensed Content Publication	Nature
Licensed Content Title	Identification of stem cells in small intestine and colon by marker gene Lgr5
Licensed Content Author	Nick Barker et al
Licensed Content Date	Oct 14, 2007
Type of Use	Thesis/Dissertation
Requestor type	academic/university or research institute
Format	print and electronic
Portion	figures/tables/illustrations
Number of figures/tables/illustrations	1
High-res required	n/a
Will you be translating?	no
Circulation/distribution	1 - 29
Author of this Springer Nature content	no
Title	Molecular Mechanisms of M Cell Signalling
Institution name	University of South Australia
Expected presentation date	Jul 2022
Portions	Figure 1

Requestor Location	Ms. Ana Klisuric [redacted] [redacted] [redacted] Australia Attn: Ms. Ana Klisuric
Total	0.00 USD

Chapter 2

Klisuric A, Thierry B, Delon L, Prestidge CA, Gibson RJ. Identifying human and murine M cells in vitro. Experimental Biology and Medicine. 2019;244(7):554-564. doi:10.1177/1535370219838674

The published version is available at:
https://journals.sagepub.com/doi/10.1177/1535370219838674

Author	Wrote Manuscript	Revised Manuscript	Designed Research	Performed Research	Analysis of Data	Data Interpretation
A Klisuric	✓	✓	✓	✓	✓	✓
B Thierry		✓	✓			
L Delon		✓	✓			
CA Prestidge		✓	✓			
RJ Gibson		✓	✓			

This published manuscript has been reproduced for this thesis under the “gratis reuse” clause of Springer Nature guidelines.

Chapter 3

This chapter is currently unpublished.

Author	Wrote Manuscript	Revised Manuscript	Designed Research	Performed Research	Analysis of Data	Data Interpretation
A Klisuric	✓	✓	✓	✓	✓	✓
JB Ephraim		✓	✓			
Z Jia		✓	✓			
RJ Gibson		✓	✓			
CA Prestidge		✓	✓			
B Thierry		✓	✓			
H Clevers		✓	✓			

Chapter 4

This chapter is currently unpublished.

Author	Wrote Manuscript	Revised Manuscript	Designed Research	Performed Research	Analysis of Data	Data Interpretation
A Klisuric	✓	✓	✓	✓	✓	✓
H Clevers		✓	✓			

Chapter 5

This chapter is currently unpublished.

Author	Wrote Manuscript	Revised Manuscript	Designed Research	Performed Research	Analysis of Data	Data Interpretation
A Klisuric	✓	✓	✓	✓	✓	✓
JB Ephraim		✓	✓			
B Thierry		✓	✓			
H Clevers		✓	✓			

Chapter 6

This chapter is currently unpublished.

Chapter 7

This chapter is currently unpublished.

Author	Wrote Manuscript	Revised Manuscript	Designed Research	Performed Research	Analysis of Data	Data Interpretation
A Klisuric	✓	✓	✓	✓	✓	✓
RJ Gibson		✓	✓			
CA Prestidge		✓	✓			
Z Jia		✓	✓			
M Winter		✓	✓			
B Thierry		✓	✓			